Investigating the pathways required for TGF-β_1 stimulated mTORC1 activation and collagen I synthesis

Mr Matthew Redding

A thesis submitted to University College London for the degree of Doctor of Philosophy

Centre for Inflammation and Tissue Repair

UCL Respiratory

Division of Medicine

University College London

Acknowledgements

I would like to thank my academic supervisors Professor Rachel Chambers and Dr Paul Mercer and my industrial sponsor supervisors at GlaxoSmithKline, Dr David Budd and Dr Andy Blanchard. The knowledge and wisdom you have imparted over the years will be invaluable throughout my future career and life. I look forward to continuing to work with you in the future.

To my colleagues at UCL, you have been fantastic, supportive and fun. Even through the hard times, you have always been there to advise me, cheer me up and remind me to be me. In particular, David Pearce, Deborah Chong and Gabby Szylar your help, support, sound logic and smiles got me through many difficult situations. You truly are great friends. I wish you all the best of luck for the future.

To my family, this PhD would not have been completed without you. Especially my parents I could ask for no more, you are both such wonderful parents, the time, energy and endless support you have invested into me is beyond words, and to say a simple thank you doesn't speak the volumes I would require to 'truly' say thank you. Over the years you have picked me up, dusted me off, and sent me on to complete this very important milestone in my life. For this, I will be eternally grateful.

Declaration

I confirm that the work presented in this thesis is entirely my own.

Abstract

Idiopathic pulmonary fibrosis (IPF) is a chronic progressive lung scarring disease. The abnormal and aberrant wound healing response leads to excess matrix production. The aetiology of IPF is unknown, the prognosis is poor and current treatments are ineffective.

Transforming growth factor-β is a critical cytokine which is increased in IPF patients, due to repetitive epithelial injury. TGF-β_1 is responsible for driving the progression of the disease through the activation and differentiation of local and recruited fibroblast populations. TGF-β_1 initiates signalling pathways within the fibroblasts which drives their differentiation programme into the myofibroblast and the deposition of matrix proteins, in particular collagen I.

TGF-β_1 regulates genes involved in fibrogenesis. It does this by regulating several transcription factors as well as promoting the translation of the mRNA. Critically, it mediates the transcription of the collagen I gene through the activation of SMAD 3 and the translation of this gene via mammalian target of rapamycin complex 1 (mTORC1) activation. The mechanism of TGF-β_1 stimulated mTORC1 activation is currently unknown in primary human lung fibroblasts. To examine the TGF-β_1 stimulated pathway required for mTORC1 activation I employed pharmacological, siRNA and gene editing techniques.

This study defined the mechanisms of mTOR phosphorylation at the amino acid residue site S2448 and ruled it was not required for TGF-β_1 mediated collagen synthesis. This study delineated that ras homology enriched in brain (RHEB) was critical for mTORC1 activation. However, the role of RHEBs regulatory complex, comprised of tuberous sclerosis 1 and tuberous sclerosis 2 (TSC1/2), still remains ambiguous. Finally, it identified that mothers against decapentaplegic (SMAD) 3 was required for early mTORC1 activation through an unknown transcriptionally regulated protein.

The work reported in this thesis raises the possibility that there is a protein acting as a link between SMAD 3 and the mTORC1 regulatory components TSC1/2 and RHEB which could be a potential drug target for the treatment of IPF. There could be additional benefits of inhibiting this target rather than directly inhibiting TGF-β_1, the TGF-β_1 receptors or mTORC1 which have

unwanted and serious side-effects. The niche targeting of a SMAD 3 transcriptionally regulated protein that enhances mTORC1 signalling downstream of TGF-β_1 should in theory minimise these unwanted side-effects. Finally, the implications of SMAD 3 and mTORC1 activation downstream of TGF-β_1 are relevant in other fibrotic diseases adding to the potential of a translatable drug between diseases.

Impact statement

This thesis describes several aspects revolving around TGF-β_1 stimulated mTORC1 activation and collagen I synthesis in primary human lung fibroblasts. In this study, I have described the mechanisms of mTOR phosphorylation. Specifically, the S2448 site on mTOR was phosphorylated by TGF-β_1 stimulation at early time-points which correlated with the phosphorylation of its substrates 4E-BP1 and P70S6K. The initial investigation delineated that the mTOR S2448 phosphorylation was independent of the well characterised pathway PI3K/AKT. Next, I established that the mTOR kinase activity acted as a feedback loop to facilitate its own phosphorylation. Furthermore, I established that it must be mTORC1 kinase activity that was required because the inhibition of P70S6K prevented S2448 phosphorylation. Finally, for the first time, I established that PDK1 was also required for the phosphorylation of S2448. This mechanism highlights the importance of both PDK1 and mTORC1 signalling converging on P70S6K to activate it. The histological analysis of this site revealed low signalling in the fibroblast. However, there is large amounts of staining in the epithelium, suggesting that this site may be important for epithelial cell signalling. Furthermore, S2448 could be a useful biomarker in clinical studies for distinguishing active mTORC1 signalling and perhaps looking at the difference between the epithelium and the myofibroblasts.

This investigation built upon the role of SMAD 3 signalling, highlighting its requirement for TGF-β_1 stimulated mTORC1 activation. The identification that TGF-β_1 activates SMAD 3 to transcribe a protein to activate mTORC1 is interesting conceptually because mTORC1 will be required for the translation of this SMAD 3 transcribed gene. This highlights that the combination of TGF-β_1 stimulated SMAD 3 and the basally activated mTORC1 facilitates increased activation of mTORC1 in a pseudo feedforward loop. Interestingly, investigations of the two known SMAD 3 to mTOR activation pathways were ruled out in our primary human lung fibroblasts. Therefore, there is a novel protein or signalling pathway that remains unidentified. To identify a SMAD 3 dependent transcribed protein, RNAseq technology could be employed. From the host of transcribed proteins identified from this data set, a compound

screen could then be used to see which of the targets lead to mTORC1 and collagen inhibition. This could lead to the discovery of a novel protein for mTORC1 activation leading to future therapeutic opportunities. Additionally, identifying early SMAD 3 regulated genes may identify new proteins that are important to other aspects of the disease IPF.

Finally, the GTPase RHEB was found to be critical for TGF-β_1 stimulated mTORC1 activation and collagen I synthesis. Interestingly, knock-down of TSC1/2 highlights its complex relationship with mTORC1 suggesting that it not only works synergistically with TGF-β_1 but also functions in an independent manner because knock-down increases mTORC1 signalling independent of TGF-β_1. However, it also shifts the TGF-β_1 curve in favour of increased mTORC1 activation. The investigation of the TSC1/2-RHEB axis revealed that this pathway is independent of several kinases in isolation and there may be compensatory pathways in place which need to be blocked in parallel in order to inhibit TGF-β_1 stimulated collagen I synthesis. This may suggest TGF-β_1 stimulated collagen synthesis needs to be conceived as a more complex model rather than singular isolated signalling pathways. Therefore, combinatorial compound studies targeting these kinase will be critical for ruling out their importance in this response. This research has been important in ruling out these singular signalling pathways and future research offers opportunities that other kinases may be responsible for the phosphorylation and inhibition of the TSC1/2 complex which could present novel therapeutic targets.

Table of Contents

List of Figures

List of Tables

List of Abbreviations

4E-BP1	Eukaryotic translation initiation factor 4E binding protein 1
DAPI	4',6-diamidino-2-phenylindole, dihydrochloride
ALK5	Activin receptor-like kinase 5
α-SMA	Alpha-smooth muscle actin
ANOVA	Analysis of variance
ATP5B	ATP synthase 5B
B2M	Beta2 microglobulin
BCA	Bicinchoninic acid
BSA	Bovine serum albumin
BAL	Bronchoalveolar lavage
SMAD	*Caenorhabditis elegans* protein SMA and mothers against decapentaplegic
CDK1	Cyclin dependent kinase 1
COL1A1	Collagen, type 1, alpha 1
COL1A2	Collagen, type 1, alpha 2
CTGF	Connective tissue growth factor
DNA	Deoxyribonucleic acid
DEPTOR	DEP domain containing mTOR-interacting protein
DMSO	Dimethyl sulfoxide
DMEM	Dulbecco's modified eagle medium
ER	Endoplasmic reticulum
ELISA	Enzyme-linked immunosorbent assay
EMT	Epithelial-mesenchymal transition
Elk1	Ets domain-containing protein
eIF4A	Eukaryotic translation initiation factor 4A
eIF4B	Eukaryotic translation initiation factor 4B
eIF4E	Eukaryotic translation initiation factor 4E
eIF4G	Eukaryotic translation initiation factor 4G
ERK	Extracellular signal-regulated kinase
ECM	Extracellular matrix
FGF	Fibroblast growth factor
FKBP12	FK506 binding protein 12
FRB	FKBP-rapamycin binding domain
FBS	Foetal bovine serum

FVC	Forced vital capacity
GSK3	Glycogen synthase kinase 3
GPCR	G-protein coupled receptor
GAP	GTPase activating protein
HRCT	High-resolution computed tomography
HRP	Horseradish peroxidase
HLF	Human lung fibroblast
HEAT	Huntingtin, elongation factor 3, protein phosphatase 2A, TOR1
HCl	Hydrochloric acid
HIF-1α	Hypoxia inducible factor 1 alpha
IKκβ	Nuclear Factor NF-Kappa-B Inhibitor Kinase Beta
IIP	Idiopathic interstitial pneumonia
IPF	Idiopathic pulmonary fibrosis
IRS	Insulin receptor substrate
IGF-1	Insulin-like growth factor 1
IL-1β	Interleukin 1 beta
ILD	Interstitial lung disease
LARP	La Ribonucleoprotein domain family member
LAP	Latency associated peptide
LTBP-1	Latent TGF-β binding protein 1
LPA	Lypophosphatidic acid
MK2	Mitogen activated protein kinase-activated protein kinase 2
mLST8	mammalian lethal with sec-13 protein 8
mSIN1	Mammalian stress-activated map kinase interacting protein 1
mTOR	Mammalian target of rapamycin
MMP	Matrix metalloproteinase
miRNA	micro-RNA
MAPK	Mitogen-activated protein kinase
mAb	monoclonal antibody
MEF	Mouse embryonic fibroblast
NDRG1	N-Myc downstream regulated 1
P70S6K	P70 S6 kinase
PTEN	Phosphatase and tensin homolog
PBS	Phosphate buffered saline

PIP_3	Phosphatidylinositol 3,4,5-triphosphate
PIP_2	Phosphatidylinositol 4,5-bisphosphate
PI3K	Phosphatidylinositol-3-kinase (PI3K)
PIKK	Phosphatidylinositol-3-kinase-related kinase
PDK1	Phosphoinositide-dependent kinase 1
PDGF	Platelet-derived growth factor
PH	Pleckstrin homology domain
PAGE	Polyacrylamide gel electrophoresis
PRAS40	Proline-rich Akt substrate 40 kDa
PGE2	Prostaglandin E2
PKCα	Protein kinase C alpha
PAR1	Proteinase-mediated activated receptor 1
RT-qPCR	Real-time quantitative polymerase chain reaction
RICTOR	Rapamycin-insensitive companion of mTOR
Rheb	Ras homolog enriched in brain
ROS	Reactive oxygen species
RAPTOR	Regulatory-associated protein of mTOR
RNA	Ribonucleic acid
RSK1	Ribosomal S6 kinase
SGK1	Serum/glucocorticoid regulated kinase 1
SNP	Single nucleotide polymorphism
SBE	Smad-binding element
shRNA	small hairpin RNA
siRNA	Small interfering RNA
SD	Standard deviation
SEM	Standard error of the mean
SP-C	Surfactant protein C
SSc	Systemic sclerosis
TAK1	TGF-β activated kinase 1
TIMP	Tissue inhibitor of matrix metalloproteinase
TNFα	Tissue necrosis factor alpha
TOS	TOR signalling motif
$TGF-\beta_1$	Transforming growth factor beta 1
TCTP	Translationally controlled tumour protein

TBST	Tris-buffered saline, tween
TSC	Tuberous sclerosis
UIP	Usual interstitial pneumonia
VEGF	Vascular epithelial growth factor

1. Introduction

1.1. Interstitial lung disease

Interstitial lung disease (ILD) encompasses a large group of lung diseases. There are over 200 ILD's which are categorized by their impact on the interstitium which is a tissue network that supports the air sacs of the lungs. The aetiology is often unknown but these diseases are typically associated with tissue injury which triggers an abnormal wound healing response leading to lung scarring. This subsequently impairs gas exchange via either inflammation, scarring or oedema – which can be acute or chronic depending on the disease. Examples of these conditions include: cryptogenic organising pneumonia, sarcoidosis and notably idiopathic pulmonary fibrosis (IPF).

1.2. Idiopathic pulmonary fibrosis

Idiopathic pulmonary fibrosis patients represent 70% of the total ILD sufferers, however, prevalence does vary (Wolters et al. 2014). Epidemiological studies calculating the prevalence of IPF between continents has been approximated to represent 300,000 people in Europe, 640,000 in East Asia and 300,000 people in the United States – with an estimated 3 million people world-wide (Martinez et al. 2017). The incidence of IPF increases with age: below the age of 65, the range is 2-30 cases per 100,000 people; this increases to 400 cases per 100,000 in patients over the age of 65 (Martinez et al. 2017). Other studies also suggest that the incidence of IPF increased by 11% annually between 1991 and 2003 (Gribbin et al. 2006). Most studies also report a predominance of the disease in men although the reason why is unclear. (Gribbin et al. 2006).

The median survival for IPF patients is 3-5 years from diagnosis, which is often delayed and only apparent when there is already considerable fibrosis present. IPF patients exhibit increasing dyspnoea, a persistent and increasing dry cough and fatigue, with less common symptoms being fever, weight loss and muscle and joint pain. Initial patient diagnosis will detect lung crackles heard with a stethoscope and follow-up pulmonary function tests will detect the decreased total lung capacity and abnormal gas exchange indicative of ILD. Difficulties can arise when distinguishing between different ILDs due to

the commonality shared between the symptoms, for example a decline in lung function. Classification of IPF is established from clinical, radiographic and histological evaluation. The ATS/ERS/JRS/ALAT statement states that the diagnosis of IPF specifically requires the presence of a usual interstitial pneumonia (UIP) pattern including the exclusion of secondary causes of pulmonary fibrosis.

High-resolution computed tomography (HRCT) imaging is used to distinguish IPF from other ILDs. The HRCT image of an IPF lung reveals a heterogeneous lung architecture with honeycomb-like structures in the sub-pleural regions of the lung with a predominantly bilateral, peripheral and basal distribution; peripheral septal thickening and traction bronchiectasis (Raghu et al. 2011; Martinez et al. 2017). The presence of honeycombing with heterogeneous sub-pleural distribution has a success rate 90-100% of determining the histologic pattern of UIP (Wells 2013).

The distinction of a clear UIP pattern and the exclusion of other ILDs is made by a team of experienced radiologists/clinicians to determine if the diagnosis is IPF. From the ATS/ERS/JRS/ALAT statement, misdiagnosis from inexperienced radiologists and clinicians can lead to large variability between diagnoses when less usual HRCT UIP patterns are observed (Wells 2013). Therefore, any remaining uncertainty in diagnosis will necessitate a lung biopsy to be taken for histological analysis, unless the risk to patient health out-weighs the benefits of a clear diagnosis (Wells 2013; Martinez et al. 2017).

Histological analysis of a typical IPF lung biopsy reveals a lung that is heavily laden with extracellular matrices that are sporadically deposited throughout the lung. In particular, collagen I and collagen III make up a large portion of this excess matrix. The epithelial cell population is heterogeneous with regions of apoptosis, and areas characterized by epithelial hyperplasia. The disorganized deposition of collagen correlates with regions of epithelial cell damage, abnormal proliferation and hyperplastic type II epithelial cells (Datta et al. 2011).

A critical population of cells is the α-SMA positive myofibroblast which arises from differentiation of local and recruited fibroblast populations. A hall-mark

feature is the presence of fibrotic foci which are observed as a bulge-like protrusion into the alveolar airspace and are heterogeneously spaced throughout the lung (Katzenstein & Myers 1998). Fibrotic foci are characterised by a hyperplastic type II epithelium, dense extracellular matrix with high populations of fibroblasts and α-SMA expressing myofibroblasts (Datta et al. 2011).

Microarray studies using IPF lung tissue revealed that gene expression for proteins required for ECM turnover and inflammatory processes were increased (Zuo et al. 2002).

1.3. Treatment of IPF

The drug treatment options for IPF patients are limited and currently no drug is available that halts or resolves the disease. In all wound healing responses, the initial injury leads to inflammation and the recruitment of inflammatory cells such as macrophages. Therefore, historical treatments used immunosuppressive, anti-inflammatory and anti-oxidant drugs which are azathioprine, prednisolone and N-Acetylcysteine, respectively. In the 'PANTHER-IPF trial' the combinatorial treatment with these three drugs was investigated. The treatment was proved to be ineffective and caused an increased in the incidence of death. The increase in hospitalisation resulted in the trial discontinuing (clinicaltrials.gov identifier NCT00650091). However, this led to a better understanding of IPF. It is now believed that the point at which IPF is detected there is no longer any inflammatory response and as a result anti-inflammatory treatments are ineffective.

There are only two drugs licenced and marketed specifically for the treatment of IPF, Nintedanib and Pirfenidone, marketed as Ofev and Esbriet respectively. The first drug to be specifically licensed for the use in IPF patients was Pirfenidone in Japan in 2008. The compound was later licensed in Europe in 2011 and in the USA in 2014. The ASCEND phase III trial treated patients over a 52 week comparing Pirfenidone to a placebo group. Treatment with Pirfenidone preserved lung function as measured by forced vital capacity (FVC) and vital capacity. However, Pirfenidone only slowed the progression of the disease and lung function decline still occurred (King et al. 2014).

Pirfenidone is a well-tolerated compound but there are still significant side-effects. The early *in vivo* studies investigated the effect of Pirfenidone in the bleomycin mouse model of fibrosis (Kakugawa et al. 2004). This research observed that Pirfenidone attenuated the bleomycin induced lung fibrosis (Kakugawa et al. 2004). Pirfenidone's mode of action is not well defined. However, the compound showed decreased matrix deposition and fibroblast proliferation which is attributed to the attenuation of the heat shock protein 47 (HSP47) (Kakugawa et al. 2004).

Nintedanib was approved in 2014 in Europe and America. The INPULSIS-1 and INPULSIS-2 trials assessed a total 1066 patients (placebo and Nintedanib treated patients) and demonstrated that Nintedanib reduced the decline in IPF patient FVC (Richeldi et al. 2014). The treatment with Nintedanib has adverse effects although symptoms are easily treated and well tolerated (Richeldi et al. 2014; Hajari Case & Johnson 2017). Nintedanib was demonstrated to be anti-fibrotic in two fibrotic models, the bleomycin and the silica particle administration mouse models (Wollin et al. 2014) which meant it was taken forward for clinical trials. Furthermore, the *in vitro* studies have demonstrated that the mechanism of action of Nintedanib is as a triple receptor tyrosine kinase inhibitor targeting the receptors for vascular epithelial growth factor (VEGF), platelet-derived growth factor (PDGF) and fibroblast growth factor (FGF) which can supress the sarcoma kinases (Src) pathway showing decreased proliferation and differentiation of human lung fibroblasts (Hilberg et al. 2008; Wollin et al. 2014; Wollin et al. 2015). Therefore, this has given some insight in the underlying cell signalling pathways important for the synthesis of collagen and the progression of the disease. However, neither compound is capable of halting or preventing the terminal outcome of the disease. Recent evidence from the NCT02598193 clinical trial has demonstrated that the combined treatment of Pirfenidone and Nintedanib is well tolerated in patients. Whether the combined treatment will be effective in IPF patients over the single dose treatment has yet to be been determined (Flaherty et al. 2017). The current drug treatments with either Pirfenidone and Nintedanib are only partially effective for the treatment of IPF but they do improve the length of survival. Therefore, development of new therapeutic

treatments is essential. There are more than fifty IPF clinical trials including: a monoclonal antibody targeting the integrin αVβ6 (clinical trials identifier NCT01371305); Lysophophatidic acid (clinical trials identifier NCT01766817); PI3K/mTOR inhibitor (clinical trials identifier NCT01725139); JNK inhibitor (clinical trials identifier NCT03142191). Although these clinical trials hold potential for the treatment of the disease there is still a high drop-out rate of compounds from clinical trials and they may have the problem of unwanted side-effects. Therefore, by further understanding IPF, research will further the development of new therapeutic treatments.

1.4. Aetiology of IPF

The diagnosis of IPF occurs in the late stages of the disease and therefore its aetiology is currently unknown and the exact underlying pathophysiological mechanisms of IPF are poorly understood. However, a number of theories have been proposed. The most popular and prevailing theory is the disease is caused by repetitive epithelial injury. The causes of epithelial cell injury have been attributed to several factors: viral infections, smoking and certain co-morbidities or genetic risks (Oh et al. 2012; Camelo et al. 2014). These factors lead to epithelial cell apoptosis. Increased apoptosis is observed as evidenced by increased markers of apoptosis (p53, p21, bcl-2 bax and caspase 3) in alveolar and bronchial epithelial cells in IPF patient biopsies (Plataki et al. 2005). In addition, evidence has also been gathered from animal models. The most common animal model of fibrosis is the bleomycin mouse model. Mice are administered with bleomycin which leads to a similar pathology as the IPF lung, including increased transforming growth factor β_1 (TGF-β_1), the recruitment and differentiation of the fibroblasts and the excessive production of matrix proteins. In this mouse model, apoptotic markers are also observed, giving further evidence that epithelial cell damage is initiating the fibrotic response (X. Li et al. 2003).

The genetic factors do not cause the underlying epithelial cell damage in IPF. However, it is believed that gene mutations may pre-dispose or increase the susceptibility of the epithelial cells to injury, infection or damage. This will contribute to epithelial cell apoptosis. This evidence comes from studies identifying mutations in familial or sporadic cases of IPF. The gene variants

identified are mainly associated with the familial form of the disease. A cluster of genes regulating telomeres has been identified: *TERT*, *TERC*, *TINF2*, *DKC1*, *RTEL1*, *PARN* and *NAF* (Martinez et al. 2017; Armanios et al. 2007; Tsakiri et al. 2007; Kropski et al. 2014; Alder et al. 2015; Stuart et al. 2015; Stanley et al. 2016). Telomeres loss or shortening is felt to be one potential mechanism by which alveolar type II cells become unstable. Cell instability can lead to cell apoptosis and this releases the fibrotic mediators that can lead to the progressive lung scarring.

Variants in the *MUC5B* promoter occurs in both familial and sporadic cases of IPF (Seibold et al. 2011). *MUC5B* mutations prevent correct cell defence from infection. However, the exact reason why *MUC5B* mutations increase lung susceptibility to infection is not known. *TOLLIP* and *SP-C* are genes that encode proteins which are implicated in sporadic cases of IPF. Mutations in both genes lead to increased ER stress which subsequently leads to increased epithelial cell damage (Tanjore et al. 2012). Therefore, the injured cells release pro-fibrotic mediators. This is why continuous epithelial cell apoptosis is believed to underlie the aetiology of the disease.

Epigenetic changes have been identified in IPF patients. The loss of histones, deregulation of micro-RNAs (miRNAs) and DNA methylation lead to the dysregulation of cell signalling pathways in IPF patients (Martinez et al. 2017). MicroRNA (miRNA) is important for regulating the levels of their target mRNAs. They do this by targeting the mRNA for degradation. Several dysregulated miRNA's have been identified in epithelial cells; let-7d, miR-200, and miR-26a and these may be responsible for the aetiology of IPF, or the pathogenesis of the disease (Pandit et al. 2010; Li et al. 2016; Yang et al. 2012; Li et al. 2014).

1.5. Pathogenesis of IPF

Normal wound healing occurs in four generalised stages: Haemostasis, inflammation, proliferation or granulation (including ECM deposition) and matrix remodelling or maturation. The initial injury to the lung causes the release of several inflammatory mediators recruiting inflammatory cells (macrophages and neutrophils) to the site of injury. These cells release the critical mediators that promote the expansion of the fibroblast population. One

key mediator, TGF-β_1, stimulates the fibroblasts to differentiate into myofibroblasts which deposit large quantities of extracellular matrix and they contract alpha-smooth muscle actin (α-SMA) stress fibres. The contraction of the stress fibres pull the wound together. This allows re-epithelisation of the wound followed by apoptosis of the myofibroblast population. Over a period of weeks the extracellular matrix is remodelled leading to wound resolution. In contrast, IPF represents an aberrant wound healing response whereby normal resolution does not occur. There is no re-epithelialization of the wound and the myofibroblast population does not apoptose. Continued matrix production, epithelial cell apoptosis and the release of more pro-fibrotic mediators leads to the perpetual cycle of fibroblast recruitment, epithelial cell death and matrix production in the IPF lung.

The repetitive alveolar epithelial type I cell injury leads to an imbalance between apoptosis and mitosis of two cell types, the epithelial cells and the fibroblasts. This imbalance is one driver of disease progression. This is evidenced by histological stains which show regions of hyperplastic type II epithelium and a complete loss of the alveolar epithelial type I cells (Datta et al. 2011). This is caused by the continual death of (alveolar) epithelial type I cells which are then replaced with epithelial type II cells. This begins to change the architecture of the lung promoting further cells loss and aberrant cell signalling (Selman 2006; Zoz et al. 2011; Kelly et al. 2003). A cell type recruited to the site of epithelial type I apoptosis is the fibroblast. The fibroblast is responsible for the deposition of the extracellular matrix (ECM) and it does this in response to the pro-fibrotic mediators released by the epithelial cells to begin the wound healing process. The disproportional and continued release of these mediators leads to an imbalance between fibroblast apoptosis and epithelial apoptosis. The fibroblasts no longer apoptose and the epithelial cells continue to die. One protein that is believed to underlie this imbalance in apoptosis is prostaglandin E2 (PGE2). PGE2 is an anti-fibrotic agent which has been investigated *in vitro* and *in vivo* and can have different effects depending on the cell type. This protein is decreased in IPF which promotes fibroblast cell survival but leads to increased epithelial cell death leading to the ‘apoptosis – paradigm’ (Lama et al. 2002; Keerthisingam et al. 2001; Borok et

al. 1991; Maher et al. 2010). Critically, it is the apoptosis of the epithelial cells that recruit and drive the proliferation of the fibroblasts and other cell types contributing to the disease pathogenesis.

Understanding of the pro-fibrotic mediators is believed to help develop the understanding of disease progression and intervention of these mediators may halt or slow the perpetual cycle of epithelial type I cell apoptosis and fibroblast recruitment and proliferation. Several key pro-fibrotic mediators have been measured from IPF patients' bronchiolar lavage which revealed several pro-fibrotic mediators were increased in comparison to healthy controls. These proteins were: PDGF, FGF, TGF-β_1, CTGF, angiotensin, MMPs, TNF, CCL2 and CXCL12 (Selman 2006; Zoz et al. 2011; Kelly et al. 2003). The release of these pro-fibrotic mediators led to the recruitment, proliferation and differentiation of cells including macrophages, neutrophils, fibroblasts and platelets which are believed to underlie the development of the disease. In particular, it is the relationship between TGF-β_1 and the fibroblast that can drive the disease pathogenesis (TGF-β_1 signalling is discussed in more detail below 1.6). Fibroblasts are recruited to the sites of wound injury in the lung via the secreted mediators; their imbalanced cross-talk to the epithelial cells leads to increased levels ROS and angiotensin which leads also leads to further epithelial type I cell death (Wang et al. 1999). Another cause of the epithelial type I cell death is the fibroblasts depositing excessive matrix proteins, which causes changes in matrix tension and the dense fibrotic areas make it difficult for the epithelial cells to repopulate them. This complex cross-talk between the damaged epithelium and recruited fibroblasts leads to a feed-forward mechanism that acts to perpetuate the disease (Wang et al. 1999). The research within our group focuses on the fibroblast/myofibroblast since we believe that halting the matrix production would prove an effective method of treating the disease. Therefore, the remaining sections will focus on their role in IPF and their relationship to TGF-β_1 which is a driver or matrix production and fibroblast differentiation.

1.5.1. The myofibroblast

A key effector cell type involved in pathogenesis of IPF is the fibroblast and its differentiated form the myofibroblast. The expansion and differentiation of the

fibroblast is what promotes the progressive deposition of matrix proteins leading to the aberrant lung scarring and to the cells dominating the lung. The population of fibroblasts is heterogeneous in the fibrotic foci. The identification of these observed sub-populations of fibroblasts comes from their expression of different proteins including type I collagen, Thy-1, α-SMA, cyclooxygenase 2 (COX-2), telomerase and caveolin-1 (Derdak et al. 1992; Hagood et al. 2005; Zhang et al. 1996; Wilborn et al. 1995; Nozaki et al. 2000; Wang et al. 2006). The expression of these different markers is evidence to suggest that more than one source can contribute to the fibroblast/myofibroblast cell population in IPF lungs (Hung et al. 2013). Resident lung fibroblasts are believed to be the primary source for their expansion and differentiation in response to epithelial cell damage. However, other types of cells have been investigated and are believed to give rise to the population of fibroblasts and myofibroblasts. Firstly, epithelial to mesenchymal transition (EMT), which is a process where endothelial cells lose their markers (e.g. E-cadherin) and begin expressing mesenchymal markers (e.g. fibroblast-specific protein-1 and critically α-SMA) (Grünert et al. 2003). Experimentally, EMT can occur in an *in vitro* setting when exposed for long periods with TGF-β on a provisional wound matrix (Willis et al. 2005). Secondly, there is emerging literature that endothelial to mesenchymal transition (EdMT) may contribute to the fibroblast population. It was shown from capillary endothelial cells that they gave rise to a fibroblast population through mesenchymal transition in the bleomycin induced mouse model (Hashimoto et al. 2010). Thirdly, Foxd1-derived pericytes have been demonstrated to expand in bleomycin injured mice and may contribute to the population of myofibroblasts. Fourthly, fibrocytes have also been implicated in IPF, on the basis that CXCL12 is increased in IPF lung which is a key migratory chemokine that recruits fibrocytes to areas of wound healing (Strieter & Mehrad 2009; Bucala et al. 1994; Phillips et al. 2004). This cell type has also been identified in BALF fluid of IPF patients (Borie et al. 2013). There is evidence, however, against the role of the fibrocyte in IPF with CXCL12-CXCR4 targeted treatment proving ineffective in bleomycin-induced mouse fibrosis (Chow et al. 2016) and the inability to grow fibrocytes from BALF fluid (Chow et al. 2016; Borie et al. 2013). Collectively this research

suggests that several populations of cells can give rise to the fibroblast population contributing to the pathogenesis of IPF.

In IPF lungs, the myofibroblasts expressing α-SMA are Thy-1 and caveolin-1 negative, indicating they play a role in lung fibrosis. It has been reported in fibroblasts Thy-1 expressing cells are less fibrogenic than Thy-1 negative cells, considering myofibroblast's are negative in Thy-1 this helps explain their fibrogenic nature (Hagood et al. 2005). Furthermore, caveolin-1 negative fibroblasts display similar fibrogenic properties as the Thy-1 negative cell (Wang et al. 2006). Importantly, the α-SMA expressing myofibroblast's are the pre-dominant source of ECM and contribute to a considerable amount of the fibrogenic/inflammatory cytokines in the fibrotic lesions (Phan 2008). TGF-β_1 regulates all three of these proteins. The stimulation of fibroblasts with TGF-β_1 down-regulates both caveolin-1 and Thy-1, whilst upregulating the expression of α-SMA (Sanders et al. 2015; Neveu et al. 2015). The majority of the deposited ECM in IPF lungs is contributed by the α-SMA positive myofibroblast's, making TGF-β_1 a critical regulator of the fibroblast and this is why the following sections (sections to 1.6 – 1.9) will focus on the cytokine TGF-β_1.

1.6. TGF-β

The TGF-β cytokine family consists of over 30 members that are evolutionary conserved between mammals which include TGF-β, activins and BMPs amongst others (Derynck & Miyazono 2008). TGF-β family members' functions include regulation of tissue homeostasis, inflammation, wound resolution and embryo development (Derynck & Miyazono 2008). Furthermore, specifically, the TGF-β cytokines maintains a tight control over cell growth, DNA repair and protein synthesis. Due to its range of functions TGF-β_1's effects have been studied in cell types including macrophages, neutrophils, epithelial cells, B cells, T cells, endothelial cells, fibroblasts and myofibroblasts.

TGF-β_1 homeostasis is important because of its broad range of effects. Therefore, the dysregulation of TGF-β_1 signalling leads to several different diseases. The increases or decreases in the levels of TGF-β have been

implicated in diseases such as: cancer, hypertension, diabetes, Marfan's syndrome and several fibrotic conditions (Akhurst 2004). In this smaller subset of TGF-β cytokines there are three isoforms, TGF-β_1, TGF-β_2 and TGF-β_3. TGF-β_1 is extensively studied in fibrotic diseases, particularly IPF, (including liver and kidney fibrosis) due to its implications in matrix synthesis, notably collagen.

1.7. TGF-β_1 in IPF

TGF-β_1 is increased in IPF patients and is a key mediator involved in the pathogenesis of IPF (Leask & Abraham 2004). TGF-β_1 protein levels were compared between healthy and IPF lung from bronchoalveolar lavage which identified raised levels of TGF-β_1 in the disease (Hagimoto et al. 2002). In addition, lung biopsies taken from IPF patients for immunohistological staining reveal that TGF-β_1 is localised to the dense regions of extracellular matrix. The source of this TGF-β_1 is primarily believed to be from the epithelial cells and macrophages (Khalil et al. 1996). TGF-β_1 is a pro-fibrotic mediator in IPF and this fact is further supported because it contributes to the pathogenesis of other fibrotic diseases such as kidney and liver fibrosis (Choi et al. 2012; Böttinger & Bitzer 2002; Dooley & ten Dijke 2012). Hence, there is evidence to support that TGF-β_1 is a driving force in the pathogenesis of the disease.

TGF-β_1 driven fibrosis has also been implicated in animal models of fibrosis such as the bleomycin mouse model and the bleomycin hamster model of lung fibrosis. In both models, TGF-β_1 protein expression and mRNA levels are increased (Gurujeyalakshmi et al. 1998; Giri et al. 1993). Furthermore, TGF-β_1 has been directly implicated in driving the development of lung fibrosis when over-produced in the TGF-β_1 adenovirus mouse model (Ask et al. 2008). These models demonstrate that the increase in TGF-β_1 drives effector cell activation (fibroblasts), synthesis of collagens and recruitment of other cell types (Giri et al. 1993; Ask et al. 2008). The observations made from these animal models are comparable to the human disease and therefore, these models are often used for *in vivo* studies of IPF when investigating signalling pathways and potential compound treatments that will be progressed to clinical trials.

TGF-β_1 initiates the fibroblasts differentiation program leading to α-SMA expression, a marker of the differentiated fibroblast (the myofibroblast) and the synthesis of collagen. To regulate this differentiation program, TGF-β_1 controls signalling pathways that regulate the proliferation of the fibroblast, inhibition of apoptosis, cell metabolism, protein synthesis, differentiation and reorganisation of the cytoskeleton (Massagué 2012). The expression of α-SMA leads to the formation of stress fibres and the contraction of the matrix. In addition, the increased matrix deposition causes the formation of fibrotic foci. Together, these destroy the lung architecture and prevent normal lung function in IPF patients.

TGF-β_1 perpetuates the scarring problem in IPF by inhibiting collagen degradation. This occurs because TGF-β_1 increases the over-expression of TIMP which inhibits MMP proteins (Kang et al. 2007). Without MMPs, the matrix cannot be degraded as it would usually do during a normal wound healing response.

1.8. TGF-β_1 activation

TGF-β_1 is synthesised and secreted from cells as a latent complex which is then covalently bonded to the surrounding matrix prior to being activated. This complex consist of the mature dimeric growth factor, the latency-associated propeptide (LAP) and the latent TGF-β_1 binding protein (LTBP). The LTBP and TGF-β_1 are the same protein which is later associated with LAP by forming disulphide-bonds. When the complex is secreted from the cells the LTBP forms covalent bonds with the ECM proteins where it remains inactive until it is required (Khalil 1999).

The activation of the latent complex is important for the response to biological stimulus including to lung injury. The release of the active form of TGF-β_1 can be initiated by several mechanisms either physical or biological. Physical processes include acidification, extreme temperature changes and oxidation. These are not all typical mechanisms that occur *in vivo*. However, it may explain how asbestos can promote lung fibrosis which is believed to contribute to TGF-β_1 activation via oxidation of the latency complex. (Tatler & Jenkins 2012; Sullivan et al. 2008; Pociask et al. 2004). Biological mechanisms of

TGF-β_1 activation include mechanical stress of the extracellular matrix where the latent complex is associated to it or by protease cleavage. Several of these mechanism are believed to contribute to TGF-β_1 activation in IPF.

There are a number of enzymes and proteases that can cleave the latent form of TGF-β_1 including MMP2 and MMP9, plasmin, tryptase, elastase and integrins (Jenkins 2008; Tatler & Jenkins 2012). Integrin's are transmembrane proteins capable of signalling inside and outside the cell. The individual integrins are formed from different combinations of 26 subunits (18 α and 8 β subunits). Eight of these family members are capable of recognising the arginine-glycine-aspartate (RDG) sequence in the LAP of TGF-β_1 and TGF-β_3. The TGF-β_2 LAP does not have this sequence. Four Av-containing integrin's αvβ3, αvβ5, αvβ6, and αvβ8 can activate TGF-β_1 *in vivo* (Tatler & Jenkins 2012). αvβ6 is able to release TGF-β_1 from the latency complex to allow it to mediate its pro-fibrotic effects. In the lung, αvβ6 is only expressed by the epithelium at low levels helping to maintain tissue homeostasis and low levels of TGF-β_1 activation. Epithelial cell stress and damage in IPF, as a result of lung injury, upregulates the expression of αvβ6 leading to the increased activation of TGF-β_1 (Tatler & Jenkins 2012). Thrombin and lysophosphatidic acid (LPA) have both been implicated in IPF (Howell et al. 2005; Tager et al. 2008). Thrombin and LPA mediate their pro-fibrotic effects by inducing αvβ6 expression via PAR1 or RhoA kinases activation, respectively (Jenkins et al. 2006). Therefore, increased αvβ6 expression leads to the activation of TGF-β_1 which promotes its pro-fibrotic effects and this contributes to the progression of IPF. Increased levels of αvβ6 are associated with poor patient survival and a monoclonal antibody targeting this integrin is now in phase 2 clinical trials for the treatment of IPF (Clinical trials identifier NCT01371305).

Matrix metalloproteases (MMPs) are proteases which exist in a subfamily called endopeptidases consisting of 23 members. Some of these MMP family members can also activate TGF-β_1 by cleaving the latent TGF-β complex. In IPF, the gene expression profile of MMPs reveals that MMP-2 and MMP-9 are increased in IPF patients. MMP-2 and MMP-9 can both activate TGF-β (Rosas et al. 2008; Pardo et al. 2016; Zuo et al. 2002). Furthermore, histological investigations show MMP-2 and MMP-9 are localised to the fibrotic foci

(Selman et al. 2000). Thy-1 negative fibroblasts are capable of synthesising MMP-9 *in vitro* through the activation of the ERK1/2 pathway (Ramírez et al. 2011). Therefore, the increased expression of MMP-9 and MMP-2 is believed to be contributing to the active portion of TGF-β_1 leading to the stimulation of the fibroblast and increasing their pro-fibrotic response in IPF patients.

Finally, the release of pro-fibrotic mediators leading to the expression of MMP's and increased matrix proteins changes the architecture of the lung and causes the stiffening of the matrix. Healthy lung stiffness is around 4 kPa in comparison to the IPF lung stiffness which is near 27 kPa. Increased matrix stiffness contributes to TGF-β_1 activation (Froese et al. 2016). When myofibroblasts contract *in vitro* it leads to the activation of ECM associated TGF-β_1. This result was dependent upon the matrix stiffness *in vitro*. The myofibroblasts grown on soft matrix demonstrated no activation of TGF-β_1 and in contrast on stiff matrix TGF-β_1 became activated. The transient over-expression of TGF-β_1 in a rat model of fibrosis demonstrated that the harvested lung when mechanically stressed, releases the active form of TGF-β_1 (Froese et al. 2016). This was also demonstrated by taking slices from human lung, with a UIP pattern, and exerting a mechanical stress. This showed increased TGF-β_1 activation, which was matched with an increase in mothers against decapentaplegic (SMAD) 2 and SMAD 3 phosphorylation which are direct substrates of the TβRI/TβRII receptor (discussed in 1.9.2). In addition, SMAD 3 is a transcription factor that promotes collagen I gene expression (Froese et al. 2016). Therefore, matrix stiffness plays a critical role in activating TGF-β_1 in the IPF lung and thereby contributing to the progression of the disease.

1.9. TGF-β_1 signalling

1.9.1. TGF-β_1 receptors

TGF-β_1 stimulates its intracellular signalling cascades through the TβRI/TβRII receptor complex and this is how it stimulates matrix synthesis in fibroblasts. Evidence initially came from work in animals. Investigations in rat fibroblasts showed that TGF-β_1 mediates its effects through the TβRI receptor. The treatment with a TβRI inhibitor, SD-208, inhibits TGF-β_1 stimulated matrix synthesis, growth factors and proteinase inhibitors (Bonniaud et al. 2005).

Additionally, the TβRII receptor has been implicated in animal models. In the bleomycin induced lung fibrosis model in hamsters, the treatment with recombinant inactive TβRII led to a reduction in hydroxyl-proline levels (an amino acid present in collagen which is utilised as a measure of collagen synthesis) (Kawabata et al. 1995).

There are 7 type I receptors and 5 type II TGF-β receptors in humans (Massagué 2012). TGF-β_1 signalling is highly conserved between species due to its critical role regulating a large number of cellular processes. (Massagué 2012). The TGF-β_1 cytokine binds to the TGF-β receptor II (TβRII). This leads to an increase in the affinity of TβRII receptor for the TβRI which forms a complex consisting of two TβRI and two TβRII. Under basal conditions FK506-binding protein inhibits the TβRI, however, once the TβRI and TβRII complex has formed, the TβRII phosphorylates the TβRI in the GS domain at several sites. The phosphorylated TβRI receptor undergoes a conformational change within the GS domain which dissociates the FK506-binding protein and promotes the recruitment of MH2 containing proteins (Massagué 2012; Souchelnytskyi et al. 1996). The activation of the receptor complex therefore allows the activation of a number of downstream pathways. SMAD 2 and SMAD 3 are MH2 containing proteins which allows their recruitment and activation by the TβRI. TβRI phosphorylates SMAD 2 and SMAD 3 at Ser465/467 and Ser423/425, respectively (Massagué 2012; Shi 2006). Additionally, the receptors also activate several other signalling pathways including PI3K and mitogen activated kinases (MAPK). Several of these pathways are important to fibroblast matrix synthesis and differentiation. Figure 1.1 gives an overview of several of the TGF-β_1 signalling pathways.

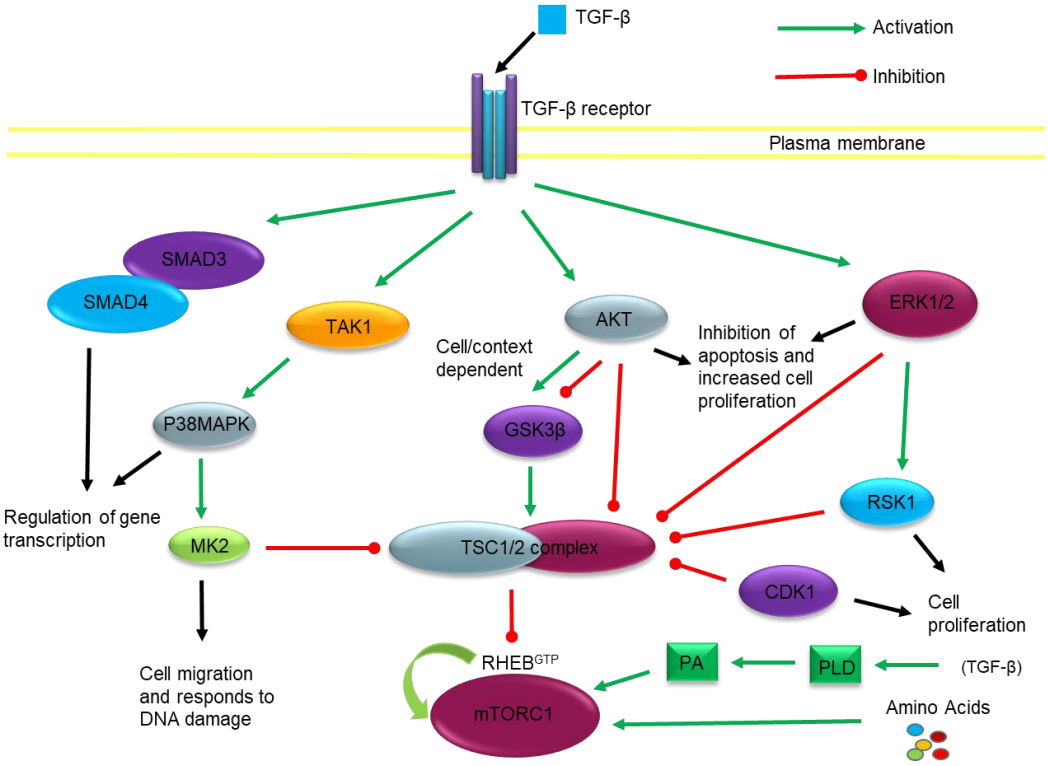

Figure 1.1: TGF-β$_1$ stimulated signalling pathways

TGF-β$_1$ stimulation of the TβRI and TβRII complex leads to the activation of several signalling cascades. These pathways have different functions within the cell which can be cell and context dependent. Some of these pathways can cross-talk and signal to the same proteins.

1.9.2. SMAD signalling

TGF-β family members are capable of activating select SMAD proteins downstream of their associated receptors to mediate gene transcription. The SMAD proteins are divided into three groups, receptor activated SMADs (R-SMADs), co-SMADs and inhibitory SMADs (I-SMADs). The R-SMADs are phosphorylated by the receptor complex and drive gene transcription with the aid of the co-SMAD, SMAD 4, and a range of co-transcription factors. The R-SMADs include SMAD 1, SMAD 2, SMAD 3, SMAD 5, SMAD 8 and SMAD 9. SMAD 6 and SMAD 7 are I-SMADs which repress SMAD signalling and are often up-regulated by R-SMADs as an inhibitory feedback loop (Das et al. 2013; Heldin & ten Dijke 1999; Jung et al. 2013; Tsuchida et al. 2003).

TGF-β$_1$ activation of the TβRI/TβRII complex mediates the activation of SMAD 2 and SMAD 3. The SMAD 2 and SMAD 3 protein structure has 3 distinct regions, the MAD homology 1 (MH1) and MAD homology 2 (MH2) domains and a region that bridges the two is the phosphor-linker region. The MH2 domain recognises and binds to the phosphorylated TβRI where it is

phosphorylated at the carboxy-terminus at the SXS motif (Shi 2006). The MH1 domain is required for DNA binding. The phosphor-linker region is phosphorylated by kinases (such as MAPKs) activated also by TGF-β_1 or other mediators. The phosphor-linker (linker) on SMAD 2 and SMAD 3 can be phosphorylated on 4 sites in response to mitogen stimulation. This can promote or prevent the SMAD complexes ability to translocate to the nucleus (Shi 2006). Therefore, this can regulate SMAD's ability to initiate transcription of its target gene (Sapkota et al. 2006; Mori et al. 2004; Kamaraju & Roberts 2005; Kretzschmar et al. 1999).

SMAD 2 and SMAD 3 exist as homodimers and upon phosphorylation they dissociate from the receptor complex and associate with SMAD 4 which promotes their translocation into the nucleus via nuclearporins (Derynck et al. 1998; Massagué 2012). The MH1 domain is then responsible for binding to the DNA either directly (SMAD 3) or indirectly (SMAD 2). SMAD 2 and SMAD 3 utilise a host of co-transcription factors to promote gene transcription (Massagué et al. 2005; J. Chen et al. 1999; Imoto et al. 2005). Key co-transcription factors involved in SMAD 2 and SMAD 3 signalling include: p300 and CREB-binding protein (CBP), jun, and AP-1 (Verrecchia & Mauviel 2002; Ghosh et al. 2000). To summarise, TGF-β_1 drives gene transcription through receptor mediated phosphorylation of the SMAD proteins which allows them to form a complex with SMAD 4. Binding with SMAD 4 allows the SMAD complex to translocate into the nucleus to drive gene transcription. A simplified schematic is represented in Figure 1.2.

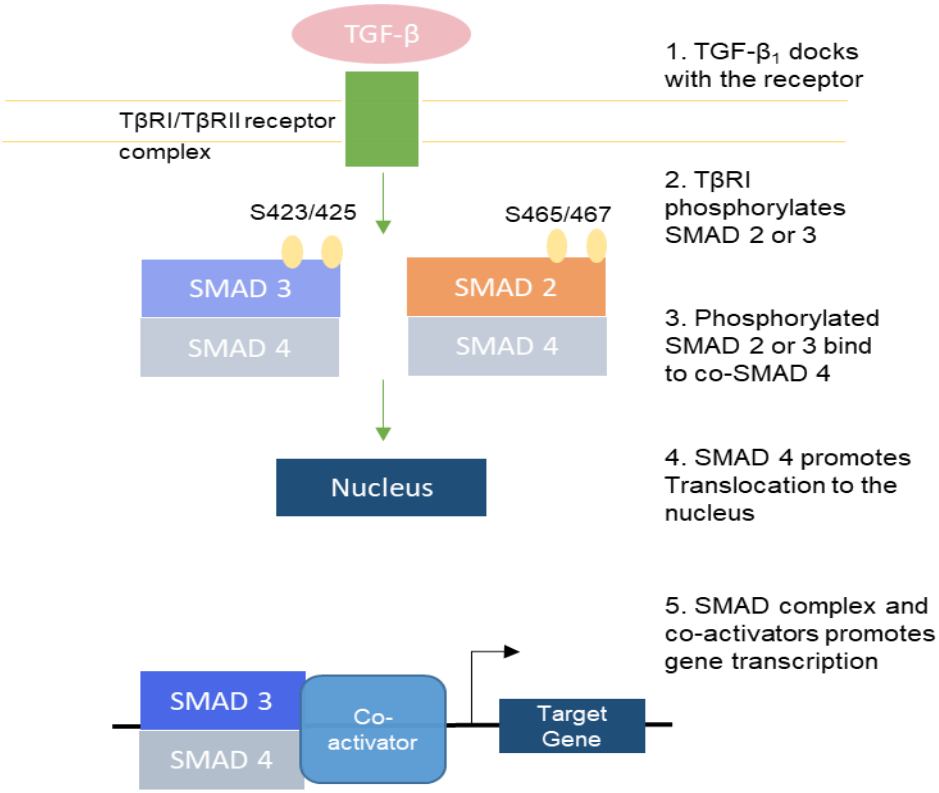

Figure 1.2: TGF-β_1 activates SMAD 2 and SMAD 3 to regulate gene transcription

TGF-β_1 signalling drives gene transcription via the translocation of the SMAD complex into the nucleus where they recognise their gene targets. Co-transcription factors aid the SMAD 2 and SMAD 3's ability to bind to the promoter region of the gene to initiate gene transcription.

1.9.3. SMAD regulation of collagen genes

The SMAD proteins have been linked to many diseases including kidney disease, chronic obstructive pulmonary disease and in most fibrotic diseases (kidney, liver, heart and lung) which are characterised by the excessive deposition of matrix proteins.

There are 19 types of collagens identified. In particular, collagen I and collagen III are the most abundant in the fibrotic lesions making up approximately 95% of the total lung parenchymal collagen and are heavily increased in IPF (Madri & Furthmayr 1980; Reynolds 1978; Verrecchia & Mauviel 2002; Last et al. 1983). The myofibroblast synthesises collagen I and collagen III concurrently (Gay et al. 1976). The collagen I fibres are used in several of our experiments to quantify the effects of TGF-β_1 stimulation on our fibroblasts. So in brief I will describe the synthesis of collagen I.

1.9.3.1. Collagen synthesis

Collagen I is composed of α1 and α2 chains, in a 2:1 ratio, which are encoded by the *COL1A1* and *COL1A2* gene, respectively (Karsenty & de Crombrugghe 1991). Collagens are made up of tandem repeats of glycine-X-Y. The X and Y positions are proline and hydroxyproline residues. Post-translational modifications and the number of repeats determine the type of collagen that is formed (Reiser & Last 1981). The pro-*COL1A1* and *COL1A2* are synthesised as polypetide chains by the myofibroblasts and enter into the endoplasmic reticulum. The proline and lysine residues are hydroxylated to form hydroxyproline and hydroxylysine, respectively (Ghosh 2002). This allows the collagen pro-chains to hydrogen bond and form the triple helix pro-collagen which is secreted by the myofibroblasts through the golgi apparatus. Finally, proteases in the extracellular space cleave the N and C terminus of the pro-peptides to form the mature collagen molecule. These mature molecules aggregate to form larger collagen fibrils and form the ECM with other matrix proteins (Ghosh 2002). The amino acid glycine makes up almost one third of the collagen protein and, therefore, the biosynthesis of glycine is critical. To manage this biosynthetic need, the glycine synthesis pathways can be upregulated. Emerging evidence is beginning to unravel several glycolytic enzymes that are required to convert glucose into glycine and meet the cell's glycine demands in response to stimuli such as insulin, serum and TGF-β_1 (DeNicola et al. 2015; Adams 2007; Seo et al. 2009; Zhu et al. 2013). The proteins that promote the conversion of glucose into glycine are PHGDH, PSAT1, PSPH and SHMT2. Activating transcription factor 4 (ATF4) is a basic leucine zipper domain containing transcription factor that regulates stress responses, amino acid metabolism and oxidative stress (Roybal et al. 2005; Yang et al. 2004; Seo et al. 2009). ATF4 is able to upregulate all of these glycolytic enzymes to increase serine and glycine synthesis. Emerging evidence from our group and others believe that TGF-β_1 upregulates ATF4 to metabolically re-programme the cells to meet the glycine requirements of the fibroblasts (Chang et al. 2018; Selvarajah unpublished data). Therefore, this helps to mediate collagen synthesis.

1.9.3.2. SMAD 3 and IPF

There are several enhancer and repressor elements in the promoter of both *COL1A1* and *COL1A2*. Within the *COL1A1* and *COL1A2* genes are TGF-β_1 responsive elements, subsequently allowing TGF-β_1 to control both genes to promote myofibroblast collagen synthesis. TGF-β_1 does this through the activation of the SMAD proteins. The promoter region of each gene has a SMAD binding element (SBE) which is made up of CAGA repeats and these repeats are recognised by SMAD 2 and SMAD 3 (Chen et al. 1999; Zawel et al. 1998; Verrecchia & Mauviel 2002). These repeats are found in *COL1A1* and *COL1A2*. In the *COL1A2* gene, these repeats are located between -263 to 258 bp (Ghosh 2002).

In the IPF lung, TGF-β_1 is mediating the transcription of the collagen genes via the activation of SMAD 3. cDNA microarray analysis has revealed a number of fibrillar collagens that are regulated by TGF-β_1 activated SMAD 3 transcriptional activity including: *COL1A1*, *COL1A2*, *COL3A1*, *COL5A2*, *COL6A1*, *COL6A3*, *COL7A1* and *TIMP-1* (Verrecchia & Mauviel 2002). Furthermore, in bleomycin induced lung fibrosis in mice, SMAD 3 expression correlates with the peak of fibrosis in the lung and this then steadily declines as the fibrotic lung injury resolves (Zhao & Geverd 2002). In addition, in SMAD 3 deficient mice, bleomycin-induced lung fibrosis is attenuated. This was attributed to a decrease in collagen mRNA and hydroxyproline levels (Zhao et al. 2002). SIS3 is a SMAD 3 inhibitor. It has been investigated in the bleomycin mouse model of lung fibrosis, demonstrating that treatment with SIS3 reduced the collagen deposition in histological slices and lowered hydroxyproline content. The decrease in hydroxyproline and collagen deposition were believed to be because of the decrease in phosphorylated SMAD 3 caused by SIS3 treatment (Shou et al. 2018). This recent evidence may suggest a potential therapeutic treatment for IPF. Finally, IPF derived lung fibroblasts demonstrate increased SMAD 2 and SMAD 3 phosphorylation and this leads to their increased nuclear localisation, this translocation is promoted by calcium influx through the $K_{Ca3.1}$ channel (Roach et al. 2015). The evidence demonstrates that in IPF, TGF-β_1 is controlling the transcription of the collagen genes through the activation of SMAD 3.

1.9.4. MAPK signalling in response to TGF-β_1

TGF-β_1 activation of the TβRI/TβRII complex also promotes the activation of mitogen activated kinases (MAPK) signalling. MAPK signalling is based on a tiered system of MAP4K (MAP Kinase kinase kinase kinase) and MAP3K (MAP kinase kinase kinase) at the top of the pathway which mediate the activation of MAP2K's and these then mediate the activation of MAPK's. The activation of MAPK's does not always have to start at the top of this tiered system but this is the general rule (Figure 1.3). The activation of MAPK is responsible for activating a number of transcription factors, such as JNK (MAPK), which activates the transcription factor c-jun. TGF-β_1 can mediate the activation of several MAPK's including: MK2, P38 MAPK, ERK and RSK (Zhang 2009). These pathways are also highlighted in Figure 1.1. The activation of these kinases can all activate a number of transcription factors and in addition can converge on the protein complex TSC1/2, which will be discussed in more detail later (section 11.1.3). Interestingly, several kinases including TAK1, MK2 and ERK1/2 have either been implicated in collagen synthesis or IPF (Liang et al. 2018; Kim et al. 2007; Bhogal & Bona 2008).

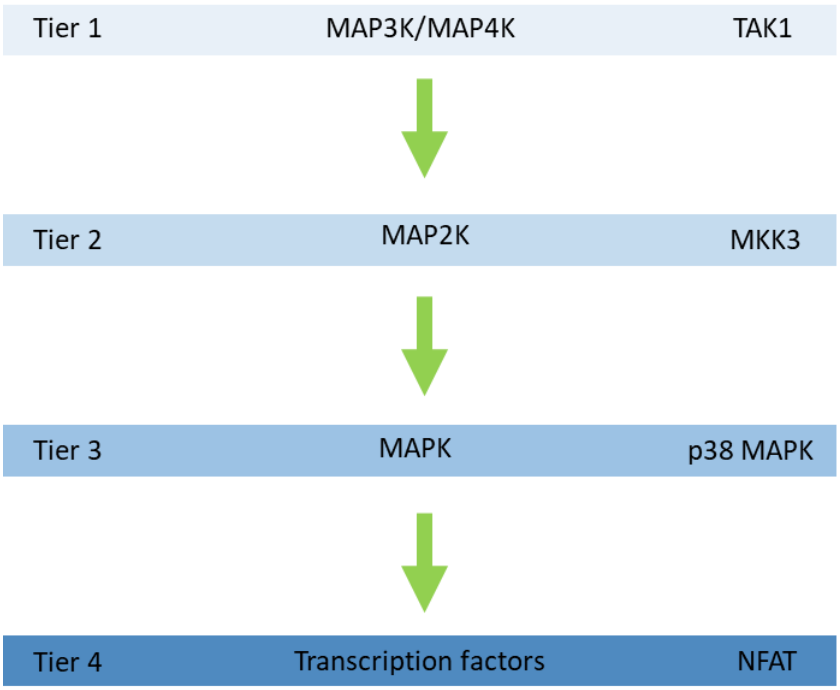

Figure 1.3: TGF-β1 signalling activates MAP3K or MAP4K to initiate signalling cascade

The activation of MAP4K's or MAPK3K's promote the activation of their down-stream substrate which leads to the activation of several transcription factors which carry out several of TGF-β_1 cellular functions .

1.9.5. PI3K/AKT

The Phosphatidylinositol 3-Kinase (PI3K) is divided into three classes: Class I, Class II, and Class III. The Class I PI3K's (through-out the thesis will be referred to as PI3K) are formed of two subunits, the P110 (α, β, γ and δ) catalytic subunit and a P85 regulator subunit, which in turn, are broadly expressed in a number of cell types including fibroblasts (Kok et al. 2009; Conte et al. 2011). PI3K activation is measured through the phosphorylation of its downstream effector AKT, which is activated after TGF-β_1 stimulation (Bakin et al. 2000). Activated PI3K catalyses the conversion of phosphatidylinositol 4,5-bisphosphate (PIP2) to phosphatidylinositol 3,4,5-triphosphate (PIP3) to recruit AKT to the membrane where it is phosphorylated by PDK1 and mammalian target of rapamycin complex 2 (mTORC2) (Figure 1.4). The PI3K/AKT signalling axis is a central regulator of cell metabolism, proliferation and survival (Engelman et al. 2006). The PI3K/AKT signalling pathway has been demonstrated to activate the mammalian target of rapamycin complex 1 (mTORC1) signalling hub, which will be discussed in more detail below (1.10). The dysregulation of the PI3K/AKT/mTORC1 axis has been implicated in a number of diseases, including cancer and fibrosis.

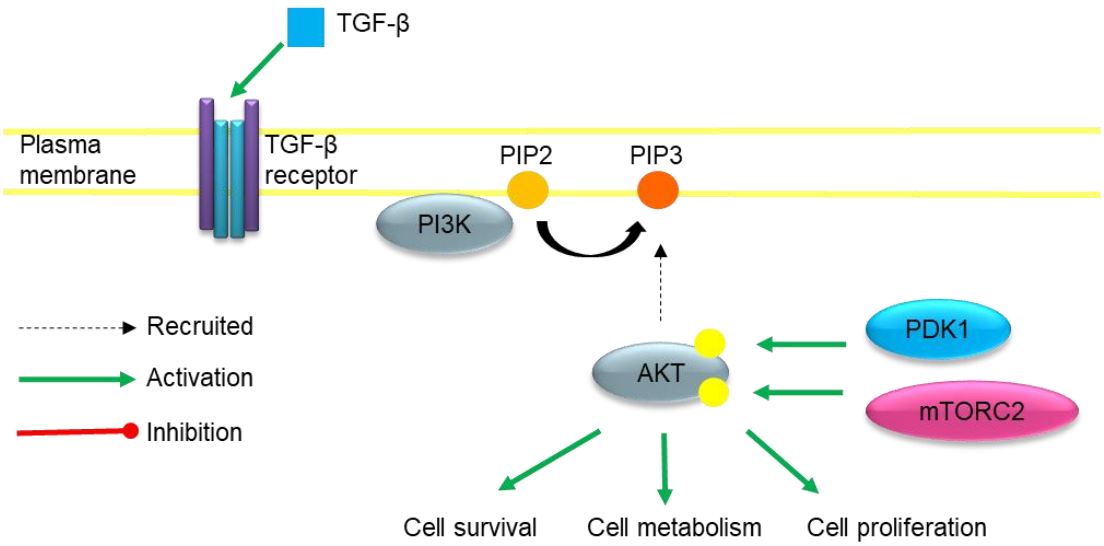

Figure 1.4: TGF-β1 stimulation of the PI3K/AKT axis

TGF-β_1 stimulation of PI3K converts PIP2 to PIP3 in the plasma membrane. PIP3 recruits Akt to the plasma membrane (via AKT's PH domain). Akt is then phosphorylated by PDK1 and mTORC2

PI3K/AKT regulates the activation of mTORC1 in several cell types and subsequently plays an important role in mediating TGF-β_1 signalling in fibroblast. More recent evidence also points to a role for a PI3K/AKT axis in IPF (Nho et al. 2013). The investigation of PI3K/AKT/mTORC1 axis with a novel PI3K/mTOR inhibitor, GSK2126458, demonstrated that the compound inhibited TGF-β_1 stimulated AKT phosphorylation and collagen I deposition (Mercer et al. 2016). Furthermore, GSK2126458 inhibited the progression of fibrosis in the bleomycin mouse model and has now progressed through phase I clinical trials for the treatment of IPF (ClinicalTrials.gov Identifier: NCT01725139). In addition, there was some indication that Rapamycin inhibition of mTORC1 attenuated both bleomycin and radiation induced pulmonary fibrosis, suggesting that this complex through the PI3K/AKT axis is important for collagen synthesis (Chung et al. 2016; Jin et al. 2014). However, our group's recent evidence has demonstrated that selective inhibition of either PI3K or AKT results in no inhibition of collagen synthesis in pHLFs (Woodcock, unpublished data). The inhibition of PI3K and AKT still prevented serum stimulated fibroblast proliferation, but was not required for TGF-β_1 stimulated collagen I synthesis. However, mTORC1 was demonstrated to be important for collagen I synthesis, which explains the effects of GSK2126458 were through the inhibition of mTORC1 and not the PI3K/AKT axis. The role of mTORC1 in collagen I synthesis is supported by studies we have conducted which demonstrate that selective inhibition of mTOR using AZD8055 inhibited TGF-β_1 stimulated collagen synthesis (Woodcock, unpublished data). mTOR is required for TGF-β_1 stimulated collagen I synthesis and its role in animal models of fibrosis identify it as a critical component in TGF-β_1 stimulated fibrosis. Therefore, I will now focus upon the mTOR kinase and its mechanisms of activation upon which this thesis is centred.

1.10. mTOR

The kinase, target of rapamycin (TOR) is named due to its sensitivity to the macrolide ester rapamycin. Rapamycin was initially used as an anti-fungal and immunosuppressant and its role in the treatment of these contexts led to the discovery of the TOR protein in Saccharomyces cerevisiae (Abraham & Wiederrecht 1996; Diggle et al. 1996). There are two copies of the TOR protein

in yeast which share approximately 60% homology. Further investigation in human cells led to the discovery of a mammalian version of TOR (known as RAFT1 at the time) which had similar homology to the yeast protein (40% shared homology). This protein was later termed mechanistic target of rapamycin (mTOR). mTOR belongs to the family of Phosphatidylinositol 3-kinase-related kinases (PIKK) which are serine/threonine kinases. These are very large proteins spanning between 280 kDa and 470 kDa in size. PIKK catalytic domains share similar homology with the PI3K families' kinase domain at around 20-30% homology, although their cellular roles are very different (Smith & Jackson 2010). This similarity means some PI3K inhibitors like GSK2126458 can inhibit PIKK family members (Liu et al. 2005; McNamara & Degterev 2011). There are six PIKK family members including: mTOR; transformation/transcription associated protein (TRRAP); DNA-dependent protein kinase catalytic subunit (DNA-PKcs); the protein product of the gene mutated in ataxia-telangiectasia (ATM); ATM Rad3-related (ATR) protein; SMG-1 (Smith & Jackson 2010). As previously discussed mTOR has emerged as a kinase involved in TGF-β_1 stimulated collagen synthesis and IPF pathogenesis.

1.10.1. mTOR structure

mTOR is a 282 kDa protein composed of 2892 amino acids. Its structure consists of regions and domains including: HEAT repeats, FAT domain, the FRB domain, kinase domain, NRD, and FATC. These domains determine the function of mTOR allowing it to associate with several proteins. Furthermore, mTOR can be phosphorylated at numerous sites (Figure 1.5). This determines the configuration of the final complex which can either be as mTORC1 or mTORC2 (Figure 1.5) which will be discussed below.

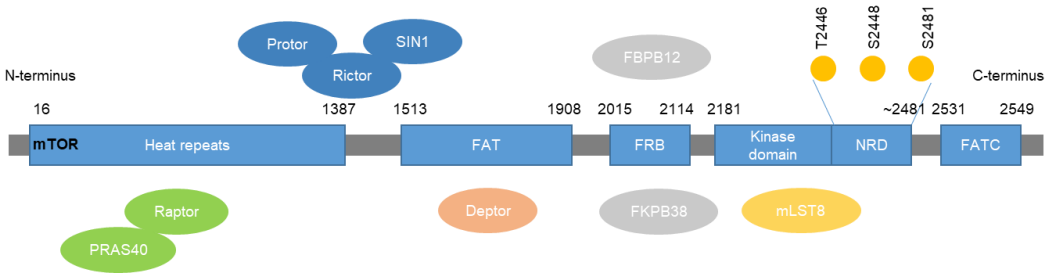

Figure 1.5: The mTOR structure.

Several regions and associated proteins are critical for determining its activation and substrate recognition of the mTOR kinase. The domains allow it to form into distinct complexes, mTORC1 and mTORC2, by binding to different accessory proteins which alters its cellular function. In addition, the mTOR structure can be phosphorylated to regulate it activity.

1.10.2. Heat domain

The Huntingtin, EF3, the alpha regulatory subunit of PP2A, and TOR (Heat) repeats are 20 repeats of 30-40 hydrophobic amino acids along the length of the N-terminal end of mTOR between the regions of 16 and 1397. This region is important for binding the mTORC1 specific protein regulatory-associated protein of mTOR (RAPTOR) and is also capable of binding to other proteins Gephrin and Ubiquilin 1. Towards the end of the Heat repeat domain and before the FAT domain is where rapamycin-insensitive companion of mammalian target of rapamycin (RICTOR) the mTORC2 associated protein can bind to. Both RICTOR and RAPTOR are critical for the function of their complexes.

1.10.3. FAT and FAT-C domain

The FRAP, ATM, and TRRAP (FAT) domain and the FRAP, ATM, and TRRAP C-terminus end (FAT-C) domain are the defining domains for PIKK family of kinases. There is not much research attributed to the function of these domains but evidence suggests these domains come together to form the overall tertiary complex (Yamashita, et al., 2001). This region serves as a binding site for the accessory protein DEP domain containing mTOR interacting protein (DEPTOR) which is common to both mTORC1 and mTORC2 complexes and is capable of inhibiting them to regulate their cellular activity.

1.10.4. FRB domain

FKBP-rapamycin complex binding (FRB) domain spans residues 2025-2114. This domain is believed to be required for mTOR catalytic activity (Vilella-Bach, et al., 1999). The FRB domain is where rapamycin binds to in association with FKBP-12 to inhibit the mTORC1 complex (Schmelzle & Hall 2000; Van Duyne et al. 1991; Choi et al. 1996). The crystal structure for this has been established in association with the rapamycin/FKBP-12 complex. Rapamycin is an allosteric inhibitor, allosteric inhibition is when a molecule binds to a protein not at its active site, and this leads to inhibition of the protein and it does this by causing structural changes. Rapamycin inhibits mTORC1 by altering its structure and this causes steric hindrance to the mTOR structure promoting a partial closing of the active site and because it is only a partial closing it allows mTORC1 to still phosphorylate some of its substrates (Yang et al. 2013; Choo & Blenis 2009).

1.10.5. NRD

The negative regulatory domain (NRD) or “repressor” domain regulates mTOR kinase activity (Sekulić et al. 2000). Deletion of the NRD domain has been shown to activate mTOR (Sekulić et al. 2000). This region has three phosphorylation sites: T2446, S2448 and S2481. In contrast to the deletion study, point mutations of the T2446 or S2448 to alanine residues has no impact on mTOR activity *in vitro* (Chiang & Abraham 2005). Structural investigation of mTOR suggests that the tertiary structure leads to the NRD domain being folded in such a way that it restricts entry into the phosphorylation sites (Chiang & Abraham 2005). Therefore, structural changes in mTOR may be required for certain phosphorylation sites to be exposed. This may then impact on mTORC1 activation. Importantly, this region impacts on mTOR’s kinase activity and these phosphorylation sites are regulated by proteins including P70S6K and AMPK (Cheng et al. 2004; Holz & Blenis 2005; Chiang & Abraham 2005).

1.10.6. mTORC1 and mTORC2

mTORC1 consists of three proteins bound to its structure: mammalian lethal with Sec13 protein 8 (mLST8), RAPTOR and DEPTOR (Peterson et al. 2009). In association with this complex, proline-rich Akt substrate of 40 kDa

(PRAS40) binds to RAPTOR to complete the mTORC1 complex (Vander Haar, et al., 2007; Sancak et al., 2007). mTORC2 consists of three accessory proteins bound to the mTOR kinase: Rictor, mLST8, DEPTOR. In addition, RICTOR associates with Protor and mSIN1 (Pearce et al. 2007). mTORC1 and mTORC2 have different downstream substrates which is determined by their associated proteins. mTORC2 is known for its regulation of AGC (termed from PK**A,** PK**G** and PK**C**, but is now known to be a large family of over 60 kinases) kinases including: PKA,PKG,PKC and SGK1. In addition, it phosphorylates AKT at the S473 site completing the full activation of AKT (Ikenoue et al. 2008). mTORC1 regulates three well known substrates 4E-BP1, P70S6K and ULK1. The proteins associated in each complex and their downstream substrates are shown in Figure 1.6.

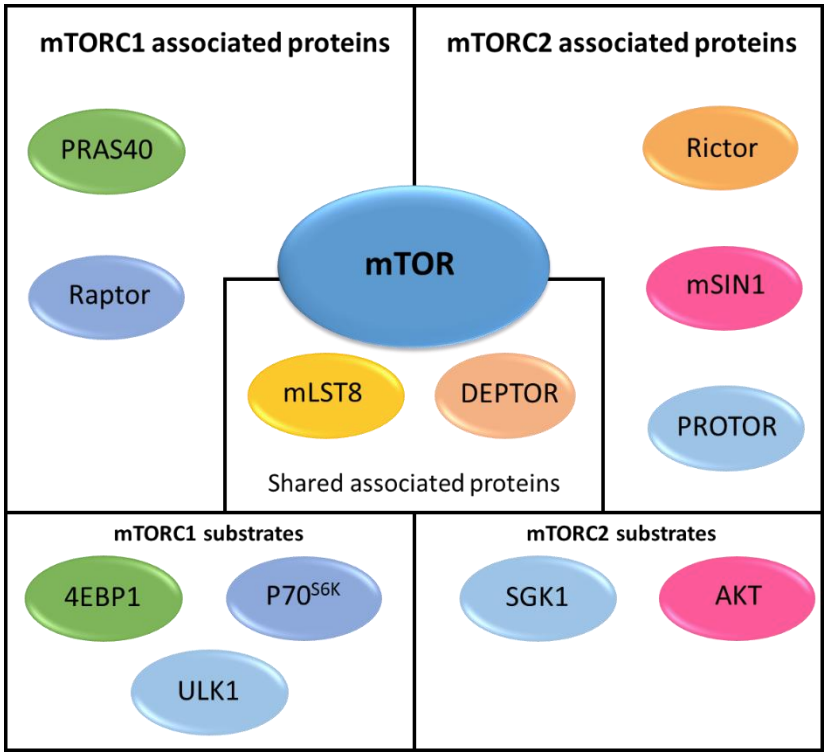

Figure 1.6: mTOR is a critical kinase in two complexes mTORC1 and mTORC2

Each complex is comprised several proteins. The overall complex dictates their ability to recognise and allow mTOR to activate the downstream substrates.

The cellular roles of each complex varies depending on their target substrates. A key distinction between the two complexes is that mTORC1 is rapamycin sensitive. In contrast, mTORC2 is only sensitive to long exposure to rapamycin which is attributed to the rapamycin complexed to mTORC1 preventing the

formation of the mTORC2 complex. This rapamycin selectivity has allowed researchers to begin to distinguish between the two complexes' cellular functions (Sarbassov et al. 2006; Lamming et al. 2012). This allows researchers to tease apart the role of mTORC1 from mTORC2. The role of mTORC1 is diverse in that it regulates: protein synthesis; lipid, nucleotide and glucose metabolism and protein turnover. mTORC2 is a key regulator of proliferation and survival and the organisation of the actin cytoskeleton (Saxton et al. 2017). Together both complexes regulate a large range of cellular functions and others are still emerging.

1.10.7. 4E-BP1

Eukaryotic translation initiation factor 4E binding protein 1 (4E-BP1) belongs to a family of eIF4E-binding proteins (4EBP 1-3). 4E-BP1 is an important inhibitor of cap-dependent translation when in its hypo-phosphorylated form by binding eukaryotic translation initiation factor 4E (EIF4E). To promote cap-dependent translation, EIF4E needs to be liberated from binding to 4E-BP1 and allowed to associate with EIF4G and EIF4A to form the complex termed as EIF4F and this initiates cap-dependent translation of mRNA. To remove the inhibition of 4E-BP1 and allow the complex to form and promote mRNA translation, 4E-BP1 is phosphorylated by mTORC1. The best characterised sites are T37/46, S65 and T70. There are other phosphorylation sites, such as S101 and S112 which are believed to be constitutively phosphorylated and important for the release of 4E-BP1 from EIF4E. S101 is also important for the phosphorylation of S65 (Wang et al. 2003). Finally there is a S83 phosphorylation site which is also believed to be involved in dissociating 4E-BP1 from the complex (Fadden et al. 1997). The T37/46 and T70 are priming sites and the phosphorylation of these sites is not sufficient to cause dissociation of 4E-BP1 from EIF4E (Gingras et al. 1999). The phosphorylation of 4E-BP1 is reported to be sequential starting with T37/46 which allows the phosphorylation of T70 and then subsequently S65 which promotes the dissociation of 4E-BP1 (Gingras, Raught & Sonenberg 2001). However, this is not always true and it is likely that a combination of the different phosphorylation sites that may regulate the dissociation of 4E-BP1 from the

mRNA. As long as 4E-BP1 is hyper-phosphorylated this will allow translation of the mRNA to occur (Velásquez et al. 2016)

1.10.8. P70S6K

S6K is a serine/threonine kinase and belongs to the AGC kinase family. There are three S6K1 isoforms, P70S6K and its alternatively spliced forms $P85^{S6K}$ and a very truncated form $P31^{S6K}$. P70S6K consists of 502 amino acids and it is localised to the cytoplasm and nucleus of the cell (Rosner & Hengstschläger 2011).To activate P70S6K, it is initially required to be primed at 4 sites: S411, S418, S241 and S424, but the kinase responsible is unknown. These sites are observed to be phopsphorylated under basal conditions (Tavares et al. 2015; Burnett et al. 1998). However, priming at these sites allows activated mTORC1 to recognise P70S6K and phosphorylate the T389 residue (Tavares et al. 2015; Burnett et al. 1998). T389 phosphorylation primes P70S6K for phosphorylation at its T229 site which is mediated by PDK1 (Pullen et al. 1998). Phosphorylation at the T229 promotes P70S6K catalytic activity and allows P70S6K to phosphorylate its key effector substrate S6. S6 promotes protein synthesis and cell survival (Pende et al. 2004). P70S6K also mediates cell survival by inhibiting pro-apoptotic proteins BAD and Mdm2 (Harada et al. 2001). In addition, P70S6K inhibits AMPK (an inhibitor of mTORC1) activity thus preventing the inhibition of mTORC1 which promotes metabolism and energy homeostasis (Dagon et al. 2012). Finally, P70S6K increases mRNA translation via S6 which promotes the assembly of the EIF3 translation initiation complex (Holz et al. 2005). Therefore, P70S6K activation allows mTORC1 to mediate several cellular functions.

1.11. Regulation of mTORC1

1.11.1. RAPTOR/PRAS40

In combination with RAPTOR, mTOR is able to mediate targeted phosphorylation of the mTORC1 substrates 4E-BP1 and P70S6K. RAPTOR is a core component of the mTORC1 complex. It is a 149 kDa protein that is well conserved in eukaryotic cells including *D. melanogaster*, *S*. *pombe*, *S. cerevisiae*, *C. elegans*, and *A. thaliana* (Kim et al. 2002; Hara et al. 2002). RAPTOR is critical for the mTORC1's ability to interact with its two key substrates P70S6K and 4E-BP1 and like mTOR, RAPTOR is able to recognise

and bind to the TOS motif (Schalm & Blenis 2002; Nojima et al. 2003). This motif exists in 4E-BP1 at the C-terminus and P70S6K at the N-terminus (Schalm & Blenis 2002). It is well described that the loss of this TOS motif prevents 4E-BP1 phosphorylation (Nojima et al. 2003). RAPTOR has been implicated in cellular processes including: Mitosis/cell cycle progression, nutrient sensing and mRNA translation because it regulates mTORC1 kinase activity, substrate recognition and cellular localisation (Kim et al. 2002; Gwinn et al. 2010; Ramírez-Valle et al. 2010)

RAPTOR is regulated by several mechanisms which determine how the mTORC1 complex functions. RAPTOR is complexed to PRAS40 which is a negative regulator of mTORC1 when it is localised to the cytoplasm (Lv et al. 2017). It accomplishes its inhibition of the complex by impeding RAPTOR's ability to bind to P70S6K and 4E-BP1. Therefore, to remove PRAS40's negative inhibition on the mTORC1 complex, it can be regulated by several mechanisms. PRAS40 has a number of phosphorylation sites at the C-terminus: Ser^{183}, Ser^{184}, Ser^{203}, Ser^{212}, Ser^{213}, Ser^{221}, Thr^{246}, and Thr^{247} (Oshiro et al. 2007; Lv et al. 2017). The phosphorylation of PRAS40 at its Ser^{183} and Thr^{246} sites inhibit the protein and alleviates its inhibitory effects on the mTORC1 complex (Kovacina et al. 2003). In addition, the phosphorylation of PRAS40 leads to its dissociation from the complex (RAPTOR) allowing it to be sequestered by the protein 14-3-3 (Kovacina et al. 2003). AKT has primarily been demonstrated to directly phosphorylate the Thr^{246} site which has been confirmed to be TGF-β_1 sensitive in our primary human lung fibroblast (pHLF) cell line (unpublished data). Additionally, mTORC1 kinase activity has also been demonstrated to regulate PRAS40 phosphorylation (Oshiro et al. 2007). TGF-β_1 also regulates PRAS40 protein expression. TGF-β_1 upregulates the gene transcription of miR-96 via SMAD 3. The increase in miR-96 targets and degrades PRAS40 mRNA leading to a decrease in PRAS40 protein levels (Siu et al. 2015). Furthermore, PRAS40 phosphorylation can also be regulated by leucine and high glucose levels (Dey et al. 2010; Sanchez Canedo et al. 2010). PRAS40 can be regulated by kinase phosphorylation upstream of mTORC1 or downstream of mTORC1 kinase activity. The phosphorylation of PRAS40 alleviates its inhibition of the complex and allows RAPTOR to recruit 4E-BP1

and P70S6K to mTORC1 making PRAS40 an important protein for mTORC1 regulation.

RAPTOR can also be regulated by phosphorylation sites which are grouped into 2 clusters; cluster 1: Ser^{696}/Thr^{706} and cluster 2: $Ser^{855}/Ser^{859}/Ser^{863}/Ser^{877}$. Several of the phosphorylation sites are regulated by the GTPase RHEB (discussed later on, 1.11.3)(Foster et al. 2010). The mechanism of how RAPTOR is regulated by RHEB is not fully defined. It is believed a number of these sites are down-stream of mTOR kinase activity suggesting that RAPTOR can receive inputs upstream of the mTORC1 complex but also mTOR can feedback to regulate its own activity through RAPTOR (Foster et al. 2010). In addition, RAPTOR plays a crucial role in energy stress conditions. Energy stress caused by low ATP or amino acid levels causes the upregulation of AMPK. AMPK can phosphorylate RAPTOR at two sites, Ser^{722} and Ser^{792} leading to an inhibition of mTOR kinase activity *in vitro and in vivo* (Gwinn et al. 2008). RAPTOR can also be phosphorylated by RSK, which recognises Ser^{719}, Ser^{721}, and Ser^{722} and this promotes Phorbol 12-myristate 13-acetate (PMA)-induced mTOR activation (Carrière et al. 2008). The regulation of RAPTOR is not only crucial for integrating different stimulatory inputs for mTORC1 activation, but also preventing its ability to function leading to mTORC1 inhibition.

1.11.2. DEPTOR

DEPTOR is a 46 kDa protein that is localised to either cytoplasmic, mitochondrial or in nuclear locations (Catena & Fanciulli 2017). DEPTOR has been implicated in a number of functions, including apoptosis, autophagy, cell growth, proliferation and inflammation (Catena & Fanciulli 2017). DEPTOR inhibits both mTORC1 and mTORC2 activity. However, overexpression of DEPTOR increases the phosphorylation of AKT residues (S473 and T308), the S473 being a substrate of mTORC2, which is contradictory to its role in suppressing mTORC2 activity. This increase is explained by the loss a mTORC1 negative feedback loop to AKT (Peterson et al. 2009).

In low energy states DEPTOR binds to mTOR and inhibits its kinase activity. In contrast, serum treatment leads to the phosphorylation of DEPTOR at Ser^{293}

and Ser^{299} which primes it for further phosphorylation from P70S6K and RSK at Ser^{286}, Ser^{287} and Ser^{291} which leads to ubiquitin E3 targeted degradation (Zhao et al. 2011; Gao et al. 2011; Duan et al. 2011; Catena & Fanciulli 2017). This allows the cell to regulate DEPTOR activity based on both kinase and energy levels, which in turn will regulate mTORC1 or mTORC2 accordingly.

There is also evidence to suggest that DEPTOR can be regulated by oxidative stress and lipid biosynthesis. PLD is a regulator of DEPTOR. PLD produces phosphatidic acid (PA) which binds to mTOR and competes with DEPTOR for binding. The competition for binding leads to dissociation of DEPTOR from mTOR. Dissociation of DEPTOR targets it for the same ubiquitin E3 ligase mediated degradation and promotes an increase in mTOR kinase activity (Yoon et al. 2015). Importantly, inhibition of DEPTOR leads to its degradation. DEPTOR is also regulated at the transcriptional level by Che-1 during oxygen deprivation, DNA damage or glucose starvation. Caenorhabditis elegans-1 (Che-1) driven DEPTOR expression then leads to mTOR inhibition which promotes the activation of ULK1 (mTORC1 substrate) which drives autophagy (Desantis et al. 2015). Finally, TGF-β_1 stimulated SMAD 3 activation also mediates cross-talk to mTORC1 leading to a depletion in DEPTOR via proteasomal degradation which promotes an increase in mTORC1 activity (Das et al. 2013). Overall several mechanisms are in place to regulate DEPTOR to control either mTORC1 or mTORC2 activity.

1.11.3. TSC complex

The tuberous sclerosis complex (TSC) is formed of three proteins TSC1, TSC2 and TBC1D7. Tuberous sclerosis is an autosomal dominant disorder which is caused by mutations in either TSC1 or TSC2. The loss of function of TSC1 or TSC2 leads to benign tumour development across several organs including the skin, kidney, brain and the heart (Young & Povey 1998). TSC mutations are also linked to the sporadic development of lymphangioleiomyomatosis (LAM) (Carsillo et al. 2000). Other serious diseases linked to TSC mutations include epilepsy, autism and renal angiomyolipomase (Huang & Manning, 2008). Therefore, this is a tightly controlled complex.

TSC1 (140 kDa) and TSC2 (200 kDa) are encoded by two different genes chromosomes 9 and 16, respectively (van Slegtenhorst et al. 1997; Nellist et al. 1993). TSC1 is formed of a coiled-coil domain, with no catalytic activity. At the N-terminal end it is predicted there is transmembrane domain (van Slegtenhorst et al. 1997). TSC1 acts as a molecular heat shock protein 90 (HSP90) co-chaperone for kinases and non-kinases which prevents them from being targeted for proteasomal degradation (Woodford et al. 2017). TSC1 is required to stabilise the TSC2 protein and prevent its ubiquitination, which is mediated by HERC1 (Benvenuto et al. 2000; Chong-Kopera et al. 2006). In addition, TBC1D7 promotes TSC1 and TSC2 binding, helping the formation of this trimeric complex (Dibble et al. 2012). TSC2 forms the active part of the complex; it has a coiled-coil domain and at the C-terminus it has its functional domain. This domain is a GTPase-activating protein (GAP) which is responsible for the hydrolysis of GTP bound proteins into GDP bound proteins which alters their function usually leading to inhibition (Nellist et al. 1993). TSC2 has several substrates including RAP1, Rab5 and Ras homologue enriched in brain (RHEB) *in vitro* (Wienecke et al. 1995; Xiao et al. 1997; Inoki 2003). However, only RHEB (out of the three substrates) is regulated by TSC1/2 *in vivo* (Huang & Manning 2008). Due to its GAP activity TSC2 is tumour suppressive because this complex negatively regulates RHEB activity to inhibit mTORC1 (Jin et al. 1996). TSC1/2 converts RHEB from its GTP bound form into its GDP bound form, making RHEB inactive.

The TSC1/2 complex was first associated with the regulation of P70S6K in an insulin receptor mediated study. The deletion of the insulin receptor prevented the phosphorylation of AKT and P70S6K. The loss of P70S6K phosphorylation was recovered by the deletion of either TSC1 or TSC2 in *Drosophila* cells (Gao & Pan 2001). This suggested that the TSC1/2 complex was capable of negatively regulating P70S6K. $RHEB^{GTP}$ is an activator of mTORC1 and a substrate of TSC2 GAP activity and this bridged the link between mTORC1 substrate activity and TSC1/2 negative regulation.

RHEB is a member of the RAS superfamily that is a highly conserved GTPase in all eukaryotic cells. RHEB was first identified in *Drosophila* cells to promote cell growth and cell cycle progression by activating mTORC1 (Patel et al.

2003). In addition, the TSC1/2 complex regulates RHEB in mammalian cells which was evidence to suggest that RHEB could regulate mTORC1. Biochemical studies have revealed that RHEB in its GTP bound form can bind to and promote mTORC1 activity in a concentration dependent manner (Sancak et al. 2007; Long, Lin, et al. 2005). However, the precise mechanism of RHEB mediated mTORC1 activation has not been fully established, although it is known that RHEB is essential for complete mTORC1 activation.

The relationship between TSC1/2-RHEB-mTORC1 dictates that for mTORC1 to become activated through this axis, TSC1/2 must be inhibited. Both TSC1 and TSC2 have more than 20 phosphorylation sites, which can be phosphorylated by several different kinases/proteins. The phosphorylation of these sites, can either inhibit or activate the complex (Figure 1.7). The TSC1/2 phosphorylation sites have been summarised in Table 1.1, (Huang & Manning 2008; Astrinidis et al. 2003; Lee et al. 2007; Ma et al. 2005; Long, Lin, et al. 2005; Dan et al. 2002; Y. Li et al. 2003; Inoki et al. 2006; Roux et al. 2004). This means the complex can integrate several pathways into one node (TSC1/2) to mediate whether mTORC1 is activated or not.

Independent of phosphorylation, TSC1/2 can also be regulated by the availability of amino acids. In amino acid depleted conditions, the proteins called Ras-related GTP-binding protein (RAGs, discussed in 1.11.4) can recruit TSC1/2 to the lysosome which is where RHEB is also located (Menon et al. 2014; Demetriades et al. 2014). As a consequence increased contact with RHEB enhances TSC1/2's ability to convert $RHEB^{GTP}$ to $RHEB^{GDP}$. In amino acid replete conditions, the TSC1/2 complex is dissociated from the lysosome, therefore, promoting mTORC1 activation via $RHEB^{GTP}$ (Demetriades et al. 2014). Subsequently, under homeostasis, amino acid availability means a good percentage of TSC1/2 will be dissociated from the lysosome allowing RHEB to activate mTORC1.

The regulation of mTORC1 can be the sum combination of a number of regulatory pathways which synergise to regulate the overall activation of mTORC1.

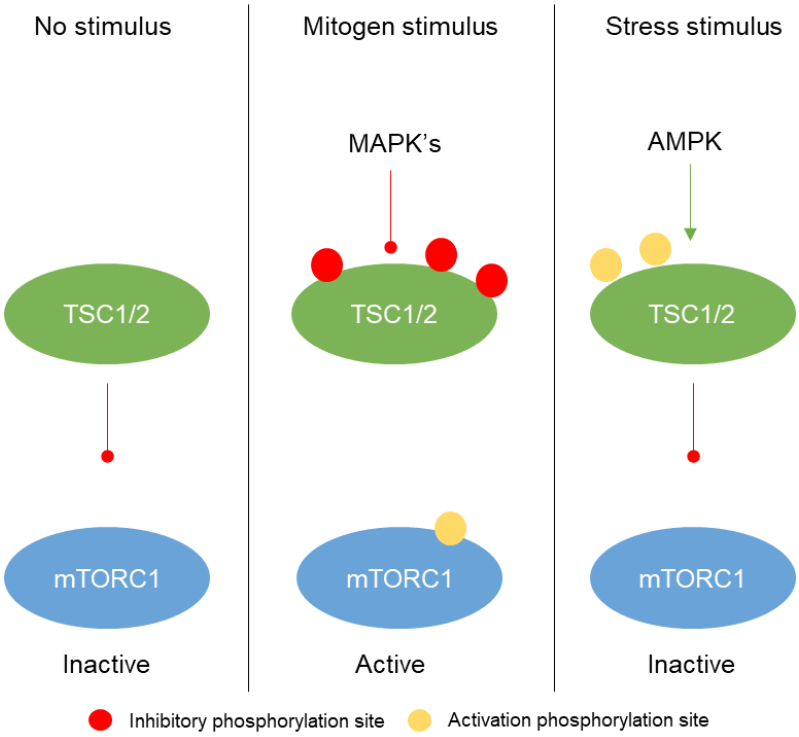

Figure 1.7: TSC1/2 negatively regulates mTORC1 activation.

Inhibition of the complex relieves the mTORC1 inhibition. Stress signals can activate the complex to inhibit mTORC1

Table 1.1 The phsophorylation sites on TSC1 or TSC2 and the kinases responsible for its phosphorylation

Phosphorylation site	Kinase that targets the site	Effects on TSC1/2 GAP activity	Effect on mTOR
TSC1 sites			
Thr^{417}	CDK1	Inhibition	Activation
Ser^{487}	IKκβ	Inhibition	Activation
Ser^{511}	IKκβ	Inhibition	Activation
Ser^{584}	CDK1	Inhibition	Activation
Ser^{1047}	CDK1	Inhibition	Activation
TSC2 sites			
Ser^{540}	ERK	Inhibition	Activation
Ser^{664}	ERK	Inhibition	Activation
Ser^{939}	AKT/RSK1	Inhibition	Activation
Ser^{1130}	AKT	Inhibition	Activation
Ser^{1132}	AKT	Inhibition	Activation
Thr^{1271}	AMPK	Activation	Inhibition
Ser^{1371}	GSK3β	Activation	Inhibition
Ser^{1375}	GSK3β	Activation	Inhibition
Ser^{1379}	GSK3β	Activation	Inhibition
Ser^{1383}	GSK3β	Activation	Inhibition
Ser^{1387}	AMPK	Activation	Inhibition
Thr^{1462}	AKT/RSK1	Inhibition	Activation
Ser^{1798}	RSK1	Inhibition	Activation
Ser^{1254}	MK2	Inhibition	Activation

1.11.4. Amino acids

Eukaryotic cells utilise the 20 available amino acids for most cellular processes. The presence of amino acids are required for mTORC1 activation (Hara et al. 1998; Wang et al. 1998). All amino acids are required to allow mTORC1 to become activated, but arginine and leucine are the most important (Hara et al. 1998; Bar-Peled & Sabatini 2014). The mTORC1 complex is recruited to the lysosome in the presence of amino acids which brings it into contact with RHEB which promotes increased mTORC1 activity (Sancak et al. 2010; Menon et al. 2014). mTORC1 is recruited to the lysosome via RAPTOR which binds to GTP bound Ras related GTP binding (RAG): A or B. RAG A or B are associated with a GDP bound RAG: C or D. The RAG dimers are

localised to the lysosome by a larger complex termed the ‘RAGULATOR’. This is a large complex comprised of 5 proteins termed late endosomal/lysosomal adaptor MAPK and mTOR activator 1-5 (LAMTOR 1-5) (Bar-Peled & Sabatini 2014; Sancak et al. 2010). The RAGULATOR has GEF activity towards RAG A and RAG B and promotes their GTP bound form which is required for mTORC1 recruitment. The RAGULATOR is only able to catalyse the addition of the phosphate group to the RAGS in the presence of amino acids (Zoncu et al. 2011; Bar-Peled & Sabatini 2014). The loss or decrease in amino acid levels subsequently leads to the hydrolysis of RAG A and RAG B into their GDP bound forms leading to the dissociation of mTORC1 from the lysosome preventing its activation (Sancak et al. 2010).

To allow the RAGULTOR and RAGs to detect the presence of amino acids, there are several other complexes involved in amino acid signalling which help regulate mTORC1 activation (through the RAGULATOR/RAG complex). The proteins/complexes are: GATOR1 (comprised of protein DEPDC5, Nprl2 and NPRL3); GATOR2 (comprised of proteins Mios, WDR24, WDR59, She 1l, Sec 13); Cellular arginine sensor for mTORC1 (CASTOR1); Sestrin2; SLC38A9; v-ATPase. These proteins and complexes are responsible for the sensing of the amino acids which in-turn dictates whether mTORC1 is localised to the lysosome. The amino acid sensing can occur in a few ways through the proteins SLC38A9, v-ATPase, Sestrin 2 and CASTOR1. The presence of leucine inhibits Sestrin 2 and Arginine inhibits CASTOR 1 which both converge on GATOR 2. In the presence of these amino acids GATOR 2 can become activated to inhibit GATOR 1 which is a negative regulator of the RAGs (Bar-Peled et al. 2013; Chantranupong et al. 2014; Chantranupong et al. 2016; Parmigiani et al. 2014; Saxton et al. 2016). GATOR 1 exerts it’s inhibition via its GAP activity towards RAG A and RAG B and converts them from the GTP bound form to the GDP bound form. Therefore, in the presence of arginine and leucine, mTORC1 can be activated through the concerted inhibition of GATOR 1.

The v-ATPase interacts with the RAGULATOR-RAG complex. It works by detecting amino acids inside the lumen of the lysosome and this allows it to promote the GEF activity of the RAGULATOR. SLC38A9 is an amino acid

transporter situated on the lysosome, where it transports arginine from the lumen into the cytoplasm. Arginine promotes the activation of GATOR 2 which subsequently promotes mTORC1 activity (Jung et al. 2015; Rebsamen et al. 2015; Wang et al. 2015).

Glutamine is utilised by proliferating cells as an energy source and a nitrogen source (Saxton et al. 2017). The mechanism is independent of RAGs, but this pathway is capable of regulating mTORC1 lysosomal localisation and its activation (Jewell et al. 2015). This mechanism utilises ADP ribosylation factor 1 (Arf1) which is a GTPase related to the RAG family (Jewell et al. 2015). The exact mechanism is not defined, but an increase in mTORC1 substrate phosphorylation can be observed. Figure 1.8 gives an overview of amino acid regulation of mTORC1.

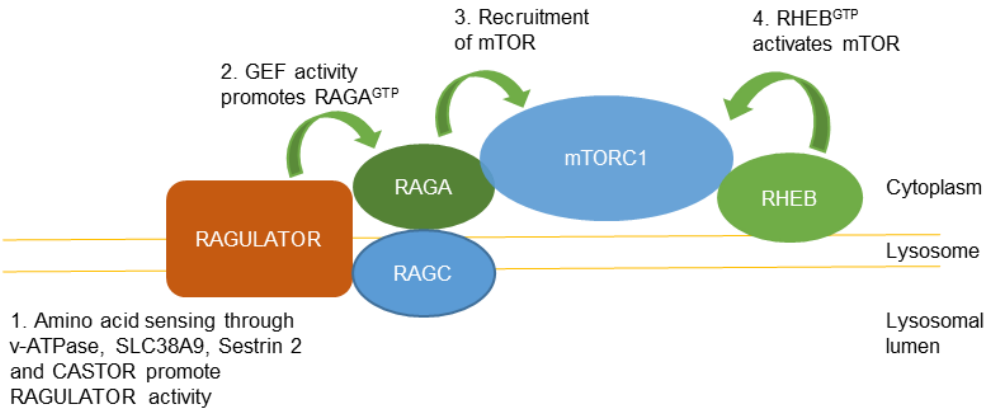

Figure 1.8: Amino acid sensing and mTORC1 activation.

Several proteins detect the levels of amino acids within the cells. This allows the activation of the RAGULATOR complex which can activate the RAG proteins A or B. Their activation leads to the recruitment of mTORC1 to the lysosome where it can come into contact with RHEB to become activated.

1.11.5. Phosphatidic acid (PA)

Phosphatidic acid is a phospholipid which can be produced by three enzymes phospholipase D, diacylglycerol kinases (DAGK) and lysophosphatidic acid-acyltransferase (LPAAT). PA has multiple roles within the cell: it acts as a precursor for lipid production; it is incorporated in the cell membrane to contribute to its properties and it can act as a second messenger. The second messenger role of PA has been associated with mTOR activation. When PLD1 is activated it produces PA which leads to mTORC1 activation (Fang et al.

2001; English et al. 1996). Increased PLD1 activity has been identified in a number of cancers. The increased PLD 1 activity produces increased PA which activates mTOR. In addition, PA promotes cancer resistance to rapamycin (Gadir et al. 2008; Shi et al. 2007). This is because PA binds to the FRB domain of mTOR which is crucial for the formation of each complex (Toschi et al. 2009).The FRB domain is the site of rapamycin interaction and PA competes with rapamycin for binding, therefore shifting the concentration at which rapamycin inhibition is effective and this promotes cancer resistance (Toschi et al. 2009). This provides some evidence that PA might be functioning to activate mTOR through a conformational change in its structure. Furthermore, RHEB is a key regulator of PLD1. RHEB in the GTP bound form binds to and promotes PLD activity, additionally this activity is inhibited by TSC1/2 (Luo et al. 1998; Fang et al. 2001).The inhibition of the TSC1/2 complex is required for PA to be produced by PLD and the presence of amino acids are also required. PLD is regulated by mitogens (serum), but some evidence shows that TGF-β_1 have also been associated to PLD activation and both promote mTORC1 activation (Sun et al. 2008; Bing Hong et al. 2000). The signalling pathways downstream of serum activation of PLD 1 suggest that PI3K is required (Sun et al. 2008). Therefore, PA under certain cellular conditions may be required for mTORC1 activation.

1.12. Hypothesis and aims

Idiopathic pulmonary fibrosis is an aberrant wound healing response characterised by the excessive deposition of matrix proteins driven by cross-talk between a number of cell types, particularly epithelial cells and fibroblasts. Central to the pathogenesis of IPF is the cytokine TGF-β_1 which promotes the fibroblast to myofibroblast differentiation and matrix protein synthesis.

TGF-β_1 exerts its cellular effects via a cascade of signalling pathways, this is mediated by SMAD signalling which is critical for the transcription of matrix proteins, specifically collagen I. The translation of the mRNA is mediated via the activation of thr mTORC1 complex. Recent evidence from our laboratory has shown that the well characterised mechanism for mTORC1 activation, the PI3K/AKT axis, is not required for TGF-β_1 induced collagen synthesis but that mTORC1 plays a key role. Therefore, the mechanism by which TGF-β_1

stimulates mTORC1 activation and collagen I synthesis in pHLFs remains undefined. The identification of the mechanism involved in both mTORC1 activation and collagen I synthesis downstream of TGF-β_1 may reveal novel therapeutic targets for the treatment of IPF.

Hypothesis: TGF-β activates mTORC1 to promote collagen I deposition in pHLFs through SMAD dependent and PI3K/AKT independent pathways

Aims:

- **To identify a TGF-β_1 sensitive phosphorylation site on mTOR that temporally correlates with mTORC1 substrate phosphorylation**
- **Investigate the cross-talk between SMAD 3 and mTORC1 activation downstream of TGF-β_1 using siRNA approaches**
- **To identify the importance of the TSC1/2 complex and investigate the kinases capable of inhibiting this complex to delineate their role in TGF-β_1 mediated mTORC1 activation and collagen I synthesis using genetic and pharmacological approaches**

2. Methods

2.1. Plasticware

Tissue culture-grade flasks, plates and disposable pipettes were all supplied by Nunc, (Denmark) unless otherwise stated. Sterile polypropylene centrifuge tubes were supplied by Falcon (New Jersey USA) and micro-centrifuge tubes were supplied by Fisher Scientific (UK).

2.2. General reagents

Reagents and buffers prepared with distilled and deionised water using a Millipore Water Purification System (Millipore R010 and Milli-Q Plus respectively, Millipore, (Germany)). Chemicals were obtained from Sigma Aldrich (UK) unless otherwise stated, all were analytical grade. Sterile cell culture reagents Dulbeco's modified eagles medium (DMEM) was supplied by Sigma-Aldrich (D6546). Sterile cell culture reagents trypsin/EDTA, antibiotics (penicillin/streptomycin) and foetal bovine serum (FBS) were supplied by Thermo Fisher scientific (UK).

2.3. Cytokines

Transforming growth factor β_1 (TGF-β_1) was purchased from R&D Biosystems (UK) and was reconstituted in 4 mM HCL/ 0.1% BSA (w/v) at 10 µg/mL. Interleukin 1β (IL1β) was purchased from Sigma Aldrich (UK) and the lyophilized recombinant human IL1β was reconstituted in sterile distilled water to a concentration of 10 µg/mL

2.4. Antibodies

Antibodies used for protein detection for western blotting were purchased from Cell Signalling Technologies (USA) see Table 2.1. The secondary antibody for western blotting was purchased from DAKO (UK). Antibodies used for immunofluorescence were either purchased from Thermofisher Scientific (UK) or Cell Signalling Technologies (USA), these are denoted in Table 2.1.

2.5. SiRNA

siRNA were used to address a number of the aims of this thesis. All siRNA used was purchased from Dharmacon (UK): TAK1 (L-003790-00-0005); SMAD3 (L-020067-00-0005), ATF4 (L-005125-00-0005), RHEB (L-009692-

00-0005), TSC2 (L-003029-00-0005), Scrambled siRNA (Invitrogen, 4390844). The siRNA was reconstituted in deionised water to 10 μM.

Table 2.1: Antibody table for western blots (wb) and Immunoflourescence (IF)

Protein Target	Code	Host species	Dilution
Primary Ab (wb)			
TAK1	5206	Rabbit	1:1000
p-P70S6K	9234	Rabbit	1:1000
P70S6K	9202	Rabbit	1:1000
p-S6K	4858	Rabbit	1:1000
S6K	2217	Rabbit	1:1000
p-T37/46 4E-BP1	2855	Rabbit	1:1000
p- S65 4E-BP1	9451	Rabbit	1:1000
p-T70 4E-BP1	13396	Rabbit	1:1000
4E-BP1	9644	Rabbit	1:1000
p-SMAD3	9520	Rabbit	1:1000
SMAD3	9523	Rabbit	1:1000
p-SMAD2	3108	Rabbit	1:1000
SMAD2	3103	Mouse	1:1000
p-T2446 mTOR	ab63552	Rabbit	1:666
p-S2481 mTOR	2974	Rabbit	1:666
p-S2448 mTOR	2971	Rabbit	1:666
mTOR	2972	Rabbit	1:666
DEPTOR	11816	Rabbit	1.2000
TSC2	3635	Rabbit	1:1000
RHEB	13879	Rabbit	1:1000
p-P38 MAPK	9215	Rabbit	1:1000
P38 MAPK	5690	Rabbit	1:1000
p-MAPKAPK2	3007	Rabbit	1:1000
MAPKAPK2	3042	Rabbit	1:1000
p-ERK1/2	9102	Rabbit	1:1000
ERK1/2	4695	Rabbit	1:1000
α-Tubulin	9099	Rabbit	1:3000
Secondary Ab (wb)			
Polyclonal Rabbit Anti-Mouse Immunoglobulins/HRP (DAKO)	PO448	Rabbit	1:1000
Polyclonal Goat Anti-Rabbit Immunoglobulins/HRP (DAKO)	PO447	Goat	1:1000
Primary Ab (IF)			
Anti-collagen type I monoclonal antibody (Sigma)	C2456	Mouse	1:1000
DAPI (Sigma)	D9542	Rabbit	1:10000
Secondary Ab (IF)			
AlexaFlour 488 (Life technologies)	A-11034	Goat	1:1000

2.6. Pharmacological inhibitors

Tool compounds were used to interrogate the aims of the thesis and are as listed: AS703026 (Selleckchem, S1475), BMS-265246 (Tocris, 5654), SL0101 (Merck, 559285), LY2584702 (Selleckchem, S7698) TAK715 (Tocris, 4254),

(5z)-7-Oxozeaenol (Cayman chemical, 17459), SB202190 (Tocris, 1264), BIRB796 (Tocris, 5989), PF3644022 (Tocris, 4279), MKIV (Merck, 475964), NG25 (Sigma, SML-1332), Actinomycin D (Tocris, 1229), CB-839 (Cayman chemicals, 22038). The inhibitors SB-525334, GSK2334470, Rapamycin, Compound 12 and AZD8055 were kindly supplied by GlaxoSmithKline, transferred under the Materials Transfer Agreement to Professor Rachel Chambers.

2.7. Fibroblast cell culture

Control explant tissue were obtained by GlaxoSmithKline from Asterand Europe (Royston, UK) and national disease research interchange (NDRI). The primary human lung fibroblasts (pHLF) (cell lines: 0311, 0110, 0610) were grown out of the explant tissue at the Centre for inflammation and tissue repair under third party transfer agreements. Briefly, human lung parenchyma was harvested as 1 mm3 – sized pieces under sterile conditions and placed in a petri dish containing 2 mL of Dulbecco's Modified Eagle Medium (DMEM) (Gibco®) supplemented with 20% foetal bovine serum (FBS) (Gibco®); 2 mM L-Glutamine (l-Glu); 50 U/ml penicillin/50µg/mL streptomycin (pen/strep) and 2.5µg/ml Amphotericin B. After the lung sections were cut, 8 mL of the supplemented DMEM was added to the petri dishes and cells were incubated at 37°C, 10% CO_2 for 24 hours. Media was replaced with 10 mL of the supplemented DMEM every 3 days. An Olympus TCK-2 inverted phase contrast light microscope (Olympus Optical Ltd., UK) was used to observe outgrowth from the parenchyma slices. Once 80-90% confluence was achieved the media was aspirated and the cells were detached from the petri dish using trypsin-EDTA (Gibco®, Life Technologies, UK) with a 5 minute incubation period at 37°C. The trypsin was neutralised using an equal volume of DMEM with FBS, the suspension was centrifuged at 300 x g for 5 minutes. The supernatant was aspirated and the cell pellet was re-suspended in 2 mM L-glutamine, 50U/µg/mL pen/strep, and 10% FBS DMEM. The cell count of the suspension was determined using the Scepter™ 2.0 Handheld Automatic Cell Counter (Millipore, Germany). The appropriate cell density was then used to seed cells for culture in flasks, plates or frozen in liquid nitrogen (DMEM supplemented with normal L-glu and pen/strep concentrations, 20% FBS and

10% DMSO (Sigma-Aldrich, UK (#D2650)). The highest passage of cells used were P8.

2.8. Routine cell culture

PHLF were passaged when confluence was reached. The media was removed from the cells followed by a wash with sterile Dulbecco's phosphate buffered saline (PBS) (Sigma-Aldrich, UK) which was aspirated as well. The cells were treated with 5 mL of trypsin-EDTA and was incubated for 5 minutes at 37°C and 10% CO2. The use of a microscope (Olympus TCK-2) confirmed the fibroblasts had detached from the flask. 5 mL of DMEM with 10% FBS was used to neutralise the trypsin-EDTA. The suspension of fibroblasts was centrifuged for 5 minutes at 300 x g. The cells were pelleted, the supernatant was removed and discarded. The pellet was re-suspended in fresh 10% FBS DMEM. Cells were counted using the Scepter™ 2.0 Handheld Automatic Cell Counter. The final cell density was determined by the amount of media added per well; 6 well plate 2 mL; 12 well plate 1 mL; 96 well plate 100 µL (black-walled:Corning, USA #3603; White-walled Perkin Elmer, USA) which were pipetted from a density of $1x10^5$ cells/mL. All cell cultures were incubated at 37°C and 10% CO_2.

2.9. Experimental cell culture

All work completed using pHLFs were derived from one control donor, with the exception of two experiments (noted in the results section). The choice to use one single primary cell culture was based upon the Chambers group prior characterisation of the fibroblast responses for these cells to several stimuli including TGF-β_1. Cells were grown until confluent or to a specified confluence (60-80% for siRNA) for the required experimental conditions. At the correct confluence the media was removed and replaced with serum starvation conditions (0% FBS DMEM) or low serum condition which was used for collagen deposition assay experiments (0.4% FBS DMEM). The cells were incubated for 24 hours in starvation conditions before treatment to stop cell proliferation and ensure any active signalling pathways were the result of TGF-β_1. The treatments were carried out under the same starvation conditions.

Pharmacological inhibitors were incubated with cells for 1 hour prior to TGF-β_1 stimulation. DMSO was the selected diluent for inhibitor preparation. The concentrations of the inhibitors were prepared in serial dilutions in DMSO followed by a final dilution factor of 1000 to provide the final inhibitor working concentration whilst ensuring the DMSO level was below toxic levels (0.1%). Samples which were not prepared with inhibitor were controlled for with the addition of DMSO (0.1% concentration).

2.10. Collagen deposition assay

A high content macromolecular crowding assay for collagen deposition has been characterised in our laboratory previously (Mercer et al., 2016). Briefly, cells were seeded in a 96 well plate format and collagen I was quantified as an end-point read-out post TGF-β_1 stimulation and inhibitor treatment. Cells were starved in 0.4% FBS DMEM 24 hours prior to treatment. At the point of treatment, macromolecular crowding was employed by preparing a macromolecular crowding media containing 0.4% FBS, L-Ascorbic acid 2-phosphate sesquimagnesium salt hydrate (ascorbic acid, 16.6µg/ml,), Ficoll® PM 70 (37.5mg/ml) and Ficoll® PM 400 (25mg/ml) (Sigma Aldrich). The cells were incubated with the pharmacological inhibitor, which was prepared in the macromolecular crowding media, for 1 hour prior to treatment with TGF-β1 at 1 ng/mL. Additionally, as a control in some experiments a TGF- β1 concentration-response curve was prepared from a 10 µM stock and prepared in serial dilutions in media followed by a final 1000 dilution to give the final working concentration in the wells.

The cells were incubated for 48 hours with treatment/inhibitor before cell fixation in ice cold methanol (VWR) for 2 minutes. The cells were washed with PBS and then permeabilised with 0.1% Triton-X-100 in PBS for a further 2 minutes. Mouse anti-collagen type I monoclonal antibody (Sigma Aldrich) was diluted at 1:1000 in PBS and was incubated with the permeabilised cells overnight at 4°C. The next day cells were washed with 0.05% Tween in PBS three times, followed by the addition of DAPI 1:10,000 (Life Technologies) and goat anti-mouse secondary antibody conjugated with AlexaFluor® 488 1:1000 (Life Technology) in PBS. The secondary antibody was incubated in the wells for 1 hour at room temperature. Finally the plates were washed with 0.05%

Tween-PBS, and then the cells were stored in 200 µL/well PBS to be imaged on the InCell 6000 (GE Healthcare Life Science, UK). The plates were stored at 4°C in the dark when not in use. High content imaging and quantitative analysis was carried out using the InCell 6000. The images were obtained at a 20x magnification, with four images taken per well. The InCell 6000 workstation was used to quantify the total collagen intensity (GE Healthcare Life Science, UK).

2.11. Generation of protein lysates

Human lung fibroblasts were cultured in a 6 or 12 well plate. Post-treatment the cells were placed on ice and the supernatant was removed at the corresponding time-point. The cells were washed with ice cold PBS which was removed and followed by the addition of 90 µL of Phosphosafe™ (Novagen®, USA) combined with protease inhibitors (complete mini, Roche). The cell layer was scraped from the plastic and transferred to 0.5 mL microcentrifuge tubes and frozen at -20°C.

2.12. BCA assay

To determine the protein concentration in each lysate the bicinchoninic acid protein assay (BCA) (Pierce, USA) was used according to manufacturer's instructions. 5µL of sample or standards was added in triplicate (standards) and duplicate (samples) on a clear 96 well plate. The standards were prepared from a stock concentration of 2 mg/mL bovine serum albumin (BSA). BCA reagent is added as 100 µL per well followed by sample mixing for 30 seconds (MixMate®, Eppendorf, Germany). The 96-well plate is then incubated for 30 minutes at 37°C. The VersaMax plate reader (Molecular Devices, USA) detected the protein absorbance at 562 nm. The averages of the replicates were taken and a standard curve was produced using the BSA standards. The standard curve was used to calculate protein concentration (Y=mx+c).

2.13. Western blotting

The loading protein concentration of each lysate was determined by the BCA assay, using a minimum of 3 µg of sample. The samples were prepared with Novex® 4X Bolt® LDS Sample Buffer, Novex® 10X Bolt® Sample Reducing Agent and water to make up the final loading volume, equal across all

samples. Samples were boiled at 80°C for 10 minutes and then centrifuged briefly at 4°C. The size of the protein determined what gel and transfer method was used.

2.13.1. Proteins 10 -150 KDa

Samples were loaded on a pre-cast 4-12% Bis-Tris Plus Gel (Novex® Bolt®) along with a 10-250 kDa protein ladder (PageRuler™ Plus Prestained Protein Ladder, Thermo Scientific, UK). Electrophoresis was performed in Bolt® MES SDS Running Buffer at 125 V for a minimum of 30 minutes (according to protein weight). The protein from the gel was heat transferred to nitrocellulose membranes which are provided in the iBlot® Transfer Stack required for the iBlot2® dry transfer system which uses a 20 V current for 7 minutes to allow sufficient transfer of the protein. To ensure the protein transfer had worked correctly the membranes were stained briefly with 2% Ponceau Red (Sigma-Aldrich, UK).

2.13.2. Proteins 150 – 300 KDa

Samples were loaded on a pre-cast 6% Tris-glycine Gel (Novex® Bolt®) along with a 40 – 300 KDa protein ladder (LC5699, Thermo Scientific, UK). Electrphoresis was performed in Bolt® Tris-glycine Running Buffer at 125 V for 1 hour. The samples were transferred by wet transfer. The Immobilon-P PVDF Membrane (Merck Millipore IPVH07850) were activated using 100% ethanol for 20 seconds followed by rinsing in MilliQ water for 1 minute. The gel, membrane and filter paper were all incubated at 4°C for 20 minutes in transfer buffer (25mM Tris-base, 192mM glycine, 10% methanol (v/v) in water). The transfer was then conducted for 16.5 hours at 30 V at 4°C.

According to the protocol set by the manufacturer, membranes were either blocked in 5% BSA or 5% Milk in TBS-0.1% Tween (TBST) for a minimum of 1 hour prior to primary antibody incubation at 4°C for 16 hours. The membranes were washed 3 times for 10 minutes for each wash. Horseradish peroxidase (HRP)-linked secondary antibody (Dako, UK) was used according to the species of the primary antibody (mouse or rabbit). The secondary antibody was incubated at room temperature for 2 hours followed by the same washing steps mentioned above. The addition of Luminata Crescendo

Western HRP Substrate (Merck Millipore, Germany) produces a luminescent derivative which can be detected on the ImageQuant4000 (GE Healthcare Life Sciences, UK). Protein loading was controlled for by either their total protein or by α-Tubulin. The α-Tubulin was already HRP-conjugated and so does not require the secondary antibody step. To probe the membrane using a new antibody the membranes were stripped using RestoreTM Plus Western Blot Striping Buffer (ThermoScientific, USA), following the antibody removal the membrane was re-blocked and probed with a different primary antibody. The protein bands were analysed using ImageJ to obtain the densitometry. The densitometry was normalised between the target protein densitometry and the reference protein densitometry to detect differences between the sample treatments. The replicates were averaged and plotted as a densitometry plot, Table 2 summarises the Antibodies used for the western blots. All antibodies were purchased from Cell Signalling Technologies.

2.14. siRNA

2.14.1. Reverse transfection

The lipofectamine RNAImax and lipofectamine 3000 were prepared as a 10 times stock and pipetted into the wells the cells were being seeded on. The cells were seeded at 1 X 10^5; 1.5 X 10^5; 2.0 X 10^5; 2.5 X 10^5 on top of the siRNA leaving the siRNA at a final 1 X concentration. The cells were seeded in 10% FBS DMEM penicillin and streptomycin. The cells were incubated for 24, 48 and 72 hours before imaging on a Zeiss axio vert A1microscope (Zeiss) using the Zen pro software (Zeiss).

2.14.2. Forward transfection

Cells were cultured in a 12 well plate or a 96 well plate in 10% FBS DMEM at 37°C in 10% CO2. At 80% cell confluence the siRNA was prepared as a 10 times working solution in DMEM and spiked into each well to give the final 1X concentration. Cells were incubated with the siRNA for 6 hours before half the media was removed followed by adding 3 parts of fresh 0% or 0.4% media to the media in the well (1 in four dilution). After 24 hours post siRNA treatment the media was removed and replaced with fresh 0% DMEM or 0.4% for the collagen deposition assay. This allowed 48 hours for the protein to be knocked-down. Post transfection period the media is replaced with fresh

DMEM and the cells were left to incubate for 1 hour prior to stimulation with 1 ng/mL TGF-β_1. The cell were lysed at the specified time point, see the above protocol and western blot protocol. For the collagen deposition assay the knock-down is the same and then the same protocol used as described above.

2.15. CRISPR-Cas9 gene editing

CRISPR guidesRNA were designed using the deskgen design platform (https://www.deskgen.com/guidebook/advanced.html). The deskgen design platform identifies the protospacer adjacent motif (PAM) site where the Cas9 gene can cleave the DNA. To target the DNA a guide RNA is required to bind to this complementary region which is adjacent to the PAM site and this is designed by the deskgene platform. 4 guideRNA were designed, Table 2.2, and run in parallel with a control guideRNA to validate them. The crRNA /guide RNA (100 µM) was mixed with tracrRNA and IDT duplex buffer. The ratio of crRNA/tracrRNA is equal to 1.2:1. The RNAs were annealed at 95°C for 5 mins. Followed by cooling at RT for 10 mins. The annealed RNA (72.5 pmol) was mixed with the Cas9 enzyme (10 µg, 60 pmol) to get a 1.2:1 RNA/cas9 ratio. After 10 mins of incubation this was mixed with (60 pmol) of electroporator enhancer (100 µM) which was incubated for 10 minutes.

Table 2.2: The guide RNA's generated for CRISPR

Target exon	CRISPR guide Sequence
1	AGATGCCGCAGTCCAAGTCC
1	ATCTTCCGGGACTTGGACTG
1	CACCGCCGCCGCGGTTGATG
3	CCAGAGGTCACTTACTTGCC

250k cells were used per condition and washed with PBS and spin at 90g for 10 min. After removal of the PBS the cells were re-suspend with 15.5 µL Nucleofactor solution P3 (Lonza). To each condition (5 including control) 4.5 µL of the RNP complex was added. The cells/RNP were pipetted into the 16-well strips, one well per condition, for electroporation. The cells were electroporated using the program CM138 in the X unit on the Lonza 4D nucleofactor (Lonza). The cells were left to rest for 5 min at RT. Following this rest period 100 µL of pre-warmed media was added to the strip and used to

transfer the cells to the pre-warmed T25 flask (5 mL of media). For validation of the guideRNA, at confluence, the cells were harvested using the lysis-western blot protocol.

To investigate the effect of CRISPR RNAguide 1 effect on the cells, they were grown in T25 to confluence and then expanded in T175. They were then plated into a 6 well plate and grown to confluence at 37^{o}C and 5% CO_2. At confluence cells were starved for 24 hours in 0% DMEM. After the starvation, the media was replaced with fresh 0% DMEM and was incubated for 1 hour prior to stimulation with 1 ng/mL TGF-β_1. The cells were stimulated with TGF-β_1 for 3 hours before being harvested before using the lysis-western blot protocol. For the collagen deposition assay the CRISPR treated cells are plated and treated under the same conditions and then the protocol described in the collagen deposition assay protocol.

2.16. Caspase 3/7 glo apoptosis assay

PHLF were seeded in 96 well plates (Perkin-Elmer, UK) and grown to confluence. Cells were exposed to low serum (0.4% FBS DMEM) for 24 hours prior to treatment. The cells were treated with (5z)-7-Oxozeaenol for 48 hours which was equivalent to the collagen deposition assay treatment time. After 48 hours the cells the manufacturer's instructions were followed using the Caspase 3/7 glo assay protocol (Promega, UK) which quantifies the activity of caspase 3 and caspase 7. In brief, 100 µL of assay buffer was added to the cell supernatant and incubated for 1 hour. Staurosporine was added as a positive control known to induce apoptosis. The cells luminescence was measured on a FLUOstar® Omega plate reader (BMG Labtech, Germany) to determine the levels of caspase 3 and caspase 7.

2.17. LDH necrosis assay

PHLF were seeded in 96 well plates (Perkin-Elmer, UK) and grown to confluence. They were exposed to low serum (0.4% FBS DMEM) for 24 hours prior to treatment. The cells were treated with (5z)-7-Oxozeaenol for 48 hours equivalent to the collagen deposition assay treatment time. After 48 hours the cells LDH levels were uded to measure cell death were tested, as per the manufacturer's instructions. In brief, 50 µL of supernatant was removed and

added to a new clear 96 well plate. A buffer including NAD+ is added to the supernatant, LDH catalyses NAD+ to NADH and H+ which then reacts with a tetrazolium salt to reduce it to a red coloured formazan which was then quantified by measuring the absorbance wavelength at 490 nm on a VersaMax plate reader. The background was measured at 680nm. This value was subtracted from the replicates to get the LDH activity reading. Then the following equation was used to calculate the cytotoxicity:

% Cytotoxicty = (Compound-treated LDH activity – Spontaneous LDH activity)/(Maximum LDH activity – Spontaneous LDH activity) * 100.

The spontaneous activity controls were TGF-β negative control which was used to only calculate the drug cytotoxicity in (5z)-7-Oxozeaenol only treated cells. The TGF-β_1 positive control was used to only calculate the drug cytotoxicity in (5z)-7-Oxozeaenol stimulated with 1 ng/mL. The maximum LDH activity was calculated by using 10 X lysis buffer provided in the kit.

2.18. RT-qPCR

2.18.1. RNA extraction

PHLF were seeded in 6-well plates and the samples were collected a select time-points. Surfaces were cleaned with RNaseZap (Sigma-Aldrich, UK). The supernatant was removed from tissue culture plates and washed with cold PBS prior to the addition of 350 µL RLT buffer (RNeasy mini kit, Qiagen). The lysed cell were scraped and transferred into 1.5 mL microcentrifuge tubes. An equal volume of 70% ethanol was added to the lysates and centrifuged for 15s at > 8000 x g. The flow-through was discarded and 700 µL of Buffer RW1 (Qiagen) was added to the column and spun the same as before. Flow-through was discarded and 500 µL RPE buffer was added to the column and re-centrifuged, and this was repeated. After the flow-through was discarded again, 50 µL RNase-free water was added to the column and centrifuged at 13000 x g to elute the RNA.

2.18.2. DNase treatment

The RNA was purified from the DNA using DNAse (Thermo-Fisher, U.S.A.) treatment. The DNAse was incubated at 37^{o}C for 10 minutes followed by heat

inactivation at 60ºC for one hour. A NanoDrop 8000 spectrophotometer (Thermo Fisher Scientific) was used to calculate the RNA concentrations.

2.18.3. cDNA synthesis

cDNA was prepared from the RNA extracts using reverse transcription using qcript cDNA supermix kit (Quanta Biosciences, USA). 500 ng of RNA from each sample was mixed with 4 µL of qscript, the volume was made up to a total of 20 µL using nuclease-free water. The samples were incubated cycling from 25ºC for 5 minutes followed by 42ºC for 30 minutes and then 85ºC for 5 minutes on a tetrad thermocycler (Bio-Rad).

2.18.4. Quantitative RT-PCR

Quantitative real-time polymerase chain reaction (qRT-PCR) was conducted using the *Power* SYBR® Green PCR Master Mix (Applied Biosystems®, Life Technologies, UK). The PCR reaction mix consisted of 2 µL cDNA, forward and reverse primers and master mix all prepared in white 96-well plates. The samples were run in duplicate. The PCR reaction was conducted on the Mastercycler® EP Realplex (Eppendorf, Germany) on the following cycle: 95° for 10 minutes, followed by 40 cycles of 95° for 15 seconds and 60° for 60 seconds. To assess the amplification of the RNA of interest the cycle threshold (Ct) is taken, which is determined from the earliest point of the linear region of the logarithmic amplification plot that reached the threshold of detection. The Ct values were normalised to the reference genes (ATP synthase 5B (ATP5B) and β2 microglubulin (B2M) to give the ΔCT. The relative expression of the gene of interest was then calculated using the equation $2^{-\Delta CT}$. The primers used are described in Table 2.3.

2.19. Click-IT assay

2500 cells were seeded in a 96 well plate (Corning). After 24 hours the cells were starved in 0% DMEM at 50% confluence for another 24 hours. The starve media was removed and replaced with either control, BMS-265246 or SL0101 (4 concentrations of each) diluted in either 10% FBS or 0% DMEM and incubated for 48 hours. 8 hours before the end of the experiment 100 µL/well EdU (Life Technologies) was spiked into each well. After the 8 hours the media was removed and replaced with ice cold methanol for 15 minutes followed by

2 PBS washes. The PBS was removed and replaced with 0.1% triton in PBS for 15 minutes at room temperature. The click-IT cocktail was prepared from: 2 x click-IT reaction buffer, CuSO4, Oregon green 488 Azide and click-IT Edu buffer additive and 50 µL of this was added to the cells and incubated for 25 minutes in the dark at room temperature. The cells were then incubated with blocking buffer (supplied by the kit (component H). After blocking, 50 µL of anti-Oregon Green HRP antibody solution was incubated in the dark for 30 minutes at room temperature. The wells were washed and followed by incubation with 100 µL of Amplex UltraRed buffer and incubated for 15 mins at room temperature in the dark. The reaction was quenched using 10 µL of Amplex UltraRed stop reagent. The plate was read at excitation 568 and emission at 585 nM on the FLUOstar® Omega plate reader (BMG Labtech, Germany)

Table 2.3: The forward and reverse primers used for PCR

Gene	Forward sequence	Reverse sequence
ATP5B	Not supplied by manufacturer (PrimerDesign, #HK-SY-hu-1200), accession number: NM_001686	
B2M	Not supplied by manufacturer (PrimerDesign, #HK-SY-hu-1200), accession number: NM_004048	
SMAD 3	Not supplied by manufacturer (PrimerDesign, #SY-hu-600), accession number: NM_005902	
COL1A1	5’ ATGTAGGCCACGCTGTTCTT 3’	5’ GAGAGCATGACCGATGGATT 3’
ATF 4	5’ TTCTCCAGCGACAAGGCTAAGG 3’	5’ CTCCAACATCCAATCTGTCCCG 3’

2.20. Statistics

The datasets are presented as mean values ± SEM. The statistical tests used were two-way-ANOVA with Tukey’s multiple comparison. The values were considered significant if $p<0.05$ (*). The graphs and statistical analysis were generated on GraphPad Prism v7.0 using the inhibition-concentration response curve model, with the four-parameter non-linear regression for the curve.

3. Results

3.1. Characterising the temporal activation of TGF-β_1 activated SMAD 3 and mTORC1 pathways

The excessive deposition of collagen is a central feature of IPF. TGF-β_1 is a key mediator that stimulates the synthesis of collagen by fibroblasts and myofibroblasts. TGF-β_1 does this by mediating gene transcription via SMAD 3. SMAD 3 activation is directly phosphorylated by the activated TβRI receptor and this allows it to bind and translocate to the nucleus with SMAD 4. SMAD 3 then mediates the transcription of the *COL1A1* gene and the translation of the collagen mRNA is regulated indirectly via mTORC1. However, at the time of investigation, it was not clear whether mTORC1 or mTORC2 were responsible for regulating the downstream pathways that led to the translation of collagen I mRNA. Collectively as a group we now know that it is mTORC1 mediated (Woodcock et al. 2019). Our evidence demonstrates that PI3K/AKT activation does not increase mTORC1 kinase activity downstream of TGF-β_1 stimulation. The inhibition of PI3K and AKT did not affect the phosphorylation of mTORC1 substrates, 4EBP1 and P70S6K (Woodcock et al. 2019). Furthermore, the inhibition of PI3K or AKT does not inhibit TGF-β_1 stimulated collagen I synthesis (Woodcock et al. 2019). This means the mechanism by which TGF-β_1 mediates mTORC1 activation is unknown. This generated the basis of my hypothesis.

The temporal phosphorylation profile of SMAD 3 and mTORC1 downstream of TGF-β_1 stimulation was established first. The temporal activation of two of the core TGF-β_1 signalling pathways is critical for understanding how TGF-β_1 stimulates mTORC1 activation. Therefore, it was determined when the initial activation of mTORC1 occurred by measuring the phosphorylation of the mTORC1 substrates 4E-BP1 or P70S6K. This would help temporally align when the phosphorylation of other proteins occurred with mTORC1 activation and this would help determine whether they could be required for the activation of mTORC1 downstream of TGF-β_1 stimulation.

Time 0 is taken 1 hour after the starvation media (0% FBS) is removed and replaced with fresh starvation media. At each time-point pHLFs are treated with or without TGF-β_1 [1 ng/mL]. In response to TGF-β_1, SMAD 3

phosphorylation peaks at 1 hour (Figure 3.1A). The phosphorylation decreases at three hours however a degree of phosphorylation can be observed for up to 12 hours. In addition, the SMAD 3 total levels of protein are decreased at 24 hours (Figure 3.1). The 4E-BP1^{S65} was investigated to assess mTORC1 activity. This has previously been demonstrated to be the most responsive site to TGF-β_1 stimulation in our pHLFs and it is directly phosphorylated by mTORC1 (Woodcock et al. 2019). There are basal levels of 4E-BP1^{S65} phosphorylation in the absence of TGF-β_1. However, in response to TGF-β_1 stimulation 4E-BP1^{S65} phosphorylation is increased from 3 hours onward and this continues for 24 hours (Figure 3.1). Using this temporal profile of SMAD 3 and mTORC1 activation, this determined the time-points for future investigations.

3.2. The mechanisms of TGF-β_1 stimulated mTOR phosphorylation

3.2.1. Introduction

mTOR is phosphorylated at several different phosphorylation sites, including S1261, S2159, T2164 T2446, S2448 and S2481 (Chen et al. 2002; S. W. Y. Cheng et al. 2004; Acosta-Jaquez et al. 2009; Ekim et al. 2011). In particular, the T2446, S2448 and S2481 are located in the NRD domain of mTOR. The deletion of this domain prevents mTORC1 from phosphorylating 4E-BP1 and P70S6K (Sekulić et al. 2000). Published work has identified different roles for each site. The T2446 is an inhibitory site that has been investigated for its role in inhibiting mTOR in response to negative stimuli, such as increased AMPK activity and a decrease in amino acid levels (Cheng et al. 2004). The S2481 site has been implicated as an mTORC2 site and its phosphorylation is regulated by mSIN1 (a component of the mTORC2 complex) (Copp et al. 2009). In addition, it is known that TGF-β_1 regulates this site to increase mTORC2 activity (Chen et al. 2002). The S2448 site is regulated by insulin and FBS and two signalling pathways have been defined. The site is argued to be either regulated by the PI3K/AKT axis or via a PDK1/P70S6K feedback loop that is dependent on mTORC1 phosphorylating P70S6K (Chiang & Abraham 2005; Cong et al. 2018; Navé et al. 1999). The S2448 site is also sensitive to TGF-β_1 stimulation, however, the signalling pathway involved is unknown. A time-course of all three sites in fibroblasts or in response to TGF-

β_1 has never been published. These sites have the potential to serve as markers of TGF-β_1 stimulation relevant to collagen synthesis and could help identify the upstream mechanism(s) required for mTORC1 (S2448) or mTORC2 (S2481) activation.

The following section aims to define the signalling pathways leading to mTOR S2448 phosphorylation in response to TGF-β_1 stimulation in pHLFs using several selective pharmacological inhibitors.

3.2.2. Investigating the effect of TGF-β_1 stimulation on the mTOR regulatory domain phosphorylation sites

The evidence from Figure 3.1 demonstrates that mTORC1 activity is increased in response to TGF-β_1 from 3 to 24 hours. The effects of TGF-β_1 on T2446, S2448 and S2481 mTOR phosphorylation sites were assessed and compared to the activity profile of mTORC1. To assess the phosphorylation states of these three sites the pHLFs were cultured in serum-free DMEM with or without TGF-β_1 [1 ng/mL] and three phosphorylation sites were analysed at selected time-points by western blotting (Figure 3.2).

The mTOR T2446 phosphorylation site is phosphorylated when amino acid availability is low (Cheng et al. 2004). Figure 3.2A indicates that the T2446 site was unresponsive to TGF-β_1 stimulation but is constitutively phosphorylated at baseline. Previous reports have identified this as an inhibitory site (Cheng et al. 2004). Therefore, observing no change in this site had not been expected and so this site was investigated further, see below, section 3.2.3 (Figure 3.3).

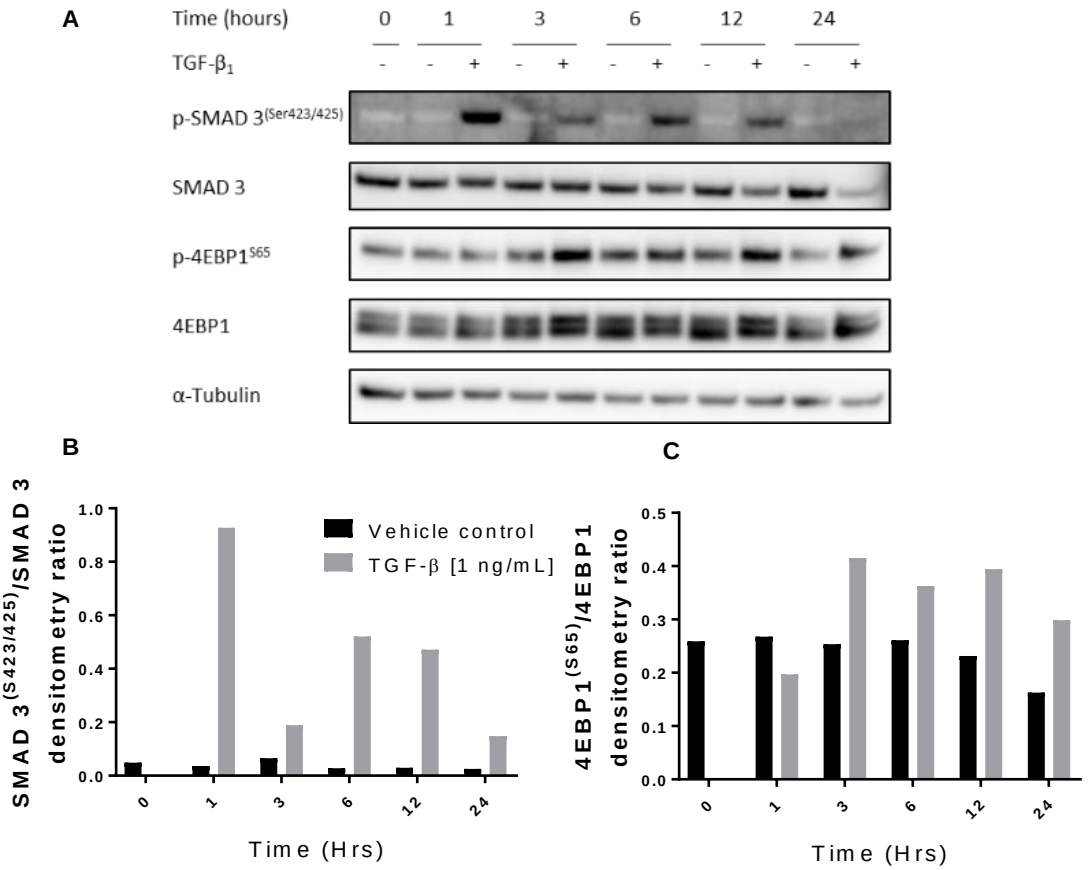

Figure 3.1: The effect of TGF-β_1 stimulation on SMAD 3 and 4E-BP1 phosphorylation over 24 hours in pHLFs

Confluent pHLFs were serum-starved prior to stimulation with 1 ng/mL TGF-β_1 for the indicated time-periods. Phosphorylated SMAD 3 and 4E-BP1 were assessed by western blotting. Protein loading was verified by blotting with anti- α-tubulin antibody. The densitometry was calculated and plotted as a phopho-protein to total protein ratio shown in Panel B. The data is representative of two independent experiments performed.

The mTOR S2481 phosphorylation site is an autocatalytic site and typically used as a marker of mTORC2 activity (Copp et al. 2009). The S2481 phosphorylation site showed a marginal increase in phosphorylation above the basal levels at 6 and 12 hours (Figure 3.2B). This delayed phosphorylation signalling is indicative of the auto-phosphorylation of S2481 which is associated with mTORC2 and occurs in line with PI3K/AKT signalling (Woodcock et al. 2019; Mercer et al. 2016). Furthermore, this site is phosphorylated by AKT downstream of PI3K activation (Copp et al. 2009; Chen et al. 2002). The delay in response demonstrated that S2481 was unlikely to be required for the TGF-β_1 stimulated activation of mTORC1 complex which occurs at three hours. Taken together with previous reports defining this as an mTORC2 specific site, the phosphorylation of S2481 on mTOR was not pursued any further.

The next site investigated was the S2448, which is used as a marker of mTORC1 activity and is responsive to exogenous stimuli, including TGF-β_1 (Chen et al. 2002). TGF-β_1 induced an increase in phosphorylation above the basal levels at 3, 6 and 12 hours (Figure 3.2C). On the first section of the blot (0-1 hours) at 0 and 15 minutes there is a higher level of phosphorylation in both TGF-β_1 stimulated and unstimulated cells compared to 30 mins and 1 hour. S2448 in HEK293 cells has been shown to be sensitive to acute changes in nutrients, therefore it is possible that these early fluctuations in phosphorylation state reflect sensitivity to media changes (Cooper et al. 2017). Therefore, when the fresh media is added to the pHLFs the availability of amino acids present in the media may contribute to the higher levels of phosphorylation at 0 and 15 minutes compared to the 30 and 1 hour time-points (Figure 3.2C).

Taken together these results shows that phosphorylation of mTOR at S2448 in response to TGF-β_1 temporally correlates with the phosphorylation of 4E-BP1^{S65}.

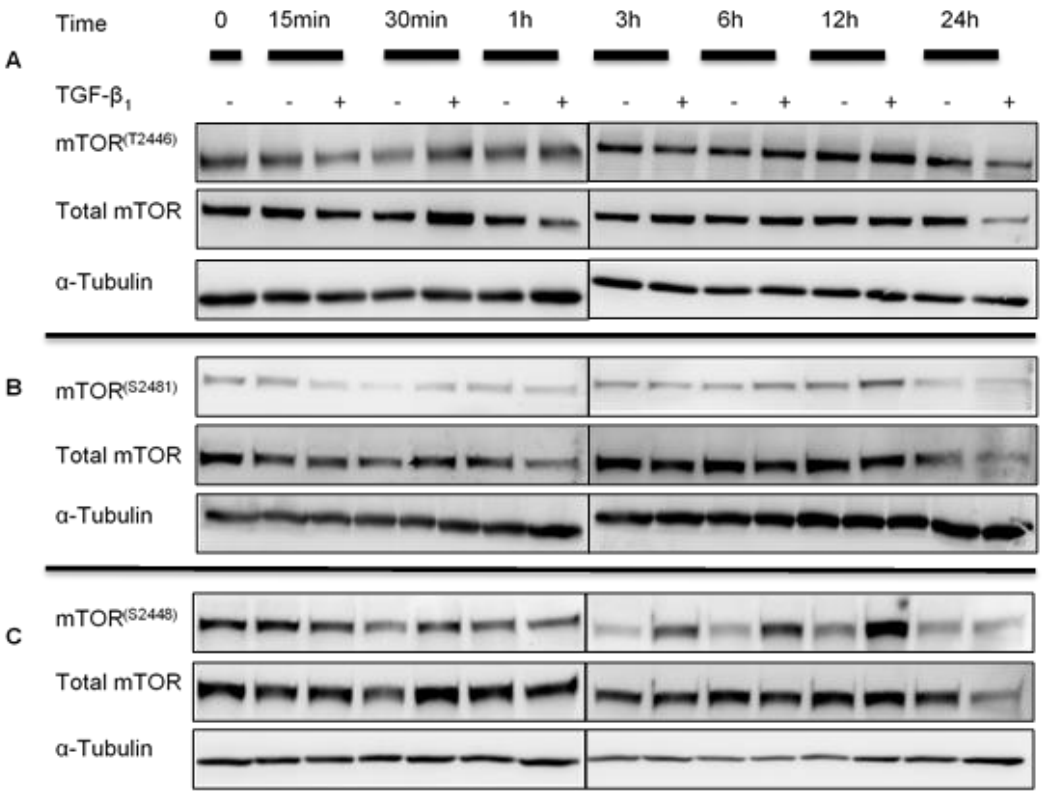

Figure 3.2: Time course of TGF-β1 stimulated mTOR phosphorylation in pHLFs

pHLFs were serum-starved prior to stimulation with 1ng/ml TGF- β1 for the indicated time periods. The different mTOR phosphorylation sites, T2446, S2481 and S2448 were assessed Western blotting panel A-C, respectively. Protein loading was verified by blotting with an anti-α-Tubulin antibody. These data are representative of two independent experiments performed.

3.2.3. The effects of amino acid starvation on T2446 phosphorylation

The T2446 phosphorylation site on mTOR is unresponsive to TGF-β_1 (Figure 3.2). This phosphorylation site is regulated by a decrease in amino acids levels and AMPK, and marks inhibited mTORC1 activity (Cheng et al. 2004). Since Figure 3.2 demonstrated constitutive phosphorylation of this site this means, according to previous reports, a portion of mTOR is inhibited. This contradicts the observed phosphorylation of 4E-BP1 and the increase in S2448 phosphorylation which are markers of mTORC1 activity (Cheng et al. 2004). To determine if the phosphorylation of T2446 is due to either a technical issue or the result of a portion of mTOR that is inhibited, pHLFs were exposed to low amino acid levels which would demonstrate sensitivity of the T2446 site to amino acid deprivation. The pHLFs were treated by removing the DMEM and replacing it with PBS and assessing the phosphorylation over a 3 hours, with

the aim of inducing a change in the phosphorylation status. Treatment with PBS increased the phosphorylation of the T2446 mTOR site after 3 hours (Figure 3.3). This indicates that T2446 was responsive to starvation conditions but is not responsive to TGF-β_1 stimulation. The S2448 site was the only site that was responsive to TGF-β_1 and was congruent with the phosphorylation of mTORC1 substrates at 3 hours. Therefore, my subsequent investigations remained focussed on the S2448 phosphorylation site.

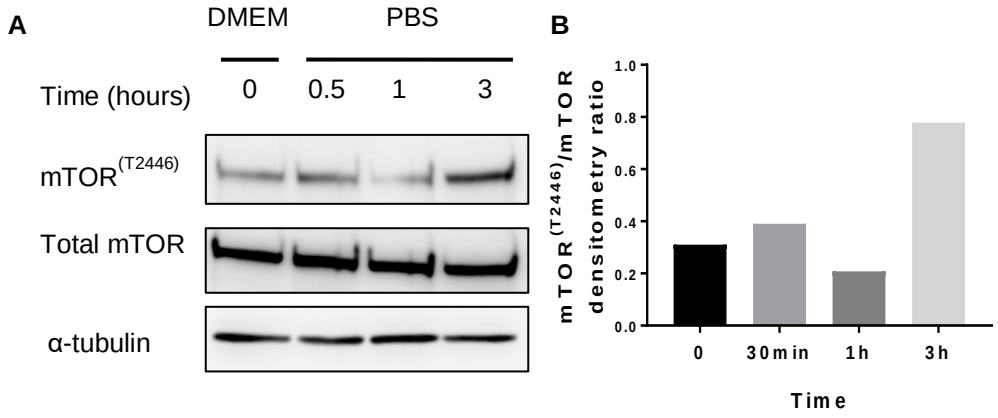

Figure 3.3: The effect of media removal and incubation with PBS on mTOR^{T2446} phosphorylation in pHLFs

pHLFs were serum-starved 24 hours prior to the media change to PBS. The phosphorylation of T2446 was assessed by Western blotting over a period of 3 hours (panel A). Protein loading was verified by blotting with an anti-α-Tubulin antibody. Densitometric analysis of T2446 phospho-protein relative to total mTOR is calculated for each time-point shown in Panel B. Data are representative of two independent experiments performed.

3.2.4. The effect of PI3K inhibition on S2448 mTOR phosphorylation

The kinases involved in TGF-β_1 induced phosphorylation of the active S2448 site which temporally coincided with the early events of mTOR substrate phosphorylation were investigated next. The difference in phosphorylation window at 3 hours between basal and TGF-β_1 stimulated conditions might not have been great enough to detect the change in phosphorylation when exposed to the pharmacological inhibitor. A time-point (6 hours) was therefore selected to ensure that temporal proximity was maintained when we know that the early activation of mTORC1 (4E-BP1 and P70S6K phosphorylation) occurs but would provide a sufficient window to detect any change in phosphorylation because of pharmacological inhibition. With this in mind, any identified mechanisms could then be explored at earlier time-points.

Previous reports have demonstrated that in response to insulin the activation of the PI3K/AKT axis leads to increased phosphorylation of the S2448 site (Reynolds et al. 2002; Navé et al. 1999). However, work within our group has demonstrated that mTOR activation and collagen synthesis occur independently of PI3K/AKT activation downstream of TGF-β_1 stimulation (Woodcock et al. 2019). This was demonstrated using the PI3K inhibitor compound 12. Therefore, it was contextually important for the phosphorylation of the S2448 residue to be independent of PI3K/AKT activity. To investigate the relationship between PI3K activation and mTOR S2448 phosphorylation, PI3K was inhibited with compound 12 which had previously been used to identify the PI3K/AKT independent mTORC1 dependent pathway (Woodcock et al. 2019).

PHLFs were incubated with either vehicle (DMSO 0.1%) or compound 12 [1 µM (0.1%DMSO)] for 1 hour prior to TGF-β_1 being spiked into the wells. After 6 hours of treatment with TGF-β_1 the cells were lysed and the S2448 phosphorylation site was interrogated to determine the effects of PI3K/AKT inhibition on S2448 phosphorylation. Figure, 3.4A shows that TGF-β_1 stimulated P70S6K phosphorylation was not inhibited by the PI3K inhibitor (compound 12), demonstrating mTORC1 activity is preserved in the presence of compound 12 and this data agrees with previously published work (Woodcock et al. 2019). Nonetheless, the demonstration that TGF-β_1 stimulated AKT phosphorylation was decreased in the presence of the inhibitor, reinforced that compound 12 was engaging its target, PI3K (Figure 3.4C). Next, the inhibition of PI3K in pHLFs did not affect TGF-β_1 stimulated S2448 phosphorylation (Figure 3.4A and B). This high-lighted that S2448, like mTORC1 acts independently of PI3K activity when stimulated with TGF-β_1. Therefore, S2448 phosphorylation may still play a role in TGF-β_1 stimulated mTORC1 activation and collagen I synthesis.

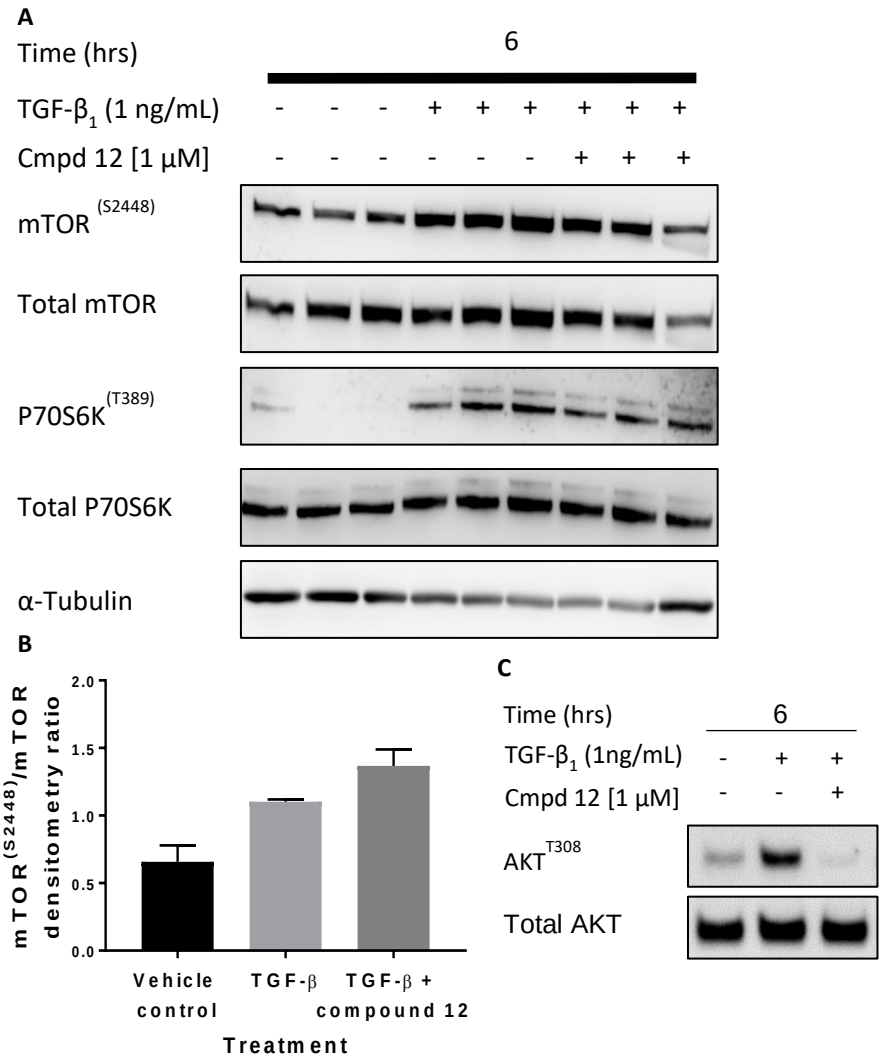

Figure 3.4: The effect on PI3K inhibition on TGF-β_1 stimulated mTOR^{S2448} phosphorylation in pHLFs

pHLFs were serum-starved prior to treatment, the cells were incubated for 1 hour with and without compound 12 (cmpd) prior to stimulation with 1ng/ml TGF- β1 for 6 hours. The mTOR S2448, P70S6K and AKT phosphorylation sites was assessed by Western blotting, panel A, panel C (AKT). Protein loading was verified by blotting with an anti-α-Tubulin antibody. Densitometric analysis of S2448 phospho-protein relative to total mTOR is calculated for each condition, panel B. These data are representative of two independent experiments performed. The replicate experiment is shown in Appendix 1

3.2.5. The effect of mTOR inhibition on S2448 mTOR phosphorylation

The phosphorylation of mTOR S2448 occurs at 3 hours and the peak of phosphorylation occurs 12 hours. In comparison between Figure 3.1 and Figure 3.2, the delay in S2448 phosphorylation compared to mTOR's substrate 4E-BP1^{S65} phosphorylation suggested that the delay in phosphorylation may

be as a result of S2448 being potentially down-stream of mTOR kinase activity. This has been previously reported in myeloma, HEK 293, MCF-7, and HeLa cells (Cirstea et al. 2014; Chiang & Abraham 2005). To examine the mechanism of mTOR S2448 site phosphorylation, I wanted to identify whether this was phosphorylated before or after mTOR kinase activation. AZD8055 is an ATP-competitive inhibitor of mTOR that is highly selective for mTOR over other PIKK family members, including the class I PI3Ks. Therefore, it does not inhibit PI3K (or AKT). This allowed for the interrogation of mTOR activity and its role in regulating the phosphorylation of the S2448 site without inhibiting the PI3K/AKT axis in pHLFs. PHLFs were treated with either vehicle (DMSO 0.1%) or AZD8055 [1 μM (0.1% DMSO)] for 1 hour prior to 6 hours of TGF-β_1. The inhibition of mTOR demonstrated that the phosphorylation of S2448 site is dependent on mTOR kinase activity at 6 hours with a decrease in phosphorylation observed back to basal levels, Figure 3.5.

The inhibition data obtained with AZD80550 confirmed that the phosphorylation of S2448 is most likely downstream of mTOR kinase activity. This could have provided an interesting mechanism by which mTOR could perhaps regulate its own activity at 3 hours and provide a mechanism for recognising its substrates. Therefore, S2448 is not required for the initial activation of mTORC1 at 3 hours.

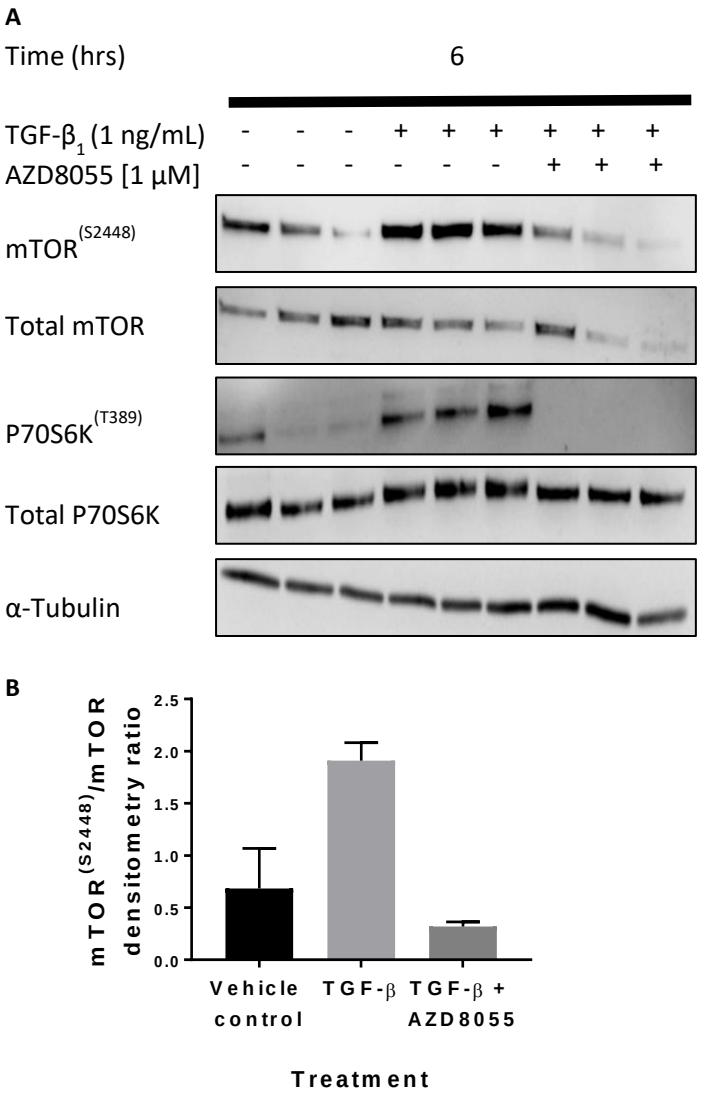

Figure 3.5: The effects of mTOR kinase activity inhibition on TGF-β_1 stimulated mTOR^{S2448} phosphorylation in pHLFs

pHLFs were serum-starved prior to treatment, the cells were incubated for 1 hour with and without compound AZD8055 prior to stimulation with 1ng/ml TGF- β1 for 6 hours. The mTOR S2448 and P70S6K phosphorylation site was assessed by Western blotting, panel A. Protein loading was verified by blotting with an anti-α-Tubulin antibody. Densitometric analysis of S2448 phospho-protein relative to total mTOR is calculated for each condition, panel B. These data are representative of two independent experiments performed. The replicate experiment are shown in Appendix 2

3.2.6. The effects of P70S6K inhibition on S2448 mTOR phosphorylation

Figure 3.5, demonstrated that S2448 phosphorylation, in response to TGF-β_1 stimulation, was downstream of mTORC1 activation and because previous evidence has shown insulin induced P70S6K activity is required for S2448

phosphorylation, it was possible that P70S6K mediates mTOR S2448 phosphorylation (Chiang & Abraham 2005). Therefore, the requirement of P70S6K to mediate the phosphorylation of the S2448 site was investigated. The P70S6K inhibitor, LY2584702, was used to interrogate this mechanism within our primary human lung fibroblasts and determine if P70S6K regulates the phosphorylation of S2448 site downstream of TGF-β_1. The potency of this compound was unknown in pHLFs. To determine an effective concentration that inhibits P70S6K the phosphorylation state of S6 was determined. S6 is directly phosphorylated by the P70S6K kinase, so a decrease in S6K phosphorylation when stimulated with TGF-β_1 and when treated with LY2584702 would indicate that P70S6K was inhibited. The pHLFS were incubated with either vehicle (DMSO 0.1%) or LY2584702 [0.1, 1 and 10 µM (0.1% DMSO)] for 1 hour prior to stimulation with TGF-β_1 for 6 hours. Figure 3.6 demonstrates that good inhibition of P70S6K is achieved with 1 and 10 µM with almost complete loss of S6 phosphorylation when compared to the TGF-β_1 treated control. The concentration of 1 µM was chosen to minimise any potential off-target effects whilst achieving good inhibition of the kinase.

Having established a working concentration of the compound, LY2584702 [1 µM] was used to investigate the effects of P70S6K inhibition on S2448 phosphorylation. Incubation of pHLFs with LY2584702 inhibited S2448 phosphorylation at 6 hours back to basal levels (Figure 3.7). In parallel P70S6K inhibition is confirmed by examining S6K phosphorylation which is also decreased by LY2584702 at 6 hours. Taking this in combination with the AZD8055 data and previous literature these indicate TGF-β_1 stimulated mTOR S2448 phosphorylation is downstream of its own activity and requires the activation of its substrate P70S6K.

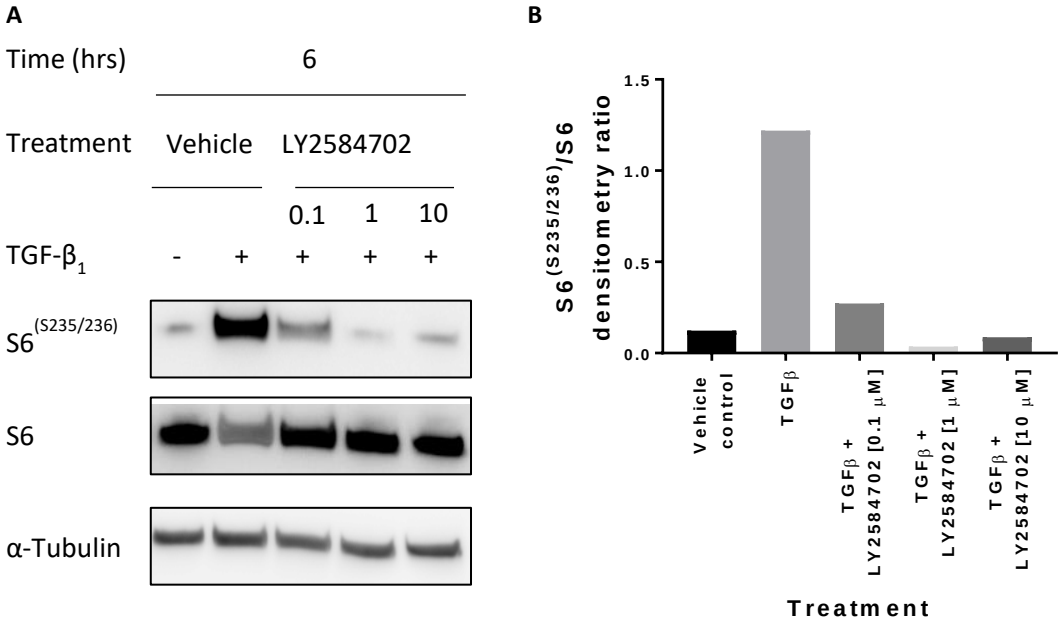

Figure 3.6: The effects of P70S6K inhibition on TGF-β_1 stimulated S6 phosphorylation in pHLFs

pHLFs were serum-starved prior to treatment, the cells were incubated for 1 hour with and without 3 concentrations of compound LY2584702 prior to stimulation with 1ng/ml TGF- β1 for 6 hours. The pS6 phosphorylation sites was assessed as a read-out for P70S6K inhibition by Western blotting, panel A. Protein loading was verified by blotting with an anti-α-Tubulin antibody. Densitometric analysis of the S2448 phospho-protein relative to total mTOR is calculated for each condition, panel B.

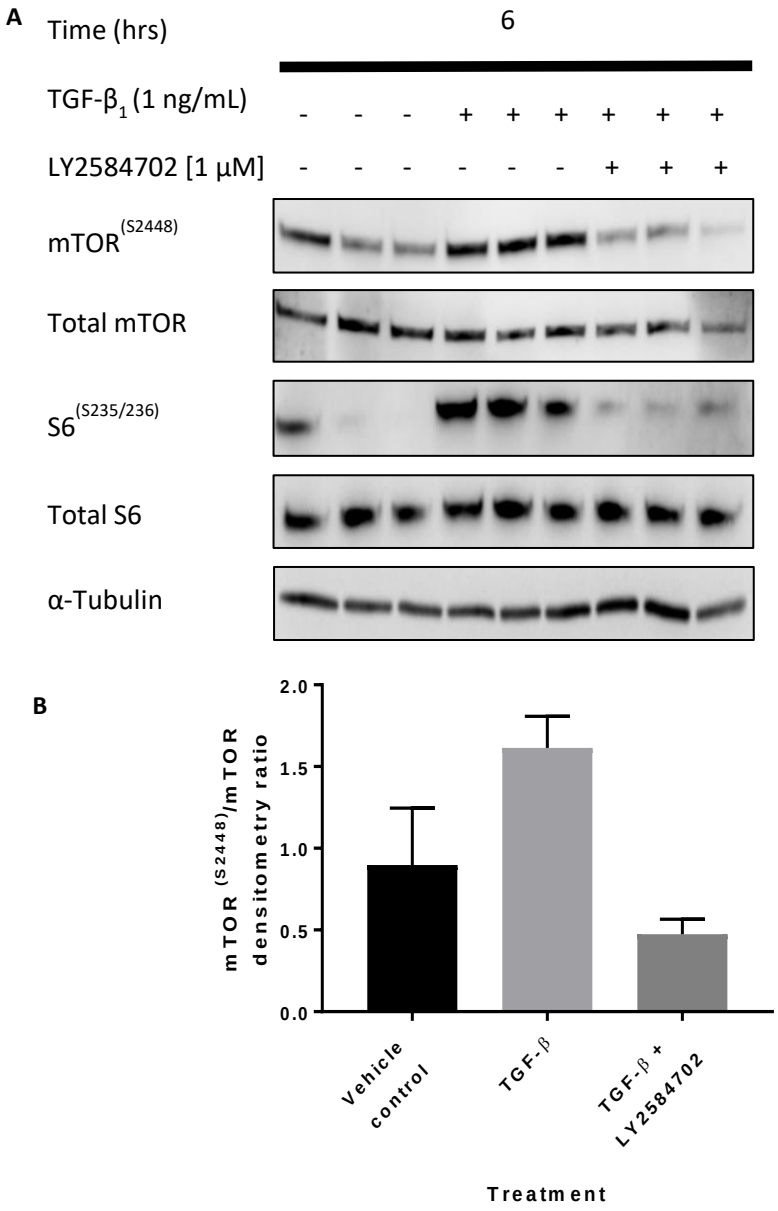

Figure 3.7: The effects of P70S6K inhibition of TGF-β_1 stimulated mTOR^{S2448} phosphorylation in pHLFs

pHLFs were serum-starved prior to treatment, the cells were incubated for 1 hour with and without compound LY2584702 prior to stimulation with 1ng/ml TGF- β1 for 6 hours. The mTOR S2448 and pS6 phosphorylation sites was assessed by Western blotting, panel A. Protein loading was verified by blotting with an anti-α-Tubulin antibody. Densitometric analysis of the S2448 phospho-protein relative to total mTOR is calculated for each condition, panel B. These data are representative of two independent experiments performed. The replicate is shown in Appendix 3

3.2.7. The effects of PDK1 inhibition of S2448 mTOR phosphorylation

The previous data highlighted that P70S6K was responsible for the mTOR S2448 phosphorylation. P70S6K is regulated by PDK1 and therefore the

requirement of PDK1 for TGF-β_1 stimulated mTOR S2448 phosphorylation was investigated. The PDK1 inhibitor, GSK2334470, inhibited the TGF-β_1 stimulated phosphorylation of P70S6K, which confirmed that PDK1 was being inhibited (Figure 3.8). Furthermore, the inhibition of PDK1 inhibited the TGF-β_1 stimulated phosphorylation of mTOR S2448 site (Figure 3.8). Work within our group has demonstrated that PDK1 does not inhibit 4E-BP1 phosphorylation suggesting that PDK1 facilitates the phosphorylation of P70S6K and mTOR S2448 phosphorylation on an alternative axis to mTOR kinase activation. This supports the notion that P70S6K is required for mTOR S2448 phosphorylation.

Other data obtained by the UCL group during the course of my PhD thesis demonstrated that the P70S6K inhibitor, LY2584702, did not inhibit collagen synthesis. In addition, the inhibition of PDK1 (which is required to stimulate P70S6K catalytic activity) did not inhibit collagen synthesis (Woodcock et al. 2019). Taken together these data suggest that mTOR S2448 phosphorylation is responsive to TGF-β_1. However, the phosphorylation of S2448 is not likely to be required for TGF-β_1 induced collagen I synthesis owing to P70S6K and PDK1's redundancy in TGF-β_1 stimulated collagen I synthesis in fibroblasts.

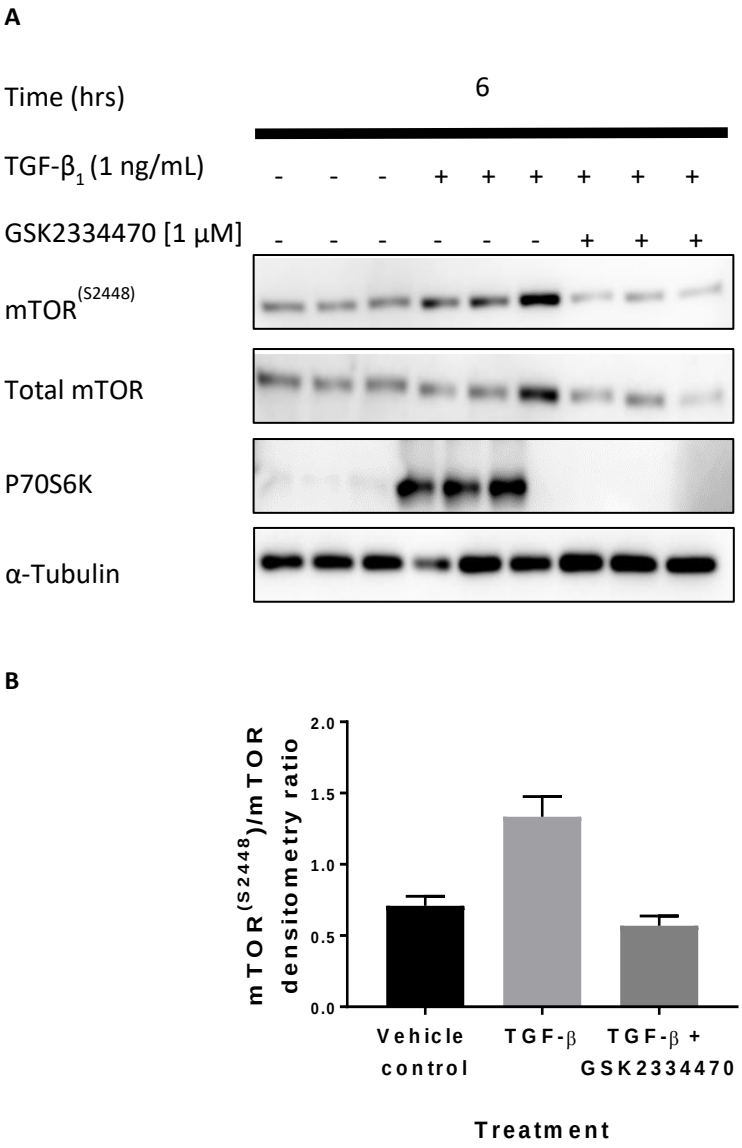

Figure 3.8: The effects of PDK1 inhibition on mTOR^{S2448} phosphorylation in pHLFs

pHLFs were serum-starved prior to treatment, the cells were incubated for 1 hour with and without compound GSK2334470 prior to stimulation with 1ng/ml TGF- β1 for 6 hours. The mTOR S2448 phosphorylation site was assessed by Western blotting, panel A. Protein loading was verified by blotting with an anti-α-Tubulin antibody. Densitometric analysis of phospho-protein relative to total mTOR is calculated for each condition, panel B. These data are representative of two independent experiments performed.

3.2.8. Summary

- All three phosphorylation sites exhibit basal levels of phosphorylation in pHLFs.

- T2446 phosphorylation is insensitive to TGF-β_1 treatment over a 24 hour period.
- S2448 and S2481 phosphorylation sites are responsive to TGF-β_1 treatment.
- S2448 phosphorylation correlates with downstream mTOR substrate phosphorylation.
- The phosphorylation of S2448 is independent of TGF-β_1 stimulated PI3K activation.
- P70S6K phosphorylation activation down-stream of TGF-β_1 activated mTOR and PDK1 is required for S2448 phosphorylation.

3.3. The role of SMAD signalling in mTORC1 activation

The role of SMAD signalling in TGF-β stimulated cells is well established for gene transcription of the collagen genes (Verrecchia et al. 2001). SMAD 3 is directly phosphorylated by TβRI which allows it to form a complex with SMAD4 and translocate to the nucleus to initiate gene transcription. There is now evidence emerging that SMAD 3 can regulate the activation of the mTORC1 complex in fibroblasts (Lampa et al. 2017; Bernard et al. 2017; Peterson et al. 2009). This series of studies aims to define the role of TGF-β_1 stimulated SMAD 3 signalling in pHLFs and to examine how this affects early mTORC1 signalling and downstream collagen I response.

3.3.1. Characterisation of the collagen deposition assay

In the following sections, an immunofluorescence based technique was employed to quantify collagen levels between conditions. The assay is termed the ‘collagen deposition assay’ or ‘Scar-in-a-jar’ and was originally developed by Chen and colleagues, 2009, and has been further optimized and validated within our group to interrogate TGF-β_1 stimulated collagen I stimulation in pHLFs.

The collagen deposition assay is well suited to demonstrate the sensitivity of pHLFs to TGF-β_1 stimulation and, unlike other assays, allows the timely conversion of pro-collagen into collagen. Therefore, the cells can be fixed after only 48 hours of incubation with TGF-β_1. Stimulation with increasing concentrations of TGF-β_1 leads to a concentration-dependent increase in collagen I deposition which is quantified by high-content imaging of collagen I immunofluorescence (Figure 3.9). The EC50 was approximately 0.5 - 0.6 ng/mL with the peak of collagen synthesis found to be achieved at 1 ng/mL TGF-β_1 in agreement with previous data from our laboratory (Woodcock et al. 2019; Mercer et al. 2016).

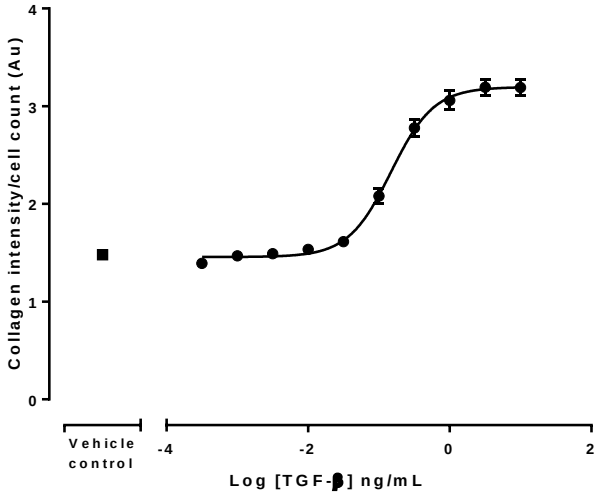

Figure 3.9: The concentration reposnse of TGF-β$_1$ on collagen 1 deposition in pHLFs

Confluent pHLFs were starved for 24 hours before being stimulated with increasing concentrations of TGF-β (1pg/ml to 30ng/ml) in DMEM containing Ficoll for 48 hours, prior to fixation and staining for type1 collagen. The individual fluorescent intensity is normalised over cell count (DAPI) per read (n=4 reads per well) and the average of the normalised replicates (n=4) was plotted. The data is plotted as arbitrary units (Au) The data is expressed as the mean (± SEM of n=4 replicate wells per condition). This is representative of two independent experiments.

In addition to being able to detect the increase in collagen deposition in response to TGF-β$_1$ the assay is also well-suited for the interrogation of the impact of inhibitors and siRNA. The TβRI receptor mediates several downstream pathways in response to the exogenous TGF-β$_1$ stimulus. These pathways, in particular SMAD and mTORC1, signal for the synthesis of collagen I. Previous reports demonstrate that by inhibiting the TβRI receptor, cells stimulated with TGF-β$_1$ are unable synthesise collagen I (Bonniaud et al. 2005). Therefore, the collagen deposition assay should be able to recapitulate these previous results by treating pHLFs with the TβRI inhibitor, SB525334. PHLFS were treated with ten concentrations of SB525334 to inhibit the TGF-β$_1$ stimulated collagen I deposition. SB525334 inhibits collagen I synthesis in a concentration-dependent manner with an IC50 of 0.17 μM (Figure 3.10A). There was no effect of the inhibitor on cell count (Figure 3.10B). This confirms a role of the TGF-β$_1$ receptor in our pHLFs and further that this assay is robust enough to investigate the effects of compounds on TGF-β$_1$ stimulation of collagen I synthesis.

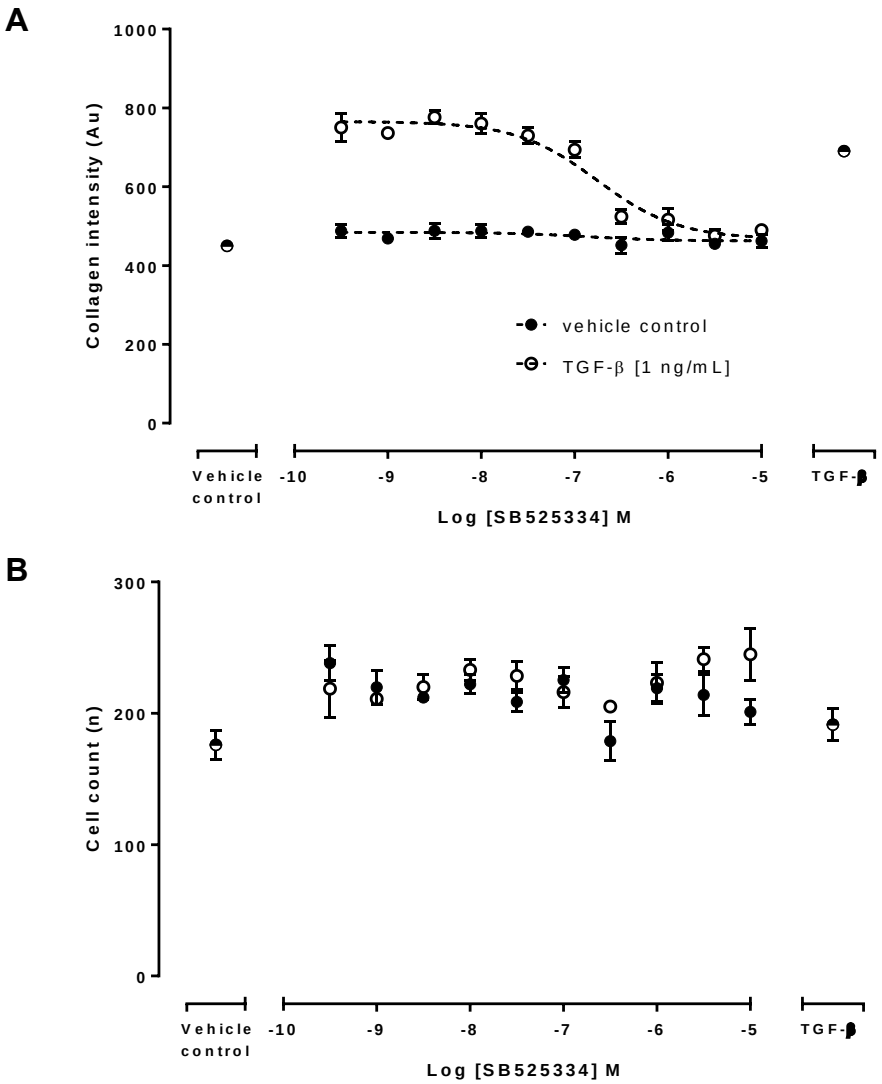

Figure 3.10: The concentration response of TβRI inhibition on TGF-β_1 stimulated collagen I synthesis

Confluent pHLFs were starved for 24 hours before being incubated with increasing concentrations of SB525334 (vehicle controls were incubated with 0.1% DMSO) in DMEM containing Ficoll for 1 hour. Following incubation cells were treated with or without TGF-β_1 [1 ng/mL] which was spiked into the wells and incubated for 48 hours, prior to fixation and staining for type1 collagen, Panel A. Cell counts were obtained from a DAPI counter stain, Panel B. Data are expressed as mean fluorescent intensity (n=4 reads per well) averaged across 4 replicates. IC_{50} values were calculated using a three-parameter non-linear regression. This is representative of two independent experiments.

Finally, the collagen deposition assay was tested for its suitability for investigating siRNA treatment and its effects on TGF-β_1 stimulated collagen I synthesis. To demonstrate this assay is suitable for siRNA treatment, a protein that we have established as a regulator of collagen down-stream of mTORC1 was investigated. ATF4 regulates collagen synthesis by upregulating the

proteins required for the conversion of glucose to glycine, and it is glycine that makes up one third of the collagen molecule (Selvarajah et al. 2019). pHLFs were treated with ATF4 siRNA [10 nM] for 48 hours followed by stimulation with TGF-β_1 [1 ng/mL] for 48 hours. Collagen deposition was quantified by high content imaging of collagen I immunofluorescence. The siCTRL treated cells demonstrated an approximate 2-fold increase in collagen I deposition (Figure 3.11). The knock-down of ATF4 inhibited TGF-β_1 stimulated collagen I deposition. This also confirmed knock-down proteins in a 96 well format can be achieved and utilised for interrogating the effects of further protein knock-down in the collagen deposition assay.

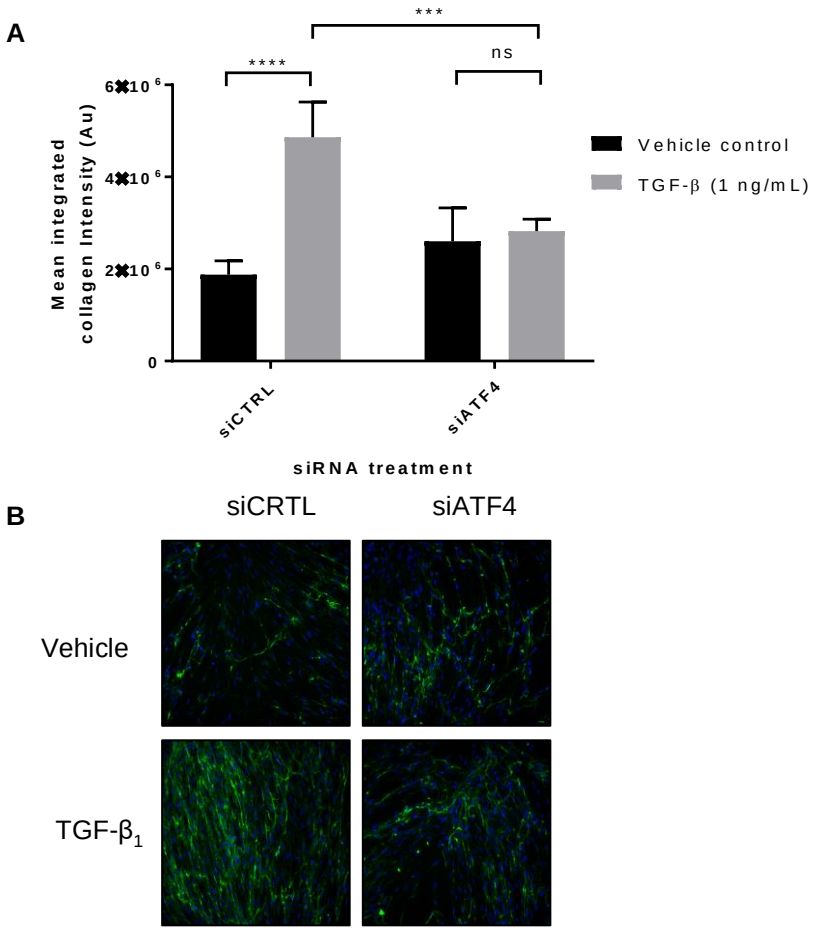

Figure 3.11: The effect of ATF4 knock-down on TGF-β_1 stimulated collagen I protein deposition in pHLFs

At 60-80% confluence pHLFs were transfected with ATF4 siRNA or control siRNA for 24 hours prior to starvation with 0% DMEM. Cells were starved for 24 hours in 0% DMEM. After starvation cells were incubated with DMEM containing Ficoll for 1 hour. Following incubation cells were treated with or without TGF-β_1 [1 ng/mL] which was spiked into the wells and incubated for 48 hours, prior to fixation and staining for type1 collagen, Panel A. The individual fluorescent intensity is normalised over cell count (DAPI) per read (n=4 reads per well) and the average of the normalised replicates (n=4) was plotted. The data is expressed as the mean (± SEM of n=4 replicate wells per condition). This is representative of two independent experiments. Panel B shows representative images from each condition.

3.3.2. A comparison of the effects of AZD8055 and Rapamycin on 4E-BP1 phosphorylation sites

TGF-β_1 stimulated collagen synthesis is mediated through 4E-BP1 which controls the translation of an unknown protein that is required for collagen I synthesis (Woodcock et al. 2019). 4E-BP1 is a repressor of translation, 4E-BP1 mediates its inhibition by preventing the formation of the translation initiation complex on mRNA. For complete inhibition of 4E-BP1, each of its phosphorylation sites are phosphorylated in a sequential manner starting with T37/T46, followed by T70 and then S65 (Gingras, Raught, Gygi, et al. 2001). For full inhibition of 4E-BP1 all three sites must be phosphorylated. Subsequently, with only partial inhibition of mTORC1, the remaining activity is still able to phosphorylate T37/T46 on 4E-BP1 to promote some translation. This can be seen when comparing the two inhibitors, rapamycin and AZD8055. AZD8055 is a highly selective ATP-competitive mTOR inhibitor, whereas rapamycin is an allosteric inhibitor of mTORC1 by binding to the FRB domain. This is believed to disrupt RAPTOR binding to 4E-BP1 and P70S6K and prevents mTORC1 from being able to phosphorylate P70S6K and the S65 phosphorylation site on 4EBP1. Other data obtained by the group during the course of my PhD demonstrated that AZD8055 inhibits collagen I synthesis in pHLFs whereas rapamycin treatment does not (Woodcock et al. 2019). This was demonstrated by the ability of AZD8055 to inhibit all of the 4E-BP1 phosphorylation sites and not just partially inhibit the S65 and T70 sites. I recapitulated this work and focussed my investigation at 3 hours. This represents the initial TGF-β_1 induced mTORC1 activation time point. Furthermore, this is also the time point when SMAD 3 phosphorylation decreases from its peak. I first characterised the effect of AZD8055 and Rapamycin on TGF-β_1 stimulated 4E-BP1 phosphorylation at the three sites: 4E-BP1$^{T37/46}$, 4E-BP1^{S65} and 4E-BP1^{70}. This data built a profile of the 4EBP1 phosphorylation states in response to two compounds, one that inhibits collagen (AZD8055) and one that does not (Rapamycin) (Woodcock et al. 2019). In addition, the phosphorylation states between the two compounds is a useful guide when investigating the effects of other pharmacological tools, siRNA or CRISPR.

PHLFs were incubated with and without either compound (AZD8055 or rapamycin) for 1 hour prior to TGF-β_1 treatment. AZD8055 was used at 1 μM and rapamycin 100 nM according to their previously characterised inhibitory concentrations in pHLFs (Woodcock et al. 2019). Treatment with TGF-β_1 stimulates an increase in 4E-BP1^{S65} and prevents the phosphorylation of 4E-BP1^{T70} (Figure 3.12 A and Figure 3.13A). Treatment of pHLFs with AZD8055 inhibits the phosphorylation of the three 4E-BP1 sites under basal and TGF-β_1 treated conditions (Figure 3.12A). The densitometry confirms the decrease in the phosphorylation of 4EBP1$^{T37/T46}$, 4EBP1^{S65} and 4EBP1^{T70} (Figure 3.12 B, C and D). In contrast, Rapamycin inhibits TGF-β_1 stimulated 4EBP1^{S65} and 4EBP1^{T70} phosphorylation. Moreover, it had no impact on the basal levels of 4EBP1 phosphorylation suggesting only partial inhibition of the mTORC1 complex (Figure 3.13). The densitometry confirms that there is a decrease in the phosphorylation of 4EBP1^{S65}, however, it did not change the phosphorylation states of either 4EBP1$^{T37/T46}$ or 4EBP1^{T70} (Figure 3.13 B, C and D). TGF-β_1 increased the expression of total 4E-BP1 levels and this was inhibited by treatment with either AZD80550 or Rapamycin (Figure 3.12E and Figure 3.13E). In particular, this shows that full inhibition of mTORC1 is required to prevent the phosphorylation of 4E-BP1 completely at all sites.

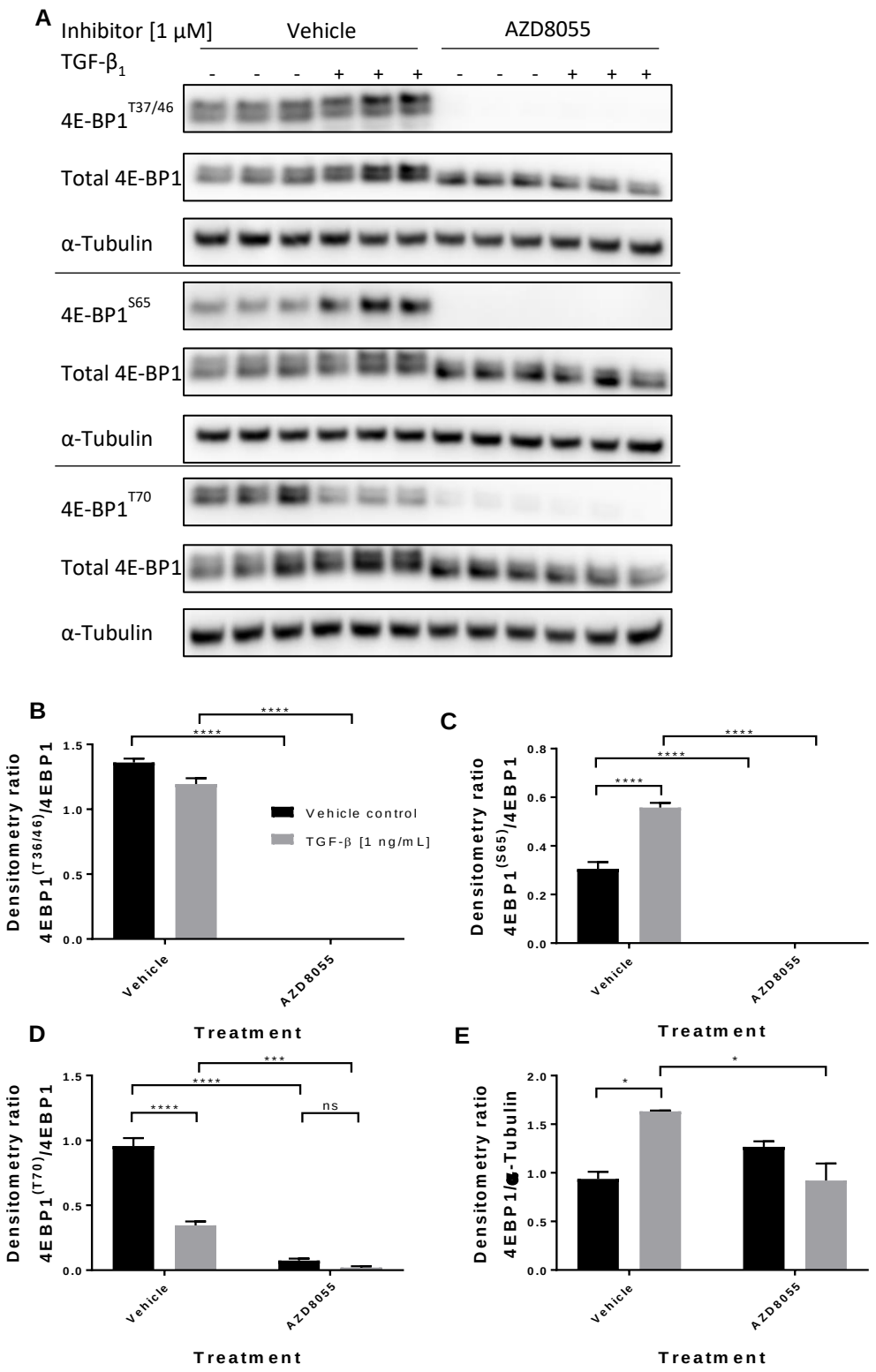

Figure 3.12: The effect of AZD8055 on TGF-β1 stimulated 4E-BP1 phosphorylation in pHLFs

Confluent pHLFs were serum-starved prior for 24 hours prior to incubation with AZD8055 for 1 hours followed by stimulation with 1 ng/mL TGF-β_1 for 3 hours. The phosphorylation of 4E-BP1$^{37/46}$, 4E-BP1^{S65} and 4E-BP1^{T70} were assessed by western blotting, Panel A. Protein loading was verified by blotting with anti- α-tubulin antibody. The densitometry (panels B-E) was calculated and plotted as a phospho-protein to total protein ratio. The data is representative of two independent experiments performed

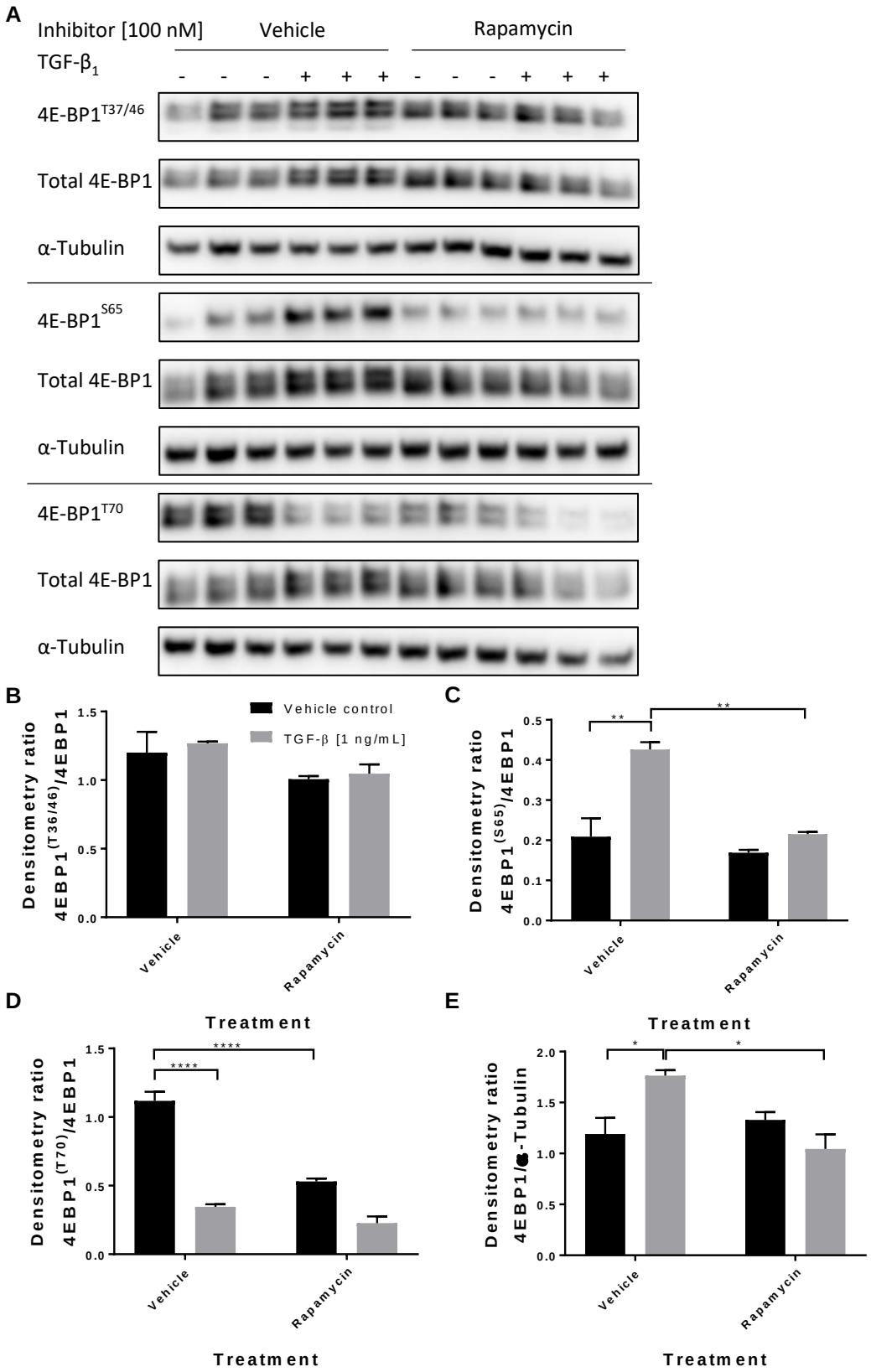

Figure 3.13: The effect of Rapamycin on TGF-β_1 stimulated 4E-BP1 phosphorylation in pHLFs

Confluent pHLFs were serum-starved prior for 24 hours prior to incubation with Rapamycin for 1 hours followed by stimulation with 1 ng/mL TGF-β_1 for 3 hours. The phosphorylation of 4E-BP1$^{37/46}$, 4E-BP1^{S65} and 4E-BP1^{T70} were assessed by western blotting, Panel A. Protein loading was verified by blotting with anti- α-tubulin antibody. The densitometry (panels B-E) was calculated and plotted as a phospho-protein to total protein ratio. These data are representative of two independent experiments performed

3.3.3. Characterising SMAD 3 knock-down in pHLFs

There are two receptor SMAD (SMAD 2 and SMAD 3) that are directly phosphorylated by the TβRI upon TGF-β_1 stimulation. The TβRI/TβRII receptor phosphorylates the SMAD homodimer. The phosphorylation at their C-terminus promotes SMAD 2 or SMAD 3 binding to the co-SMAD SMAD 4 which promotes translocation into the nucleus followed by gene transcription. Specifically, SMAD 3 can recognise several collagen gene promoters due to the CAGA repeats in this domain (Verrecchia et al. 2001). Therefore, SMAD 3 is important in IPF due to its role in facilitating collagen mRNA transcription (Zhao & Geverd 2002; Verrecchia et al. 2001). To start, SMAD 3 was assessed to identify if it was responsible for regulating collagen mRNA levels in pHLFs, since there may be differential responses between cell lines. The role of SMAD 3 was investigated by using siRNA to knock-down SMAD 3.

Knock-down of SMAD 3 was assessed by RT-qPCR at 24 hours, the time-point at which the *COL1A1* mRNA level is are at its peak (Woodcock et al. 2019). It was confirmed that treatment with SMAD 3 siRNA [10 nM] was sufficient to decrease SMAD 3 mRNA by approximately 70% (Figure 3.14A). In addition, TGF-β_1 regulates SMAD 3 mRNA levels at 24 hours post-treatment, independent of siRNA treatment. This observation was confirmed and translated at the protein level (Figure 3.14B) suggesting that TGF-β_1 potentially regulates SMAD 3 signalling in the cell by promoting the degradation of SMAD 3 mRNA. Taken together, this confirmed that SMAD 3 could be knocked-down in pHLFs.

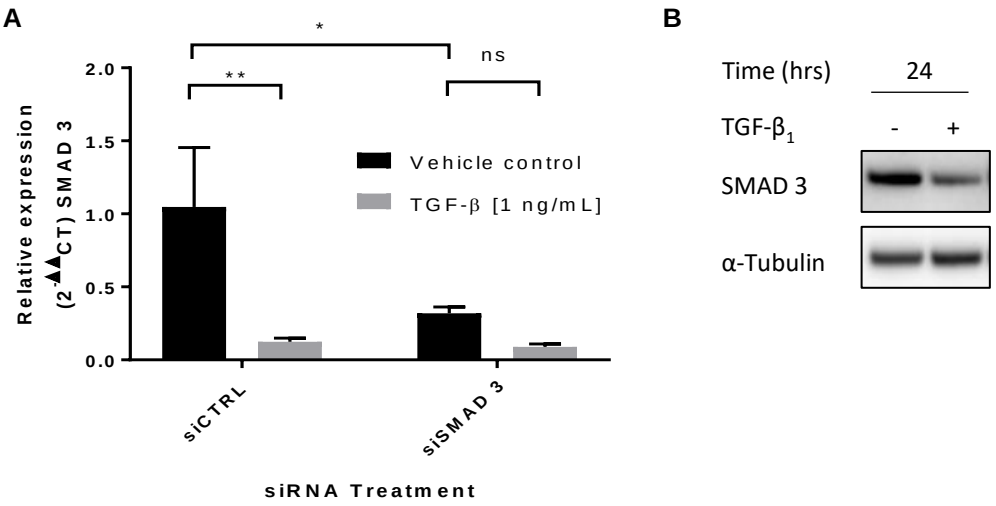

Figure 3.14: The effect of SMAD 3 knock-down on SMAD 3 mRNA levels

At 60-80% confluence pHLFs were transfected with SMAD 3 siRNA for 24 hours prior to starvation with 0% DMEM. Cells were starved for 24 hours prior to treatment with or without 1 ng/mL TGF-β_1. The cells were harvested 24 hours post stimulation. The lysates were assessed by rt-qPCR. Data are shown as gene expression of COL1A1 expression relative to the geometric mean of two housekeeping genes (mean ± SEM, n=3 replicates). This data is representative of two independent experiments performed. Differences between groups were evaluated with two-way ANOVA and Tukey multiple comparison testing. Panel B, after 24 hours of TGF-β_1 stimulation SMAD 3 total protein levels were assessed by western blot

To establish if the 70% SMAD 3 knock-down achieved with siRNA treatment was sufficient to have a functional impact on the collagen mRNA (*COL1A1*) levels the effect of the SMAD 3 siRNA was assessed, since this link has been reported on previously (Zhao & Geverd 2002; Verrecchia et al. 2001). The mRNA levels of the *COL1A1* were assessed by RT-qPCR. Treatment of TGF-β_1 increases *COL1A1* mRNA levels by approximately 6-fold in pHLFs. This increase is significantly reduced in the presence of SMAD 3 siRNA (Figure 3.15).

The depletion of the SMAD 3 protein in pHLFs inhibits the TGF-β_1 stimulated increase in *COL1A1* mRNA levels. Therefore, the effects of SMAD 3 mRNA inhibition was likely to decrease the collagen I protein levels. As previously demonstrated for ATF4 (Figure 3.11), the collagen deposition assay was capable of quantifying the effects of siRNA on collagen deposition and therefore this assay was used to investigate the effects of SMAD 3 knock-down on collagen I synthesis. The effects of siRNA knock-down completely inhibits TGF-β_1 induced collagen deposition (Figure 3.16). Taken together, this data confirms SMAD 3 is required for TGF-β_1 stimulated collagen I synthesis.

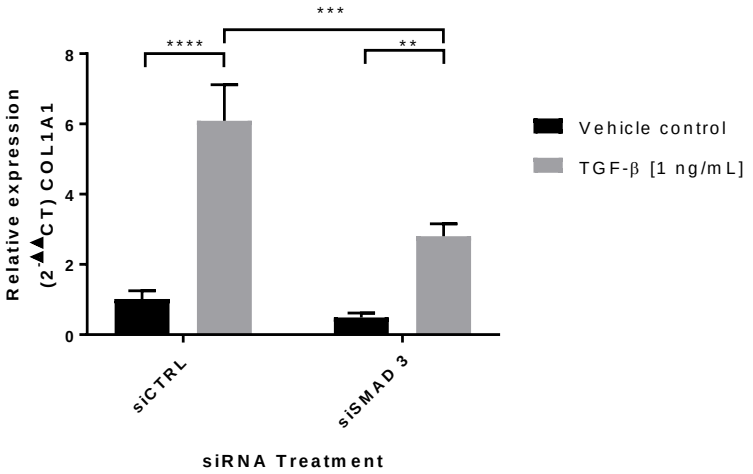

Figure 3.15: The effect of SMAD 3 knock-down on TGF-β_1 stimulated *COL1A1* gene expression and collagen I synthesis in pHLFs

At 60-80% confluence pHLFs were transfected with SMAD 3 siRNA for 24 hours prior to starvation with 0% DMEM. Cells were starved for 24 hours prior to treatment with or without 1 ng/mL TGF-β_1. The cells were harvested 24 hours post stimulation. The lysates were assessed by rt-qPCR. Data are shown as gene expression of COL1A1 expression relative to the geometric mean of two housekeeping genes (mean ± SEM, n=3 replicates). These data are representative of two independent experiments performed. Differences between groups were evaluated with two-way ANOVA and Tukey multiple comparison testing. Panel B, after 24 hours of TGF-β_1 stimulation SMAD 3 total protein levels were assessed by western blot

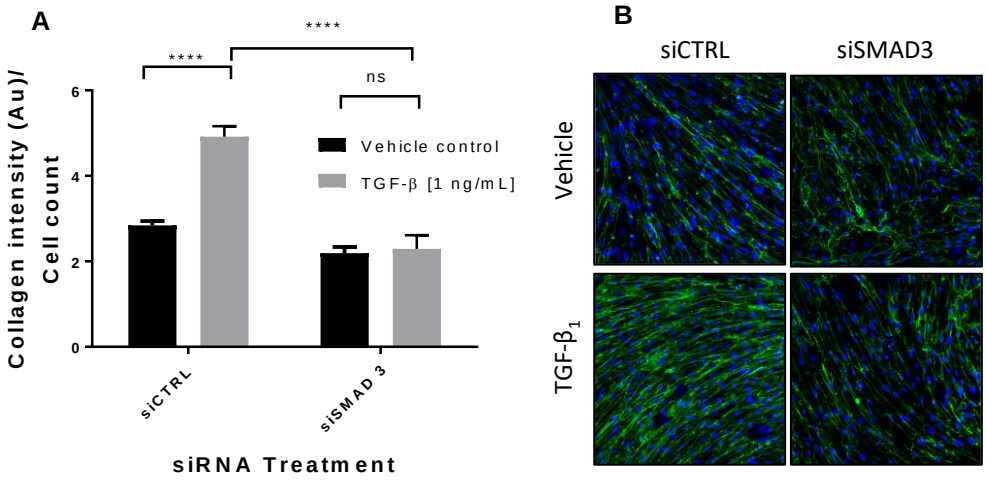

Figure 3.16: The effect of SMAD 3 knock-down on TGF-β_1 stimulated collagen I synthesis in pHLFs

At 60-80% confluence pHLFs were transfected with SMAD 3 siRNA or control siRNA for 24 hours prior to starvation with 0% DMEM. Cells were starved for 24 hours prior to treatment. After starvation cells were incubated with DMEM containing Ficoll for 1 hour. Following incubation cells were treated with or without TGF-β_1 [1 ng/mL] which was spiked into the wells and incubated for 48 hours, prior to fixation and staining for type1 collagen, Panel A. The individual fluorescent intensity is normalised over cell count (DAPI) per read (n=4 reads per well) and the average of the normalised replicates (n=4) was plotted. These data are expressed as the mean (± SEM of n=4 replicate wells per condition). These data are representative of two independent experiments. Panel B shows representative images from each condition.

3.3.4. The effect of SMAD 3 knock-down on 4E-BP1 phosphorylation

The effect of SMAD 3 knock-down was sufficient to deplete the TGF-β_1 stimulated COL1A1 mRNA levels and collagen protein deposition. Recent reports have suggested that SMAD 3 knock-down also impacts on mTORC1 activity (Das et al. 2013; Lampa et al. 2017; Bernard et al. 2017; Peterson et al. 2009). Therefore, to establish whether SMAD 3 also regulates mTORC1 activation in response to TGF-β1 in pHLFs, the mTORC1 substrate 4E-BP1 was used as a measure of mTORC1 catalytic activity by blotting for the 4E-BP1 phosphorylation sites (as described above, Figure 3.12 and Figure 3.13).

Treatment of pHLFS with SMAD 3 siRNA [10 nM] demonstrated that protein levels were decreased at three hours. The densitometry readings calculated from the western blots demonstrate 87% of the protein was knocked-down compared to the control siRNA treated pHLFs (Figure 3.17A and E). The 87% knock-down is also similar to that quantified by the RT-qPCR (Figure 3.15) showing that there is consistency between techniques. 4E-BP1$^{T37/46}$ phosphorylation was investigated. The siCTRL had no effects on the 4E-BP1$^{T37/46}$ in vehicle or TGF-β_1 treated pHLFs (Figure 3.17A and B). In the SMAD 3 siRNA treated pHLFs, the knock-down demonstrated a decrease in 4E-BP1$^{T37/46}$ phosphorylation in basal and TGF-β_1 treated conditions. This suggests that SMAD 3 may be required under basal conditions to maintain the phosphorylation of this site. However, because the phosphorylation was not completely lost, when compared with the treatment with AZD8055 (Figure 3.12), more than one protein may be required for mTORC1 activation or the remaining 13% of the SMAD 3 protein is sufficient to maintain mTORC1 activity and subsequently 4E-BP1$^{T37/46}$ phosphorylation. The second site investigated was the 4E-BP1^{S65}. Treatment with TGF-β_1 induced the phosphorylation of 4E-BP1^{S65} in control pHLFs. 4E-BP1^{S65} phosphorylation was present at basal levels and treatment with SMAD 3 siRNA inhibited both baseline and TGF-β_1 stimulated 4E-BP1^{S65} phosphorylation (Figure 3.17A and C). TGF-β_1 prevented the increase in 4E-BP1^{T70} phosphorylation which is higher in non-TGF-β_1 stimulated pHLFs. Treatment with SMAD 3 siRNA abrogated this decrease in phosphorylation (Figure 3.17A and D). However, the baseline increase was only minimal and significance was not achieved. In

addition, it was demonstrated that TGF-β_1 at three hours causes an increase in the total levels of 4E-BP1 protein which was inhibited by SMAD 3 knock-down. Therefore, this evidence suggests that TGF-β_1 regulates SMAD 3 activation to regulate the transcription of 4E-BP1 (Figure 3.17A and F). Taken together, SMAD 3 regulates all three sites on 4E-BP1, however, all in a TGF-β_1 independent manner with the exception of the 4E-BP1^{T70}.

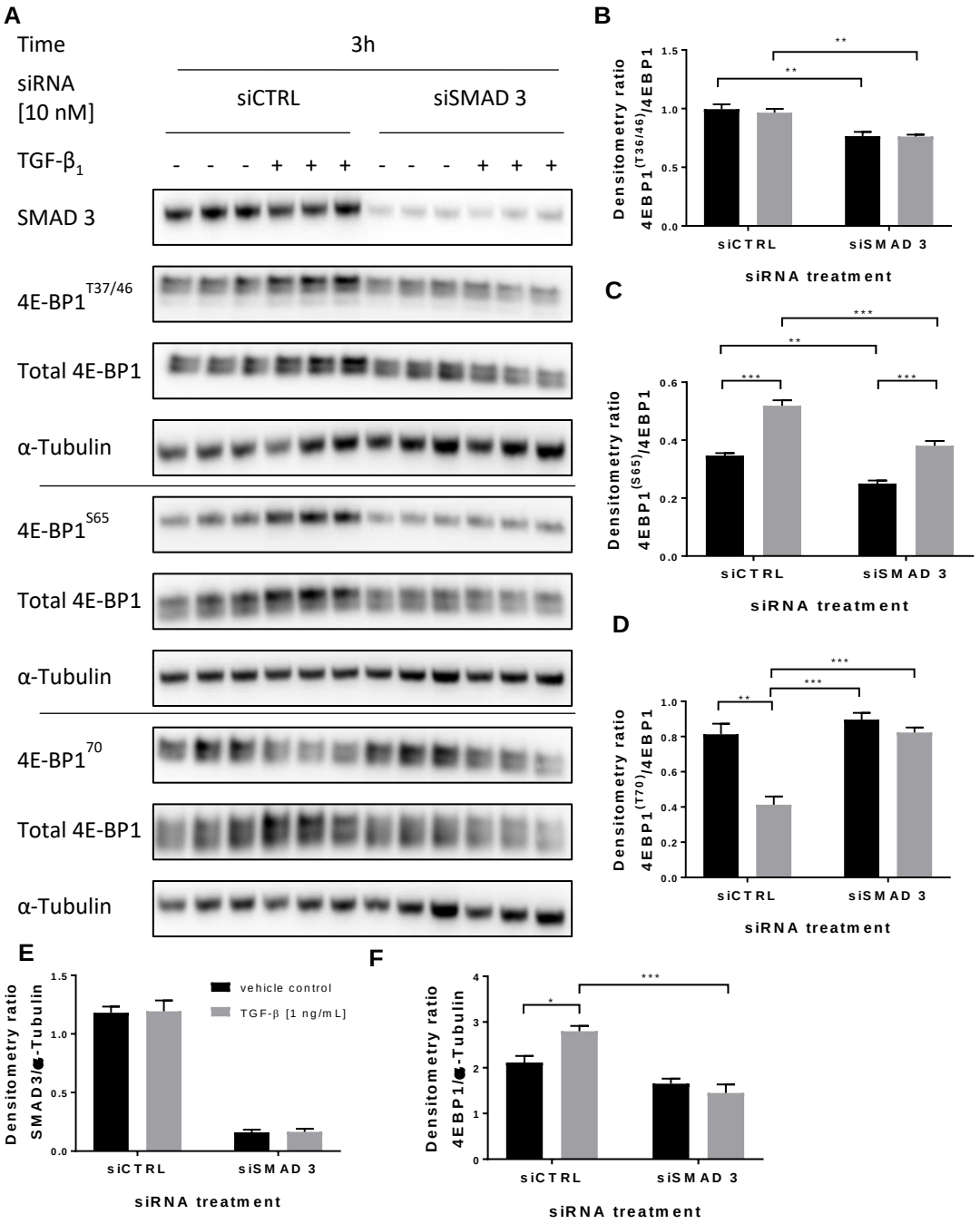

Figure 3.17: The effect of SMAD 3 knock-down on TGF-β_1 stimulated 4E-BP1 phosphorylation in pHLFs

At 60-80% confluence pHLFs were transfected with SMAD 3 siRNA for 24 hours prior to starvation with 0% DMEM. Cells were starved for 24 hours prior to treatment with or without 1 ng/mL TGF-β_1. The cells were harvested 3 hours post stimulation. The lysates were assessed by either western blotting investigating four 4E-BP1 phosphorylation sites. Protein loading was verified by blotting with an anti-α-Tubulin antibody. Densitometric analysis (panels B-F) of phosphor/protein relative to total protein or SMAD 3 total to α-Tubulin is calculated for each condition (n=3 replicates). These data are representative of two independent experiments performed. Differences between groups were evaluated with two-way ANOVA and Tukey multiple comparison testing. The replicate is shown in Appendix 4.

3.3.5. The effect of actinomycin D on TGF-β_1 stimulated mTORC1 activation

The previous evidence demonstrated that SMAD 3 was capable of regulating mTORC1 activity, however, the mechanism involved is unknown. It is possible that SMAD 3 binds to mTORC1 through an unknown mechanism to promote a conformational change to the mTORC1 structure allowing mTORC1 to bind and phosphorylate its downstream targets. However, because SMAD 3 is a transcription factor, it is more likely that it regulates mTORC1 via the transcription of a protein. To identify if SMAD 3 was transcribing a protein to regulate mTORC1 phosphorylation, 4E-BP1^{S65} was used as a measure of mTORC1 activity because this was the site most inhibited by SMAD 3 knock-down and it is a site that is highly regulated by TGF-β_1. Actinomycin D is capable of inhibiting transcription by preventing RNA chain elongation and so was used to interrogate the effect of transcription inhibition on TGF-β_1 stimulated mTORC1 activation. The first experiment was conducted to investigate if treatment of pHLFS with actinomycin D [100 nM] inhibits TGF-β_1 stimulated SMAD 3 phosphorylation, since this has been demonstrated to directly impact on mTORC1 activity. This was feasible since feedback pathways exist to inhibit SMAD 3 if transcription prevented. The effect of actinomycin D caused a small decrease in SMAD 3 phosphorylation (Figure 3.18A). However, this was not a significant decrease when analysed by the densitometry (Figure 3.18B). In addition, the treatment does not impact on the total levels of the SMAD 3 protein. Actinomycin D inhibited TGF-β_1 stimulated 4E-BP1^{S65} phosphorylation (Figure 3.18 A and D). Treatment with actinomycin D inhibited the TGF-β_1 stimulated increase in total 4E-BP1. This data suggests that the inhibition of transcription is capable of regulating TGF-β_1 stimulated mTORC1 activation. Taken together with the SMAD 3 knock-down data, this supports the notion that SMAD 3 is regulating a protein that is required for TGF-β_1 to activate mTORC1 to allow it to phosphorylate 4E-BP1.

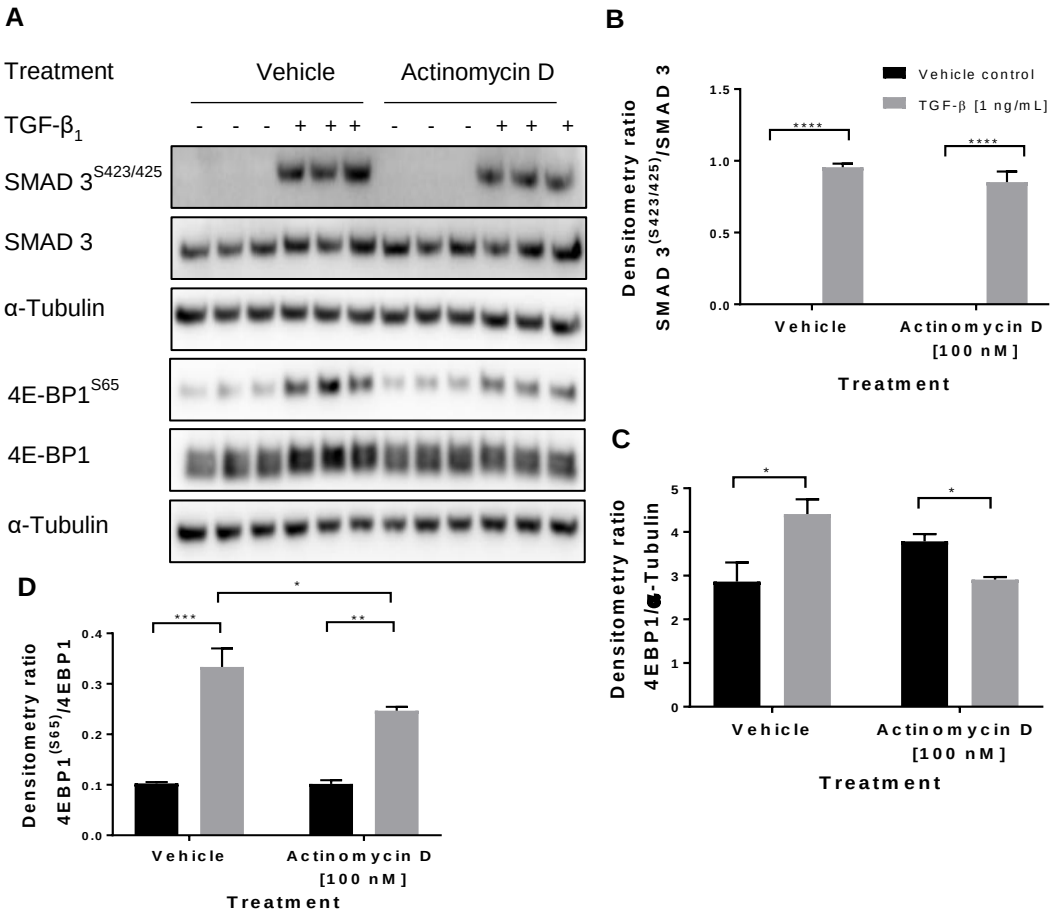

Figure 3.18: The effect of Actinomycin D on TGF-β_1 signalling in pHLFs

Confluent pHLFs were serum-starved prior for 24 hours prior to incubation with Actinomycin D for 1 hours followed by stimulation with 1 ng/mL TGF-β_1 for 3 hours. The phosphorylation of 4E-BP1$^{T37/46}$, 4E-BP1^{S65} and 4E-BP1^{T70} were assessed by western blotting. Protein loading was verified by blotting with anti- α-tubulin antibody. The densitometry (panels B-D) was calculated and plotted as a phospho-protein to total protein ratio. These data are representative of two independent experiments performed. See Appendix 5 for repeat

3.3.6. The effects of GLS inhibition on TGF-β_1 stimulated mTORC1 activation

The experiment utilising the inhibitor of transcription, actinomycin D, demonstrated that SMAD 3 may regulate mTORC1 through a transcriptionally regulated protein. There are currently two known proteins, Glutaminase (GLS) and DEPTOR that are regulated by SMAD 3 and have been shown to regulate mTORC1 (Bernard et al. 2017; Peterson et al. 2009; Das et al. 2013).

Glutaminase is an enzyme required for the conversion of glutamine to glutamate and this subsequently is used in the synthesis α-Ketoglutarate. Recent evidence demonstrates that α-Ketoglutarate is required for mTORC1 activition in pHLFs (Lampa et al. 2017). Furthermore, SMAD 3 was demonstrated to regulate GLS (Bernard et al. 2017). Therefore, there was a potential pathway where TGF-β_1 activates GLS to regulate mTORC1 activation. The effects of GLS inhibition on 4E-BP1 phosphorylation were investigated by western blot. The concentration of CB-839, a GLS inhibitor, was previously optimised within our group when investigating its effects on collagen I synthesis. PHLFs were incubated with CB-839 [1 μM] for 1 hour prior to TGF-β_1 treatment. Cells were lysed at three hours post-stimulation with TGF-β_1. Treatment with CB-839 did not inhibit the TGF-β_1 sensitive sites 4E-BP1^{S65} or 4E-BP1^{T70} (Figure 3.19A, C and D). The treatment visually did not have an effect on the 4E-BP1$^{T37/46}$ but the densitometry suggests a small decrease in phosphorylation (Figure 3.19B). Since the compound CB-839 did not change the TGF-β_1 responsive sites, next DEPTOR, another SMAD 3 regulated protein, was investigated.

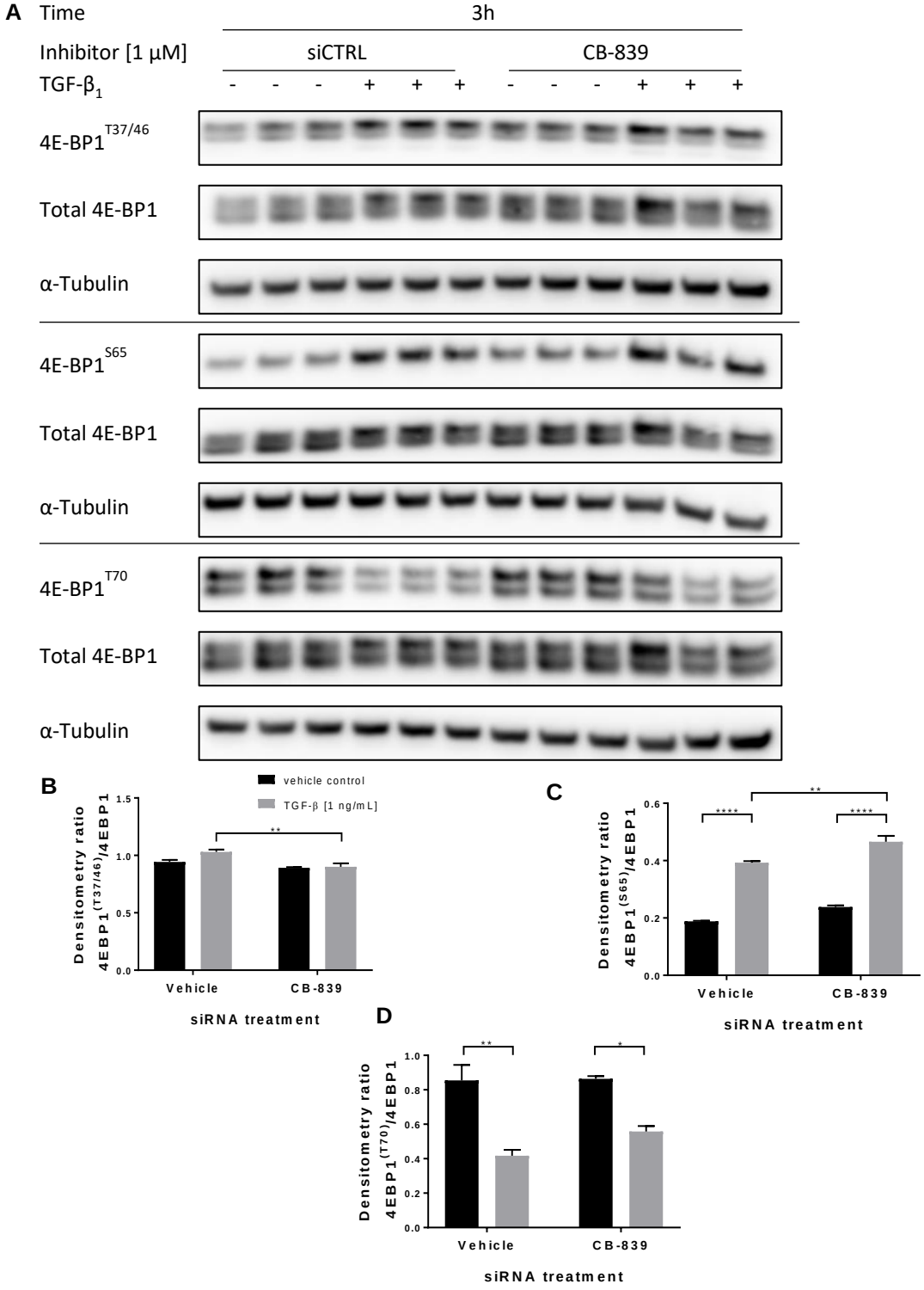

Figure 3.19: The effect of CB-839 on TGF-β$_1$ stimulated 4E-BP1 phosphorylation in pHLFs

Confluent pHLFs were serum-starved prior for 24 hours prior to incubation with CB-839 for 1 hours followed by stimulation with 1 ng/mL TGF-β$_1$ for 3 hours. The phosphorylation of 4E-BP1$^{T37/46}$, 4E-BP1^{S65} and 4E-BP1^{T70} were assessed by western blotting. Protein loading was verified by blotting with anti- α-tubulin antibody. The densitometry (panels B-D) was calculated and plotted as a phopho-protein to total protein ratio. These data are representative of two independent experiments performed.

3.3.7. The role of DEPTOR in mTORC1 activation

DEPTOR is an inhibitory component of the mTORC1 and mTORC2 complex. SMAD 3 can increase mTORC1 activation by down-regulating DEPTOR (Peterson et al. 2009; Das et al. 2013). The relationship established in both reports demonstrates that SMAD 3 transcriptionally regulates DEPTOR, and based on the actinomycin D and SMAD 3 knock-down data, this was another potential mechanism that SMAD 3 regulates TGF-β_1 stimulated mTORC1 activity in pHLFs.

To delineate the relative time-course of DEPTOR the protein levels were measured by western blot over a 24 hour period after treatment with TGF-β_1 (Figure 3.20). In the vehicle and TGF-β_1 treated pHLFs there were no changes in DEPTOR protein levels. There was no evidence to show that this mechanism is required for SMAD 3 regulated mTORC1 activity.

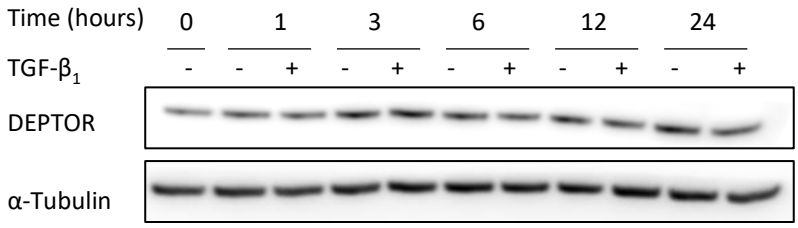

Figure 3.20: The effect of TGF-β_1 stimulation on DEPTOR protein expression over 24 hours in pHLFs

Confluent pHLFs were serum-starved prior to stimulation with 1 ng/mL TGF-β_1 for the indicated time-periods. DEPTOR was assessed by western blotting. Protein loading was verified by blotting with anti-α-tubulin antibody. The densitometry was calculated and plotted as DEPTOR to α-tubulin antibody ratio. These data are representative of two independent experiments. See Appendix 6 for the repeat.

3.3.8. Summary

- AZD8055 and Rapamycin both have different inhibitory profiles on 4E-BP1 phosphorylation. AZD8055 shows complete inhibition of all 4E-BP1 phosphorylation whereas Rapamycin only shows partial inhibition
- SMAD 3 knock-down inhibits both collagen gene transcription and collagen I deposition
- SMAD 3 protein and mRNA expression is decreased at 24 hours by TGF-β_1 treatment
- TGF-β_1 regulates total 4E-BP1 levels at 3 hours

- SMAD 3 and mTORC1 are required for TGF-β_1 stimulated increase in 4E-BP1 levels
- SMAD 3 is required for TGF-β_1 stimulated 4E-BP1^{S65} and 4E-BP1^{T70} phosphorylation
- GLS and DEPTOR are not required for early mTORC1 activation
- SMAD 3 is required for TGF-β_1 stimulated activation of mTORC1, however, the mechanism remains unknown.

3.4. The role of the TSC1/2-RHEB axis and TGF-β_1 stimulated mTORC1 activation

3.4.1. Introduction

TSC2 forms a heterotrimer with TSC1 and TBC1D7 and together they form a complex that negatively regulates the activation of mTORC1. Critically, TSC2 has GAP activity and is able to hydrolyse $RHEB^{GTP}$ into $RHEB^{GDP}$, therefore preventing RHEB from activating the mTORC1 complex. This following section aims to define the role of the TSC2 complex in mTORC1 activation downstream of TGF-β_1 stimulation. Furthermore, it aims to investigate kinases that are capable of inhibiting the TSC1/2 complex (promoting mTORC1 activation) using selective pharmacological inhibitors. In addition, this complex could bridge the link between SMAD 3 signalling and mTORC1 activation since several kinases (ERK1/2, MK2, CDK1 and RSK1) that regulate the TSC1/2 complex can also regulate SMAD signalling (Shi 2006).

3.4.2. The effect of TSC2 knock-down on TGF-β_1 stimulated 4E-BP1 phosphorylation

The TSC1/2 complex inhibits RHEB, which means knocking-down or inhibiting either TSC1 or TSC2 will lead to an increase in mTORC1 activity due to the increased availability of $RHEB^{GTP}$. This observed increase in mTORC1 activity is well-characterised in tumour growth (harmartomas) which has decreased TSC activity, caused by a mutation in either TSC1 or TSC2 (Kohrman 2012). I rationalised that by generating a TGF-β_1 response curve, with TSC2 knock-down in pHLFs, and looking at the shift in the curve it would help identify whether TGF-β_1 was acting through the TSC1/2 complex or via an alternative mechanism. TSC2 was the protein target since TSC1 is also known to have a role in shuttling proteins in cells, which could have unforeseen effects in our fibroblasts (Woodford et al. 2017). In contrast, TSC2 has only been identified to be associated with TSC1 with the sole function of regulating mTORC1 activity. The effect of TSC2 knock-down was assessed along with increasing concentrations of TGF-β_1 and this was evaluated by western blot measuring the phosphorylation of the mTORC1 substrate 4E-BP1. The knock-down of TSC2 in pHLFs was established, finding that TSC2 siRNA [100 nM] knocked-down TSC2 efficiently (Figure 3.21). Next, pHLFs were treated with TSC2 or

control siRNA for 48 hours prior to treatment with 4 concentrations of TGF-β_1 (0.03, 0.1, 0.3, 1, 3 ng/mL). The pHLF were stimulated with TGF-β_1 across two time-points, 3 and 6 hours. 3 hours was selected because this is when the increase 4E-BP1 phosphorylation is first detected in response to TGF-β_1 (Figure 3.1). In addition, the 6 hour time-point was selected because this would detect any changes in the curve missed at the earlier time-point. Treatment with TGF-β_1 has no effect on the TSC2 protein levels at 3 hours in pHLFs treated with the control siRNA (Figure 3.21A and B). PHLFs treated with TSC2 siRNA demonstrates that the knock-down of the protein was decreased about 6-fold in comparison to the control siRNA, confirming good knock-down was achieved. At 3 hours, TSC2 siRNA treated cells demonstrates that 4E-BP1^{S65} phosphorylation is increased in comparison to the control cells, whilst still showing a TGF-β_1 dependent increase in 4EBP1^{S65} phosphorylation (Figure 3.21 A and C). At 6 hours, the curve was more pronounced for the control cells. However, the TSC2 knock-down cells still demonstrates a shift in the curve and a shift in the maximum phosphorylation observed (Figure 3.21 A and D). The shift suggests pHLFs with TSC1/2 knocked-out have increased sensitivity to TGF-β_1 stimulation and therefore TGF-β_1 potentially regulates the TSC2 complex to mediate TGF-β_1 stimulated mTORC1 activation. Other reports show that mutated TSC2 leads to hyper-activated mTORC1 and the inhibition of RHEB prevents this both of which support this data (Mahoney et al. 2018).

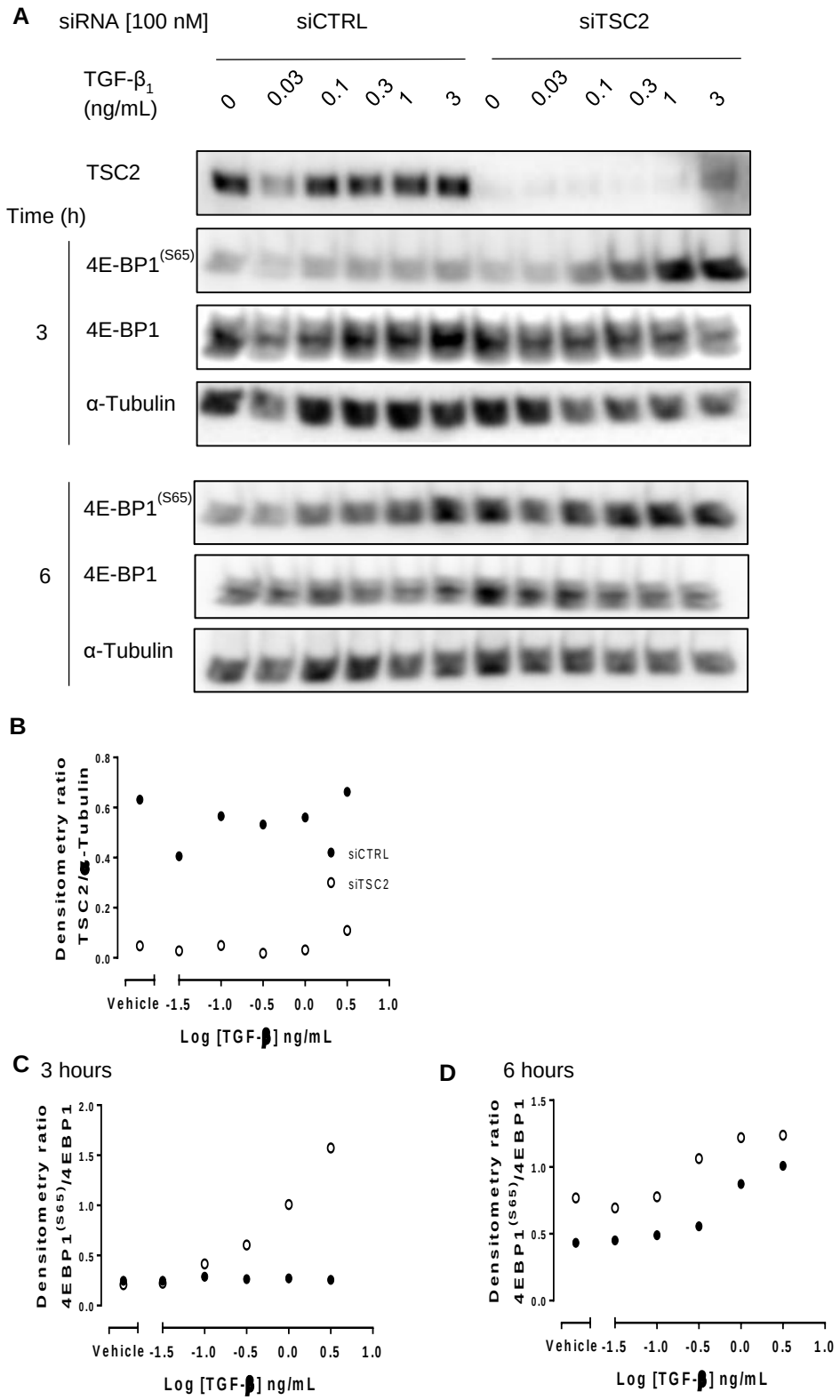

Figure 3.21: The effect TSC2 knock-down on TGF-β_1 stimulation of 4E-BP1 in pHLFs

At 60-80% confluence pHLFs were transfected with TSC2 siRNA for 24 hours prior to starvation with 0% DMEM. Cells were starved for 24 hours prior to treatment with a range of TGF-β_1 concentrations (0.03-3 ng/mL). The cells were harvested 3 and 6 hours post stimulation. The lysates were assessed by either western blotting investigating 4E-BP1^{S65} phosphorylation site. Protein loading was verified by blotting with an anti-α-Tubulin antibody. Densitometric (panels B-D) analysis of phosphor/protein relative to total protein or TSC 2 total to α-Tubulin is calculated for each condition.

3.4.3. The effect of RHEB knock-down on TGF-β_1 stimulated 4E-BP1 phosphorylation

RHEB is a GTP-binding protein which is required for mTOR activation in response to amino acids and MAPK. Since RHEB is a positive regulator of mTORC1 (negatively regulated by TSC1/2 complex), reduction or deletion of RHEB should lead to mTORC1 inhibition. RHEB siRNA and CRISPR knock-outs were used to investigate the relationship between TGF-β_1 stimulated mTORC1 activation and RHEB.

PHLFS were treated with RHEB siRNA (50 nM) or control siRNA for 48 hours (Figure 3.22A). Following the knock-down period, the cells were then stimulated with TGF-β_1. The effects of the knock-down on RHEB protein expression and 4E-BP1^{S65} phosphorylation were assessed by western blot. Treatment with RHEB siRNA was sufficient to reduce the protein levels by around 5.5 to 6.5-fold (Figure 3.22A and B). Visually, very little RHEB protein remains in the RHEB treated knock-down cells. TGF-β_1 had no impact on RHEB protein levels and increased the phosphorylation of 4E-BP1 in the siRNA control cells. In contrast 4EBP1^{S65} phosphorylation was decreased when RHEB was knocked-down (Figure 3.22A and C) .Taken together these data suggest that RHEB is required for TGF-β_1 stimulated 4E-BP1 phosphorylation.

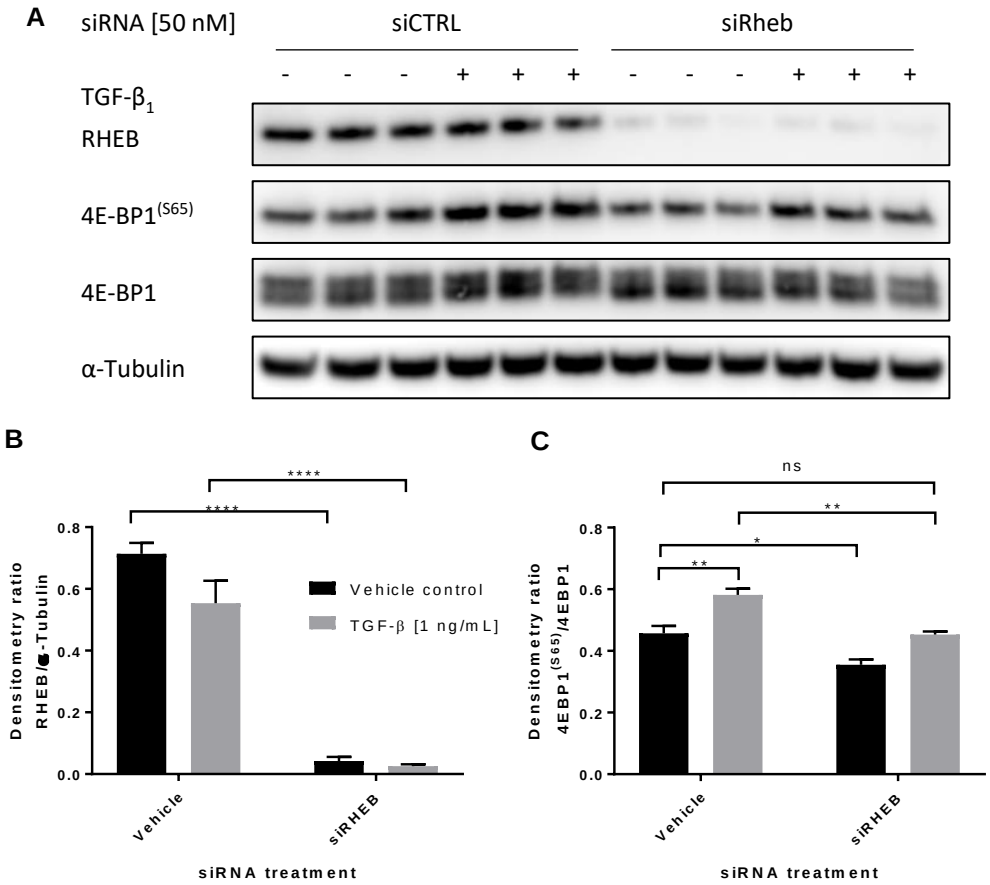

Figure 3.22: The effect of RHEB knock-down on TGF-β_1 stimulated 4E-BP1 phosphorylation in pHLFs

At 60-80% confluence pHLFs were transfected with RHEB siRNA for 24 hours prior to starvation with 0% DMEM. Cells were starved for 24 hours prior to treatment with or without 1 ng/mL TGF-β_1. The cells were harvested 3 hours post stimulation. The lysates were assessed by western blotting investigating the 4E-BP1^{S65} phosphorylation site. Protein loading was verified by blotting with an anti-α-Tubulin antibody. Densitometric analysis (panels B-C) of phosphor/protein relative to total protein or RHEB total to α-Tubulin is calculated for each condition (n=3 replicates). These data are representative of two independent experiments performed. Differences between groups were evaluated with two-way ANOVA and Tukey multiple comparison testing. See repeat Appendix 7.

In addition to siRNA, a CRISPR approach was taken since pharmacological tools were not available at the time. However, there is now a small molecule, NR1, available for the inhibition of RHEB (Mahoney et al. 2018). CRISPR is a tool for editing DNA at specifically targeted locations using the Cas9 enzyme and a guide RNA sequence. Together they form the Cas9 complex. The guide RNA targets the Cas9 enzyme to its complementary region on the DNA which then allows the Cas9 enzyme to cut the DNA at specific sites called protospacer adjacent motif (PAM) sites which correspond of the sequence 'NGG' of nucleotides (where N can be any nucleotide). The repair mechanisms

of the cells will then introduce mistakes into the cut regions as they are repaired, leading to insertions, deletions, or mutations. Typically for CRISPR experiments, CRISPR treated cells are single cell sorted allowing the culture of a homogenous population with the gene of interest knocked-out. However, since single cell isolation is not possible due to the slow growth of fibroblasts and restrictions based around Hayflick's constant (which leads to primary cells becoming senescent), the knock-out is conducted on a heterogeneous population of pHLFs. Therefore, like siRNA, the RHEB knock-out is based on the efficiency of transfecting the guide RNA into the pHLFs and the recognition of guide RNA for its target. Four guide RNA sequences were generated to target different regions of the RHEB DNA and were investigated for their ability to knock-out RHEB. These guide RNAs targeted different regions on the exons or different exons.

pHLFs were treated with the Cas9 guideRNA complex via electroporation and then grown to confluence. Using a fluorescent probe which is incorporated onto the Cas9 enzyme, this established that electroporation has occurred in the pHLFs and how well this corresponds to the cells visually using fluorescent microscopy. The fluorescent signal can be seen evenly spread across the images and is located in regions populated by cells which is seen by visible light, Figure 3.23.

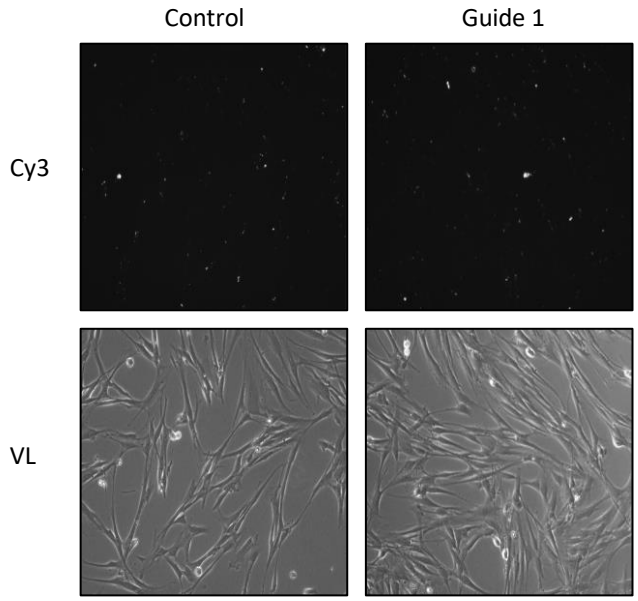

Figure 3.23: Electroporated CAS9enzyme in pHLFs

250,000 cells were harvested per condition and electroporated with their guideRNA and the CAS9 enzyme. The Cas9 enzyme has a fluorescent probe which can be visualized by using the cy3 fluorescent channel on a fluorescent microscope.

The efficiency of knock-out was assessed by quantifying RHEB protein levels in pHLFs by western blot. The four guide RNA were assessed in comparison to a control guide. Guides 1 and guide 2 demonstrated decreased RHEB protein levels. Therefore, Guide 1 was taken forward for further investigation with TGF-β_1 stimulation because it consistently was the most effective at decreasing RHEB protein levels (Figure 3.24).

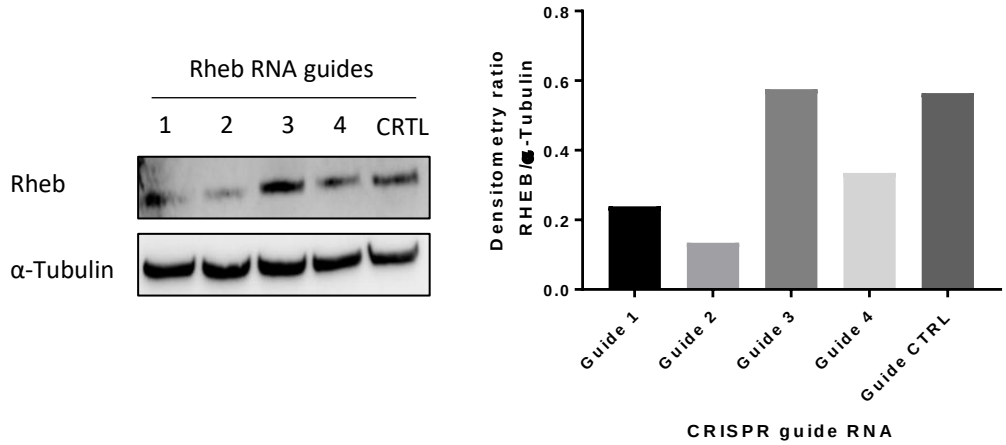

Figure 3.24: The comparison between 5 CRISPR guide RNA's effect on RHEB knock-out

pHLFs were electroporated with individual guide/CAS9 complex. The cells were then seeded into a 6 well plate and cultured until confluence. The pHLFs were harvested and the lysates were assessed by either western blotting investigating RHEB total protein levels. Protein loading was verified by blotting with an anti-α-Tubulin antibody. Densitometric analysis of RHEB total to α-Tubulin is calculated for each condition. These data are representative of two independent experiments performed.

To investigate whether RHEB is required for TGF-β_1 stimulated mTORC1 activation, the phosphorylation of 4E-BP1 was assessed when RHEB was knocked out. The treatment with the RNA guide 1 gave an almost complete loss of the RHEB protein across the 6 replicates (including – and + TGF-β_1 conditions) (Figure 3.25). In the control guide treated cells, treatment with TGF-β_1 increased the phosphorylation of 4E-BP1^{S65}. In comparison, in cells with RHEB knocked-out, the TGF-β_1 stimulated phosphorylation was inhibited. Therefore, RHEB is required for TGF-β_1 stimulated mTORC1 activation in pHLFs. Taken together, the siRNA knock-down and CRISPR knock-out demonstrate that pHLFs with reduced RHEB protein levels are inhibited from activating mTORC1 when treated with TGF-β_1. Furthermore, this supports the data that the TSC1/2 complex is important in pHLFs for inhibiting RHEB

activity and is inhibited upon TGF-β_1 stimulation to allow mTORC1 to become activated. These data are also supported by recent literature evidence, which shows the importance of the TSC1/2-RHEB axis in the kidney cell line TRI102 which have a mutated TSC2 protein leading to increased mTORC1 activation. In this report the inhibition of RHEB with NR1 results in decreased mTORC1 activation reversing the effects of the TSC1/2 mutation (Mahoney et al. 2018). Furthermore in MCF-7 cell RHEB inhibition inhibits insulin and EGF stimulated mTORC1 activation (Mahoney et al. 2018).

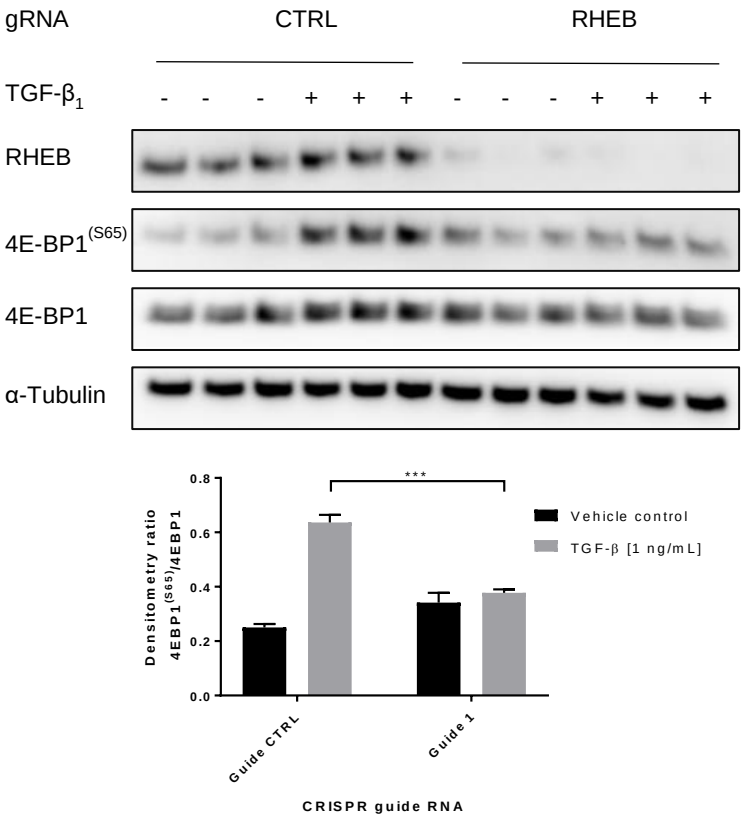

Figure 3.25: The effect of RHEB knock-out on TGF-β_1 stimulated 4E-BP1 phosphorylation in pHLFs

pHLFs were electroporated with individual RHEB guide1/CAS9 complex. The cells were then seeded into a T25 cultured until confluence. The cells were treated with trypsin and re-seeded in 6 well plates. Cells were starved for 24 hours prior to treatment with or without 1 ng/mL TGF-β_1. The cells were harvested 3 hours post stimulation. The lysates were assessed by western blotting investigating the total levels of RHEB and 4E-BP1^{S65} phosphorylation site. Protein loading was verified by blotting with an anti-α-Tubulin antibody. Densitometric analysis of phosphor/protein relative to total protein or RHEB total to α-Tubulin is calculated for each condition (n=3 replicates). These data are representative of two independent experiments performed. Differences between groups were evaluated with two-way ANOVA and Tukey multiple comparison testing

The previous evidence high-lighted the importance of the TSC1/2-RHEB axis for TGF-β_1 stimulated mTORC1 activation. To investigate the potential

importance of RHEB for TGF-β_1 stimulated collagen synthesis RHEB knock-out pHLFs were used (Figure 3.26). TGF-β_1 stimulation induced an increase collagen deposition in control guide cells. In contrast the CRISPR cells which had reduced RHEB protein levels were inhibited from synthesising collagen I.

Collectively, these data support that the TSC1/2-RHEB axis regulates TGF-β_1 induced mTORC1 activation as measured by phosphorylation of 4E-BP1^{S65}. Moreover, RHEB is required for collagen synthesis downstream of TGF-β_1 stimulation.

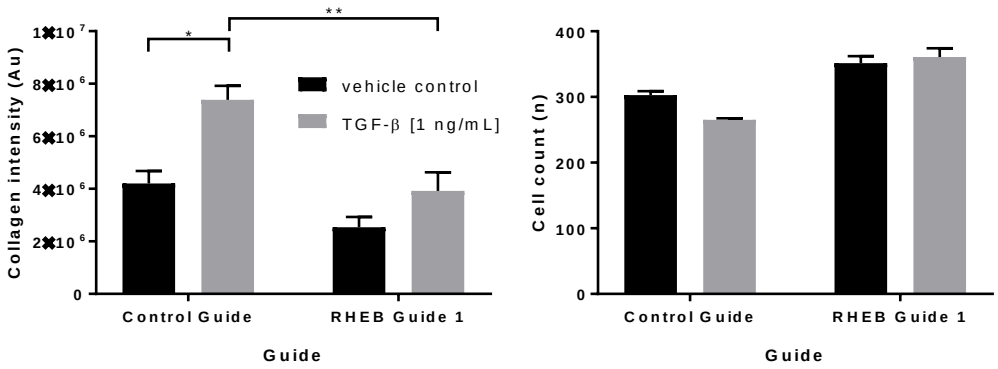

Figure 3.26: The effect of RHEB knock-out on TGF-β_1 stimulated collagen I synthesis in pHLFs

pHLFs were electroporated with individual RHEB guide1/CAS9 complex. The cells were then seeded into a T25 cultured until confluence. The cells were treated with trypsin and re-seeded in 96 well plates in 10% DMEM. At confluence the pHLFs were starved for 24 hours prior to treatment. After starvation cells were incubated with DMEM containing Ficoll for 1 hour. Following incubation cells were treated with or without TGF-β_1 [1 ng/mL] which was spiked into the wells and incubated for 48 hours, prior to fixation and staining for type1 collagen (left column) and cell counts (right column) were obtained from a DAPI counter stain. Data are expressed as mean fluorescent intensity or cell count (n=4 reads per well) averaged across 4 replicates. These data are representative of two independent experiments. Differences between groups were evaluated with two-way ANOVA and Tukey multiple comparison testing. This was done in collaboration with Dr D.Guillotin. See Appendix 8

3.4.4. The inhibition of TSC2 upstream kinases, MK2 CDK1, ERK and RSK and its effect on TGF-β_1 stimulated mTORC1 activation and collagen synthesis

The initial TSC2 data was ambiguous (Figure 3.24). However, the RHEB knock-out and knock-down data demonstrated that RHEB regulates mTORC1 activity and inhibits TGF-β_1 stimulated collagen I synthesis. RHEB is the only known substrate of TSC1/2 *in vivo* and because of previously reported data and the data presented in this thesis, this implicates the TSC1/2 complex in TGF-β_1 induced mTORC1 activation (Huang & Manning 2008). In addition, previous reports have shown that TSC2 is tumour suppressive because this

complex negatively regulates RHEB activity to inhibit mTORC1 (Jin et al. 1996; Huang & Manning 2008; Gao & Pan 2001; Patel et al. 2003). Therefore, TSC1/2 and its role in TGF-β_1 stimulated mTORC1 activation was pursued next.

TSC1 and TSC2 are both large proteins and have several phosphorylation sites (Table 1.1). The phosphorylation sites determine the activity of the complex as a whole. TSC1 is critical for the stability of TSC2 and the phosphorylation of TSC1 can cause it to dissociate from TSC2. TSC1 dissociated from TSC2 means TSC2 is targeted for proteasomal degradation, which promotes increased mTORC1 activity. 14-3-3 proteins can target and inhibit or sequester TSC1/2 when it is phosphorylated at specific sites. All inhibitory sites lead to a decrease or loss of TSC2 GAP activity. Finally, some phosphorylation sites on TSC1/2 lead to an increase in its activation. The complex can receive input from multiple different kinases to determine its final GAP activity. The aim was to identify the pathway between TGF-β_1 activating the receptor and the TSC1/2 complex which is negatively regulating RHEB, knowing that RHEB is critical for mTORC1 activation and collagen I synthesis (Figure 3.25 and Figure 3.26). Therefore, the kinases investigated in this thesis are the upstream inhibitors of the TSC1/2 complex. In addition, if a kinase was identified its relationship with SMAD 3 could also be explored since this regulates mTORC1 activation. Furthermore, the identified kinase could be a potential therapeutic target.

3.4.5. The investigation of the effects of the MK2/TSC1/2 node

3.4.6. The effects of (5z)-7-Oxozeaenol inhibition of pHLF collagen I synthesis

TGF-β_1 Activated Kinase 1 (TAK1) has been identified as a mediator of several TGF-β_1 stimulated pathways in several cell types and can be directly phosphorylated by the TβRI receptor. This kinase sits upstream of P38 MAPK which is a critical activator of MK2 and it is MK2 that can inhibit TSC1/2. TAK1 was an optimal target because it was at the top of the pathway and has also been identified as a kinase required for collagen synthesis (Kuk et al. 2015; Li et al. 2017; Grillo et al. 2015; Guo et al. 2013; Ono et al. 2003).

The effects of TAK1 inhibition on TGF-β_1 stimulated collagen synthesis using (5z)-7-Oxozeaenol (a TAK1 inhibitor) were investigated (Figure 3.27). The collagen deposition assay was used to investigate the treatment of pHLFs with a concentration range of (5z)-7-Oxozeaenol (0.3 nM – 10 μM). The pHLFs were incubated for 1 hour with each concentration prior to TGF-β_1 stimulation. The collagen deposition was quantified after 48 hours using high content imaging of collagen I immunofluorescence. (5z)-7-Oxozeaenol significantly inhibited TGF-β_1 induced collagen I deposition with an IC_{50} of 0.24 μM (Figure 3.27). In addition, a reduction in cell count was observed with an IC_{50} of 11 μM, indicating that higher concentrations are toxic to the cells. The loss in cell count suggested that this may be driving the decrease in collagen synthesis and perhaps not the compound inhibiting pathways for collagen I synthesis. However, the difference in IC_{50} values suggests that there is a separation between the inhibitory effects of the compound on collagen synthesis versus the effect on the loss in cell count. Visibly, during the experiment, no rounding or floating cells were detected. Therefore, to investigate whether the decrease in collagen deposition was driven by pHLF cell death or driven through TAK1 inhibition, two assays that detect cell death were used. The assays used were LDH assay (quantifies apoptosis and necrosis) and caspase 3/7 glo assay (quantifies cell apoptosis) (Figure 3.28). For both assays, staurosporine was utilised as a positive control because it acts as a pan kinase inhibitor that leads to the activation of apoptotic pathways. The LDH and caspase 3/7 glo assays both demonstrate high levels of cell death when treated staurosporine [100 nM] (positive control), with just over a 2-fold increase in luminescence signal for the Caspase 3/7 glo assay and a 30-fold increase in absorbance for the LDH assay. Treatment with (5z)-7-Oxozeaenol for 48 hours demonstrated no increase in cell death in comparison to the vehicle control. This meant that decrease in collagen synthesis measured by the treatment of (5z)-7-Oxozeaenol was not likely driven by cell death.

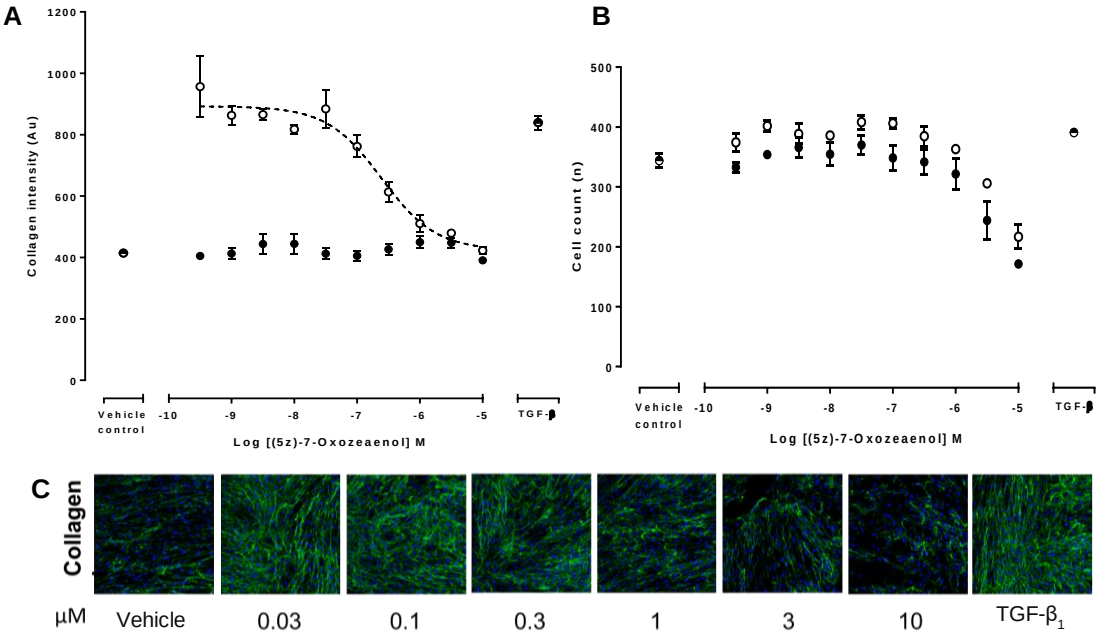

Figure 3.27: The effects of TAK1 inhibition on TGF-β_1 stimulated collagen I synthesis

Confluent pHLFs were starved for 24 hours before being incubated with increasing concentrations of (5z)-7-Oxozeaenol (the vehicle controls were incubated with 0.1% DMSO) in DMEM containing Ficoll for 1 hour. Following incubation cells were treated with or without TGF-β1 [1 ng/mL] which was spiked into the wells and incubated for 48 hours, prior to fixation and staining for type1 collagen, Panel A. Cell counts were obtained from a DAPI counter stain, Panel B. Data are expressed as mean fluorescent intensity (n=4 reads per well) averaged across 4 replicates. IC_{50} values were calculated using a three-parameter non-linear regression. Panel C shows representative images from each condition. These data are representative of two independent experiments.

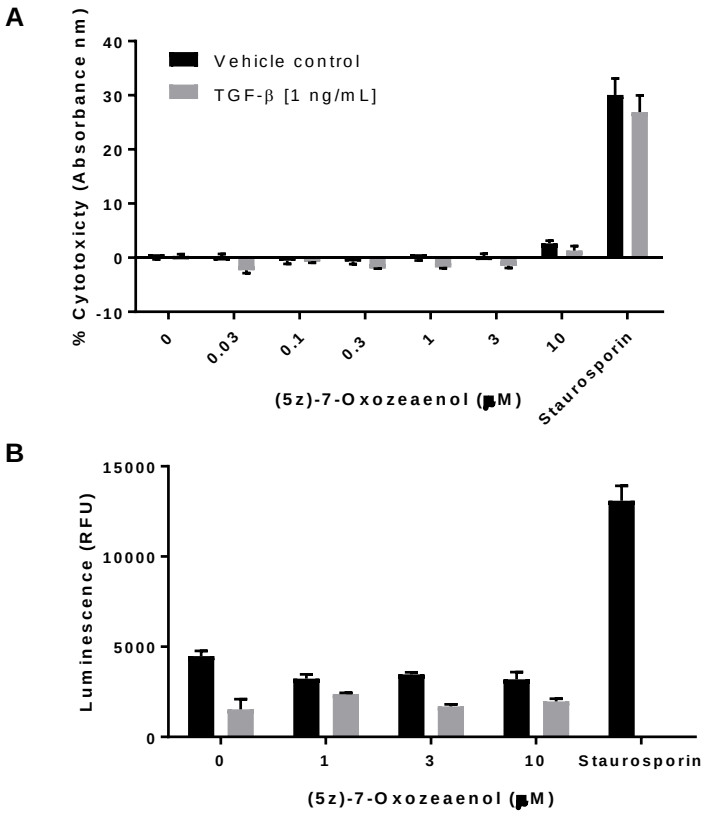

Figure 3.28: The effect on (5z)-7-Oxozeaenol on cell death

Confluent pHLFs were starved for 24 hours before being incubated with increasing concentrations of (5z)-7-Oxozeaenol (excluding the vehicle controls 0.1% DMSO) or staurosporine in DMEM containing Ficoll for 1 hour. Following incubation cells were treated with or without TGF-β1 [1 ng/mL] which was spiked into the wells and incubated for 48 hours. Panel A, caspase 3/7 glo assay buffer was added to the wells and luminescence was quantified. Panel B, LDH buffer was added and the absorbance (490 nm) was read. The data were plotted as ± SEM of n=4 replicate wells per condition (Panel A and B).

Before further investigation continued into the mechanisms of (5z)-7-Oxozeaenol, It was important to ensure the effect seen was observable in other pHLF cell lines as well. Two pHLF cell lines were used (0611 and 0110). The pHLF were incubated with (5z)-7-Oxozeaenol one hour prior to the treatment with TGF-β_1. Treatment with (5z)-7-Oxozeaenol demonstrated a concentration dependent decrease in collagen I intensity (Figure 3.29). The compound IC50 from the other cell lines were 1.5 μM and 1.2 μM respectively. This is 5-fold higher than the 0311 cell line (0.24 μM). In addition, no cell loss observed in these cell lines which may explain the shift in the concentration curve. This suggests that there is variability between cell lines in terms of sensitivity to the compound.

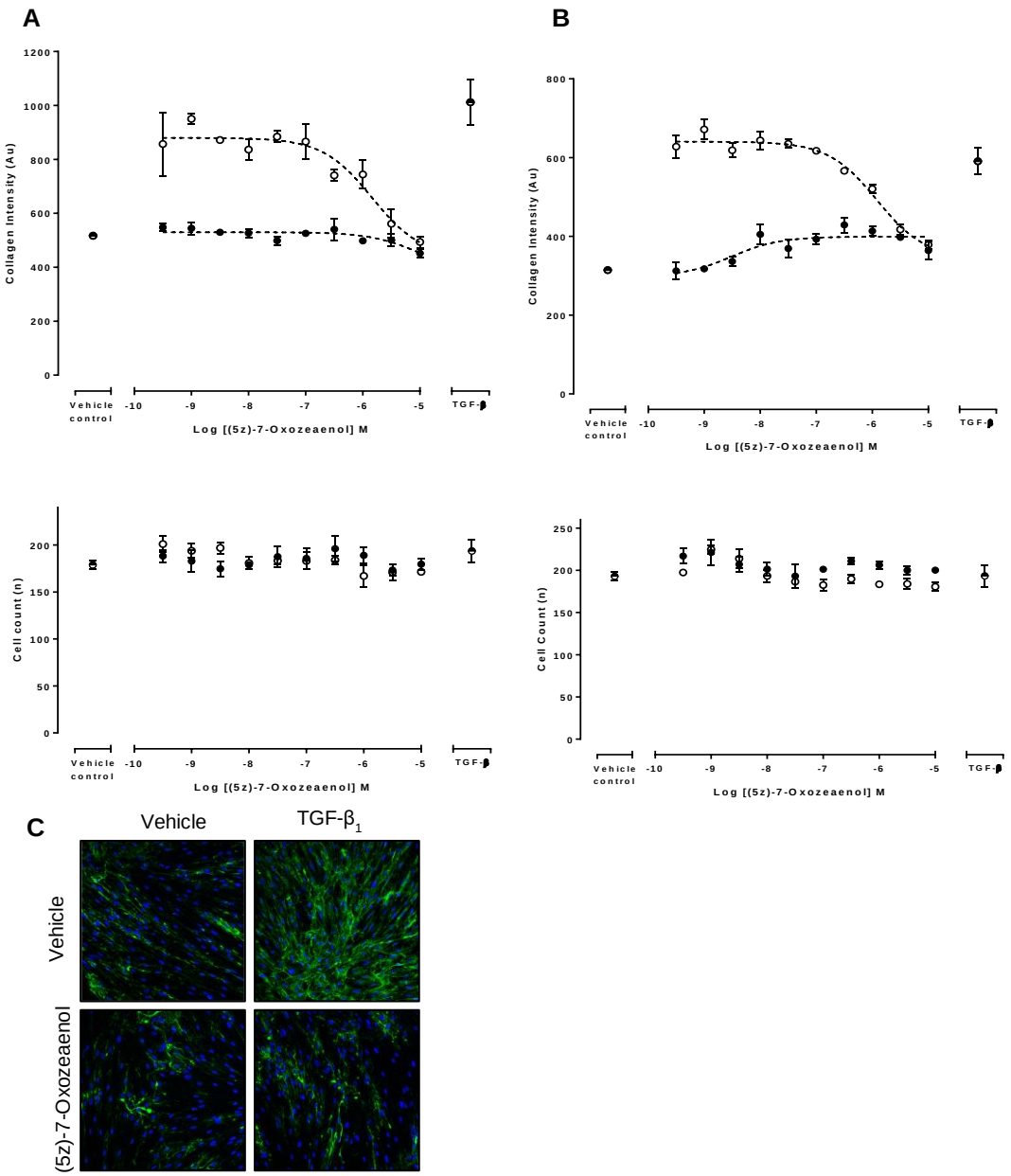

Figure 3.29: The effect of (5z)-7-Oxozeaenol on TGF-β stimulated collagen I synthesis in pHLF additional cell lines

Confluent pHLFs were starved for 24 hours before being incubated with increasing concentrations of (5z)-7-Oxozeaenol (including the vehicle controls 0.1% DMSO) in DMEM containing Ficoll for 1 hour. Following incubation cells were treated with or without TGF-β1 [1 ng/mL] which was spiked into the wells and incubated for 48 hours, prior to fixation and staining for type1 collagen and cell counts were obtained from a DAPI counter stain. Panel A and B are representative of two different cell lines. The data are expressed as mean fluorescent intensity or cell count (n=4 reads per well) averaged across 4 replicates. Panel C shows representative images from each condition of Panel A. This is representative of two independent experiments.

3.4.7. The effects of (5z)-7-Oxozeaenol on TGF-β_1 stimulated mTORC1 activation

P38 MAPK is activated by different stimuli including IL1β, EGF and TGF-β_1. A time-course of P38 MAPK phosphorylation was used to identify the time frame that this kinase becomes activated and determine whether it correlates with the temporal activation of mTORC1 downstream of TGF-β_1 stimulation. Secondly, it was used to establish a time frame to asses if (5z)-7-Oxozeaenol was engaging its target, TAK1, which would be observed by a loss of P38 MAPK phosphorylation.

To establish the temporal activation of P38 MAPK, the effect of stimulation on P38 MAPK phosphorylation was assessed over 24 hours by western blot (Figure 3.30). TGF-β_1 stimulates P38 MAPK phosphorylation at as early as 3 hours and this prolonged for 24 hours (Figure 3.30). TβRI does not phosphorylate P38 MAPK directly. Therefore, the active TβRI receptor is likely activating a kinase required for P38 MAPK phosphorylation. In addition, this signalling cascade resulting in P38 MAPK phosphorylation temporally coincides with mTORC1 substrate 4E-BP1 phosphorylation, which has been demonstrated previously (Figure 3.1).

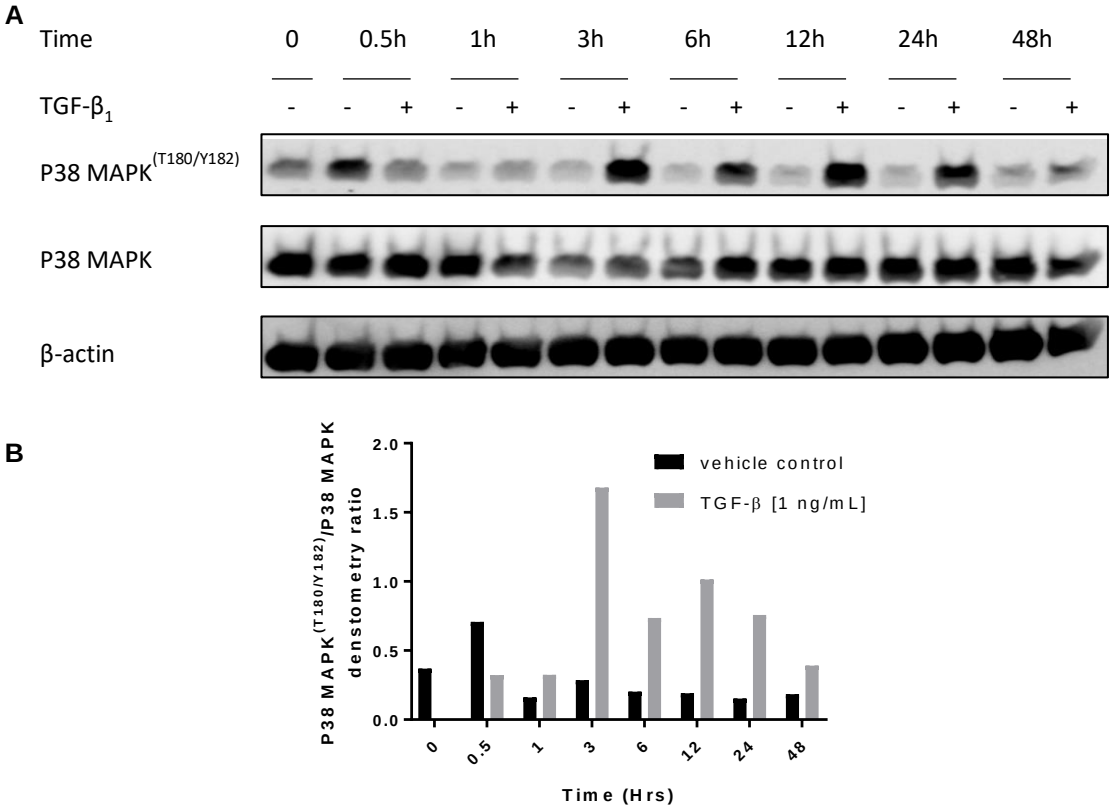

Figure 3.30: The effect of TGF-β_1 stimulation on P38 MAPK phosphorylation over 48 hours in pHLFs

Confluent pHLFs were serum-starved prior to stimulation with 1 ng/mL TGF-β_1 for the indicated time-periods. Phosphorylated p38 MAPK was assessed by western blotting. Protein loading was verified by blotting with anti- α-tubulin antibody. The densitometry was calculated and plotted as a phopho-protein to total protein ratio shown in Panel B. The data is representative of two independent experiments performed.

Knowing that P38 MAPK is being phosphorylated when pHLFs are induced with TGF-β_1 the next investigation was whether (5z)-7-Oxozeaenol was able to inhibit this TAK1 signalling pathway since P38 MAPK is a downstream kinase of TAK1. This was assessed by quantifying the p38 MAPK phosphorylation state in the presence of the inhibitor. PHLFs were incubated with (5z)-7-Oxozeaenol and a time-course of P38 MAPK phosphorylation was measured by western blot. (5z)-7-Oxozeaenol inhibits P38 MAPK phosphorylation from 3 hours onwards (Figure 3.31A and B). This demonstrated (5z)-7-Oxozeaenol was inhibiting a target required for P38 MAPK and this was most likely TAK1. To examine the role of TAK1 kinase in

mTORC1 activation in pHLFs the same lysates were used to assess the effects of (5z)-7-Oxozeaenol on 4E-BP1 and P70S6K phosphorylation. (5z)-7-Oxozeaenol decreased the phosphorylation of 4E-BP1^{S65} and P70S6K from 3 hours onwards, temporally coinciding with the loss in P38 MAPK phosphorylation (Figure 3.31A, C and D).

Collectively, these data support the notion that TAK1 mediates TGF-β_1 activation of mTORC1 and it is required for collagen I synthesis.

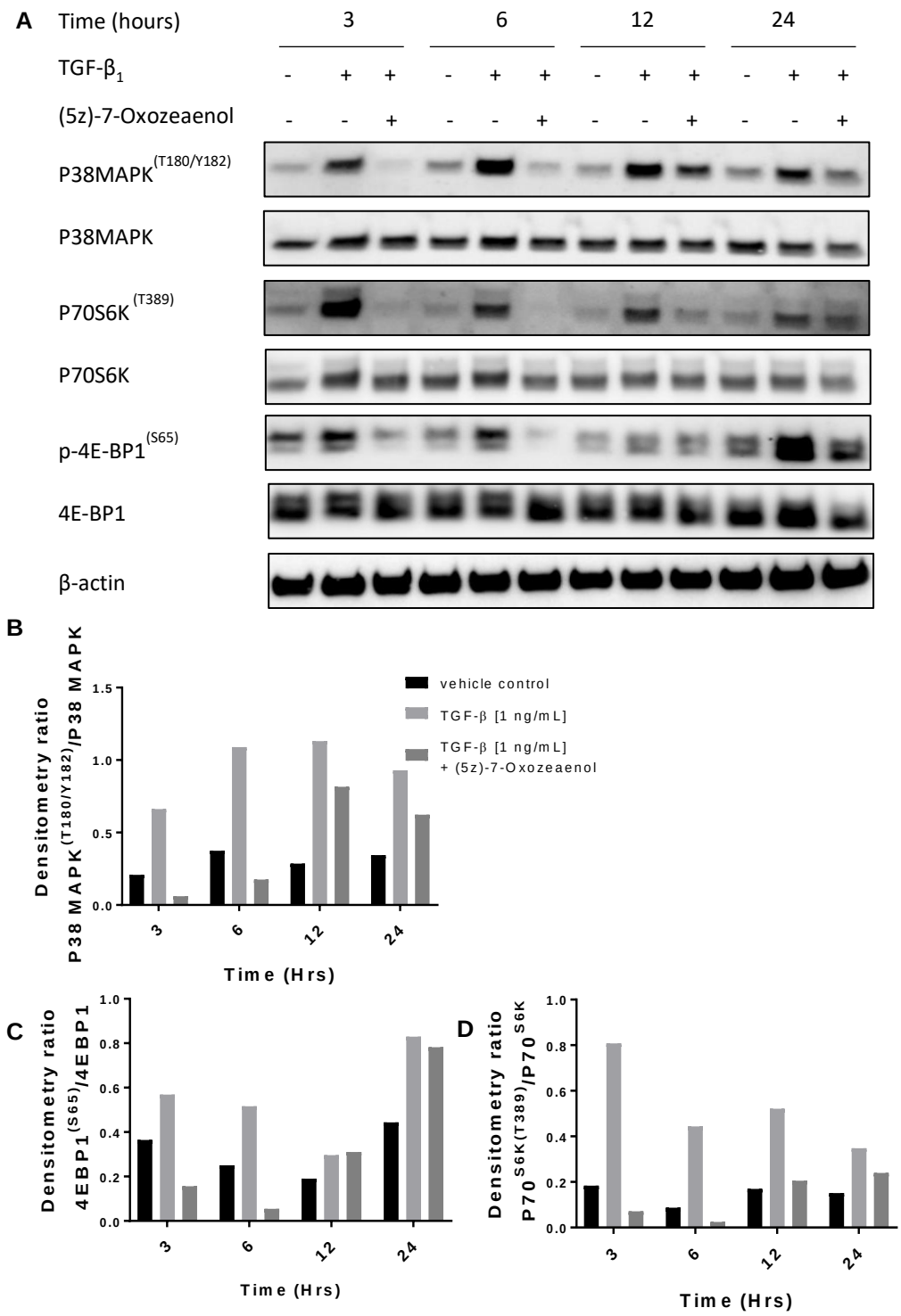

Figure 3.31: The effect of (5z)-7-Oxozeaenol on TGF-β$_1$ stimulated P38 MAPK and mTORC1 phosphorylation over 24 hours in pHLFs

Confluent pHLFs were serum-starved prior for 24 hours prior to incubation with 1 μM (5z)-7-Oxozeaenoll for 1 hours and then stimulation with 1 ng/mL TGF-β$_1$ for the indicated time-periods. Phosphorylation of p38 MAPK, P70S6K and 4E-BP1 were assessed by western blotting. Protein loading was verified by blotting with anti- α-tubulin antibody. The densitometry (panels B-D) was calculated and plotted as a phopho-protein to total protein ratio shown in Panel B. The data is representative of three independent experiments performed. Replicate data is presented in appendix 9

3.4.8. The effect of P38 MAPK or MK2 inhibition on TGF-β_1 stimulated collagen I synthesis

The previous figures showed that (5z)-7-Oxozeaenol inhibited collagen I synthesis and mTORC1 substrate phosphorylation (Figure 3.27, 3.29 and 3.31). This suggested that the TAK1 kinase facilitates collagen synthesis down-stream of TGF-β_1 stimulation. mTORC1, P38 MAPK and MK2 were investigated to understand how TAK1 mediates their activation. P38 MAPK is a kinase downstream of TAK1 activation and MK2 is a substrate of P38 MAPK. Previous reports have provided evidence that MK2 can activate the mTORC1 complex by inhibiting the TSC1/2 complex (phosphorylation of the S1210 site) (Y. Li et al. 2003).

The effect of MK2 and P38 MAPK inhibition was assessed by screening a range of compounds for both kinases. There are 4 isoforms of P38 MAPK (α, β, δ and γ) and there is some evidence that they can compensate for each other (Krementsov et al. 2013). Therefore, three compounds were selected to inhibit P38 MAPK to cover its range of isoforms, Table 3.1. In addition, two compounds were selected to inhibit MK2, which both showed different mechanisms of inhibition. PF-3644022 is an ATP-competitive inhibitor and MKIV is a reversible and non-ATP-competitive inhibitor, Table 3.1.

Table 3.1 P38 MAPK and MK2 inhibitors

Target (isoform)	Compound	IC50 (nM)
P38 MAPK (α)	TAK715	7.1
P38 MAPK (α,β)	SB202190	50 and 100
P38 MAPK (α/β/γ/δ (pan))	BIRB796	38, 65 , 200 and 520
MK2	PF-3644022	5.2
	MKIV	110

The effect of the three P38 MAPK inhibitors TAK715, BIRB796 and SB202190 on collagen deposition was evaluated in the collagen deposition assay. Unlike (5z)-7-Oxozeaenol inhibition, P38 MAPK inhibition did not inhibit TGF-β_1

stimulated collagen I synthesis (Figure 3.32). There is a decrease in collagen deposition with the compound TAK715, however this is associated with by a decrease in cell loss.

The inhibition of MK2 was investigated using PF-3644022 and MKIV and the collagen deposition was measured using high content imaging of collagen I immunofluorescence. TGF-β_1 stimulated collagen deposition was not inhibited by pHLF treatment with PF-3644022 or MKIV (Figure 3.33). Taken together, these data suggested that TAK1 mediated activation of P38 MAPK and MK2 was not required for TGF-β_1 stimulated collagen synthesis.

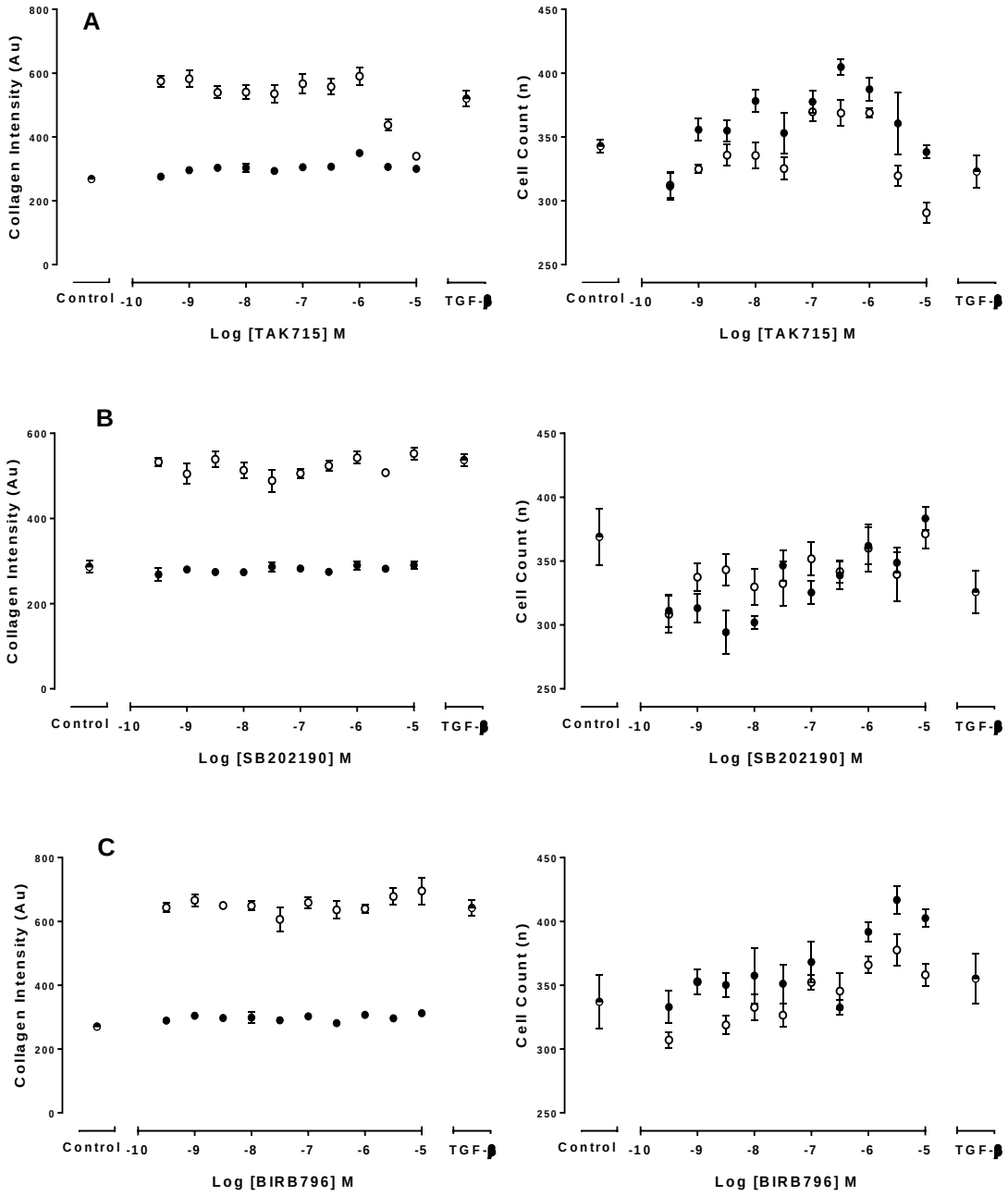

Figure 3.32: The effect of P38 MAPK inhibition on TGF-β_1 stimulated collagen I synthesis in pHLF

Confluent pHLFs were starved for 24 hours before being incubated with increasing concentrations of either TAK715 (Panel A), SB202190 (Panel B) or BIRB796 (Panel C) (vehicle controls were incubated with 0.1% DMSO) in DMEM containing Ficoll for 1 hour. Following incubation cells were treated with or without TGF-β_1 [1 ng/mL] which was spiked into the wells and incubated for 48 hours, prior to fixation and staining for type1 collagen (left column) and cell counts (right column) were obtained from a DAPI counter stain. Data are expressed as mean fluorescent intensity or cell count (n=4 reads per well) averaged across 4 replicates. These data are representative of two independent experiments

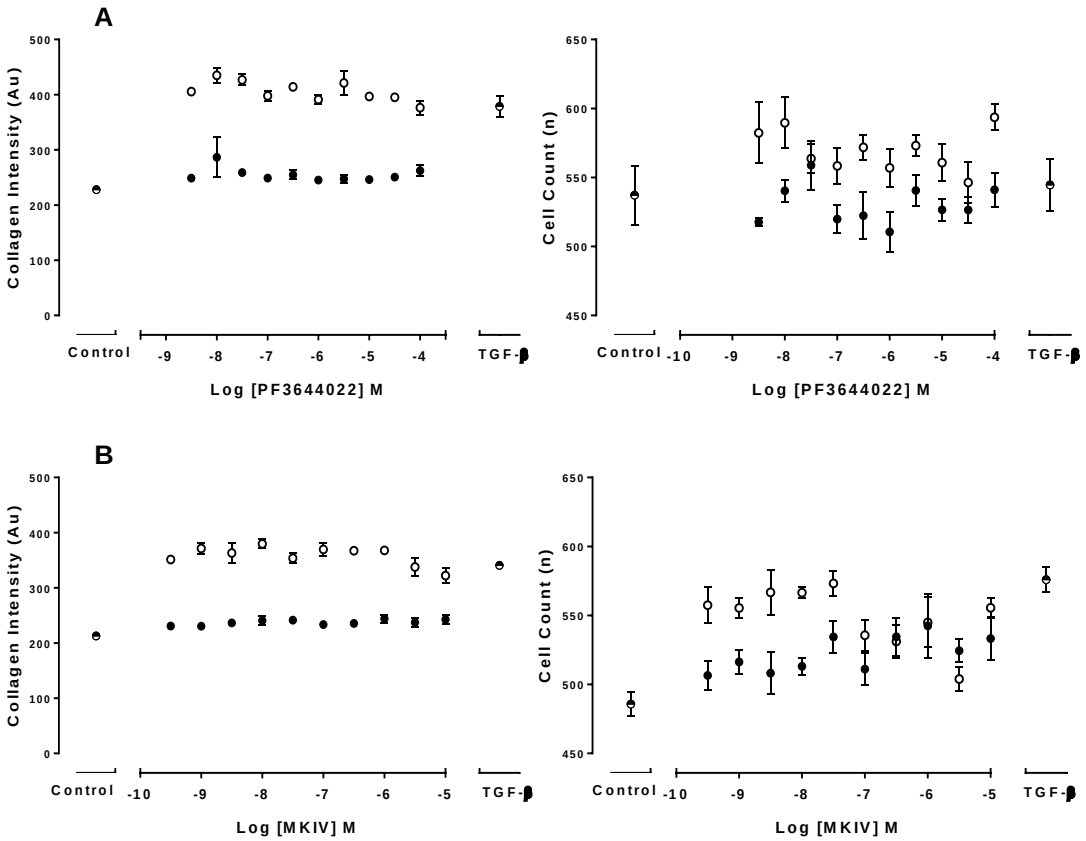

Figure 3.33: The effect of MK2 inhibition on TGF-β_1 stimulated collagen I synthesis in pHLF

Confluent pHLFs were starved for 24 hours before being incubated with increasing concentrations of either PF3644022 (Panel A) or MKIV (Panel B) (vehicle controls were incubated with 0.1% DMSO) in DMEM containing Ficoll for 1 hour. Following incubation cells were treated with or without TGF-β_1 [1 ng/mL] which was spiked into the wells and incubated for 48 hours, prior to fixation and staining for type1 collagen (left column) and cell counts (right column) were obtained from a DAPI counter stain. Data are expressed as mean fluorescent intensity or cell count (n=4 reads per well) averaged across 4 replicates. These data are representative of two independent experiments

3.4.9. Investigating TGF-β_1 stimulated MK2 phosphorylation

The inhibition of MK2 and P38 MAPK did not affect TGF-β_1 stimulated collagen synthesis. An explanation for the lack of effect could have been because the compounds were not engaging their targets. However, the compounds used in Table 3.1 were used around 100-fold higher than their IC50 and more than one compound was used for P38 MAPK and MK2. To support the inhibitor data and to rule out MK2 as a kinase involved in TGF-β_1 stimulated collagen I synthesis, the phosphorylation state of MK2 in pHLFs was investigated when stimulated with TGF-β_1. The phosphorylation of MK2 is a marker of its catalytic activity.

MK2 has been shown to be phosphorylated by TGF-β_1 stimulation at the T334 site (Xu et al. 2006). MK2 phosphorylation was measured across 3 hours period. This time period was selected because P38 MAPK is activated as early as 30 minutes and published evidence suggests that MK2 can be phosphorylated as early as 10 minutes under some conditions (Xu et al. 2006). Previous reports show IL1β and anisomycin stimulate MK2 phosphorylation. These stimuli were included as additional controls in this investigation to show that MK2 phosphorylation can be detected (Y. Li et al. 2003). In addition, TGF-β_1 was used at an increased concentration which had been used in previous reports (Xu et al. 2006). Four time-points were assessed: 5, 10, 30 minutes and 3 hours in combination with either TGF-β_1 treatment ([1 ng/mL and 5 ng/mL]); IL1β ([10 ng/mL]) and anisomycin ([10 µg/mL]). $MK2^{T334}$ phosphorylation was assessed in response to these stimuli by western blot, (Figure 3.34). The treatment of pHLFs with anisomycin and IL1β induced MK2 phosphorylation at several time-points. IL1β stimulates the phosphorylation of MK2 between 5 minutes with the peak of phosphorylation at 10 minutes. The phosphorylation persists for up to 3 hours. Treatment of pHLFs with Anisomycin induces MK2 phosphorylation at 10 minutes and peaked at 30 minutes. The phosphorylation had declined by 3 hours post anisomycin stimulation. In comparison, the treatment with TGF-β_1, even at the higher concentration [5 ng/mL], did not induce MK2 phosphorylation at any time-point (Figure 3.34).

Taken together with the inhibitory data from the collagen deposition assay and these western blots, this would suggest that (5z)-7-Oxozeaenol inhibition of mTORC1 and collagen deposition is not mediated through a TAK1-P38 MAPK-MK2 axis. Therefore, based upon this evidence it is possible that TAK1 is acting independently of P38 MAPK and MK2, via other kinases such as MKK4 and MKK6.

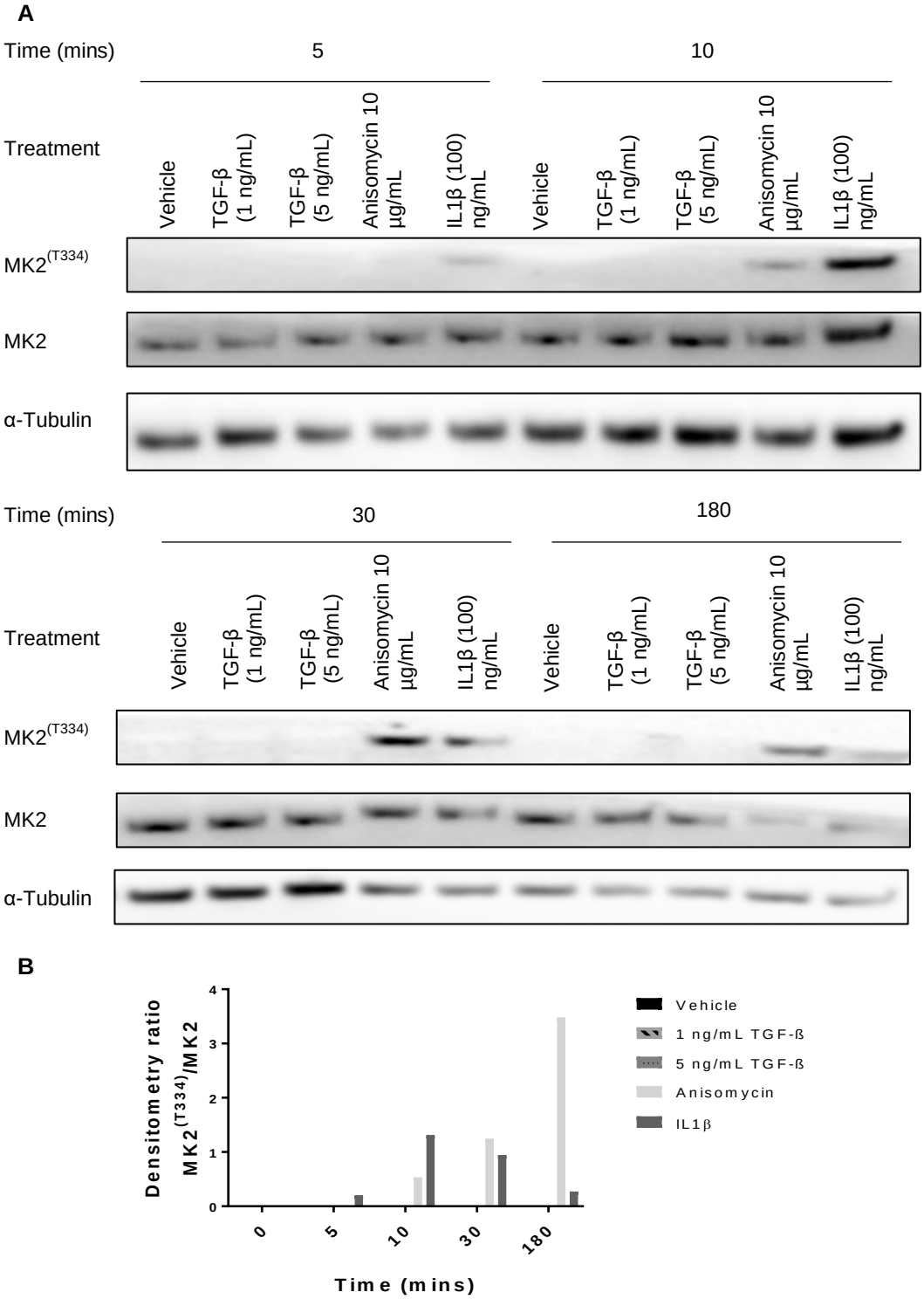

Figure 3.34: Comparing the effects of various stimuli on MK2 phosphorylation in pHLFs

Confluent pHLFs were serum-starved prior to stimulation with four different stimulus, TGF-β_1 [1 ng/mL], TGF-β_1 [5 ng/mL], Anisoymcin [10 µg/mL], IL1β [100 ng/mL] for the indicated time-periods. Phosphorylated MK2 was assessed by western blotting, Panel A. Protein loading was verified by blotting with anti- α-tubulin antibody. The densitometry was calculated and plotted as a phopho-protein to total protein ratio shown in, Panel B. These data are representative of two independent experiments performed

3.4.10. Investigation of TAK1 knock-down on TGF-β_1 stimulated mTORC1 activation and collagen I synthesis

The down-stream substrate of TAK1, MK2, failed to demonstrate any phosphorylation in response to TGF-β_1 stimulation. In addition, the inhibitors of MK2 and P38 MAPK had no effect on TGF-β_1 induced collagen synthesis. Therefore, how TAK1 was mediating mTORC1 activation in response to TGF-β_1 stimulation was yet to be determined. Before investigations went further, it was important to solidify the data demonstrating that TAK1 was responsible for mediating TGF-β_1 stimulated collagen I synthesis, since the data for MK2 and P38 MAPK (its only substrates linking it to TSC1/2) were not involved in TGF-β_1 stimulated collagen I synthesis.

The effect of TAK1 knock-down was used to investigate the effects TGF-β_1 stimulated collagen I synthesis. In parallel, the knock-down of TAK1 was assessed by western blot to ensure that knock-down was achieved at the time of TGF-β_1 treatment and that knock-down was maintained at the end of the experiment when the cells are fixed for the collagen deposition assay. The treatment of pHLFs with TAK1 siRNA did not inhibit TGF-β_1 stimulated collagen synthesis. Between control and knock-down cells a 1.5-fold increase in TGF-β_1 stimulated collagen deposition remained (Figure 3.35 Panel A). The knock-down of TAK1 during the experimental period was shown, with TAK1 knock-down confirmed to be decreased at the start and end of the collagen deposition assay (Figure 3.35 Panel B).

Next, TAK1 knock-down effects were was assessed on TGF-β_1 stimulated mTORC1 substrate (4EBP1 and P70S6K) phosphorylation. The western blot confirmed that pHLFs treated with TAK1 siRNA have a decrease of 70-80% of the TAK1 protein. TAK1 knock-down did not prevent the TGF-β_1 stimulated phosphorylation of P38 MAPK, P70S6K and 4E-BP1 (Figure 3.35 Panel C).

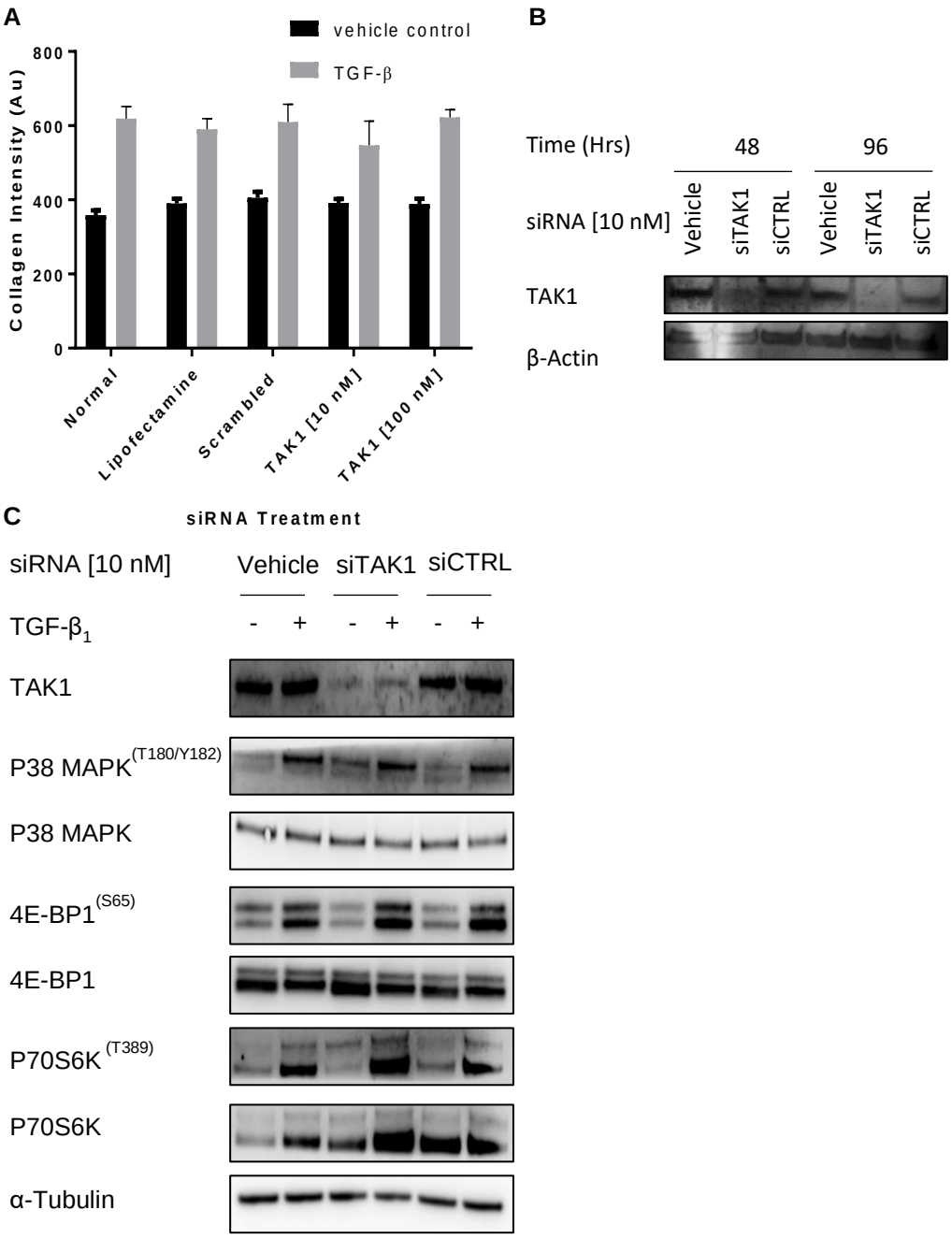

Figure 3.35: The effect of TAK1 knock-down on TGF-β_1 stimulated P38 MAPK and mTORC1 signalling

At 60-80% confluence pHLFs were transfected with TAK1 siRNA or control siRNA for 24 hours prior to starvation with 0% DMEM. Cells were starved for 24 hours prior to treatment. Panel A, after starvation cells were incubated with DMEM containing Ficoll for 1 hour. Following incubation cells were treated with or without TGF-β_1 [1 ng/mL] which was spiked into the wells and incubated for 48 hours, prior to fixation and staining for type1 collagen. The individual fluorescent intensity is normalised over cell count (DAPI) per read (n=4 reads per well) and the average of the normalised replicates (n=4) was plotted. The data is expressed as the mean (± SEM of n=4 replicate wells per condition). Panel B, an additional two 6 well plates were run in the same conditions to the collagen deposition assay but were harvested pre-TGF-β_1 stimulation, 48 hours and 96 hours and TAK1 protein expression was assessed by western blot. Total Protein loading was verified by blotting with an anti-α-Tubulin antibody. Panel C, post knock-down and starvation steps cell were treated with or without TGF-β_1 and harvested 3 hours post stimulation. P38 MAPK, 4E-BP1 and P70S6K phosphorylation were assessed by western blot. Protein loading was verified by blotting with an anti-α-Tubulin antibody. These data are representative of two independent experiments performed.

3.4.11. The effect of NG25 on TGF-β_1 stimulated collagen I synthesis

The siRNA data contradicted the data obtained with (5z)-7-Oxozeaenol, so a third approach was taken to further understand why the compound inhibits TGF-β_1 stimulated mTORC1 activation and collagen I synthesis but the siRNA was not. A second pharmacological inhibitor was used, NG25, as an alternative to (5z)-7-Oxozeaenol. NG25 was considered a good choice because it is a different chemotype and has a different mechanism of action to (5z)-7-Oxozeaenol, minimising the risk of inhibiting over-lapping kinase targets.

The effects on NG25 inhibition were assessed on TGF-β_1 stimulated collagen deposition (Figure 3.36). In line with the siRNA data, treatment with NG25 did not have a significant effect on TGF-β_1 stimulated collagen synthesis (Figure 3.36).

Collectively, these data do not support a role for TAK1 signalling in mediating the pro-fibrotic effects of TGF-β_1 and suggests that (5z)-7-Oxozeaenol inhibits a target other than TAK1 to block TGF-β_1-induced collagen I synthesis.

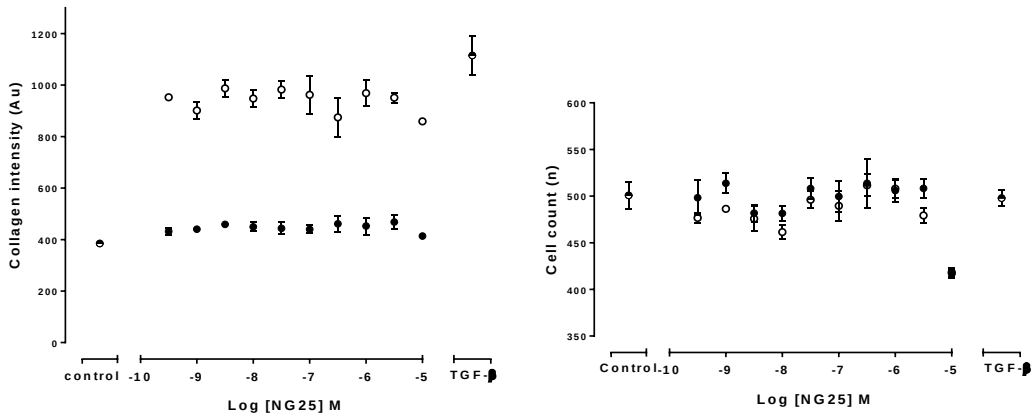

Figure 3.36: The effect of NG25 on TGF-β_1 stimulated collagen I synthesis in pHLF

Confluent pHLFs were starved for 24 hours before being incubated with increasing concentrations of NG25 (vehicle controls were incubated with 0.1% DMSO) in DMEM containing Ficoll for 1 hour. Following incubation cells were treated with or without TGF-β_1 [1 ng/mL] which was spiked into the wells and incubated for 48 hours, prior to fixation and staining for type1 collagen (left column) and cell counts (right column) were obtained from a DAPI counter stain. Data are expressed as mean fluorescent intensity or cell count (n=4 reads per well) averaged across 4 replicates. These data representative of two independent experiments

3.4.12. (5z)-7-Oxozeaenol regulates SMAD 2 and SMAD 3 phosphorylation

The siRNA experiments and NG25 data suggest that TAK1 was not likely to be required for TGF-β_1 stimulated mTORC1 activation or collagen synthesis. This suggests that (5z)-7-Oxozeaenol is eliciting its effect through another mechanism that isn't TAK1.

TGF-β_1 activation of the TβR complex (TβRI + TβRII) leads to the direct phosphorylation of SMAD 2 and SMAD 3 at sites S423/425 and S465/467, respectively. This subsequently leads to the binding of SMAD4 and the translocation of this complex into the nucleus to regulate gene transcription (Abdollah et al. 1997). Before investigating the kinase that (5z)-7-Oxozeaenol is targeting, the effect of (5z)-7-Oxozeaenol inhibition on SMAD 2 and SMAD 3 phosphorylation was assessed. (5z)-7-Oxozeaenol was incubated with pHLFS and the phosphorylation status of TGF-β_1 stimulated SMAD 2 and SMAD 3 was assessed by western blot across several time-points. (5z)-7-Oxozeaenol treatment was found to inhibit TGF-β_1 stimulated SMAD 2 (S423/425) and SMAD 3 (S465/467) phosphorylation across a range of time-points (Figure 3.37A, B and C).

TβRI directly phosphorylates SMAD 2 and SMAD 3. How (5z)-7-Oxozeaenol inhibits TGF-β_1 stimulated SMAD2 and SMAD 3 phosphorylation remains unknown. However, an explanation for this was that (5z)-7-Oxozeaenol directly engages and inhibits the TβRI/TβRII receptor complex. Regardless, taken together the data suggest that TAK1 was not the kinase of interest.

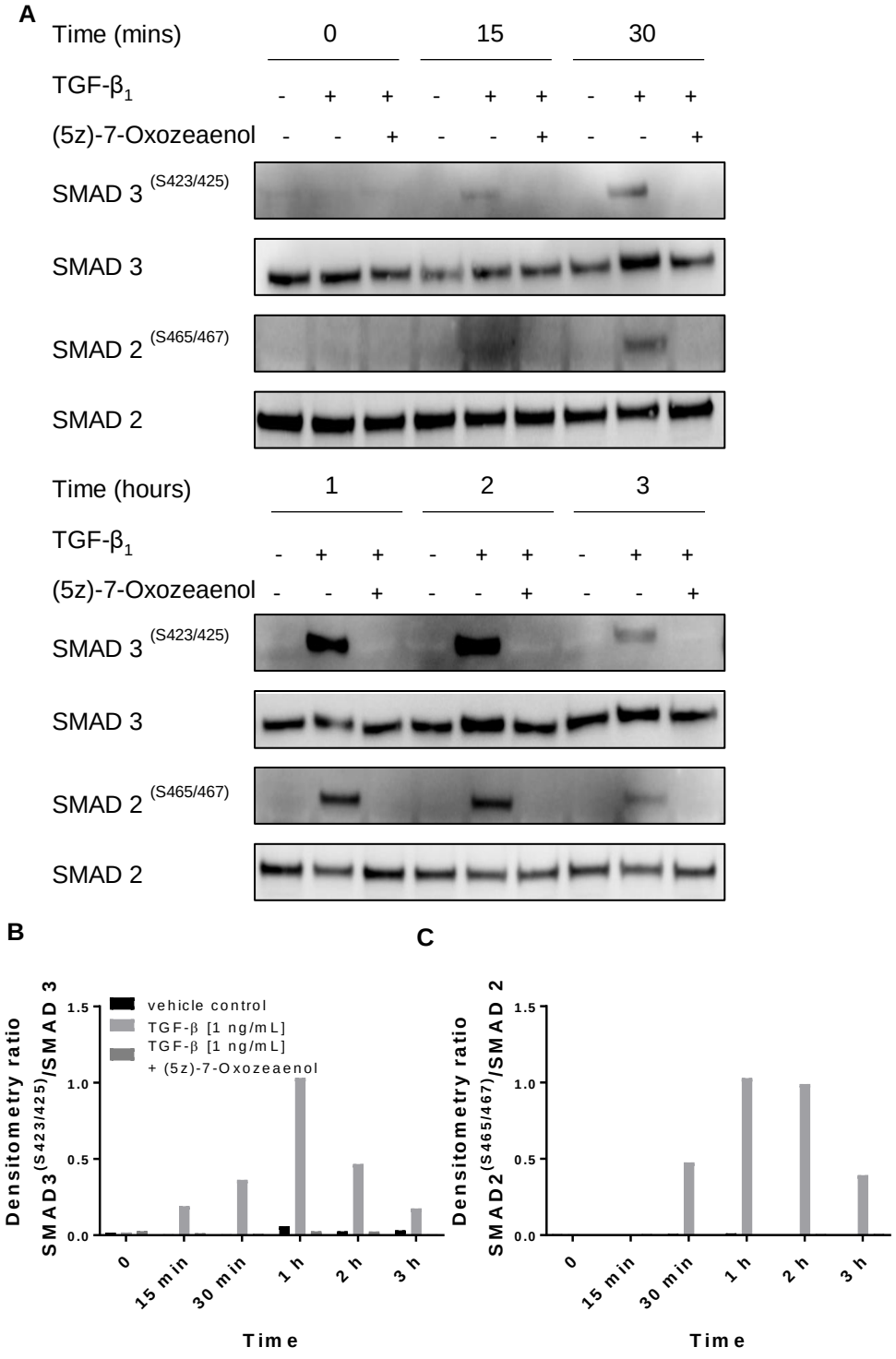

Figure 3.37: The effect of (5z)-7-Oxozeaenol on TGF-β_1 stimulation of SMAD 2 and SMAD 3 in pHLFs

Confluent pHLFs were serum-starved prior for 24 hours prior to incubation with (5z)-7-Oxozeaenol for 1 hours and then stimulation with 1 ng/mL TGF-β_1 for the indicated time-periods. Phosphorylation of SMAD 2 and SMAD 3 were assessed by western blotting.. The densitometry was calculated and plotted as a phopho-protein to total protein ratio shown in Panel B. The data is representative of two independent experiments performed

3.4.13. (5z)-7-Oxozeaenol analysis of potential targets

The inhibitory effect of (5z)-7-Oxozeaenol on TGF-β_1 stimulated collagen synthesis are likely to be mediated through the inhibition of SMAD 2 and SMAD 3 phosphorylation. One report identifies an amino acid sequence that the compound can recognise on TAK1 kinase, which makes up part of the ATP-binding pocket and is targeted by (5z)-7-Oxozeaenol (Ohori et al. 2007). The sequence needs to be similar to: **HRD**L**K**PSNLLLNTTCDLKICDFGLARVADP. The letters highlighted in **bold** are common to most MAPK's, the red C marks the important cysteine residue which needs to be approximately at position 20, from the start of that sequence, for (5z)-7-Oxozeaenol to recognise and form a covalent bond to its target (Ohori et al. 2007). This is what makes (5z)-7-Oxozeaenol an irreversible inhibitor. Table 3.2, highlights a number of MAPK's that could be targeted by this compound. Additionally, an MRC screen has clarified an activity profile of (5z)-7-Oxozeaenol inhibition including a range of proteins (Figure 3.38). It is likely however, that the compound may be inhibiting the TGF-β_1 receptor (Tan et al. 2017). Taken together, these data suggest (5z)-7-Oxozeaenol mediates its inhibition through the TGF-β_1 receptor.

Table 3.2: Indentfication of MAPK's that have the required consensus sequence and the cysteine residue required for (5z)-7-Oxozeaenol to recognise the kinase

MAPK Tier	NAME	Sequence	C residue
MAPK	MAPK1(ERK1)	HRDLKPSNLLLNTTCDLKICDFGLARVADP	Yes
	MAPK3(ERK2)	HRDLKPSNLLINTTCDLKICDFGLARIADP	Yes
	MAPK7(ERK5)	HRDLKPSNLLVNENCELKIGDFGMARGLCT	Yes p15
MAP2K	MAP2K1(MEK1)	HRDVKPSNILVNSRGEIKLCDFGVSGQLID	Yes
	MAP2K2(MEK2)	HRDVKPSNILVNSRGEIKLCDFGVSGQLID	Yes
	MAP2K3(MKK3)	HRDVKPSNVLINKEGHVKMCDFGISGYLVD	Yes
	MAP2K4(MKK4)	HRDIKPSNILLDRSGNIKLCDFGISGQLVD	Yes
	MAP2K5	HRDVKPSNMLVNTRGQVKLCDFGVSTQLVN	Yes
	MAP2K6(MKK6)	HRDVKPSNVLINALGQVKMCDFGISGYLVD	Yes
	MAP2K7(MKK7)	HRDVKPSNILLDERGQIKLCDFGISGRLVD	Yes
MAP3K	MAP3K1(MEKK1)	HRDVKGANLLIDSTGQRLRIADFGAAARLA	No
	MAP3K2	HRDIKGANILRDSTGNVKLGDFGASKRLQT	No
	MAP3K3	HRDIKGANILRDSAGNVKLGDFGASKRLQT	No
	MAP3K4(MEKK4)	HRDIKGANIFLTSSGLIKLGDFGCSVKLKNN	Yes p24
	MAP3K5(ASK1)	HRDIKGDNVLINTYSGVLKISDFGTSKRLA	No
	MAP3K6	HRDIKGDNVLINTFSGLLKISDFGTSKRLA	No
	TAK1(MAP3K7)	HRDLKPPNLLLVAGGTVLKICDFGTACDIQ	Yes
	MAP3K8	HHDIKPSNIVFMSTKAVLVDFGLSVQMTED	No
	MAP3K9	HRDLKSSNILILQKVENGDLSNKILKITDF	No
	MAP3K10	HRDLKSINILILEAIENHNLADTVLKITDF	No
	MAP3K11	HRDLKSNNILLLQHIESDDMEHKTLKITDF	No
Serine/Threonine kinase	ALK5	HRDLKSKNILVKKNGTCCIADLGLAVRHD	P17 and P18

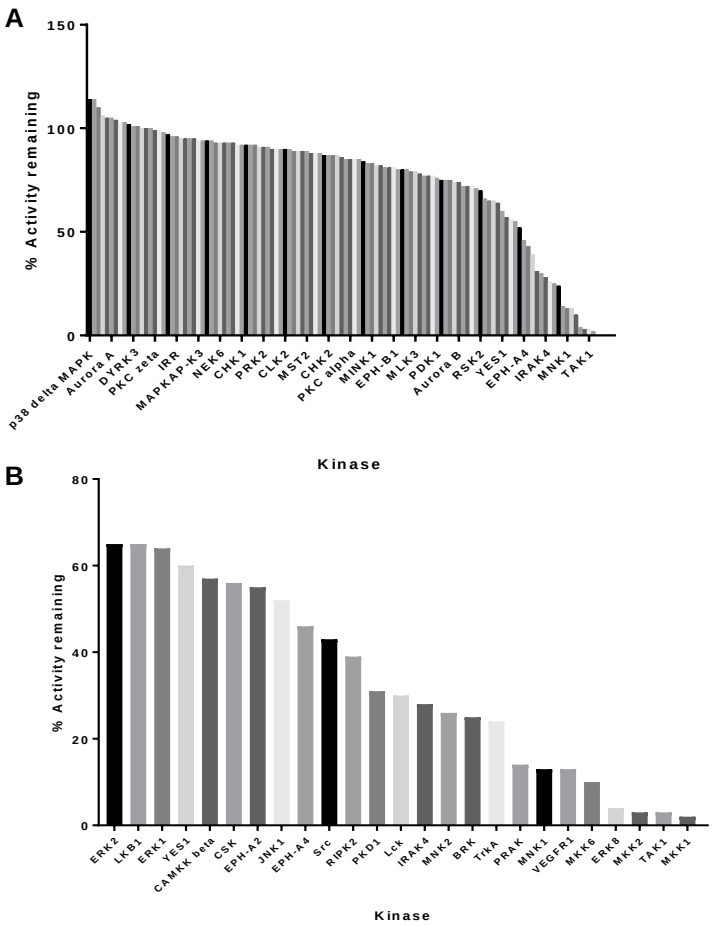

Figure 3.38: (5z)-7-Oxozeaenol inhibition of a panel of kinases

In a cell free assay the MRC have screen hundreds of kinases and quantified their activity in the presence of the inhibitor (5z)-7-Oxozeanol at 1 μM, Panel A is all the kinases plotted. Panel B, zoomed in on the most inhibited kinases. The data was taken from the screen from the website: http://www.kinase-screen.mrc.ac.uk/kinase-inhibitors last assessed: 11/9/18 and plotted as a graph in Graphpad prism 7.0.

Having established that MK2 does not mediate the effects of TGF-β_1 stimulated mTORC1 activation and collagen synthesis, there were other kinases capable of inhibiting the TSC1/2 complex to consider. The effects of inhibitors on each of these kinases were investigated to quantify their effects on TGF-β_1 stimulated mTORC1 activity and collagen I synthesis.

3.4.14. CDK1

CDK1 is well documented for its role in cell cycle progression, which was demonstrated by the inhibition of CDK1 which stopped cell division and the expansion of the pHLF population (Enserink & Kolodner 2010). This mechanism was used to investigate whether the inhibitor of CDK1 was engaging its target. The click-it assay measures newly synthesised DNA to

detect changes in cell proliferation. The click-it assay works by using EDU (5-Ethynyl-2'-Deoxyuridine) which incorporates itself into newly synthesised DNA. A fluorescent azide dye detects the EDU and the fluorescent signal can be quantified. Using the click-it assay, cell proliferation in the presence of the compound, BMS-265246, when stimulated with FBS (used to promote cell proliferation) was assessed. PHLFs were grown to 50% confluence before starving for 24 hours (Figure 3.39). This stops the cells from any further proliferation and allows any treatment that inhibits proliferation to be detected when the cells are reintroduced to FBS. Following the starvation period, cells were incubated with 3 concentrations of BMS-265246 (0.01, 0.1 and 1 μM) for one hour prior to being stimulated with 10% FBS for 24 hours, in addition, the EDU reagent is spiked into the wells to allow it to be incorporated into any proliferating cells. The effect of BMS-265246 treatment was demonstrated to inhibit FBS stimulated cell proliferation in a concentration dependent manner. The vehicle treated cells demonstrate a clear increase when comparing between FBS treated and non-FBS treated cells. At the top concentration of BMS-265246, 1 μM, no cell proliferation was observed when compared to baseline and this was approximately 3.5 fold less proliferation when compared to the FBS treated vehicle control. Therefore, this suggests BMS-265246 [1 μM] completely inhibits CDK1.

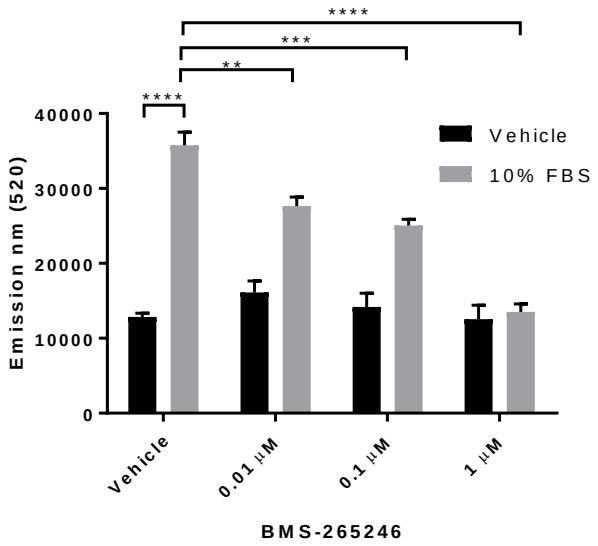

Figure 3.39: The effect of BMS-265246 on FBS induced pHLF proliferation

pHLF were grown to 50% confluence before starving them for 24 hours. The cells were then incubated with BMS-265246 [1 μM] with or without 10% FBS for 40 hours (control cells received 0.1% DMSO). Cells were then incubated with click-it buffer for 8 hours before fixing in methanol. Click-IT assay buffer was then added to the cells after fixation and the emission at 520 was read to determine the change in proliferation between conditions (n=4 replicates). Differences between groups were evaluated with two-way ANOVA and Tukey multiple comparison testing.

The inhibition of CDK1 on TGF-β_1 stimulated 4E-BP1 phosphorylation was investigated (Figure 3.40). Treatment of pHLFs with BMS-265246 had no impact on $4EBP^{T37/46}$ (Figure 3.40A and B), whereas in contrast BMS-265246 treatment increased both basal and TGF-β_1 treated $4E\text{-}BP1^{S65}$ stimulation (Figure 3.40A and C). BMS-265246 treatment also increased basal levels of $4E\text{-}BP1^{T70}$ phosphorylation (Figure 3.40A and D). This data suggests that CDK1 regulates mTORC1 independent of TGF-β_1 stimulation.

In parallel to this, the effects of the compound were assessed on TGF-β_1 stimulated collagen synthesis in the collagen deposition assay (Figure 3.41). BMS-265246 did not inhibit TGF-β_1 stimulated collagen synthesis. There were no changes in the collagen I synthesis in non-TGF-β_1 stimulated cells. Collectively, this suggests that TGF-β_1 does not engage CDK1 to regulate mTORC1 activation or collagen I synthesis. Taken together the inhibitor had no impact on collagen deposition and increased 4E-BP1 signalling

independent of TGF-β_1 stimulation, therefore, it is not likely to play a role in regulating the inhibition of TSC1/2 in response to TGF-β_1 stimulation.

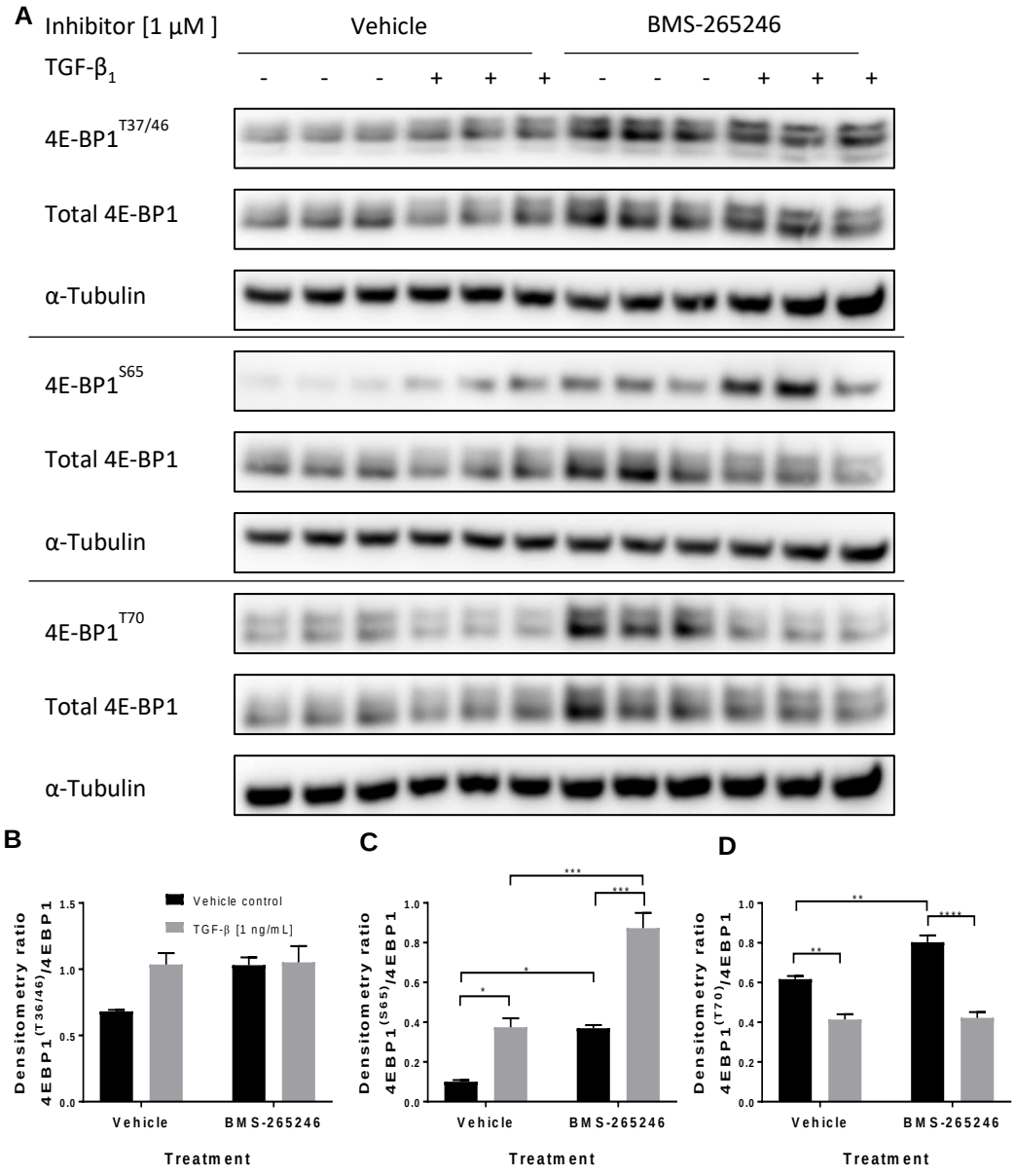

Figure 3.40: The effect of BMS-265246 on TGF-β_1 stimulated 4E-BP1 phosphorylation in pHLFs

Confluent pHLFs were serum-starved prior for 24 hours prior to incubation with BMS265246 for 1 hours followed by stimulation with 1 ng/mL TGF-β_1 for 3 hours. The phosphorylation of 4E-BP1$^{37/46}$, 4E-BP1^{S65} and 4E-BP1^{T70} were assessed by western blotting. Protein loading was verified by blotting with anti- α-tubulin antibody. The densitometry (panels B-D) was calculated and plotted as a phospho-protein to total protein ratio. These data are representative of two independent experiments performed.

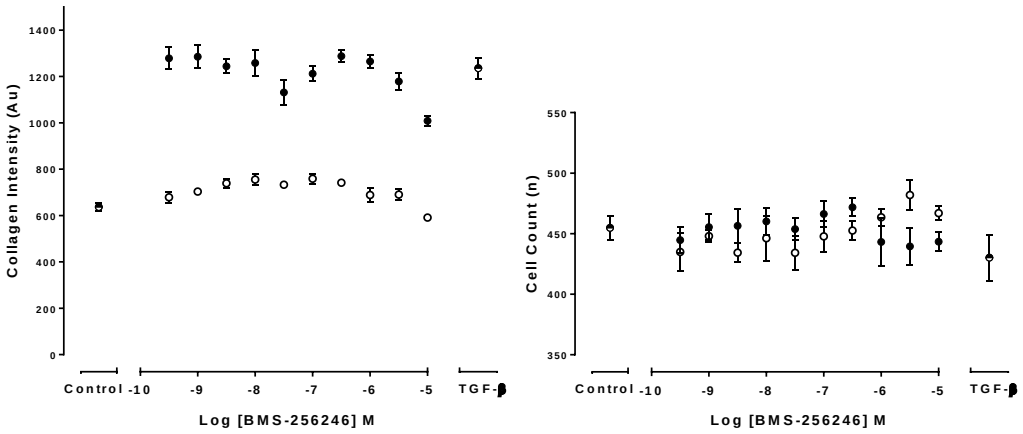

Figure 3.41: The effect of BMS-256246 on TGF-β_1 stimulated collagen I synthesis in pHLF

Confluent pHLFs were starved for 24 hours before being incubated with increasing concentrations of BSM-256246 (vehicle controls were incubated with 0.1% DMSO) in DMEM containing Ficoll for 1 hour. Following incubation cells were treated with or without TGF-β_1 [1 ng/mL] which was spiked into the wells and incubated for 48 hours, prior to fixation and staining for type1 collagen (left column) and cell counts (right column) were obtained from a DAPI counter stain. Data are expressed as mean fluorescent intensity or cell count (n=4 reads per well) averaged across 4 replicates. These data are representative of two independent experiments. Replicate data is shown in Appendix 10.

3.4.15. MEK1/2

MEK1/2 are the direct upstream kinases responsible for mediating ERK1/2 phosphorylation. To investigate if ERK1/2 is required for TGF-β_1 stimulated mTORC1 activation and collagen I synthesis MEK1/2 was targeted with an inhibitor, since the compounds available were more selective and potent. To ensure that MEK1/2 was inhibited and therefore ERK1/2, ERK1/2 phosphorylation was investigated when treated with the inhibitor. The loss of ERK1/2 phosphorylation would suggest that MEK1/2 was inhibited and can no longer phosphorylate its substrate ERK1/2 compounds. Therefore, suggesting the compound is able engage its target MEK1/2. TGF-β_1 treatment increased the phosphorylation of ERK1/2. The treatment with AS703026 completely abolished the phosphorylation of vehicle and TGF-β1 treated cells. A decrease of approximately 10-fold in ERK1/2 phosphorylation was seen for the compound when comparing the TGF-β_1 treated control and TGF-β_1 treated cells with compound (Figure 3.42).

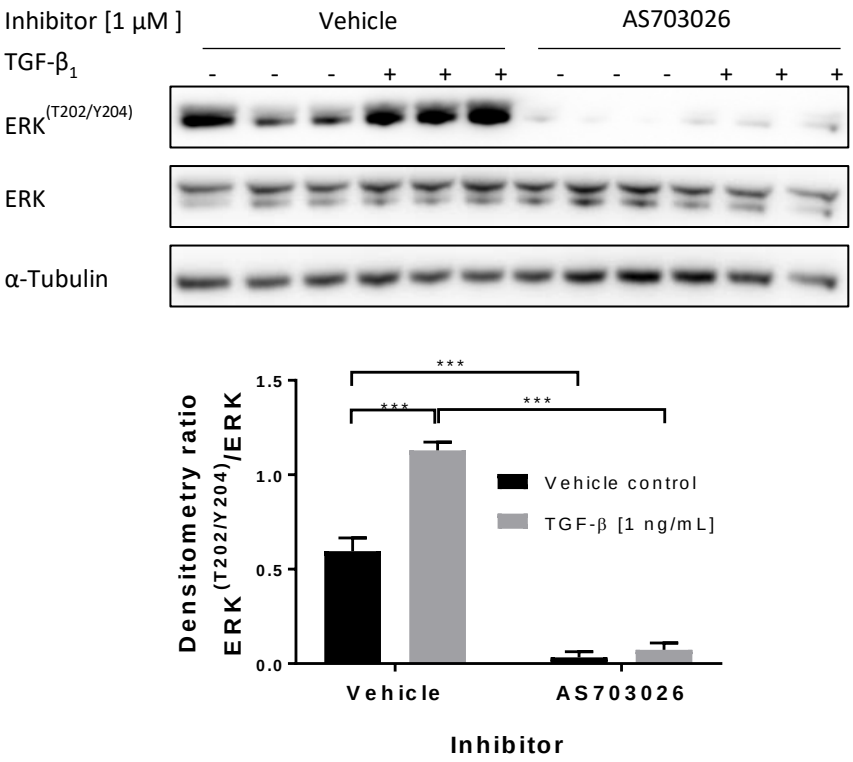

Figure 3.42: The effect of AS703026 on TGF-β_1 stimulated collagen I synthesis in pHLF

Confluent pHLFs were serum-starved prior for 24 hours prior to incubation with AS703026 for 1 hours followed by stimulation with 1 ng/mL TGF-β_1 for 3 hours. The phosphorylation of ERK1/2 were assessed by western blotting. Protein loading was verified by blotting with anti- α-tubulin antibody. The densitometry was calculated and plotted as a phopho-protein to total protein ratio. The data is representative of two independent experiments performed.

The previous experiment demonstrated that AS703026 engages its target kinase MEK1/2 in the pHLFs. The effect of MEK1/2 (ERK1/2) inhibition with AS703026, on TGF-β_1 stimulated 4E-BP1 was investigated (Figure 3.43A). AS703026 had a marginal amount of inhibition on the 4E-BP1$^{T37/47}$ site (Figure 3.43A and B). It did not inhibit TGF-β_1 stimulated phosphorylation of 4E-BP1^{S65} (Figure 3.43A and C). Finally, it led to the increase in 4E-BP1^{T70} phosphorylation in TGF-β_1 treated cells (Figure 3.43A and D). Taking the three sites together, the western blots suggest inhibition of the ERK kinase alone does not affect TGF-β_1 stimulated 4E-BP1 phosphorylation.

The effect of the compound was also assessed in the collagen deposition assay (Figure 3.44). Treatment with AS703026 did not inhibit the TGF-β_1 stimulated increase in collagen I deposition, Figure 3.44. However, in vehicle treated cells in the presence of AS703026, the top two concentrations showed a small increase in collagen deposition. This suggests that ERK1/2 is not

required for TGF-β_1 stimulated collagen deposition. Taken together the inhibitor had no impact on TGF-β_1 stimulated collagen deposition or 4EBP1 signalling, therefore, it is not likely to play a role in inhibiting TSC1/2 in response to TGF-β_1 stimulation.

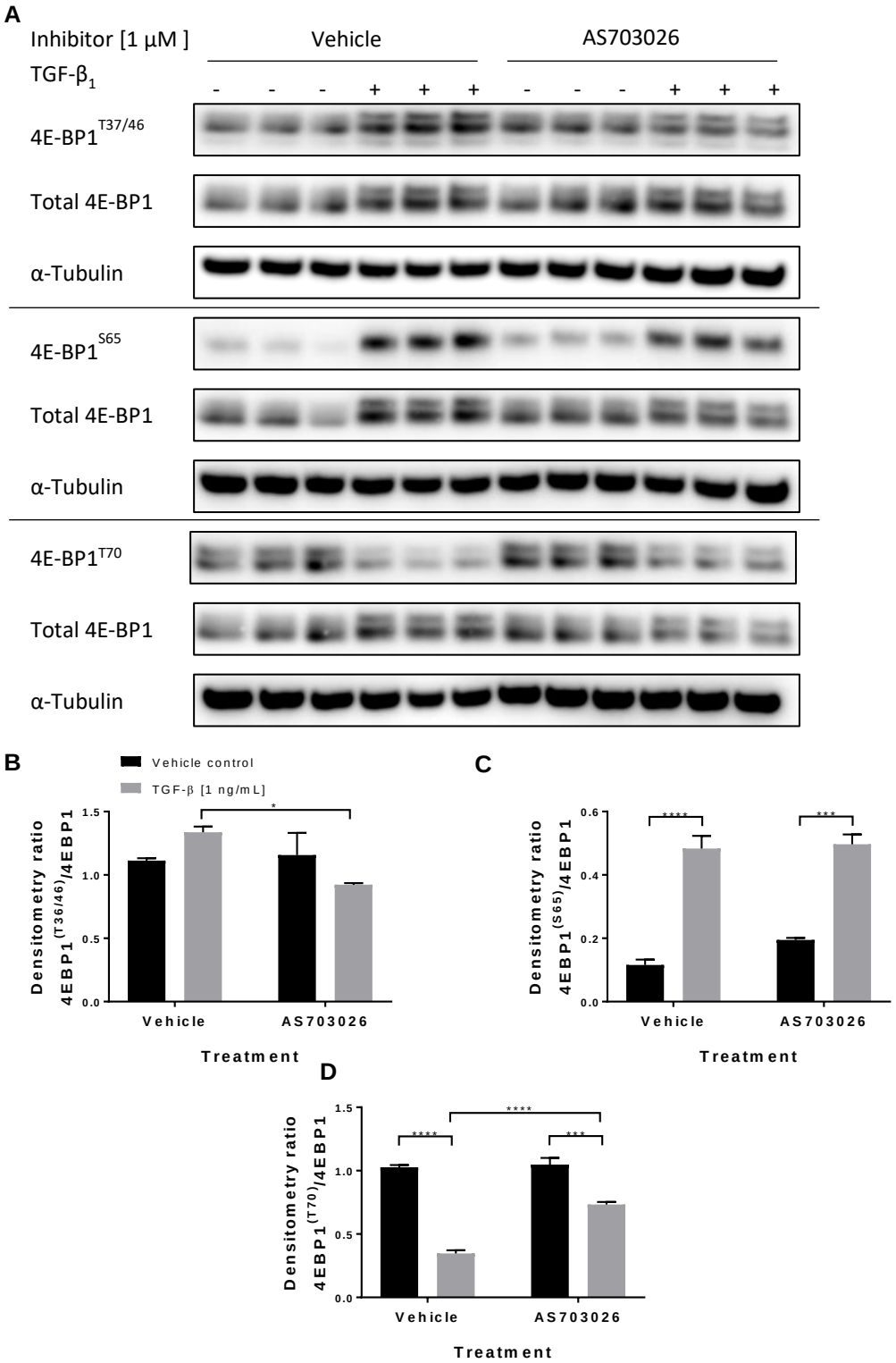

Figure 3.43: The effect of AS703026 on TGF-β_1 stimulated 4E-BP1 phosphorylation in pHLFs

Confluent pHLFs were serum-starved prior for 24 hours prior to incubation with AS703026 for 1 hours followed by stimulation with 1 ng/mL TGF-β_1 for 3 hours. The phosphorylation of 4E-BP1$^{37/46}$, 4E-BP1^{S65} and 4E-BP1^{T70} were assessed by western blotting. Protein loading was verified by blotting with anti- α-tubulin antibody. The densitometry (panels B-D) was calculated and plotted as a phopho-protein to total protein ratio. These data are representative of two independent experiments performed.

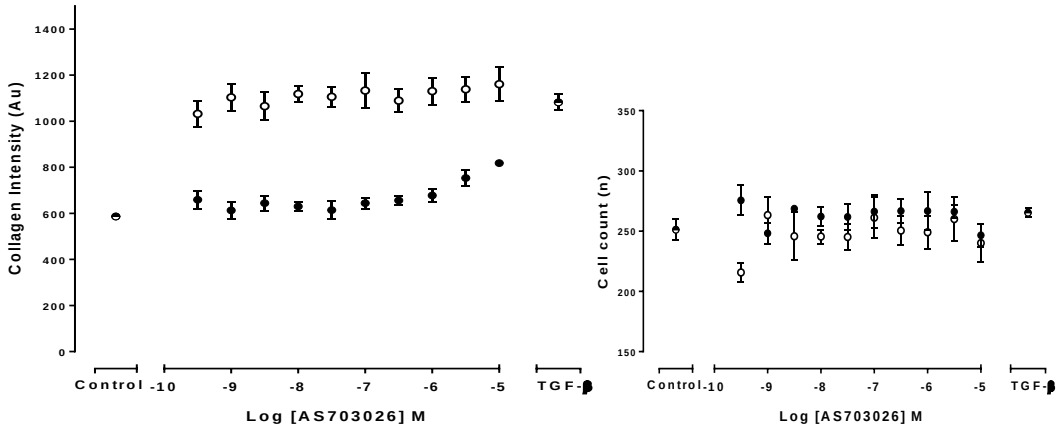

Figure 3.44: The effect of AS703026 on TGF-β_1 stimulated collagen I synthesis in pHLF

Confluent pHLFs were starved for 24 hours before being incubated with increasing concentrations of AS703026 (vehicle controls were incubated with 0.1% DMSO) in DMEM containing Ficoll for 1 hour. Following incubation cells were treated with or without TGF-β_1 [1 ng/mL] which was spiked into the wells and incubated for 48 hours, prior to fixation and staining for type1 collagen (left column) and cell counts (right column) were obtained from a DAPI counter stain. Data are expressed as mean fluorescent intensity or cell count (n=4 reads per well) averaged across 4 replicates. These data are representative of two independent experiments. Replicate data is presented as Appendix 11

3.4.16. RSK1

RSK is a substrate of ERK1/2, but it can also be activated by other ERK such as ERK5. To ensure that RSK was not acting independently from ERK1/2 activation, RSK was inhibited using the compound SL0101. RSK, like CDK1, has been implicated in regulating cell proliferation, so the click-it assay was used, as before (Figure 3.39), to test the effects of the compound on cell proliferation and ensure that SL0101 engaged its target, RSK (Figure 3.45). Treatment of pHLFs with SL0101 inhibited FBS stimulated pHLF proliferation at the top two concentrations 0.1 and 1 μM. This suggests that the compound was engaging its target mechanism by inhibiting RSK to which prevented cell proliferation.

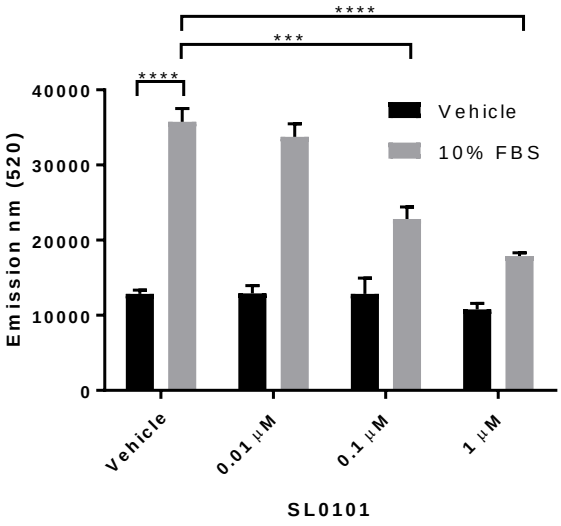

Figure 3.45: The effect of SL0101 on FBS induced pHLF proliferation

pHLF were grown to 50% confluence before starving them for 24 hours. The cells were then incubated with SL0101 [1 μM] with or without 10% FBS for 40 hours (control cells received 0.1% DMSO). Cells were then incubated with click-it buffer for 8 hours before fixing in methanol. Click-IT assay buffer was then added to the cells after fixation and the emission at 520 was read to determine the change in proliferation between conditions (n=4 replicates). Differences between groups were evaluated with two-way ANOVA and Tukey multiple comparison testing

To investigate the effect of RSK1 inhibition on TGF-β_1 stimulated 4E-BP1 phosphorylation, pHLFS were incubated with SL0101 (Figure 3.46A). Treatment with SL0101 did not inhibit TGF-β_1 stimulated 4E-BP1$^{T37/46}$ or 4E-BP1^{T70} phosphorylation (Figure 3.46A, B and D). In contrast, SL0101 increased basal and TGF-β_1 stimulated phosphorylation of 4E-BP1^{S65}, (Figure 3.46A and C).

The effect of the compound was also assessed in the collagen deposition assay. Treatment with SL0101 did not inhibit the TGF-β_1 stimulated increase in collagen I deposition (Figure 3.47). In addition, the SL0101 inhibitor had no effect on the baseline collagen synthesis. This suggests that inhibition of RSK alone is not sufficient to inhibit TGF-β_1 stimulated collagen synthesis. Taken together these data demonstrate SL0101 had no impact on TGF-β_1 stimulated collagen deposition or 4EBP1 phosphorylation, therefore, it is not likely to play a role in inhibiting TSC1/2 in response to TGF-β_1 stimulation.

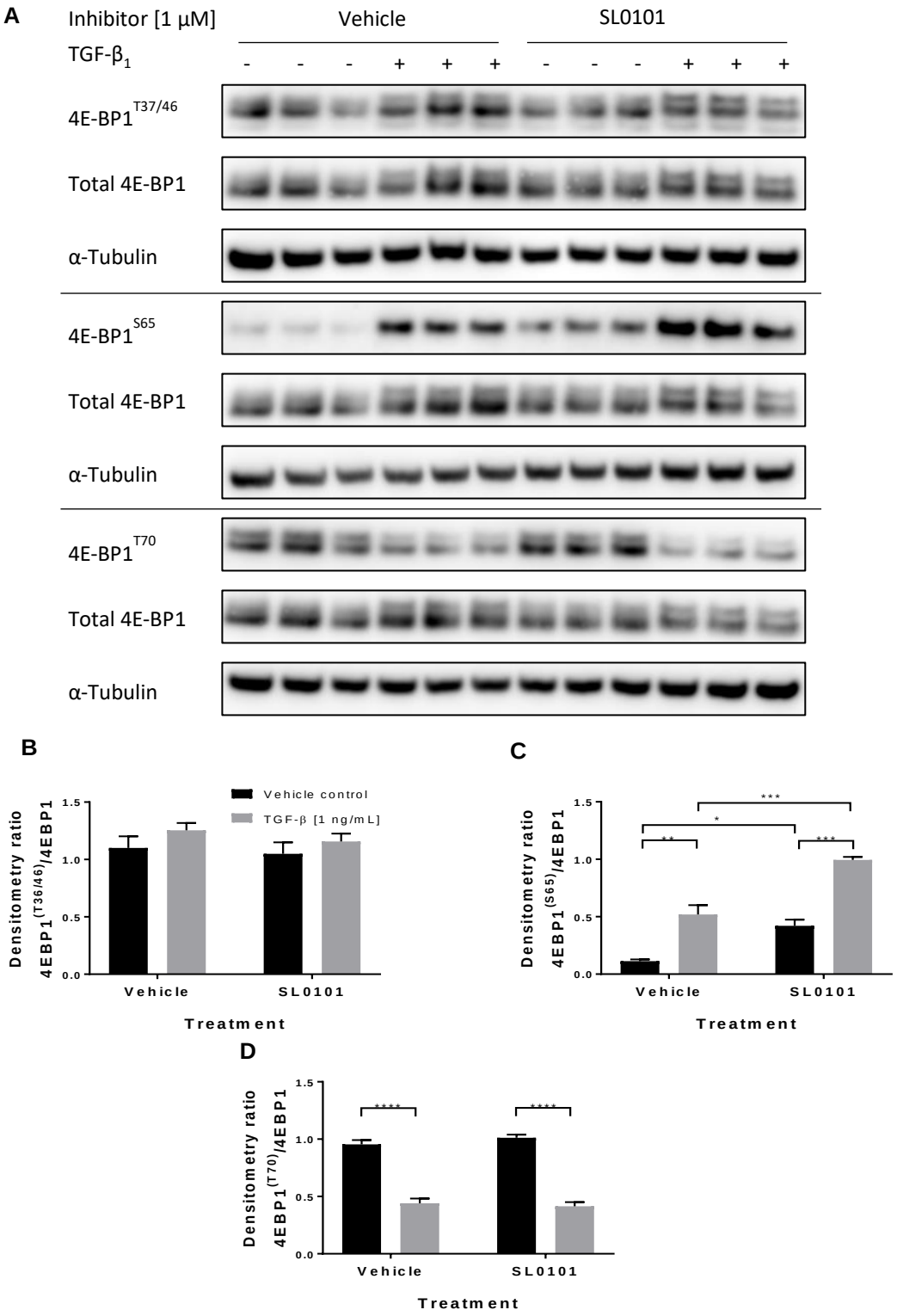

Figure 3.46: The effect of SL0101 on TGF-β_1 stimulated 4E-BP1 phosphorylation in pHLFs

Confluent pHLFs were serum-starved prior for 24 hours prior to incubation with SL0101 for 1 hours followed by stimulation with 1 ng/mL TGF-β_1 for 3 hours. The phosphorylation of 4E-BP1$^{37/46}$, 4E-BP1^{S65} and 4E-BP1^{T70} were assessed by western blotting. Protein loading was verified by blotting with anti- α-tubulin antibody. The densitometry (panel B-D) was calculated and plotted as a phopho-protein to total protein ratio. These data are representative of two independent experiments performed.

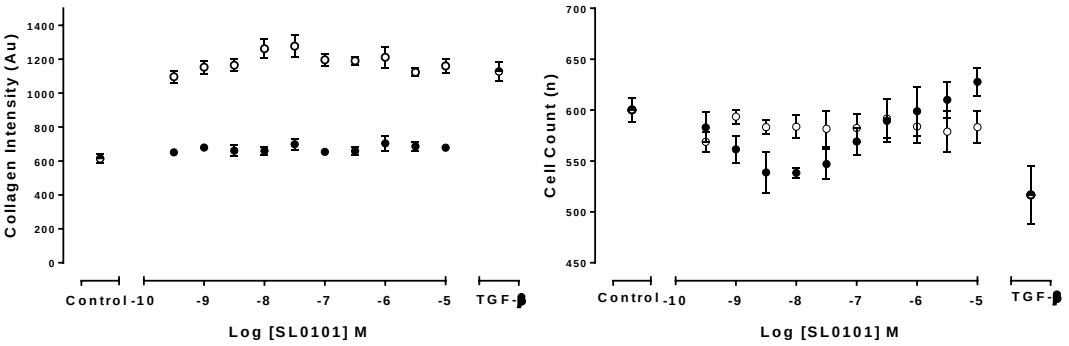

Figure3.47: The effect of SL0101 on TGF-β_1 stimulated collagen I synthesis in pHLF

Confluent pHLFs were starved for 24 hours before being incubated with increasing concentrations of AS703026 (vehicle controls were incubated with 0.1% DMSO) in DMEM containing Ficoll for 1 hour. Following incubation cells were treated with or without TGF-β_1 [1 ng/mL] which was spiked into the wells and incubated for 48 hours, prior to fixation and staining for type1 collagen (left column) and cell counts (right column) were obtained from a DAPI counter stain. Data are expressed as mean fluorescent intensity or cell count (n=4 reads per well) averaged across 4 replicates. This is representative of two independent experiments. See Appendix 12 for replicate data

Each of the compounds had no impact on collagen synthesis, even at concentration 10-fold higher than that used to engage their target kinases. The compound AS703026, did seem to have some effects on the phosphorylation of 4E-BP1 going against the effect of TGF-β_1 on 4E-BP1^{T70} phosphorylation and inhibited marginally the 4E-BP1$^{T37/46}$ site. It was possible that the signalling was compensated by other kinases. A combination of the PI3K inhibitor and MEK1/2 inhibitor was used to assess the effects on collagen synthesis. The combination compound 12 [1 μM] of and a dose response curve of AS703026 had no impact on TGF-β_1 stimulated collagen synthesis (Figure 3.48). Therefore, this demonstrated that the inhibition of PI3K and ERK1/2 together does not in inhibit TGF-β_1 stimulated collagen I synthesis.

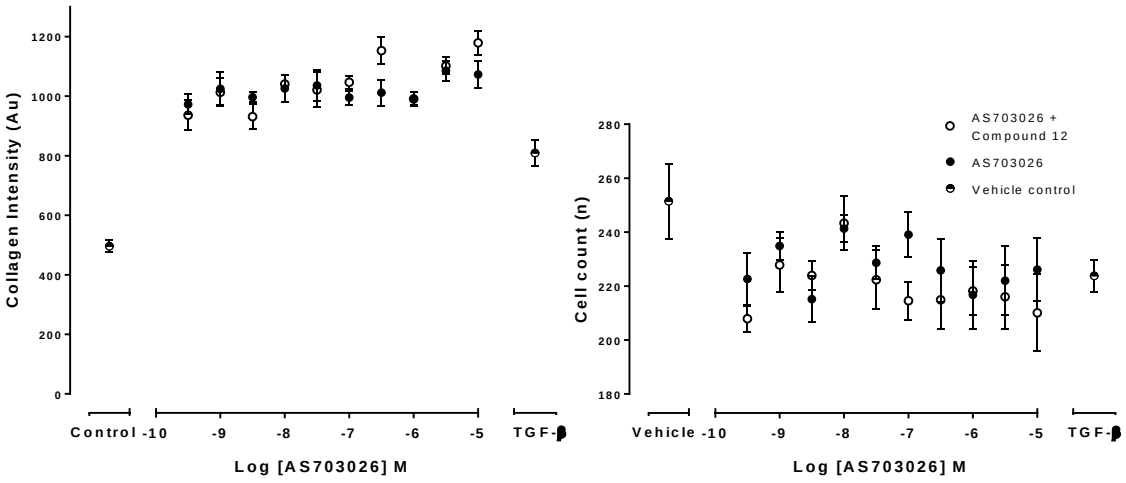

Figure 3.48: The effect of combined inhibition with AS703026 and compound 12 on TGF-β_1 stimulated collagen I synthesis in pHLF

Confluent pHLFs were starved for 24 hours before being incubated with increasing concentrations of AS703026 with or without compound 12 [1 μM] in DMEM containing Ficoll for 1 hour. Following incubation cells were treated with or without TGF-β_1 [1 ng/mL] which was spiked into the wells and incubated for 48 hours, prior to fixation and staining for type1 collagen (left column) and cell counts (right column) were obtained from a DAPI counter stain. Data are expressed as mean fluorescent intensity or cell count (n=4 reads per well) averaged across 4 replicates. These data are representative of two independent experiments.

3.4.17. Summary

- TSC1/2 regulates mTORC1 activity in pHLFs
- RHEB is required for TGF-β_1 stimulated mTORC1 activation and collagen I synthesis
- (5z)-7-Oxozeaenol inhibits TGF-β_1 stimulated mTORC1 activation and collagen I synthesis but these effects are not mediated by the inhibition of TAK1 since the siRNA knock-down and NG25 shows no effect
- (5z)-7-Oxozeaenol inhibits collagen I synthesis and mTORC1 activation by inhibiting the TβRI/TβRII receptor complex and preventing SMAD 2 and SMAD 3 phosphorylation
- P38 MAPK and MK2 are not required for TGF-β_1 stimulated collagen synthesis
- Pharmacological inhibition of ERK, CDK1 and RSK1 does not inhibit TGF-β_1 stimulated mTORC1 activation or collagen I synthesis
- Combined inhibition of PI3K and ERK does not inhibit TGF-β_1 stimulated collagen I synthesis

4. Discussion

4.1. Introduction

Idiopathic pulmonary fibrosis (IPF) is an interstitial lung disease characterised by an aberrant wound healing response believed to be caused by repetitive epithelial lung injury, however, the exact aetiology still remains unknown. The IPF lung is characterised by the chronic production of extracellular matrix, in particular collagen I.

TGF-β_1 is central to the pathogenesis of IPF and promotes the recruitment, proliferation and differentiation of fibroblasts and causing type I epithelial cell apoptosis. This subsequently releases more pro-fibrotic mediators which perpetuate the aberrant wound healing response.

Understanding the core TGF-β_1 signalling pathways underlying the differentiation of the fibroblast to the myofibroblast and the synthesis of collagen I and may provide novel opportunities for therapeutic intervention.

Our understanding of TGF-β_1 signalling has grown. SMAD 3 signalling is the transcriptional driver of several matrix genes including *COL1A1* and *COL1A2*. We and others have identified mTORC1 downstream of TGF-β_1 is a key axis required for collagen I deposition. However, the signalling pathway between TGF-β_1 stimulation and mTORC1 activation in pHLFs is unknown. This pathway is critical for controlling downstream pathways that lead to the translation of the collagen I mRNA, this still needs further investigation (Woodcock et al. 2019). Our understanding of this pathway has lead us to believe that mTORC1 by inhibiting 4EBP1 allows for a critical protein(s) to be translated which is then sufficient to promote collagen I mRNA translation. Our investigations in pHLFs and their response to TGF-β_1 demonstrate that mTORC1 is activated at as early as 3 hours and this activation is prolonged for 48 hours post-stimulation (Woodcock et al. 2019). During this time our group has highlighted several TGF-β stimulated, mTORC1 dependent pathways including the upregulation of ATF4 which is essential for collagen I deposition (Selvarajah, unpublished data also see Figure 3.11). The pathway between TGF-β_1 activating the pHLFS TβRI/TβRII receptors at the membrane and the internal signal that leads to mTORC1 remains unknown. Several

groups believe that the PI3K/AKT axis is important for mTORC1 activation (Hinault et al. 2004; Yoon et al. 2011; Garami et al. 2003), however, others have highlighted other mechanisms for mTORC1 activation (Carrière et al. 2008; Y. Li et al. 2003). Critically, our group has highlighted that this pathway which promotes mTORC1 activation and collagen I synthesis is independent of PI3K/AKT in TGF-β_1 stimulated pHLF activation. Therefore, identifying the pathway was a key focus of my research.

During the course of my thesis, work in pHLFs using the inhibitory compounds 12 (PI3K) and MMK205 (AKT) has confirmed that TGF-β_1 stimulated mTORC1/mTORC2 activation and collagen I synthesis is PI3K and AKT independent. However, the mTOR inhibitor AZD8055 inhibits TGF-β_1 stimulated collagen I synthesis. Previously, it was unknown which mTOR complex was mediating the synthesis of collagen in response to TGF-β_1 stimulation. mTORC1 was identified as the critical complex. This was demonstrated by the inhibition of mTORC2 associated AGC kinases, such as SGK1. When AGC kinases were inhibited, there was no effect on collagen I synthesis. Furthermore, the mTORC1 substrate 4E-BP1 was demonstrated to be an inhibitor of collagen synthesis, likely by preventing the translation of 'protein X' which is required for the mediation of translation *COL1A1* mRNA (Woodcock et al. 2019). mTORC1 is required in response to TGF-β_1 to hyper-phosphorylate 4E-BP1 to promote translation and subsequently lead to the downstream synthesis of collagen I. The other mTORC1 substrate P70S6K was identified to not be required for translation. Our group investigated P70S6K inhibition (the inhibitor used was LY2584702) and demonstrated that it's inhibition did not inhibit TGF-β_1 stimulated collagen synthesis (Woodcock et al. 2019). The critical experiment conducted by our group that identified 4E-BP1 inhibition was required for collagen synthesis was through the use of siRNA. This experiment demonstrated that AZD8055 inhibited mTORC1 mediated collagen I synthesis but this could be recovered by siRNA knock-down of 4E-BP1 (since 4E-BP1 is an inhibitor of translation).

Investigations are on-going to identify which 4E-BP1 phosphorylation sites are critical for its inhibition and are required for TGF-β_1 to stimulate translation. The important phosphorylation sites have begun to be delineated through the

comparison between the treatments with either AZD8055 or rapamycin. In addition, investigation of point-mutations of each site may yield information on which sites are important for inhibiting 4EBP1 to allow for the downstream regulation for COL1A1 mRNA through a factor which is still to be discovered. However, a large gap in our knowledge still remained which was the signalling pathway between TGF-β_1 stimulation and mTORC1 activation.

Hypothesis: TGF-β activates mTORC1 to promote collagen I deposition in pHLFs through SMAD dependent and PI3K/AKT independent pathways

Aims:

- **To identify a TGF-β_1 sensitive phosphorylation site on mTOR that temporally correlates with mTORC1 substrate phosphorylation**
- **Investigate the cross-talk between SMAD 3 and mTORC1 activation downstream of TGF-β_1 using siRNA approaches**
- **To identify the importance of the TSC1/2 complex and investigate the kinases capable of inhibiting this complex to delineate their role in TGF-β_1 mediated mTORC1 activation and collagen I synthesis using genetic and pharmacological approaches**

4.2. The mechanisms of TGF-β_1 induced mTOR phosphorylation in pHLFs

4.2.1. Introduction

The mTOR kinase has three phosphorylation sites in its regulatory domain, T2446, S2448 and S2481 and this domain is known to regulate mTOR activity (Sekulić et al. 2000). The S2481 and S2448 are the better characterised sites and have often been used as markers for mTOR kinase activity. In contrast the T2446 is used as a marker for mTOR inhibition. The S2481 site has been mainly linked with mTORC2 activity or auto-kinase activity and the S2448 is linked with mTORC1 activity. Both sites can be phosphorylated in response to the same stimuli such as follicle stimulating hormone (FSH), PDGF-BB and insulin (Chen et al. 2002; Cong et al. 2018; Copp et al. 2009). The S2481 and

S2448 sites are also responsive to TGF-β_1 (Chen et al. 2002). T2446 had been characterised by others that in response to inhibitory stimuli such as AICAR, DNP, decrease in amino acids or an increase in adenosine monophosphate (AMP), leads to the activation of AMPK (Cheng et al. 2004; Abooali et al. 2015). The increase in AMPK activity leads to mTOR phosphorylation at the T2446 site which leads to a decrease in downstream mTOR substrate phosphorylation (mTOR inhibition) (Cheng et al. 2004).

In this study, the phosphorylation pattern of all three residues was investigated in response to TGF-β_1 over a 24 hour periods. The TGF-β_1 responsive site, S2448, was investigated further and the signalling pathways for its phosphorylation were identified and its likely redundancy for collagen I synthesis.

4.2.2. The temporal phosphorylation profile of the mTOR kinase regulatory domain

The results outlined in Figure 3.2 demonstrated the temporal time-course of the phosphorylation of three mTOR phosphorylation sites (S2481, S2448 and T2446).

The T2446 site was not TGF-β_1 sensitive. There have been no previous reports of T2446 sensitivity to TGF-β_1. Previous evidence reports T2446 is strongly linked to increased AMPK activity and depleted amino acid levels (Cheng et al. 2004). To support my data and demonstrate that this was likely to be an inhibitory site, I demonstrated that nutrient starvation or cell stress increased T2446 phosphorylation. Interestingly, since this site is a marker for AMPK or amino acid deprivation, it would not have been unexpected to demonstrate that T2446 phosphorylation is increased at later time points in pHLFs post TGF-β_1 stimulation. As a result this may suggest that the pHLFs amino acid depletion does not decrease sufficiently to inhibit mTORC1 in pHLFs and this may be the result of the amino acid levels being sufficiently maintained. The mechanism by which T2446 was being phosphorylated in PBS treated conditions was not investigated because TGF-β_1 stimulation had no impact on T2446 phosphorylation. Therefore, this mechanism was not felt to be relevant to IPF which is a TGF-β_1 driven disease.

The S2481 site on mTOR demonstrated some sensitivity to TGF-β_1 stimulation with an observable increase in phosphorylation at 6 and 12 hours. Previous reports have demonstrated that S2481 is TGF-β_1 sensitive in rat granuloma cells (Chen et al. 2002). However, S2481 phosphorylation observed here did not coincide with the early activation of mTORC1 (observed by the phosphorylation of its substrates) and reports have attributed S2481 to mTORC2 autocatalytic activity because in immunoprecipitation studies RICTOR, but not RAPTOR, is pulled down with S2481 (Copp et al. 2009). mSIN1, a protein that binds to mTOR to form part of the mTORC2 complex, is required for S2481 phosphorylation. In mSIN1 knock-down MEFs, S2481 phosphorylation is inhibited (Copp et al. 2009). This suggests that the phosphorylation I observed is associated with mTORC2 and not mTORC1 activation.

With respect to the role of mTORC2 during TGF-β_1 stimulated collagen synthesis, our group has strong evidence to support that mTORC1 mediates it's effects through the inhibition of 4E-BP1 and is therefore mTORC2 independent (Woodcock et al. 2019). This evidence of mTORC2 independence is supported by our group's demonstration that collagen inhibition with AZD8055 is recovered by 4E-BP1 knock-down in TGF-β_1 stimulated pHLFs. Since this site shows late activation and is linked to mTORC2 activity, there was not enough evidence to support that S2481 was required for early mTORC1 activation or collagen I synthesis. Therefore, S2481 phosphorylation would not inform about the TGF-β_1 stimulated pathways required for early mTORC1 activation in TGF-β_1 mediated collagen synthesis.

Further research into this site in the future may still be informative. The temporal disconnect between S2448 and S2481 phosphorylation might allow mTORC1 and mTORC2's functions to be separated, which is often difficult to achieve because there is no selective tool for mTORC2 and the selective mTORC1 compound rapamycin is only a partial inhibitor. In addition, in our pHLFs, mTORC1 and mTORC2 substrates are activated by TGF-β_1 at the same time making the functional separation between the two even more difficult.

In contrast, the phosphorylation of S2448 was induced by TGF-β_1 at the early time point of 3 hours. The phosphorylation of S2448 correlates well with the mTORC1 substrate phosphorylation time-course, Figure 3.2. In contrast, other reports have demonstrated increases in S2448 phosphorylation at earlier time-points. In HEK293 cells which were stimulated with 200 nM of insulin demonstrated increased mTOR S2448 phosphorylation was captured at 5 minutes (Copp et al. 2009). In contrast NSCLC cells and mesenchymal stem cells had increased S2448 phosphorylation in response to stimulation with 20 ng/mL of TGF-β_1 at 30 minutes and 60 minutes, respectively (Cong et al. 2018; Cooper et al. 2017). These differences may be explained by the use of different cell types and the use of stimuli. Additionally, the use of high TGF-β_1 concentrations (20 ng/mL) is likely to be driven by increased receptor occupancy (Dijke & Hill 2004). These high concentrations are not required within our cells since the peak of collagen synthesis in pHLFs cells and at 1 ng/mL TGF-β_1. Although differences in timings were found for the phosphorylation of mTORC1, the temporal phosphorylation aligns well with what was expected. Therefore, I investigated the mechanisms of S2448 phosphorylation with the concept that it may play a functional role during early mTORC1 activation and shed light on the upstream pathways required for mTORC1 activation.

4.2.3. Pharmacological interrogation delineates the mechanisms of TGF-β_1 induced S2448 phosphorylation

The mechanism of TGF-β_1 stimulated S2448 phosphorylation has not been delineated and most literature has only implied this site is AKT-dependent.

In previous studies within our group we demonstrated that PI3K and AKT are not required for TGF-β_1 stimulated activation of mTORC1 or for collagen I synthesis. My work was focussed on interrogating the mechanisms of S2448 phosphorylation to identify how upstream proteins may be influencing the early activation of mTOR (3 hours) and collagen I synthesis. A kinase identified for regulating this site could then be analysed for its role in mTORC1 activation and collagen synthesis. Therefore, before I continued investigations further, I wanted to demonstrate that S2448 phosphorylation in response to TGF-β_1 was PI3K/AKT independent.

The treatment of pHLF's with the PI3K inhibitor, compound 12, did not inhibit TGF-β_1 stimulated S2448 phosphorylation and this was matched to a decrease in AKT phosphorylation, which is a good marker of inhibited AKT enzyme activity. Therefore, in our cells this S2448 phosphorylation was independent of the PI3K/AKT axis. Previous reports demonstrate that S2448 phosphorylation was dependent on PI3K and AKT activation (Cheng et al. 2004; Navé et al. 1999). The difference between my work and the previous reports may be explained by the choice of compound used between studies. In previous reports, it has been demonstrated that S2448 was sensitive to treatment with wortmannin, an inhibitor of PI3K (Cheng et al. 2004; Navé et al. 1999). Others have reported that wortmannin also inhibits Polo-like Kinases, DNA-PKcCs and mTOR. As a consequence, inhibition of mTOR or another kinase may explain why wortmannin inhibits S2448 phosphorylation (McNamara & Degterev 2011; Liu et al. 2005). This is also supported by my data and other reports show this site is sensitive to mTOR inhibition, Figure 3.5 (Ferguson et al. 2017; Cirstea et al. 2014). Therefore, it is likely that this site is PI3K/AKT insensitive and previous reports report the consequence of mTOR kinase inhibition, which is required to phosphorylate this site.

In support of my work, others have demonstrated that S2448 phosphorylation is sensitive to wortmannin but independent of AKT (Chiang & Abraham 2005). Other investigators demonstrated that S2448 phosphorylation was attributable to P70S6K activation downstream of mTOR activation and this observation was also supported by a second group (Chiang & Abraham 2005; Holz & Blenis 2005). The previous investigations believed this was explained by the compound's ability to inhibit PI3K which is required for PDK1 recruitment (independent of AKT activity). Therefore, by inhibiting PI3K this would lead to the inhibition of PDK1 and prevent P70S6K becoming activated and phosphorylating the S2448 site (Chiang & Abraham 2005). However, this was not experimentally demonstrated. Another group demonstrated that mTORC1 activation is independent of PI3K and AKT and believe that mTORC1 is mediating P70S6K activation in synergy with PDK1 (Holz & Blenis 2005). This supports my observation that the phosphorylation of S2448 was independent of PI3K and AKT and it was still possible that the effects of wortmannin

observed by Chiang & Abraham (2005) were mediated by mTOR inhibition. I have confidence in my observations because the pharmacological tool utilised in my work, compound 12, exhibits much greater selectivity for PI3K in comparison to mTOR with an IC50 of 40 nM and 50 μM, respectively. The 1000-fold increase in selectively allows PI3K to be assessed independently of mTOR and demonstrated that S2448 phosphorylation of mTOR is independent of PI3K. This was confirmed because TGF-β_1 stimulated AKT phosphorylation is inhibited by compound 12 whilst P70S6K phosphorylation was still maintained, Figure 3.4. Therefore, the effects of wortmannin are not likely mediated through the PI3K/AKT axis, but by the compound inhibiting mTOR directly in other studies.

The role of mTOR kinase activity was investigated in order to determine if S2448 was being phosphorylated downstream mTORC1 activation when pHLFs are stimulated with TGF-β_1. PHLF's treated with an mTOR inhibitor, AZD8055, inhibited the increase in mTORC1 S2448 phosphorylation. This confirmed that S2448 phosphorylation is likely temporally situated downstream of mTORC1 activation. Reports confirm that AZD8055 is able to inhibit the phosphorylation of this phosphorylation site (Cirstea et al. 2014) along with other mTOR inhibitors (Ferguson et al. 2017).

Treatment with LY2584702 (P70S6K inhibitor) also confirmed that mTOR activity is required for the phosphorylation of S2448 via the P70S6K. A number of reports support this feed-back mechanism driven by P70S6K and this is sensitive to mTOR inhibition via rapamycin treatment (Chiang & Abraham 2005; Holz & Blenis 2005; Cirstea et al. 2014). This further supports the previous argument that wortmannin likely mediates its effect through the inhibition of mTOR thus preventing it from activating P70S6K to mediate the phosphorylation of the S2448 site.

The compound wortmannin is also believed to be able to inhibit the phosphorylation of S2448 via inhibition of PI3K (Chiang & Abraham 2005). PI3K activation is required for PDK1 recruitment because it converts PIP2 to PIP3 at the cell membrane which recruits PDK1, AKT and P70S6K via their PH (pleckstrin homology) domains and brings the three kinases into close

contact allowing PDK1 to phosphorylate AKT and P70S6K. PDK1 is responsible for phosphorylating P70S6K at the T229 site in the kinase domain to promote P70S6K catalytic activity. Therefore, I wanted to understand if PDK1 was required for P70S6K activation to allow the phosphorylation of S2448.

Treatment with GSK2334470 (PDK1 inhibitor) inhibited the phosphorylation of the mTOR S2448 amino acid site. Previous reports show that PDK1 is essential for the activation of P70S6K by phosphorylating P70S6K's activation loop which promotes kinase activity. Therefore, inhibiting PDK1 with GSK2334470 identified the requirement of the PDK1 to P70S6K axis in TGF-β_1 stimulated mTORC1 S2448 phosphorylation. Interestingly this inhibitory data from Figure 3.4 and Figure 3.8, demonstrate that PDK1 is acting independently of PI3K recruitment in our pHLFs. In addition to my own data, I was confident that compound 12 was inhibiting AKT via PI3K, since I could see a decrease in AKT phosphorylation and others within the group have also shown it completely inhibits AKT phosphorylation and cell proliferation at 1 μM (Woodcock et al. 2019). Therefore, I believe that PDK1 is acting independently from PI3K activation. To explain this, PDK1 is known to be active under basal conditions. This suggested that PDK1 does not need to be localised to the cell membrane to sufficiently activate P70S6K or that another mechanism promotes its recruitment to the membrane. Furthermore, mTORC1 under amino acid replete conditions is also believed to be localised to the lysosome and this may support a role for an alternative pathway that leads to PDK1 recruitment to the lysosome (Bar-Peled et al. 2012). There are also reports which support the notion that PDK1 can be regulated independently of PI3K (Caohuy et al. 2014), but the mechanism still remains elusive. My work provides a number of potential insights within our cells that could be explored in the future by identifying the signalling pathways that regulate PDK1 and subsequently regulate P70S6K phosphorylation/activity.

A Previous report demonstrated a dual mechanism involving PDK1 and P70S6K whereby mTORC1 can be activated in an AKT-independent manner in cancer cells and demonstrated resistance to PI3Kα inhibition (Castel et al. 2016). Their work identified two mechanisms that regulate the S2448 site on

mTOR requiring both PDK1 and P70S6K suggesting they may play a role in mediating mTORC1 activity and this could have been required for collagen I synthesis. These cancer cells compensate for this inhibition by driving mTORC1 activation via SGK1 and PDK1 (Castel et al. 2016). However, work within our group demonstrated that using the same inhibitors for PDK1, P70S6K or SGK1, there was no effect on TGF-β_1 stimulated collagen I synthesis (Woodcock et al. 2019). This suggests that this site is phosphorylated for alternative reasons which are not linked to TGF-β_1 stimulated collagen I synthesis. An alternative method of measuring the activity of mTORC1 would be to use a radioactive kinase assay on co-immunoprecipitations of Raptor. This would pull-down specifically mTORC1 and not mTORC2. This would allow the quantitation of different inhibitor treatments and how they impact the kinase activity of mTORC1.

Summary

Taking together the data obtained with these four inhibitors, the kinases required for the phosphorylation of mTOR at the S2448 site are P70S6K, mTORC1 and PDK1. Importantly, this work has also supported that TGF-β_1 activation mTORC1 is independent of the PI3K/AKT axis. This data also sheds light on the PDK1 to P70S6K axis which is independent of PI3K but dependent on TGF-β_1 stimulation that can lead to the phosphorylation of the S2448 on mTORC1. In addition to previous reports, my data has helped align the temporal order of these kinases to lead to the increased phosphorylation of the S2448 site in response to TGF-β_1 stimulation. Figure 4.1 represents a model that shows the known kinases important for the phosphorylation of S2448 based upon the inhibitory data presented in this thesis.

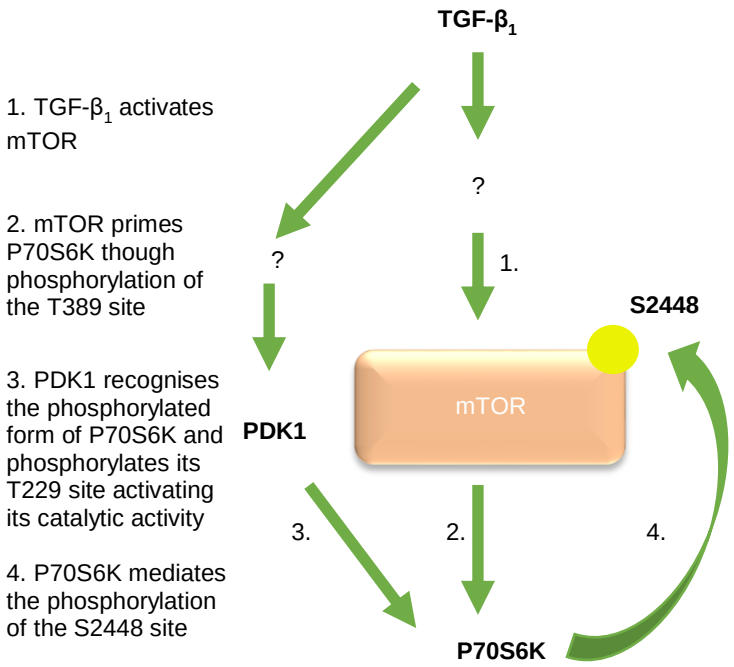

Figure 4.1: The TGF-β_1 stimulated mechanism of mTOR S2448 phosphorylation in pHLFs

1. TGF-β_1 activates mTOR through and unknown mechanism. 2. The activation of mTOR kinase activity leads to mTORC1 targeted phosphorylation of P70S6K at the T389 site. 3. This allows P70S6K to be targeted by PDK1 which phosphorylates P70S6K at the T229 site which is located in the activation loop and subsequently leads to increased P70S6K catalytic activity. 4. The activated P70S6K then mediates the phosphorylation of mTOR at the S2448 site.

4.3. SMAD3 is required for TGF-β_1 mTORC1 activation

4.3.1. Introduction

TGF-β_1 binds to the TβRII receptor which increases its affinity for TβRI receptors which leads to the formation of the TβRI/TβRII receptor complex. TβRII activates the TβRI through phosphorylation allowing TβRI to then directly phosphorylate SMAD 2 and SMAD 3. The phosphorylation of either transcription factor promotes their binding to SMAD 4 allowing them to translocate into the nucleus and promote gene transcription. Early work on SMAD 3 regulated genes identified that it can regulate a number of collagen genes, including *COL1A1*, implicating SMAD 3 in most TGF-β_1 driven pro-fibrotic responses (Tsuchida et al. 2003; Verrecchia et al. 2001). mTOR has also been implicated as a pro-fibrotic hub, regulating the translation of the mRNA of several pro-fibrotic proteins in response to TGF-β_1 stimulation (Platé, unpublished data; Woodcock et al. 2019;Rozen-Zvi et al. 2013). Finally, evidence has emerged that there may be cross-talk between SMAD activation

and mTORC1 (Rozen-Zvi et al. 2013). In the present study, the contribution of SMAD 3 signalling and gene transcription to the activation of mTORC1 was evaluated using a range of techniques including siRNA knock-down and selective pharmacological inhibitors in pHLFs.

4.3.2. A comparison of the effects of two mTOR inhibitors on TGF-β_1 stimulated 4E-BP1 phosphorylation

Rapamycin and AZD8055 are both inhibitors of the mTORC1 complex. However, both show different pharmacological mechanisms of inhibition. AZD8055, like Torin-1, is an ATP-competitive inhibitor of mTOR and is, therefore, capable of inhibiting mTORC2 substrate phosphorylation as well. In contrast, rapamycin is an allosteric inhibitor of mTORC1. Crystal structure analysis revealed that rapamycin and FKBP12 forms a complex to bind to the FRB domain on mTOR (Choi et al. 1996). These differences in rapamycin and AZD8055 mean that AZD8055 can inhibit the phosphorylation of all 4E-BP1 sites, however, 4E-BP1 has both rapamycin-sensitive and insensitive sites. It is well documented that rapamycin is capable of influencing the phosphorylation of 4E-BP1^{S65} and 4E-BP1^{T70}, yet 4EBP$^{T37/46}$ is rapamycin insensitive (Walker et al. 2016; Kang et al. 2013; Thoreen et al. 2009). The differences in site-specific sensitivity are most likely explained by the negative impact rapamycin may have on substrate conformational binding to the mTOR active site, preventing the phosphorylation of the 4E-BP1^{S65} site and P70S6K (Kang et al. 2013). Furthermore, phosphoproteomic studies have demonstrated that mTORC1 has a much higher affinity for the 4E-BP1$^{T37/46}$ sites, but, is much weaker for the 4E-BP1^{S65} and 4E-BP1^{T70} sites and P70S6K. This means mTORC1 can still phosphorylate the 4E-BP1$^{T37/46}$ site in the presence of rapamycin (Kang et al. 2013; Thoreen et al. 2009).

These differences between rapamycin and ATP-competitive mTOR inhibitors was recapitulated in our pHLFs; whereas AZD8055 was capable of inhibiting all three 4E-BP1 sites, rapamycin only inhibited the effects of TGF-β_1 stimulation of 4E-BP1^{S65} and 4E-BP1^{T70}. This served as a strong basis when comparing the effects of both pharmacological inhibitors and siRNA on mTORC1 activation, importantly because AZD8055 inhibits collagen synthesis, whereas rapamycin does not (Woodcock et al. 2019).

4.3.3. Characterisation of SMAD 3 knock-down in pHLFs

TGF-β_1 stimulated SMAD 3 phosphorylation is a direct event that is driven by TβRI phosphorylating SMAD 3 in the MH2 domain. This allows it to translocate to the nucleus after binding to SMAD 4. The MH1 domain of SMAD 3 recognises the CAGA repeats in the *COL1A1* gene to drive transcription (Verrecchia et al. 2001).

The aim of my initial experiments was to ensure that good knock-down of SMAD 3 was achieved in pHLFs and that the knock-down recapitulates the known contribution of SMAD 3 for *COL1A1* gene transcription. The effect of SMAD 3 siRNA knock-down inhibited TGF-β_1 stimulated COL1A1 mRNA levels and this was recapitulated at the protein level, with a decrease in TGF-β_1 stimulated collagen deposition observed. It has been reported in numerous fibroblast cell lines that TGF-β_1 regulates collagen synthesis through the activation of the SMAD pathway, in particular SMAD 3, to promote its pro-fibrotic effects (Zhang et al. 2011; Higashiyama et al. 2007; Tsuchida et al. 2003; Verrecchia et al. 2001).

I next demonstrated after 24 hours following TGF-β_1 stimulation, TGF-β_1 negatively regulates SMAD 3 mRNA and protein levels in pHLFs. Reports support this evidence, and it has been well-documented as a regulatory mechanism to inhibit continued SMAD 3 signalling. TGF-β_1 down-regulates SMAD 3 gene transcription through an as yet unknown mechanism and SMAD 3 luciferase reporter activity drops significantly when glomerular mesangial cells are treated with TGF-β_1 (Poncelet et al. 2007). TGF-β_1 has also been shown to regulate SMAD 3 protein levels through targeted ubiquitination by F-box/WD repeat-containing protein 1a (Fbw1a) in COS7 cells (Fukuchi et al. 2001). There is also evidence that has implicated a signalling axis involving Protein inhibitor of activated STAT (PIAS) 4 and fibrosis-inducing E3 ligase 1 (FIEL1) (Lear et al. 2016). PIAS4 is an important inhibitor of TGF-β signalling, which supresses SMAD 3 signalling via SMAD 3 degradation, complex binding and recruitment of histone deacetylase 1 (HDAC1) which supresses SMAD 3 transcription (Long et al. 2003; Imoto et al. 2004). FIEL1 is a direct negative regulator of PIAS4 which promotes its degradation and prolongs TGF-β_1 stimulated activation of SMAD 3. Interestingly, a small molecule inhibitor of

FIEL 1 has been shown to promote increased survival and reduced collagen levels in mice following bleomycin induced lung fibrosis (Lear et al. 2016). Considering in our pHLFs, SMAD 3 is being degraded, this has no relevance for early mTORC1 activation mediated collagen synthesis, but in the disease context may promote the prolonged transcription of the collagen I gene.

4.3.4. SMAD 3 regulates TGF-β_1 stimulated mTORC1 activation through the transcription of an unknown protein

The requirement for TGF-β_1 stimulated SMAD 3 signalling and the collagen I gene expression is well-established. However, the cross-talk between SMAD 3 and mTORC1 activation has only just recently begun to emerge. SMAD 3 knock-down was assessed across the four 4E-BP1 phosphorylation sites, of which 4E-BP1^{S65} and 4E-BP1^{T70} show TGF-β_1 dependence. Treatment with SMAD 3 siRNA in pHLFs strongly inhibited 4E-BP1^{S65} at baseline and under TGF-β_1 stimulated conditions. Conversely SMAD 3 siRNA treatment increased 4EBP^{70} phosphorylation, preventing the TGF-β_1 regulated inhibition. The effect on 4E-BP1$^{T37/46}$ was only marginal although it was statistically significant when quantified by densitometry. Treatment with actinomycin D supported the notion that this response was indeed transcriptionally regulated for the TGF-β_1 sensitive site 4E-BP1^{S65}. Reports support that SMAD 3 is capable of regulating mTORC1 activation, however, these reports differ slightly in selected time-points examined (Das et al. 2013; Lampa et al. 2017; Bernard et al. 2017). These reports also link two SMAD 3 transcriptionally regulated proteins that have the capability to modulate mTOR activity, DEPTOR and GLS. DEPTOR negatively regulates mTOR complexes (mTORC1 and mTORC2). The first report identified DEPTOR as a SMAD 3 regulated protein but this regulation was down-stream of mTORC1 in glomerular mesangial cell (Das et al. 2013). This observation was not recapitulated in pHLFs which demonstrated that DEPTOR is not down-regulated by TGF-β_1. Considering this evidence, it is likely that the pHLF do not require the mTORC1 regulated decrease in DEPTOR to prolong mTORC1 activation for 48 hours post stimulation with TGF-β_1. The explanation for this may be that sufficient nutrients are being supplied, allowing pHLFs to maintain mTORC1 activation or the differences in cell type examined.

Work within our group has demonstrated that glycolysis is a core metabolic pathway that is upregulated in pHLFs stimulated with TGF-β1 (Selvarajah, unpublished data). The upregulation of these glycolytic pathways are driven by the TGF-β_1 dependent upregulation of ATF4. ATF4 has been investigated within our group and its upregulation occurs at 6 hours and peaks at 24 hours (Selvarajah, unpublished data). Figure 3.11, highlights how the knock-down of ATF4 using siRNA inhibits TGF-β_1 stimulated collagen I deposition in pHLFs. This suggested that a protein or metabolite involved in glycolysis could be responsible for the TGF-β_1 stimulated activation of mTORC1. Previous reports support this idea, and report that the glycolytic inhibitor 3PO attenuated bleomycin induced fibrosis (Xie et al. 2015). GLS, an enzyme that converts glutamine to glutamate which is then converted to α-Ketoglutarate by glutamate dehydrogenase (Yang et al. 2014). The α-Ketoglutarate produced as a result of the upregulation of GLS is capable of mediating increased mTORC1 activity through the RAG complex (discussed in the next paragraph) (Durán et al. 2012). In addition, it was reported that breast cancer cells incubated with CB-839, a GLS inhibitor, for a period 24 hours had decreased levels of P70S6K and 4E-BP1^{T70} phosphorylation (Lampa et al. 2017). This compound has now been entered into clinical phase I trials for the treatment of cancer (Clinical trials identifier: NCT02071927). Importantly, it has been identified that SMAD 3 transcriptionally regulates GLS (Bernard et al. 2017). This highlighted GLS as potential target within our pHLFS. It was theorised that TGF-β_1 could be transcriptionally regulating GLS via SMAD 3 and the subsequent increase in GLS expression would increase the synthesis of α-Ketoglutarate, therefore promoting RAG mediated activation of mTORC1.

In contrast to what was observed in these previous reports, my investigation of CB-839 demonstrated it has no effect on two of the TGF-β_1 sensitive 4E-BP1 sites: 4E-BP1^{T70} and 4E-BP1^{S65}. There was a very marginal effect on 4E-BP1$^{T37/46}$ based upon the densitometry but the western blot visually does not look decreased. The difference between the reported literature and what I observed is likely due to the early time point I selected. The previous reports discussed above examined time points at 24-48 hours which is much later than the early activation seen with mTORC1 (Xie et al. 2015; Bernard et al. 2017;

Lampa et al. 2017). One explanation for the observation seen is that over the 48 hour period, mTORC1 activation requires the maintenance of amino acids and other influences required for its activation and hence it up-regulates a number of glycolytic enzymes. The 4E-BP1$^{T37/46}$ is well characterised as a high affinity site that is recognised by mTORC1 (Kang et al. 2013; Thoreen et al. 2009). This site acts as a priming site for the other two sites allowing for their phosphorylation (Gingras et al. 1999). This site has also been demonstrated to be regulated by glutaminolysis which produces α-ketoglutarate which is required to keep RAGB in its GTP bound form (Durán et al. 2012). The RAG proteins RAG A-D are all critical proteins that are required for mTORC1 activation. In the GTP bound form, RAG A or RAG B associate with either RAG C or RAG D in their GDP bound form. The RAG proteins are tethered to the lysosome to a complex termed the RAGULATOR. Along with tethering the RAGS to the lysosome, the RAGULATOR is a GEF. This exchanges the RAG A or RAG B GDP for GTP which allows mTORC1 to be recruited. In the absence of amino acids, the GTP is converted to the GDP bound form, preventing mTORC1 from remaining localised to the lysosome. Therefore, prolonged treatment with the compound CB-839 over a 24 hour period would lead to the depletion of α-ketoglutarate which is critical for maintaining basal levels of mTORC1 activity which can be demonstrated by quantifying the phosphorylation 4E-BP1$^{T37/46}$ which is primed ready so the other 4EBP1 sites can be phosphorylated. So, while α-ketoglutarate is critical for maintaining mTORC1 localisation at the lysosome and mTORC1 basal levels of activity, this is independent of TGF-β_1 stimulated early mTORC1 activation, which is required for the increased phosphorylation of 4EBP^{S65} and 4EBP1^{T70}. In our culture conditions, over a four hour exposure period with CB-839, this is not sufficient to deplete the levels of α-ketoglutarate and therefore this leads to the reduction of 4E-BP1$^{T37/46}$ phosphorylation. This also may explain why there is only a marginal effect on this site at the 3 hour time-point. This does not discount that TGF-β_1 in our cells may up-regulate glutaminolysis and GLS expression (to produce α-ketoglutarate) to maintain mTORC1 baseline activity which is required to allow TGF-β_1 driven mTORC1 activation. Considering this information, the upregulation of ATF4 in our cells and its requirement for collagen synthesis, Figure 3.11, ATF4s ability to upregulate glycolytic

enzymes (Appendix 14) may be sufficient to keep mTORC1 activated and therefore does not need DEPTOR to be down-regulated in pHLFs. This has been evidenced in other reports, which show mTORC1 balances amino acid levels through the upregulation of ATF4 and in turn this maintains mTORC1 activity (Park et al. 2017). To conclude I believe that α-ketoglutarate is required for the maintenance of mTORC1 basal activity. The synthesis of α-ketoglutarate by GLS is required to promote the availability of mTORC1 at the lysosome which subsequently allows it to be fully activated by other stimuli such as TGF-β_1. Therefore, α-ketoglutarate and DEPTOR are not required for the early activation of mTORC1 in response to TGF-β_1 stimulation in pHLFS.

Our group use the TGF-β_1 sensitive 4E-BP1 phosphorylation sites and use a secondary read-out which is collagen I deposition. This supports that we are inhibiting collagen I and this is likely through mTORC1. TGF-β_1 activates SMAD 3 in pHLFs to mediate the transcription of the collagen I gene. The evidence that only SMAD 3, downstream of TGF-β_1, is required to activate mTORC1 is ambiguous, Figure 3.17. Although it demonstrates that SMAD 3 knock-down regulates the mTORC1 there was still large amounts of 4EBP1 phosphorylation remaining at each of the sites, making the results more comparable to rapamycin which does not inhibit collagen compared to AZD8055 which does. In light of this I wanted to explore other known mechanisms that regulate mTORC1 and it would not be too far to assume that SMAD 3 still had the potential to regulate or feed into this other pathway which was the TSC1/2 complex.

4.4. TSC1/2

4.4.1. Introduction

The TSC1/2 complex is a large negative regulatory complex. The complex is formed of three proteins, TSC1, TSC2 and TBC1D7. Mutations in these tumour suppressor genes encoding either TSC1 or TSC2 leads to tuberous sclerosis, a disease characterised by the formation of hamartoma's. Mutations in the TSC1 or TSC2 genes have also linked to sporadic cases of lymphangioleiomyomatosis (Carsillo et al. 2000). The loss of function of TSC2 and the development of these conditions was attributed to TSC1/2 being required as a negative regulator of the protein RHEB, which is required for

mTORC1 activation (Carsillo et al. 2000; Inoki 2003; Huang & Manning 2008; Demetriades et al. 2014).

TSC1 and TSC2 are both large proteins with a large number of phosphorylation sites, particularly TSC2. The various phosphorylation sites on TSC1 or TSC2 can either inhibit or activate overall activity of the complex. A number of stimulatory signals including amino acids, TGF-β_1 and EGF can lead to the inhibition of this complex to promote mTORC1 activation, which occurs through the activation of select kinases that phosphorylate and inhibit the complex or by changing its localisation.

4.4.2. The TSC1/2 complex and RHEB are required for mTORC1 activation

The results outlined in Figures 3.21, 3.22, 3.25 and 3.26 demonstrate that the TSC2-RHEB axis is critical for TGF-β_1 stimulated 4E-BP1^{S65} phosphorylation and collagen I synthesis. The results regarding TSC2 were difficult to interpret owing to its ability to shift the TGF-β_1 curve to the left and also increase the Emax which was investigated by western blot analysis. This may be explained because the relationship between TSC1/2 complex and mTORC1 is multifaceted. TSC2 can be regulated by both amino acids and numerous kinase inputs (Huang & Manning 2008; Demetriades et al. 2014). My results suggest I may be enhancing both amino acid inhibition and kinase inputs inhibition of the TSC2 complex. This suggests that the loss of TSC2 can increase mTORC1 activity and this observation is well supported by the current literature (Demetriades et al. 2014; Huang et al. 2008; Carsillo et al. 2000; Garami et al. 2003).

In amino acid rich conditions, a large portion of TSC2 is dissociated from the lysosome, however, not completely (Demetriades et al. 2014). The knock-down in pHLFs promotes an increase in mTORC1 activity as seen by an increase in 4EBP1^{S65} phosphorylation, Figure 3.21. Taking the demonstration of the previous report (Demetriades et al. 2014) into account the knock-down in my pHLF's could be acting with the amino acids synergistically by removing the remaining TSC2 complex from the lysosome, therefore, theoretically promoting RHEB^{GTP} formation, which would explain the increase in Emax,

Figure 3.21. However, Figure 3.21, demonstrates there is also a leftward shift in the response of 4E-BP1^{S65} to TGF-β_1, the curve suggests TSC2 regulation is TGF-β_1 dependent. This indicates TGF-β_1 may be capable of increasing 4E-BP1^{S65} phosphorylation through the inhibition of the TSC1/2, this supports previous observations that external stimuli can inhibit this complex (Demetriades et al. 2014; Huang et al. 2008; Carsillo et al. 2000; Garami et al. 2003).

To better link the role of the TSC1/2 complex to TGF-β_1 and its role in activating mTORC1, RHEB was selected as a target for CRISPR and siRNA. RHEB has been well established as a substrate of TSC2's GAP activity (Inoki et al. 2003). RHEB is critical for the activation of mTORC1 and has been established to be responsible for fibroblast collagen synthesis in kidney fibrosis (Jiang et al. 2013) and lung mesenchymal cells (Walker et al. 2016). Using siRNA and CRISPR techniques, I demonstrated that RHEB was required for TGF-β_1 stimulated mTORC1 activation for the phosphorylation of 4E-BP1^{S65} and for the synthesis of collagen I. Taken together this suggests that RHEB and TSC2 are required for TGF-β_1 stimulated 4E-BP1 phosphorylation and for collagen synthesis. Interestingly, CRIPSR and siRNA had no effect on the basal levels of 4E-BP1 phosphorylation, which could be explained by residual levels of RHEB remaining in both the CRISPR and siRNA treated cells as demonstrated by the western blots. Previous reports have suggested that RHEB regulates mTORC1 activity by increasing mTORC1's binding to 4E-BP1 (Sato et al. 2009). This may explain why we also see differences between the 4E-BP1 phosphorylation sites. mTORC1 has a high avidity for the 4E-BP1$^{T37/46}$ phosphorylation site (Kang et al. 2013; Thoreen et al. 2009). Therefore, mTORC1 binding to RHEB mediated by TGF-β_1 stimulation in our pHLFs promote mTORC1 recognition of the low affinity 4E-BP1 phosphorylation sites, 4E-BP1^{S65} and 4E-BP1^{T70}.

4.5. The role of MK2 signalling in modulating the fibrotic response following TGF-β_1 stimulation of pHLFs.

4.5.1. Introduction

MK2 is a serine/threonine kinase encoded by the MAPKAPK2 gene on chromosome 1. The protein expression is fairly ubiquitous, but it is mainly

expressed by immune cells, particularly dendritic cells. MK2 is a substrate of P38 MAPK and TAK1, and has been implicated in regulating cellular processes including: stress, DNA damage and cell migration (Holtmann et al. 2001; Liang et al. 2018; Yang et al. 2011).

TAK1, is a MAP3K which is best known for its ability to initiate signalling cascades in response to TNF-α, whereby TAK1 mediates the activation of NF-κB in inflammatory disorders and cancer (Sakurai 2012). Stimuli including TGF-β_1, IL1β, and TNF-α can initiate other signalling pathways including TAK-MKK3/6-P38 MAPK; TAK1-MKK4/7-JNK; TAK1-MEK1/2-ERK (Sakurai 2012). Anisomycin is a tool used to investigate P38 MAPK activity and subsequently its substrate MK2. (Y. Li et al. 2003). Anisomycin treatment activates MK2 activity which phosphorylates and inhibits TSC2 (Y. Li et al. 2003).

TAK1 is a direct target of TβRI and has been implicated in regulating TGF-β_1 driven gene expression and in collagen I synthesis (Ono et al. 2003; Yamaguchi et al. 1995). To explore the pro-fibrotic role of TAK1 in pHLFs and its effects on SMAD and mTORC1, (5z)-7-Oxozeaenol and siRNA were used to explore their effects on mTORC1 activation and collagen I synthesis. The two approaches yeilded conflicting results, which will be discussed below.

4.5.2. (5z)-7-Oxozeaenol inhibits TGF-β_1 stimulated collagen I synthesis

Treatment with (5z)-7-Oxozeaenol demonstrated a significant inhibitory effect on TGF-β_1 induced collagen I deposition in pHLFs, Figure 3.27 and 3.29. Previous studies have suggested that (5z)-7-Oxozeaenol inhibits TAK1 which leads to a decrease in TGF-β_1 stimulated collagen synthesis across several cell types (Kuk et al. 2015; Li et al. 2017; Grillo et al. 2015; Guo et al. 2013; Ono et al. 2003). To determine whether (5z)-7-Oxozeaenol was engaging its target, TAK1, I demonstrated that it inhibited the phosphorylation of P38 MAPK. This has been used by various groups to demonstrate TAK1 is being inhibited by the compound (Refaat et al. 2015; Ninomiya-Tsuji et al. 2003) However, in these previous reports identifying TAK1 as a mediator of collagen synthesis, there was no data implicating (5z)-7-Oxozeaenol as a regulator of mTORC1 activation (Kim et al. 2009; Li et al. 2017; Grillo et al. 2015; Ono et al. 2003). In pHLFs, treatment with (5z)-7-Oxozeaenol inhibited the TGF-β_1

induced phosphorylation of mTORC1 substrates, 4E-BP1^{S65} and P70S6K. This was the first time that this compound had been linked to mTORC1 regulation in response to TGF-β_1 signalling. Interestingly, in contrast to my data, others report that (5z)-7-Oxozeaenol inhibition of TAK1 leads to an increase in mTORC1 activity by preventing bacteria induced TAK1 activation of AMPK (an inhibitor of mTORC1) in HeLa cells (Liu et al. 2018). This difference may be contextual and dependent on the stimulus and cell type. Due to the compound selectivity, the immediate evidence suggested that TAK1 may be critical for regulating TGF-β_1 stimulated mTORC1 activation to regulate collagen I synthesis. In light of other subsequent data my observations may be driven by compound polypharmacology (discussed below 4.5.3).

4.5.3. TAK1, P38 MAPK and MK2 are not required for TGF-β_1 stimulated collagen I synthesis

Treatment of pHLFs with TAK1 siRNA did not recapitulate the findings that were demonstrated with (5z)-7-Oxozeaenol. This was true for both TGF-β_1 stimulated collagen synthesis and mTORC1 activation. I had confidence in the siRNA data since good knock-down was obtained. However, complete removal of a protein can have unexpected effects within cells and this may lead to compensatory mechanisms becoming activated. Several reports contrast with my results: studies using mouse KO, siRNA and CRISPR CAS9 knock-down of TAK1 or TAK1 DN demonstrate that TAK1 is required for TGF-β_1 stimulated collagen synthesis (Kuk et al. 2015; Li et al. 2017; Grillo et al. 2015; Kim et al. 2007). To explain these differences to those obtained in my studies, it is worth commenting that there is a large variation of TGF-β_1 concentrations used, ranging from 2 ng/mL to 10 ng/mL across these studies. In addition, the cell types are all different, and most of these experiments are conducted in rodent cells and although they can be a useful alternative, species differences means they will not always recapitulate what will be found using human cells. Together this may account for discrepancies between my data and what is published in the literature. In contrast and in support of my TAK1 knock-down data, Sapkota, 2013 demonstrated that TGF-β_1 used at 1 ng/mL, as used in my studies, did not activate TAK1. Furthermore, it was

reported that TAK1 mediated siRNA knock-down in mouse embryonic fibroblasts and HaCAT cells did not inhibit P38 MAPK phosphorylation and it was suggested that the phosphorylation could be mediated by other MAP3Ks (MA3K4 and MAP3K10) (Sapkota 2013).

Through verbal communication with Dr Holmes (a previous collaborator at UCL), it transpires that for Dr Holmes also experienced the same observations as I did using scleroderma derived fibroblasts. Dr Holmes' group also showed that TGF-β_1 mediated the increase in collagen I synthesis, which was inhibited by (5z)-7-Oxozeaenol, whilst TAK1 siRNA knock-down had no impact (unpublished data).

To delineate whether TAK1 was implicated in collagen I and mTORC1 activation, the work investigating the downstream targets of TAK1, MK2 and P38 MAPK showed that their inhibition did not block TGF-β_1 stimulated collagen I synthesis. This was supported by a minimum of two compounds for each kinase resulting in the same outcome. Furthermore, MK2 phosphorylation could not be achieved by TGF-β_1 stimulation, but could with other stimuli, including IL1β and anisomycin.

It has been reported that MK2 is involved in collagen-induced arthritis, a predominantly inflammatory-driven disease. The mice used in this study are deficient in the MK2 gene and demonstrated improvements in disease phenotype. However, the role of MK2's in collagen synthesis were unclear (Hegen et al. 2006). Interestingly, MK2 knock-out mice develop increased fibrosis in response to the bleomycin-induced lung fibrosis, suggesting MK2 may potentially be part of the wound resolution response. In addition, MK2 knock-out mice demonstrated decreased migration of fibroblasts (Kayyali et al. 2009). Notably, a recent report has demonstrated increased MK2 staining in the human IPF and bleomycin mouse lung, suggesting MK2 may be important in IPF pathogenesis. Treatment with an MK2 inhibitor reduced collagen content in the bleomycin-induced mouse lung fibrosis model, which was attributed not to the inhibition of collagen synthesis but to inhibiting fibroblast migration to the wound (Liang et al. 2018). Collectively, this may explain why there is a difference between data obtained with cultured fibroblast

and the *in vivo* data. This also supports my siRNA observations, suggesting that both TAK1 substrates MK2 and P38 MAPK are not required for TGF-β_1 stimulated collagen synthesis in pHLFs.

In an attempt to explain how (5z)-7-Oxozeaenol is mediating its inhibition of collagen synthesis, observations about its mechanism of action are important, as it is for the use of all inhibitors.

Studying the structure of (5z)-7-Oxozeaenol has revealed its mechanism as an irreversible inhibitor (Wu et al. 2013) and the covalent bond between (5z)-7-Oxozeaenol and the target kinase requires a cysteine residue within the ATP binding socket (Ohori et al. 2007). Table 3.2, in the results section, highlights the MAPKs which I identified as having this cysteine residue in the ATP binding socket. Interestingly, the kinases I identified correlated well to two independent screens. A screen from the MRC and kinomeScan DiscoverX by Gray et al., 2017, demonstrated that (5z)-7-Oxozeaenol exhibits poly-pharmacology. Both screens and Miyake et al., 2007, demonstrated that (5z)-7-Oxozeaenol has strong selectivity for several MAP2K's, in particular MKK6 which is required for P38 MAPK phosphorylation. This might explain why inhibition of P38 MAPK in the presence of (5z)-7-Oxozeaenol can be observed in pHLFs used here. Finally, the most interesting observation from the kinomeScan DicoverX screen was that (5z)-7-Oxozeaenol can highly inhibit the TβRII which is required to phosphorylate and promote TβRI kinase activity. Therefore, this would inhibit the entire TGF-β_1 signalling pathway. This would explain why (5z)-7-Oxozeaenol inhibits SMAD 2 and SMAD 3 phosphorylation in pHLFs, particularly since these sites are directly phosphorylated by the TβRI receptor (Shi 2006; Massagué 2012). This would also explain why (5z)-7-Oxozeaenol inhibits mTORC1 activation and collagen I synthesis.

Taken together, it is very likely that (5z)-7-Oxozeaenol has poly-pharmacology which has been observed in a number of studies (MRC, (Tan et al. 2017; Ohori et al. 2007) and my own (SMAD 2 and SMAD 3 inhibition) and this was likely mediating the effects seen within our cells. The effects of the siRNA knock-down suggests that TAK1 is not required for TGF-β_1 mediated mTORC1 activation or collagen I synthesis, which is further supported by the P38 MAPK

and MK2 inhibitory data. The most likely target of (5z)-7-Oxozeaenol inhibition is TβRII.

The evidence suggesting the requirement of the TSC1/2-RHEB axis led me to investigate the remaining kinases that had the ability to inhibit the TSC2 complex, since AKT and MK2 had no effect on collagen synthesis. It was crucial in this investigation to examine the 4E-BP1 phosphorylation sites and collagen synthesis together. None of the three kinases investigated inhibited collagen synthesis. Interestingly, they each did modulate 4E-BP1 phosphorylation in some ways, albeit only marginally.

4.5.4. The effect of CDK1 inhibition on TGF-β_1 induced mTORC1 signalling in pHLFs

CDK1 is better known for its role in cell cycle progression (Enserink & Kolodner 2010); this kinase has over 70 targets, including TSC1. Considering its role within the cell, I utilised this to test whether the CDK1 inhibitor BMS-265246 was capable of inhibiting cell proliferation when stimulated with 10% FBS. We observed that at 1 μM the compound demonstrated near full inhibition of cell proliferation when compared to baseline. The ability of BSM-265246 to give full inhibition of proliferation is reported in the literature, demonstrating the cells stop proliferating and are halted in the G_2 phase of the cell cycle (Sutherland et al. 2011). The mTORC1 complex has also been implicated in cell cycle progression and this mechanism is driven through CDK1 inhibition of the TSC1 protein at three phosphorylation sites (Astrinidis et al. 2003). Therefore, it was possible that a novel mechanism exists whereby CDK1 inhibited TSC1 to promote mTORC1 activation and collagen synthesis. However, inhibition with CDK1 had no effect on collagen I synthesis. Interestingly, treatment with BMS-265246 induced a baseline increase of 4E-BP1^{T70} phosphorylation and an increase in the phosphorylation of the 4E-BP1^{S65} site in TGF-β_1 and non-TGF-β_1 treated conditions. There may be a tenuous link to explain this data, in a report that has linked CDK1 to directly phosphorylating 4E-BP1 during mitosis (Shuda et al. 2015). Therefore, complex cross-talk may exist between mTORC1 and CDK1 whereby inhibition of CDK1 under certain conditions leads to an increase in mTORC1 activation or access to directly phosphorylate 4E-BP1.

4.5.5. The effect of MEK1/2 inhibition on TGF-β_1 induced mTORC1 signalling in pHLFs

ERK1/2 signalling influences a broad range of cellular processes including: cell survival/apoptosis, proliferation, differentiation, DNA synthesis and collagen synthesis (Gille & Downward 1999; Lu & Xu 2006; Lim et al. 2003). ERK1/2 are broadly expressed proteins that have been investigated in a number of cell types, including fibroblasts.

The activation of the TβRII through the ligation of TGF-β_1 leads to the autophophorylation of certain tyrosine residues, although it is primarily a serine/threonine kinase. The three phosphorylation sites are: Y259, Y336 and Y424 (Lawler et al. 1997). The phosphorylation of these tyrosine residues is critical for the recruitment and complex formation of shcA-Grb2-SOS, which also require the kinase activity of TβRI. Together this complex is able to promote RAS^{GTP} formation which leads to the activation of the kinase cascade: RAS-RAF-MEK1/2-ERK1/2-RSK1. ERK regulates various proteins downstream of its kinase activity. Including transcription factors and kinases. In particular, I was interested in its relationship with TSC2. Active ERK1/2 phosphorylates TSC2 at two sites Ser^{540} and Ser^{664}. In addition, ERK1/2 activates RSK. Interestingly, RSK is also capable of phosphorylating the TSC2 complex at two sites Ser^{939} (also shared with AKT) and Thr^{1462} (Ma et al. 2005).

The inhibitor AS703026 has completed phase 2 clinical trials in patients for the treatment of N-ras mutated cutaneous melanoma (NCT01693068) and was well suited to inhibit ERK phosphorylation due to it selectivity and inhibition of MEK1/2. Figure 3.43 demonstrates the effects of this compound were found to be minimal on 4E-BP1 phosphorylation in pHLFs, yet at this concentration it almost completely inhibited MEK, which is observed by looking at its substrate phosphorylation (ERK1/2). The concentration selected for this compound to interrogate its effect on mTORC1 activity was 1 μM which gave near maximal inhibition. Reports support this observation using 2 μM as the top concentration to get full inhibition of ERK phosphorylation (Kim et al. 2010). In the collagen deposition assay, I utilised a high concentration of 10 μM which is 10-fold higher than what was required to fully inhibit the MEK1/2 kinases and this did not inhibit collagen I synthesis. Taken together these data support

that ERK1/2 is being inhibited by the compound but does not inhibit collagen and only inhibits 4EBP1 phosphorylation minimally.

In contrast, reports have shown that ERK1/2 can inhibit TSC2 to promote mTORC1 activation of P70S6K (Ma et al. 2005). However, this was linked to the promotion of cell proliferation and there was no evidence demonstrating an increase in collagen synthesis. Furthermore, this report did not address the effects of ERK activation and TSC2 inhibition on 4E-BP1 phosphorylation. The differences in results might also be explained by the use of stimulus (PMA) and the cell type (HEK393) used in this study (Ma et al. 2005), suggesting that the role of ERK1/2 may be context dependent. In human dermal fibroblasts ERK1/2 mediates collagen gene expression (Bhogal & Bona 2008). Treatment with IL-4 and IL-13 both lead to an increase in EKR1/2 phosphorylation and an increase in gene expression. In addition, IL4 and IL13 both increase TGF-β_1 levels which leads autocrine signalling in human dermal fibroblasts (Bhogal & Bona 2008). Critically, the stimulus required for the activation of ERK1/2 was not addressed, suggesting that either IL4/IL13 or TGF-β_1 could be responsible (Bhogal & Bona 2008). Furthermore, the ERK1/2 phosphorylation may be important for TGF-β_1 synthesis and its autocrine signalling is what leads to the activation of the SMAD pathway to promote the increase in collagen gene expression.

4.5.6. The effect of RSK inhibition on TGF-β_1 induced mTORC1 signalling in pHLFs

RSK1 is not only a down-stream kinase of ERK1/2, but also a substrate of ERK5 which acts independently or synergistically with ERK2 (Pearson et al. 2001). Critically, RSK1 is also able to phosphorylate TSC2 to enhance PI3K/AKT induced mTORC1 activation (Roux et al. 2004). RSK1 has been implicated in cell proliferation which is inhibited by the compound SL0101 (Lu & Xu 2006; Zaru et al. 2015; Hilinski et al. 2012). The inhibition of proliferation was reproduced within pHLFs using the same inhibitor which suggests that SL0101 was engaging the mechanism within our cells.

RSK1 has been established to increase mTORC1 activity along with increased ERK1/2 activity to promote melanoma growth (Romeo et al. 2013). The reports

demonstrate that treatment with SL0101 inhibits P70S6K activity. Furthermore, they established that RSK was downstream of ERK activity (Romeo et al. 2013). In contrast, treatment with SL0101 in pHLFs demonstrated that SL0101 did not inhibit 4E-BP1 phosphorylation, yet mediated an increase in 4E-BP1^{S65} phosphorylation. The explanation for this difference in regulation of mTORC1 activity may be stimulus-dependent. In the previous study, ERK and RSK activity was driven by a mutation in RAS, rendering RAS constitutively active. Interestingly, the pathway RAS-RAF-MEK1/2-ERK1/2 has a number of critical feedforward and feedback loops which regulate their activity (Arkun & Yasemi 2018). This may explain why there is a partial increase in 4E-BP1^{S65} phosphorylation at baseline and TGF-β_1 treated pHLFs, since inhibition of RSK1 may promote increased ERK1/2 activity which may feed into the TSC1/2 complex, in a TGF-β_1 independent manner. Taking the previous point into consideration, this could also be true for ERK or AKT inhibition as well. In an attempt to explain why the inhibition of these kinases did not impact on TGF-β_1-induced collagen I synthesis I considered that feedback loops may be in place to compensate for the loss of one kinase or another. This particularly makes sense when putting it into the context of a wound healing response. The loss of one of these pathways could be highly detrimental to the organism when activated in response to a stimulus triggered by a wound. Open wounds are at high risk of infection, which can subsequently lead to sepsis and death. Therefore, considering these implications, from an evolutionary perspective, cells may have developed alternative mechanisms to compensate for the loss of one kinase by using another. This is well observed for the RAS-RAF-MEK1/ERK1/2 pathway, and interestingly the mTORC1 pathway feeding back to AKT (Arkun & Yasemi 2018; Breuleux et al. 2009). Furthermore, reports have established a synergy between both ERK and PI3K signalling, one report suggests that both PI3K and ERK are required for collagen I-III production in fibroblasts (Lim et al. 2003). In addition, the full inhibition of TSC2 in HEK293 cells as measured by P70S6K was achieved by a combination of wortmannin (PI3K inhibitor) and UO126 (ERK inhibitor). Together the inhibitors fully abolish P70S6K phosphorylation. However, it is important to consider that wortmannin is

capable of inhibiting mTOR, therefore, the inhibition of PI3K may instead be mTOR being inhibited.

Interestingly, ERK inhibition and RSK1 inhibition demonstrated some marginal effects on mTORs ability to phosphorylate 4EBP1. This posed the question of whether TSC2 needed input from a number of kinases to promote inhibition of the complex and allow for mTORC1 activation, or whether inhibition of one pathway could be compensated for another? Investigations are ongoing into this question and initial data assessed the effect of dual inhibition of PI3K and ERK in the collagen deposition assay. The results in Figure 3.48 were negative, however, further investigation is needed before further conclusions can be drawn.

Finally, $TSC2^{-/-}$ mice suggest that amino acid regulation of mTORC1 at all 4E-BP1 phosphorylation sites can act independently of TSC2 knock-down (Smith et al. 2005). This also suggests that it is possible that the TSC1/2 complex is not required in our TGF-β_1 stimulated response, considering the ambiguous data received from the knock-down in combination with the TGF-β_1 curve. Alternative mechanisms of mTORC1 activation are discussed below. These could prove to be pathways that are activated downstream of TGF-β_1 stimulation and be required to activate mTORC1 and mediate collagen I synthesis.

4.6. Other potential factors that could contribute to TGF-β_1 regulated mTORC1 activation and collagen I synthesis

mTORC1 is a large complex that can be regulated by various stimuli, including cytokines, mitogens, nutrients, cell stress and ROS. Although this study has begun to rule out a number of potential inputs into mTOR, it is still important to recognise that there are many more possibilities. SMAD 3 is capable of regulating mTORC1 and ERK1/2 and RSK were also able to marginally decrease mTORC1 mediated 4E-BP1 phosphorylation. In addition, within our group, a regulator of TSC1/2, AMPK, was investigated. The work demonstrated that the inhibition of AMPK had no impact on our PHLF's at basal or when stimulated with TGF-β_1 (Selvarajah, unpublished). In addition, when AMPK was over expressed there was also no impact on mTORC1

kinase activity or collagen I deposition (Selvarajah, unpublished). There are still a number of mechanisms that have not been investigated in pHLFs as discussed below.

4.6.1. Amino acids

There are 20 amino acids found in eukaryotic cells, each playing important functions within the cell. They can fall into three categories essential, non-essential and partially essential amino acids. Our group and others have shown there is a well-established need for glycine synthesis for the production of collagen synthesis at later time-points when collagen mRNA is at its peak and we begin to observe an increase in deposited collagen. At early time-points, this increase has not been extensively investigated, with the exception of GLS inhibition, as previously described (results section 3.36 and discussion section 4.34).

As a global regulator of translation, it is unsurprising, therefore, to find that mTORC1 is regulated by the presence of amino acids. Amino acids are critical for the activation mTORC1 and it has been well-documented that, in the absence of amino acids, mTORC1 cannot be activated (Hara et al. 1998; Wang et al. 1998). Individual amino acids were investigated, showing that arginine and leucine are critical for mTORC1 activation, but only if the 18 other amino acids were also present (Hara et al. 1998; Bar-Peled & Sabatini 2014). This suggests that the role of amino acids is permissive, meaning potentially that in their absence, other pathways cannot enhance mTORC1 activation in pHLF's. In the absence of serum stimulation, all three sites on 4E-BP1 and P70S6K show some level of phosphorylation, which is important for maintaining cellular homeostasis within the cell which requires the translation of mRNA. Furthermore, the removal of amino acids leads to the increased phosphorylation of the inhibitory phosphorylation site T2446 on mTOR, which is also likely attributed to the slow depletion of amino acids in the culture medium until they can be returned to sufficient levels.

mTORC1 activity is regulated by amino acids through the amino acid sensing capabilities of the RAG/RAGULATOR complex as previously discussed. The RAGs are also well linked to the TSC2 complex and RHEB (Groenewoud &

Zwartkruis 2013; Long, Ortiz-Vega, et al. 2005). Amino acid withdrawal does not affect the GTP loading of RHEB which is primarily located on the lysosome, but does prevent mTORC1's ability to become activated (Long, Ortiz-Vega, et al. 2005). This was later discovered to be due to the RAG/RAGULTOR complexes ability to recruit mTORC1 to the lysosome only when amino acids are present (Sancak et al. 2010). Attachment of a lysosomal localisation marker to RAPTOR critically overcomes amino acid starvation, suggesting that RAPTORS role is to localise mTORC1 to the lysosome.

As previously discussed, in the presence of amino acids, the RAGULATOR provides the GEF activity for RAGS which allows RAG A or RAG B to recruit mTORC1 via RAPTOR to the lysosome. Another layer of regulation to this is GATOR 1, which is essential in the absence of amino acids and provides GAP activity towards GTP bound RAGs, therefore inhibiting their ability to recruit mTORC1 to the lysosome. In the presence of amino acids, GATOR2, is capable of detecting the amino acids levels and therefore inhibits GATOR 1. Amino acids regulate TSC1/2 lysosomal localisation and in amino acid-rich conditions TSC2 becomes dissociated from the lysosome, preventing it from inhibiting RHEB. RAG is able to recruit TSC2 which is mediated by the removal of amino acids (Demetriades et al. 2014).

Taking the above into consideration, it is possible that TGF-β_1 might promote an influx of amino acids at 3 hours. I have shown that 4E-BP1 phosphorylation mediated by the TGF-β_1 stimulated axis is dependent on the presence on SMAD 3. This could potentially be explained by the transcriptional control over a number of amino acid transporters or proteins involved in regulating the RAGs/RAGULATOR complex at the lysosome. However, in my opinion this is unlikely, even in amino acid-rich conditions as there is still likely some TSC1/2 localised to the lysosome (Demetriades et al. 2014). This means it is likely that there is a pool of $RHEB^{GTP}$ and $RHEB^{GDP}$ which exist in equilibrium. To respond to an injurious stimulus, the release of TGF-β_1 and this stimulate the pHLFs to increase mTORC1 activation, therefore, TGF-β_1 signalling pathways achieve this through further TSC2 inhibition (on top of what the amino acids already maintain). This response to injury needs to be rapid to avoid prolonged compromise to the organism and wound resolution needs to occur rapidly. To

upregulate amino acid transporters, it is likely to be too slow for the rapid response required, however kinases such as MEK1/2 can become activated as quickly as 5 mins allowing for a rapid response. Furthermore, it seems counterintuitive for this to be the TGF-β_1 responsive mechanism, since there is no guarantee of sufficient amino acids in the extracellular milieu in a wound to support this rapid requirement of activation. Although it is possible that the amino acids could be supplied by the blood.

Taking into consideration that amino acids are still required for the initial priming of mTORC1, as seen by the basal levels of the 4E-BP1$^{T37/46}$ phosphorylation site (TGF-β_1 independent), we observe in pHLFs an increase in the expression of a number of amino acid transporters (Platé, unpublished data) and the upregulation of a glycolytic enzymes, PSAT1, PHGDH and SHMT2, which are regulated by ATF4. This will therefore support the supply of amino acids which are being depleted by the production of new proteins, especially collagen. Furthermore, this supply of amino acids is needed to keep mTORC1 localised to the lysosome to maintain mTORC1s prolonged activation of 24-48 hours after the initial signalling cascade at 3 hours post-TGF-β_1 stimulation.

4.6.2. PA

Phosphatidylcholine (PC)-specific phospholipase D (PLD) converts phosphatidyl choline into phosphoatidic acid (PA) which is required for lipid metabolism. There are three enzymes capable of generating PA which are, PLD, LPAAT and DAG. PLD has been extensively investigated owing to its implication in Parkinson's, Alzheimer's and cancer (Bravo et al. 2018; Ahn et al. 2002; Chen et al. 2003).

There are currently two known mammalian PLD enzymes PLD1 and PLD2. PLD is important for a number of cellular processes: cytoskeletal reorganisation, exocytosis, cell migration and membrane trafficking (Foster et al. 2014). Most PLD mediated functions are through PA's secondary role acting as a lipid second messenger. PLD production of PA has been attributed to the binding and activation of the mTOR kinase (English et al. 1996; Fang et al. 2001; Sun & Chen 2008; Sun et al. 2008)

PLD1 activation is regulated by GTPases, specifically RHEB and RalA (Luo et al. 1998; Fang et al. 2001). In response to mitogen stimulation, PLD1 can bind to RHEB where it can not only promote mTORC1 activation, but has also been recognised to activate mTORC2 (Fang et al. 2001; Toschi et al. 2009). Additionally, in response to amino acids, RHEB can also bind to PLD1 to promote its activity. However, what functional role this plays has not been identified (Sun et al. 2008; Fang et al. 2001). Exogenous treatment with PA has been demonstrated to phosphorylate 4E-BP1 and increase P70S6K activity (Fang et al. 2001). Interestingly, in the absence of amino acids, stimulation with PA is unable to stimulate mTORC1 activation, building upon the concept that amino acids are permissive in allowing further mTORC1 activation (Fang et al. 2001).

Furthermore, PLD1 is regulated by TSC2 activity, likely through its link with RHEB which is also negatively regulated by TSC2 (Sun et al. 2008). This report also demonstrates that PLD1 is sensitive to PI3K inhibition (Sun et al. 2008). Interpretation is ambiguous due to the selectivity of wortmannin (also inhibits mTOR) which was utilised to interrogate its effects on PLD1 activity. Considering that PLD1 inhibition leads to reduced mTORC1 activation, it is likely, therefore, that PLD1 is downstream of PI3K. In addition the overexpression of PIP3 (the product of PI3K's conversion of PIP2) increases PLD1 activity (Sun et al. 2008). Stimulation of HEK293 cells with phosphatidic acid is rapamycin-sensitive leading to a decrease in P70S6K activity and a loss of 4E-BP1 phosphorylation. Interestingly, the mobility shift seen with the 4E-BP1 on the western blot presented in this article is not completely lost compared to untreated cells, suggesting that some sites on 4E-BP1 may still be phosphorylated, such as 4E-BP1$^{T37/46}$ (Sun et al. 2008). PLD can also be regulated by amino acid levels, via the amino acid sensing capabilities of the class III PI3K Vps34. Vps34 is activated by the availability of amino acids in the lysosome, which is where Vps34 is located. Activated Vps34 produces PtdIns(3)P which recruits PLD to the lysosome where it can be activated by RHEB. However, experiments conducted within our laboratories demonstrated that the inhibition of Vps34 in pHLFs did not inhibit TGF-β_1 stimulated mTORC1 activation or collagen I synthesis (Woodcock, unpublished data).

Interestingly, increased PLD activity and increased PA promotes rapamycin resistance in cells, owing to competition for binding at the FRB domain on mTOR (Toschi et al. 2009; Chen et al. 2003). There is one report linking increased PLD activity and PA production to TGF-β_1 (Bing Hong et al. 2000). This report demonstrated that the TGF-β_1 response was variable between different cell lines, with some cell lines showing very little increase in PA. Considering pHLFs are resistant to rapamycin, unresponsiveness to MAPK inhibition but sensitive to the loss of RHEB in terms of TGF-β_1-induced collagen synthesis, this could suggest a role of PLD synthesis of PA in our fibroblasts and therefore, might explain the inability of the compounds used, to inhibit 4E-BP1 and collagen synthesis. However, the association between PA, PLD and collagen has not yet been established.

4.7. Conclusion

TGF-β activates mTORC1 to promote collagen I deposition in pHLFs through SMAD-dependent and PI3K/AKT independent pathways.

This study identified the mechanism required for mTOR S2448 phosphorylation, which was mediated through a PDK1, P70S6K and mTOR axis.

I also show that SMAD 3 activation is critical for TGF-β_1 induced transcription of the collagen gene and early mTORC1 activation.

Finally, RHEB and the inhibition of its negative regulator, TSC2, are required for the early activation of mTORC1 but this is independent of AKT, ERK1/2, RSK, MK2, P38 MAPK and TAK1 when acting in isolation, but it is unknown whether they compensate for each other or act in synergy.

This present study supports a model (Figure 4.3) whereby TGF-β_1 stimulated SMAD 3 and RHEB regulate the early activation of mTORC1. A single kinase inhibition approach (ERK1/2, TAK1, MK2, RSK and P38 MAPK) failed to identify the upstream kinase involved in regulating TSC1/2/RHEB.

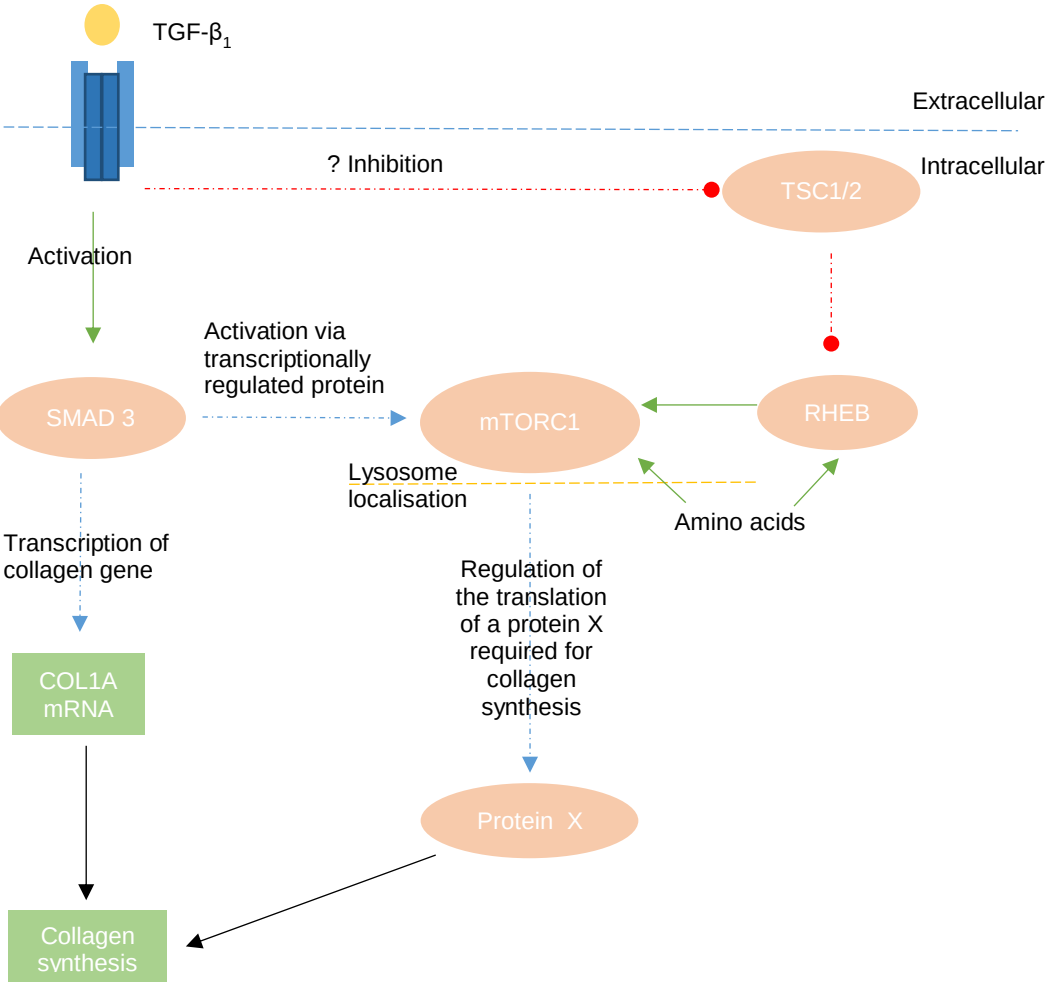

Figure 4.3: Proposed model for TGF-β1 stimulated collagen synthesis in pHLF

TGF-β1 stimulates the activation of the pHLF mediating collagen gene through the activation of the SMAD 3 pathway. The activation of mTORC1 is dependent on SMAD 3 activation and the RHEB/TSC1/2 axis, with amino acids activing as a permissive signal. mTOR mediates the translation of an unknown protein, 'protein x', which helps mediate collagen I synthesis.

4.8. Future work

While the present study has begun to unravel the mechanisms for TGF-β1 stimulated mTORC1 activation, the precise mechanism involved remains undefined. Future investigation would be directed towards assessing SMAD 3, TSC1/2 complex and mTORC1 localisation.

During the course of these investigations, I identified that SMAD 3 regulates TGF-β1 stimulated mTORC1 activation. Due to the nature of this interaction, it would be interesting if this was recapitulated in other cell types. Within our group we have demonstrated that mTORC1 is important for mediating collagen synthesis in a number of cancer cell lines. It would be interesting to

identify if TGF-β_1 regulated SMAD 3 activation was required for mTORC1 activation in these other cell lines.

Furthermore, how SMAD 3 promotes mTORC1 activation in pHLFs was not delineated. This could be investigated by using RNAseq technology, TGF-β_1 regulated mRNA's could be compared between untreated and SMAD 3 knock-pHLFs. This pool of SMAD 3 responsive genes could perhaps help delineate proteins known to be involved in mTOR regulation. Using weighted correlation network analysis (WGCNA) on this data set would allow modules or network nodes to be established.

The TSC1/2 and RHEB axis was identified in pHLFs for the TGF-β_1 response and mTORC1 activation. Kinases impacting on TSC2 inhibition reported in the literature individually did not inhibit mTORC1 activation or collagen synthesis. Further investigation of combined inhibitors to identify if multiple inhibitory inputs are required to fully inhibit the TSC1/2 complex or prevent compensatory mechanisms are now needed.

The two proteins, TSC1 or TSC2, have more than 20 phosphorylation sites which either inhibit or activate the complex. Investigation of each site may also help reveal which sites are TGF-β_1 responsive. Additionally, a time-course of the phosphorylation sites may reveal different integration patterns from different kinases phosphorylating different sites. The availability of antibodies for each site is limited. To overcome this, point mutations could be introduced at each phosphorylation site to interrogate their role for TGF-β_1 and TSC1/2 complex activity. To further complement this, the GTP/GDP ratio of RHEB could be measured to determine if this changes in response to TGF-β_1.

Translational controlled tumour protein (TCTP) is a highly conserved protein throughout all eukaryotic organisms (Bommer 2017). Interestingly, the conversion of $RHEB^{GDP}$ to $RHEB^{GTP}$ requires the GEF activity of TCTP protein (Dong et al. 2009; Hsu et al. 2007). However, this has been disputed (Wang et al. 2008). TCTP is a TGF-β_1 regulated protein which has been reported to be required for EMT and cytoskeletal reorganisation (Mishra et al. 2018). Interestingly, TCTP is translationally regulated by mTOR (Bommer et al. 2015), which could signal a potential feed forward loop that perpetuates

mTORC1 activation through increased conversion of $RHEB^{GDP}$ to $RHEB^{GTP}$ via the GEF activity of TCTP.

RHEB, TSC1/2 and mTORC1 are regulated by cellular localisation, critically the lysosome where RHEB is believed to be located along with TSC2. Investigation of mTORC1 localisation in response to TGF-β_1 may reveal changes in its localisation temporally. This would also be interesting for other components: 4E-BP1, P70S6K, TSC1/2 and RHEB since their localisation can regulate their activity.

14-3-3 proteins are one way of sequestering TSC1/2 activity, however, these normally require the phosphorylation of the inhibitory sites (Huang & Manning 2008; Astrinidis et al. 2003; Lee et al. 2007; Ma et al. 2005; Long, Lin, et al. 2005; Dan et al. 2002; Y. Li et al. 2003; Inoki et al. 2006; Roux et al. 2004). A potential mechanism could be delineated to determine if SMAD 3 is capable of regulating the expression of a 14-3-3 protein which could bridge the link between SMAD 3 and TSC2, creating a novel SMAD 3-14-3-3–TSC1/2–mTORC1 axis.

Finally, the knowledge surrounding amino acid sensing components and regulator components is expanding. It would be interesting to investigate whether TGF-β_1 can mediate rapid influxes of amino acids to regulate components such as SESTRIN and CASTOR to increase mTORC1 activity.

References

Abdollah, S. et al., 1997. TbetaRI phosphorylation of Smad2 on Ser465 and Ser467 is required for Smad2-Smad4 complex formation and signaling. *The Journal of biological chemistry*, 272(44), pp.27678–85. Available at: http://www.ncbi.nlm.nih.gov/pubmed/9346908 [Accessed August 7, 2018].

Abooali, M. et al., 2015. Crucial involvement of xanthine oxidase in the intracellular signalling networks associated with human myeloid cell function. *Scientific Reports*, 4(1), p.6307. Available at: http://www.nature.com/articles/srep06307 [Accessed July 19, 2018].

Abraham, R.T. & Wiederrecht, G.J., 1996. IMMUNOPHARMACOLOGY OF RAPAMYCIN. *Annual Review of Immunology*, 14(1), pp.483–510. Available at: http://www.annualreviews.org/doi/10.1146/annurev.immunol.14.1.483 [Accessed July 24, 2018].

Acosta-Jaquez, H.A. et al., 2009. Site-specific mTOR phosphorylation promotes mTORC1-mediated signaling and cell growth. *Molecular and cellular biology*, 29(15), pp.4308–24. Available at: http://mcb.asm.org/content/29/15/4308.abstract [Accessed May 18, 2015].

Adams, C.M., 2007. Role of the transcription factor ATF4 in the anabolic actions of insulin and the anti-anabolic actions of glucocorticoids. *The Journal of biological chemistry*, 282(23), pp.16744–53. Available at: http://www.ncbi.nlm.nih.gov/pubmed/17430894 [Accessed August 1, 2018].

Ahn, B.-H. et al., 2002. α-Synuclein Interacts with Phospholipase D Isozymes and Inhibits Pervanadate-induced Phospholipase D Activation in Human Embryonic Kidney-293 Cells. *Journal of Biological Chemistry*, 277(14), pp.12334–12342. Available at: http://www.ncbi.nlm.nih.gov/pubmed/11821392 [Accessed August 24, 2018].

Akhurst, R.J., 2004. TGFβ signaling in health and disease. *Nature Genetics*, 36(8), pp.790–792. Available at: http://www.nature.com/articles/ng0804-790 [Accessed August 30, 2018].

Alder, J.K. et al., 2015. Exome Sequencing Identifies Mutant TINF2 in a Family With Pulmonary Fibrosis. *Chest*, 147(5), pp.1361–1368. Available at: http://www.ncbi.nlm.nih.gov/pubmed/25539146 [Accessed August 29, 2018].

Arkun, Y. & Yasemi, M., 2018. Dynamics and control of the ERK signaling pathway: Sensitivity, bistability, and oscillations M. Thattai, ed. *PLOS ONE*, 13(4), p.e0195513. Available at: http://dx.plos.org/10.1371/journal.pone.0195513 [Accessed August 22, 2018].

Armanios, M.Y. et al., 2007. Telomerase Mutations in Families with Idiopathic Pulmonary Fibrosis. *New England Journal of Medicine*, 356(13), pp.1317–1326. Available at: http://www.nejm.org/doi/abs/10.1056/NEJMoa066157 [Accessed August 29, 2018].

Ask, K. et al., 2008. Progressive pulmonary fibrosis is mediated by TGF-beta isoform 1 but not TGF-beta3. *The international journal of biochemistry & cell biology*, 40(3), pp.484–95. Available at: http://www.ncbi.nlm.nih.gov/pubmed/17931953 [Accessed August 30, 2018].

Astrinidis, A. et al., 2003. Cell cycle-regulated phosphorylation of hamartin, the product of the tuberous sclerosis complex 1 gene, by cyclin-dependent kinase 1/cyclin B. *The Journal of biological chemistry*, 278(51), pp.51372–9. Available at: http://www.ncbi.nlm.nih.gov/pubmed/14551205 [Accessed February 24, 2018].

Bakin, A. V. et al., 2000. Phosphatidylinositol 3-Kinase Function Is Required for Transforming Growth Factor β-mediated Epithelial to Mesenchymal Transition and Cell Migration. *Journal of Biological Chemistry*, 275(47), pp.36803–36810. Available at: http://www.ncbi.nlm.nih.gov/pubmed/10969078 [Accessed August 31, 2018].

Bar-Peled, L. et al., 2013. A Tumor Suppressor Complex with GAP Activity for the Rag

GTPases That Signal Amino Acid Sufficiency to mTORC1. *Science*, 340(6136), pp.1100–1106. Available at: http://www.ncbi.nlm.nih.gov/pubmed/23723238 [Accessed March 16, 2017].

Bar-Peled, L. et al., 2012. Ragulator is a GEF for the rag GTPases that signal amino acid levels to mTORC1. *Cell*, 150(6), pp.1196–208. Available at: http://www.pubmedcentral.nih.gov/articlerender.fcgi?artid=3517996&tool=pmcentrez&rendertype=abstract [Accessed October 24, 2016].

Bar-Peled, L. & Sabatini, D.M., 2014. Regulation of mTORC1 by amino acids. *Trends in cell biology*, 24(7), pp.400–6. Available at: http://www.ncbi.nlm.nih.gov/pubmed/24698685 [Accessed August 24, 2018].

Benvenuto, G. et al., 2000. The tuberous sclerosis-1 (TSC1) gene product hamartin suppresses cell growth and augments the expression of the TSC2 product tuberin by inhibiting its ubiquitination. *Oncogene*, 19(54), pp.6306–6316. Available at: http://www.ncbi.nlm.nih.gov/pubmed/11175345 [Accessed August 28, 2018].

Bernard, K. et al., 2017. Glutaminolysis controls myofibroblast differentiation Glutaminolysis is Required for TGF-β1-Induced Myofibroblast Differentiation and Activation. Available at: http://www.jbc.org/cgi/doi/10.1074/jbc.RA117.000444 [Accessed August 16, 2018].

Bhogal, R.K. & Bona, C.A., 2008. Regulatory Effect of Extracellular Signal-Regulated Kinases (ERK) on Type I Collagen Synthesis in Human Dermal Fibroblasts Stimulated by IL-4 and IL-13. *International Reviews of Immunology*, 27(6), pp.472–496. Available at: http://www.tandfonline.com/doi/full/10.1080/08830180802430974 [Accessed August 22, 2018].

Bing Hong, Z. et al., 2000. *Activation of phospholipase D activity in transforming growth factor-beta-induced cell growth inhibition*, Available at: https://www.nature.com/articles/7290043.pdf?origin=ppub [Accessed August 24, 2018].

Bommer, U.-A. et al., 2015. Growth-factor dependent expression of the translationally controlled tumour protein TCTP is regulated through the PI3-K/Akt/mTORC1 signalling pathway. *Cellular Signalling*, 27(8), pp.1557–1568. Available at: http://www.ncbi.nlm.nih.gov/pubmed/25936523 [Accessed August 27, 2018].

Bommer, U.-A., 2017. The Translational Controlled Tumour Protein TCTP: Biological Functions and Regulation. In *Results and problems in cell differentiation*. pp. 69–126. Available at: http://www.ncbi.nlm.nih.gov/pubmed/29149404 [Accessed August 27, 2018].

Bonniaud, P. et al., 2005. Progressive Transforming Growth Factor β1–induced Lung Fibrosis Is Blocked by an Orally Active ALK5 Kinase Inhibitor. *American Journal of Respiratory and Critical Care Medicine*, 171(8), pp.889–898. Available at: http://www.ncbi.nlm.nih.gov/pubmed/15563636 [Accessed August 31, 2018].

Borie, R. et al., 2013. Detection of Alveolar Fibrocytes in Idiopathic Pulmonary Fibrosis and Systemic Sclerosis O. Eickelberg, ed. *PLoS ONE*, 8(1), p.e53736. Available at: http://dx.plos.org/10.1371/journal.pone.0053736 [Accessed February 3, 2018].

Borok, Z. et al., 1991. Augmentation of Functional Prostaglandin E Levels on the Respiratory Epithelial Surface by Aerosol Administration of Prostaglandin E. *American Review of Respiratory Disease*, 144(5), pp.1080–1084. Available at: http://www.ncbi.nlm.nih.gov/pubmed/1952435 [Accessed October 15, 2018].

Böttinger, E.P. & Bitzer, M., 2002. TGF-beta signaling in renal disease. *Journal of the American Society of Nephrology : JASN*, 13(10), pp.2600–10. Available at: http://www.ncbi.nlm.nih.gov/pubmed/12239251 [Accessed August 30, 2018].

Bravo, F.V. et al., 2018. Phospholipase D functional ablation has a protective effect in an Alzheimer's disease Caenorhabditis elegans model. *Scientific Reports*, 8(1), p.3540. Available at: http://www.ncbi.nlm.nih.gov/pubmed/29476137 [Accessed August 24, 2018].

Breuleux, M. et al., 2009. Increased AKT S473 phosphorylation after mTORC1 inhibition is rictor dependent and does not predict tumor cell response to PI3K/mTOR inhibition. *Molecular cancer therapeutics*, 8(4), pp.742–53. Available at: http://www.ncbi.nlm.nih.gov/pubmed/19372546 [Accessed September 6, 2018].

Bucala, R. et al., 1994. Circulating fibrocytes define a new leukocyte subpopulation that mediates tissue repair. *Molecular medicine (Cambridge, Mass.)*, 1(1), pp.71–81. Available at: http://www.ncbi.nlm.nih.gov/pubmed/8790603 [Accessed February 3, 2018].

Burnett, P.E. et al., 1998. RAFT1 phosphorylation of the translational regulators p70 S6 kinase and 4E-BP1. *Proceedings of the National Academy of Sciences of the United States of America*, 95(4), pp.1432–7. Available at: http://www.ncbi.nlm.nih.gov/pubmed/9465032 [Accessed July 26, 2018].

Camelo, A. et al., 2014. The epithelium in idiopathic pulmonary fibrosis: breaking the barrier. *Frontiers in Pharmacology*, 4, p.173. Available at: http://journal.frontiersin.org/article/10.3389/fphar.2013.00173/abstract [Accessed October 31, 2016].

Caohuy, H. et al., 2014. Activation of 3-phosphoinositide-dependent kinase 1 (PDK1) and serum- and glucocorticoid-induced protein kinase 1 (SGK1) by short-chain sphingolipid C4-ceramide rescues the trafficking defect of ΔF508-cystic fibrosis transmembrane conductance regulator (ΔF508-CFTR). *The Journal of biological chemistry*, 289(52), pp.35953–68. Available at: http://www.ncbi.nlm.nih.gov/pubmed/25384981 [Accessed July 21, 2018].

Carrière, A. et al., 2008. Oncogenic MAPK signaling stimulates mTORC1 activity by promoting RSK-mediated raptor phosphorylation. *Current biology : CB*, 18(17), pp.1269–77. Available at: http://www.ncbi.nlm.nih.gov/pubmed/18722121 [Accessed July 27, 2018].

Carsillo, T., Astrinidis, A. & Henske, E.P., 2000. Mutations in the tuberous sclerosis complex gene TSC2 are a cause of sporadic pulmonary lymphangioleiomyomatosis. *Proceedings of the National Academy of Sciences of the United States of America*, 97(11), pp.6085–90. Available at: http://www.ncbi.nlm.nih.gov/pubmed/10823953 [Accessed August 21, 2018].

Castel, P. et al., 2016. PDK1-SGK1 Signaling Sustains AKT-Independent mTORC1 Activation and Confers Resistance to PI3Kα Inhibition. *Cancer cell*, 30(2), pp.229–242. Available at: http://www.ncbi.nlm.nih.gov/pubmed/27451907 [Accessed September 5, 2018].

Catena, V. & Fanciulli, M., 2017. Deptor: not only a mTOR inhibitor. *Journal of experimental & clinical cancer research : CR*, 36(1), p.12. Available at: http://www.ncbi.nlm.nih.gov/pubmed/28086984 [Accessed July 27, 2018].

Chang, J.C. et al., 2018. Abstract 2035: Knockdown of TGFβ-activated ATF4 inhibits triple negative breast cancer metastases independently of cellular stress. *Cancer Research*, 78(13 Supplement), pp.2035–2035. Available at: http://cancerres.aacrjournals.org/content/78/13_Supplement/2035.short [Accessed August 2, 2018].

Chantranupong, L. et al., 2016. The CASTOR Proteins Are Arginine Sensors for the mTORC1 Pathway. *Cell*, 165(1), pp.153–164. Available at: http://www.ncbi.nlm.nih.gov/pubmed/26972053 [Accessed August 27, 2018].

Chantranupong, L. et al., 2014. The Sestrins Interact with GATOR2 to Negatively Regulate the Amino-Acid-Sensing Pathway Upstream of mTORC1. *Cell Reports*, 9(1), pp.1–8. Available at: http://www.ncbi.nlm.nih.gov/pubmed/25263562 [Accessed August 27, 2018].

Chen, J. et al., 1999. cDNA cloning and sequencing of MH2 domain of Smad2 from human dental pulp cells. *The Chinese journal of dental research : the official journal of the*

Scientific Section of the Chinese Stomatological Association (CSA), 2(2), pp.14–8. Available at: http://www.ncbi.nlm.nih.gov/pubmed/10863401 [Accessed August 30, 2018].

Chen, S.-J. et al., 1999. Stimulation of Type I Collagen Transcription in Human Skin Fibroblasts by TGF-β: Involvement of Smad 3. *Journal of Investigative Dermatology*, 112(1), pp.49–57. Available at: http://linkinghub.elsevier.com/retrieve/pii/S0022202X15403707 [Accessed February 19, 2018].

Chen, Y.-J. et al., 2002. *Signaling Mechanism of Fsh and Tgf B 1 in Stimulating Steroidogenesis in Rat Ovarian Granulosa Cells*, Available at: https://pdfs.semanticscholar.org/c3b6/8a0c32d0f219738c661186e0154376389024.pdf [Accessed September 12, 2018].

Chen, Y., Zheng, Y. & Foster, D.A., 2003. Phospholipase D confers rapamycin resistance in human breast cancer cells. *Oncogene*, 22(25), pp.3937–3942. Available at: http://www.ncbi.nlm.nih.gov/pubmed/12813467 [Accessed August 24, 2018].

Cheng et al., 2004. T2446 is a Novel mTOR Phosphorylation Site Regulated by Nutrient Status. , 17. Available at: http://www.jbc.org/ [Accessed July 21, 2018].

Cheng, S.W.Y. et al., 2004. Thr2446 is a novel mammalian target of rapamycin (mTOR) phosphorylation site regulated by nutrient status. *The Journal of biological chemistry*, 279(16), pp.15719–22. Available at: http://www.ncbi.nlm.nih.gov/pubmed/14970221 [Accessed June 23, 2018].

Chiang, G.G. & Abraham, R.T., 2005. Phosphorylation of mammalian target of rapamycin (mTOR) at Ser-2448 is mediated by p70S6 kinase. *The Journal of biological chemistry*, 280(27), pp.25485–90. Available at: http://www.jbc.org/content/280/27/25485.abstract [Accessed February 1, 2017].

Choi, J. et al., 1996. Structure of the FKBP12-rapamycin complex interacting with the binding domain of human FRAP. *Science (New York, N.Y.)*, 273(5272), pp.239–42. Available at: http://www.ncbi.nlm.nih.gov/pubmed/8662507 [Accessed July 25, 2018].

Choi, M.E., Ding, Y. & Kim, S. Il, 2012. TGF-β signaling via TAK1 pathway: role in kidney fibrosis. *Seminars in nephrology*, 32(3), pp.244–52. Available at: http://www.pubmedcentral.nih.gov/articlerender.fcgi?artid=3407377&tool=pmcentrez&rendertype=abstract [Accessed September 10, 2015].

Chong-Kopera, H. et al., 2006. TSC1 stabilizes TSC2 by inhibiting the interaction between TSC2 and the HERC1 ubiquitin ligase. *The Journal of biological chemistry*, 281(13), pp.8313–6. Available at: http://www.jbc.org/content/281/13/8313.full?sid=3179f590-0b36-44f3-964d-57f12ec4b9ad [Accessed April 2, 2016].

Choo, A.Y. & Blenis, J., 2009. Not all substrates are treated equally: Implications for mTOR, rapamycin-resistance, and cancer therapy. *Cell Cycle*, 8(4), pp.567–572. Available at: http://www.tandfonline.com/doi/abs/10.4161/cc.8.4.7659 [Accessed July 25, 2018].

Chow, L.N. et al., 2016. Impact of a CXCL12/CXCR4 Antagonist in Bleomycin (BLM) Induced Pulmonary Fibrosis and Carbon Tetrachloride (CCl4) Induced Hepatic Fibrosis in Mice. *PloS one*, 11(3), p.e0151765. Available at: http://www.ncbi.nlm.nih.gov/pubmed/26998906 [Accessed February 3, 2018].

Chung, E.J. et al., 2016. Mammalian Target of Rapamycin Inhibition With Rapamycin Mitigates Radiation-Induced Pulmonary Fibrosis in a Murine Model. *International journal of radiation oncology, biology, physics*, 96(4), pp.857–866. Available at: http://www.ncbi.nlm.nih.gov/pubmed/27663762 [Accessed August 31, 2018].

Cirstea, D. et al., 2014. Delineating the mTOR Kinase Pathway Using a Dual TORC1/2 Inhibitor, AZD8055, in Multiple Myeloma. Available at: www.aacrjournals.org [Accessed July 19, 2018].

Cong, X.X. et al., 2018. Activation of AKT-mTOR Signaling Directs Tenogenesis of Mesenchymal Stem Cells. *STEM CELLS*, 36(4), pp.527–539. Available at: http://doi.wiley.com/10.1002/stem.2765 [Accessed July 18, 2018].

Conte, E. et al., 2011. Inhibition of PI3K Prevents the Proliferation and Differentiation of Human Lung Fibroblasts into Myofibroblasts: The Role of Class I P110 Isoforms H. W. Chu, ed. *PLoS ONE*, 6(10), p.e24663. Available at: http://dx.plos.org/10.1371/journal.pone.0024663 [Accessed August 31, 2018].

Cooper, J.M. et al., 2017. TBK1 Provides Context-Selective Support of the Activated AKT/mTOR Pathway in Lung Cancer. *Cancer research*, 77(18), pp.5077–5094. Available at: http://www.ncbi.nlm.nih.gov/pubmed/28716898 [Accessed July 21, 2018].

Copp, J., Manning, G. & Hunter, T., 2009. TORC-specific phosphorylation of mammalian target of rapamycin (mTOR): phospho-Ser2481 is a marker for intact mTOR signaling complex 2. *Cancer research*, 69(5), pp.1821–7. Available at: http://www.ncbi.nlm.nih.gov/pubmed/19244117 [Accessed December 1, 2016].

Dagon, Y. et al., 2012. p70S6 kinase phosphorylates AMPK on serine 491 to mediate leptin's effect on food intake. *Cell metabolism*, 16(1), pp.104–12. Available at: http://www.ncbi.nlm.nih.gov/pubmed/22727014 [Accessed July 26, 2018].

Dan, H.C. et al., 2002. Phosphatidylinositol 3-Kinase/Akt Pathway Regulates Tuberous Sclerosis Tumor Suppressor Complex by Phosphorylation of Tuberin. *Journal of Biological Chemistry*, 277(38), pp.35364–35370. Available at: http://www.ncbi.nlm.nih.gov/pubmed/12167664 [Accessed August 28, 2018].

Das, F. et al., 2013. Transforming growth factor β integrates Smad 3 to mechanistic target of rapamycin complexes to arrest deptor abundance for glomerular mesangial cell hypertrophy. *The Journal of biological chemistry*, 288(11), pp.7756–68. Available at: http://www.ncbi.nlm.nih.gov/pubmed/23362262 [Accessed July 9, 2018].

Datta, A., Scotton, C.J. & Chambers, R.C., 2011. Novel therapeutic approaches for pulmonary fibrosis. *British journal of pharmacology*, 163(1), pp.141–72. Available at: http://www.ncbi.nlm.nih.gov/pubmed/21265830 [Accessed January 12, 2018].

Demetriades, C., Doumpas, N. & Teleman, A.A., 2014. Regulation of TORC1 in response to amino acid starvation via lysosomal recruitment of TSC2. *Cell*, 156(4), pp.786–99. Available at: http://www.pubmedcentral.nih.gov/articlerender.fcgi?artid=4346203&tool=pmcentrez&rendertype=abstract [Accessed January 23, 2017].

DeNicola, G.M. et al., 2015. NRF2 regulates serine biosynthesis in non-small cell lung cancer. *Nature genetics*, 47(12), pp.1475–81. Available at: http://www.ncbi.nlm.nih.gov/pubmed/26482881 [Accessed August 1, 2018].

Derdak, S. et al., 1992. Differential collagen and fibronectin production by Thy 1+ and Thy 1- lung fibroblast subpopulations. *American Journal of Physiology-Lung Cellular and Molecular Physiology*, 263(2), pp.L283–L290. Available at: http://www.ncbi.nlm.nih.gov/pubmed/1355333 [Accessed October 15, 2018].

Derynck, R. & Miyazono, K., 2008. *The TGF-β Family*, Cold Spring Harbor. Available at: https://cshmonographs.org/index.php/monographs/issue/view/087969752.50 [Accessed August 30, 2018].

Derynck, R., Zhang, Y. & Feng, X.H., 1998. Smads: transcriptional activators of TGF-beta responses. *Cell*, 95(6), pp.737–40. Available at: http://www.ncbi.nlm.nih.gov/pubmed/9865691 [Accessed August 30, 2018].

Desantis, A. et al., 2015. Che-1-induced inhibition of mTOR pathway enables stress-induced autophagy. *The EMBO Journal*, 34(9), pp.1214–1230. Available at: http://www.ncbi.nlm.nih.gov/pubmed/25770584 [Accessed July 27, 2018].

Dey, N. et al., 2010. PRAS40 acts as a nodal regulator of high glucose-induced TORC1

activation in glomerular mesangial cell hypertrophy. *Journal of cellular physiology*, 225(1), pp.27–41. Available at: http://www.ncbi.nlm.nih.gov/pubmed/20629086 [Accessed July 27, 2018].

Dibble, C.C. et al., 2012. TBC1D7 Is a Third Subunit of the TSC1-TSC2 Complex Upstream of mTORC1. *Molecular Cell*, 47(4), pp.535–546. Available at: http://linkinghub.elsevier.com/retrieve/pii/S1097276512005047 [Accessed March 16, 2017].

Diggle, T.A. et al., 1996. Both rapamycin-sensitive and -insensitive pathways are involved in the phosphorylation of the initiation factor-4E-binding protein (4E-BP1) in response to insulin in rat epididymal fat-cells. *The Biochemical journal*, 316 (Pt 2)(Pt 2), pp.447–53. Available at: http://www.ncbi.nlm.nih.gov/pubmed/8687386 [Accessed July 24, 2018].

Dijke, P. ten & Hill, C.S., 2004. New insights into TGF-β–Smad signalling. *Trends in Biochemical Sciences*, 29(5), pp.265–273. Available at: http://linkinghub.elsevier.com/retrieve/pii/S0968000404000775 [Accessed July 21, 2018].

Dong, X. et al., 2009. Molecular Basis of the Acceleration of the GDP-GTP Exchange of Human Ras Homolog Enriched in Brain by Human Translationally Controlled Tumor Protein. *Journal of Biological Chemistry*, 284(35), pp.23754–23764. Available at: http://www.ncbi.nlm.nih.gov/pubmed/19570981 [Accessed August 27, 2018].

Dooley, S. & ten Dijke, P., 2012. TGF-β in progression of liver disease. *Cell and tissue research*, 347(1), pp.245–56. Available at: http://www.ncbi.nlm.nih.gov/pubmed/22006249 [Accessed August 30, 2018].

Duan, S. et al., 2011. mTOR Generates an Auto-Amplification Loop by Triggering the βTrCP- and CK1α-Dependent Degradation of DEPTOR. *Molecular Cell*, 44(2), pp.317–324. Available at: http://www.ncbi.nlm.nih.gov/pubmed/22017877 [Accessed July 27, 2018].

Durán, R.V. et al., 2012. Glutaminolysis Activates Rag-mTORC1 Signaling. *Molecular Cell*, 47(3), pp.349–358. Available at: http://www.ncbi.nlm.nih.gov/pubmed/22749528 [Accessed March 16, 2017].

Van Duyne, G. et al., 1991. Atomic structure of FKBP-FK506, an immunophilin-immunosuppressant complex. *Science*, 252(5007), pp.839–842. Available at: http://www.ncbi.nlm.nih.gov/pubmed/1709302 [Accessed July 25, 2018].

Ekim, B. et al., 2011. mTOR kinase domain phosphorylation promotes mTORC1 signaling, cell growth, and cell cycle progression. *Molecular and cellular biology*, 31(14), pp.2787–801. Available at: http://www.ncbi.nlm.nih.gov/pubmed/21576368 [Accessed March 13, 2017].

Engelman, J.A., Luo, J. & Cantley, L.C., 2006. The evolution of phosphatidylinositol 3-kinases as regulators of growth and metabolism. *Nature Reviews Genetics*, 7(8), pp.606–619. Available at: http://www.ncbi.nlm.nih.gov/pubmed/16847462 [Accessed August 31, 2018].

English, D., Cui, Y. & Siddiqui, R.A., 1996. Messenger functions of phosphatidic acid. *Chemistry and physics of lipids*, 80(1–2), pp.117–32. Available at: http://www.ncbi.nlm.nih.gov/pubmed/8681423 [Accessed August 23, 2018].

Enserink, J.M. & Kolodner, R.D., 2010. An overview of Cdk1-controlled targets and processes. *Cell Division*, 5(1), p.11. Available at: http://celldiv.biomedcentral.com/articles/10.1186/1747-1028-5-11 [Accessed August 21, 2018].

Fadden, P., Haystead, T.A. & Lawrence, J.C., 1997. Identification of phosphorylation sites in the translational regulator, PHAS-I, that are controlled by insulin and rapamycin in rat adipocytes. *The Journal of biological chemistry*, 272(15), pp.10240–7. Available at: http://www.ncbi.nlm.nih.gov/pubmed/9092573 [Accessed July 26, 2018].

Fang, Y. et al., 2001. Phosphatidic acid-mediated mitogenic activation of mTOR signaling. , 294(5548), pp.1942–5. Available at: http://www.ncbi.nlm.nih.gov/pubmed/11729323 [Accessed June 27, 2017].

Ferguson, K.T. et al., 2017. The Novel mTOR Complex 1/2 Inhibitor P529 Inhibits Human Lung Myofibroblast Differentiation. *Journal of Cellular Biochemistry*, 118(8), pp.2241–2249. Available at: http://doi.wiley.com/10.1002/jcb.25878 [Accessed July 18, 2018].

Flaherty, K. et al., 2017. M31 Safety of combined pirfenidone and nintedanib in patients with idiopathic pulmonary fibrosis. In *Idiopathic pulmonary fibrosis treatment update*. BMJ Publishing Group Ltd and British Thoracic Society, p. A253.2-A256. Available at: http://thorax.bmj.com/lookup/doi/10.1136/thoraxjnl-2017-210983.453 [Accessed January 29, 2018].

Foster, D.A. et al., 2014. Phospholipase D and the maintenance of phosphatidic acid levels for regulation of mammalian target of rapamycin (mTOR). *The Journal of biological chemistry*, 289(33), pp.22583–8. Available at: http://www.ncbi.nlm.nih.gov/pubmed/24990952 [Accessed March 28, 2017].

Foster, K.G. et al., 2010. Regulation of mTOR complex 1 (mTORC1) by raptor Ser863 and multisite phosphorylation. *The Journal of biological chemistry*, 285(1), pp.80–94. Available at: http://www.ncbi.nlm.nih.gov/pubmed/19864431 [Accessed July 27, 2018].

Froese, A.R. et al., 2016. Stretch-induced Activation of Transforming Growth Factor-β $_1$ in Pulmonary Fibrosis. *American Journal of Respiratory and Critical Care Medicine*, 194(1), pp.84–96. Available at: http://www.atsjournals.org/doi/10.1164/rccm.201508-1638OC [Accessed April 8, 2018].

Fukuchi, M. et al., 2001. Ligand-dependent degradation of Smad3 by a ubiquitin ligase complex of ROC1 and associated proteins. *Molecular biology of the cell*, 12(5), pp.1431–43. Available at: http://www.ncbi.nlm.nih.gov/pubmed/11359933 [Accessed August 17, 2018].

Gadir, N. et al., 2008. Defective TGF-β signaling sensitizes human cancer cells to rapamycin. *Oncogene*, 27(8), pp.1055–1062. Available at: http://www.nature.com/articles/1210721 [Accessed August 27, 2018].

Gao, D. et al., 2011. mTOR drives its own activation via SCF(βTrCP)-dependent degradation of the mTOR inhibitor DEPTOR. *Molecular cell*, 44(2), pp.290–303. Available at: http://www.ncbi.nlm.nih.gov/pubmed/22017875 [Accessed July 27, 2018].

Gao, X. & Pan, D., 2001. TSC1 and TSC2 tumor suppressors antagonize insulin signaling in cell growth. *Genes & development*, 15(11), pp.1383–92. Available at: http://www.ncbi.nlm.nih.gov/pubmed/11390358 [Accessed August 28, 2018].

Garami, A. et al., 2003. Insulin Activation of Rheb, a Mediator of mTOR/S6K/4E-BP Signaling, Is Inhibited by TSC1 and 2. *Molecular Cell*, 11(6), pp.1457–1466. Available at: https://www.sciencedirect.com/science/article/pii/S109727650300220X [Accessed August 21, 2018].

Gay, S. et al., 1976. Simultaneous synthesis of types I and III collagen by fibroblasts in culture. *Proceedings of the National Academy of Sciences of the United States of America*, 73(11), pp.4037–40. Available at: http://www.ncbi.nlm.nih.gov/pubmed/1069290 [Accessed October 15, 2018].

Ghosh, A., 2002. *MINIREVIEW Factors Involved in the Regulation of Type I Collagen Gene Expression: Implication in Fibrosis*, Available at: http://journals.sagepub.com/doi/pdf/10.1177/153537020222700502 [Accessed October 15, 2018].

Ghosh, A.K. et al., 2000. Smad-dependent stimulation of type I collagen gene expression in human skin fibroblasts by TGF-β involves functional cooperation with p300/CBP transcriptional coactivators. *Oncogene*, 19(31), pp.3546–3555. Available at: http://www.nature.com/articles/1203693 [Accessed August 24, 2017].

Gille, H. & Downward, J., 1999. Multiple ras effector pathways contribute to G(1) cell cycle progression. *The Journal of biological chemistry*, 274(31), pp.22033–40. Available at: http://www.ncbi.nlm.nih.gov/pubmed/10419529 [Accessed August 22, 2018].

Gingras, A.C., Raught, B., Gygi, S.P., et al., 2001. Hierarchical phosphorylation of the translation inhibitor 4E-BP1. *Genes & development*, 15(21), pp.2852–64. Available at: http://www.ncbi.nlm.nih.gov/pubmed/11691836 [Accessed June 21, 2019].

Gingras, A.C. et al., 1999. Regulation of 4E-BP1 phosphorylation: a novel two-step mechanism. *Genes & development*, 13(11), pp.1422–37. Available at: http://www.ncbi.nlm.nih.gov/pubmed/10364159 [Accessed June 5, 2018].

Gingras, A.C., Raught, B. & Sonenberg, N., 2001. Regulation of translation initiation by FRAP/mTOR. *Genes & development*, 15(7), pp.807–26. Available at: http://www.ncbi.nlm.nih.gov/pubmed/11297505 [Accessed July 26, 2018].

Giri, S.N., Hyde, D.M. & Hollinger, M.A., 1993. Effect of antibody to transforming growth factor beta on bleomycin induced accumulation of lung collagen in mice. *Thorax*, 48(10), pp.959–66. Available at: http://www.ncbi.nlm.nih.gov/pubmed/7504843 [Accessed August 30, 2018].

Gribbin, J. et al., 2006. Incidence and mortality of idiopathic pulmonary fibrosis and sarcoidosis in the UK. *Thorax*, 61(11), pp.980–5. Available at: http://www.ncbi.nlm.nih.gov/pubmed/16844727 [Accessed January 12, 2018].

Grillo, A.R. et al., 2015. TAK1 is a key modulator of the profibrogenic phenotype of human ileal myofibroblasts in Crohn's disease. *American Journal of Physiology-Gastrointestinal and Liver Physiology*, 309(6), pp.G443–G454. Available at: http://www.physiology.org/doi/10.1152/ajpgi.00400.2014 [Accessed August 9, 2018].

Groenewoud, M.J. & Zwartkruis, F.J.T., 2013. Rheb and Rags come together at the lysosome to activate mTORC1: Figure 1. *Biochemical Society Transactions*, 41(4), pp.951–955. Available at: http://www.ncbi.nlm.nih.gov/pubmed/23863162 [Accessed August 24, 2018].

Grünert, S., Jechlinger, M. & Beug, H., 2003. Diverse cellular and molecular mechanisms contribute to epithelial plasticity and metastasis. *Nature Reviews Molecular Cell Biology*, 4(8), pp.657–665. Available at: http://www.nature.com/articles/nrm1175 [Accessed February 17, 2018].

Guo, F. et al., 2013. TAK1 Is Required for Dermal Wound Healing and Homeostasis. *Journal of Investigative Dermatology*, 133, pp.1646–1654. Available at: www.jidonline.org [Accessed August 3, 2018].

Gurujeyalakshmi, G., Hollinger, M.A. & Giri, S.N., 1998. Regulation of Transforming Growth Factor- β_1 mRNA Expression by Taurine and Niacin in the Bleomycin Hamster Model of Lung Fibrosis. *American Journal of Respiratory Cell and Molecular Biology*, 18(3), pp.334–342. Available at: http://www.ncbi.nlm.nih.gov/pubmed/9490651 [Accessed August 31, 2018].

Gwinn, D.M. et al., 2008. AMPK phosphorylation of raptor mediates a metabolic checkpoint. *Molecular cell*, 30(2), pp.214–26. Available at: http://www.ncbi.nlm.nih.gov/pubmed/18439900 [Accessed July 27, 2018].

Gwinn, D.M., Asara, J.M. & Shaw, R.J., 2010. Raptor is Phosphorylated by cdc2 during Mitosis M. Kaeberlein, ed. *PLoS ONE*, 5(2), p.e9197. Available at: http://dx.plos.org/10.1371/journal.pone.0009197 [Accessed July 27, 2018].

Haar, E. Vander et al., 2007. Insulin signalling to mTOR mediated by the Akt/PKB substrate PRAS40. *Nature Cell Biology*, 9(3), pp.316–323. Available at: http://www.nature.com/doifinder/10.1038/ncb1547 [Accessed March 16, 2017].

Hagimoto, N. et al., 2002. TGF-beta 1 as an enhancer of Fas-mediated apoptosis of lung epithelial cells. *Journal of immunology (Baltimore, Md. : 1950)*, 168(12), pp.6470–8.

Available at: http://www.ncbi.nlm.nih.gov/pubmed/12055267 [Accessed April 3, 2018].

Hagood, J.S. et al., 2005. Loss of Fibroblast Thy-1 Expression Correlates with Lung Fibrogenesis. *The American Journal of Pathology*, 167(2), pp.365–379. Available at: http://www.ncbi.nlm.nih.gov/pubmed/16049324 [Accessed October 15, 2018].

Hajari Case, A. & Johnson, P., 2017. Clinical use of nintedanib in patients with idiopathic pulmonary fibrosis. *BMJ Open Respiratory Research*, 4(1), p.e000192. Available at: http://bmjopenrespres.bmj.com/lookup/doi/10.1136/bmjresp-2017-000192 [Accessed January 29, 2018].

Hara, K. et al., 1998. Amino acid sufficiency and mTOR regulate p70 S6 kinase and eIF-4E BP1 through a common effector mechanism. *The Journal of biological chemistry*, 273(23), pp.14484–94. Available at: http://www.ncbi.nlm.nih.gov/pubmed/9603962 [Accessed August 24, 2018].

Hara, K. et al., 2002. Raptor, a binding partner of target of rapamycin (TOR), mediates TOR action. *Cell*, 110(2), pp.177–89. Available at: http://www.ncbi.nlm.nih.gov/pubmed/12150926 [Accessed July 27, 2018].

Harada, H. et al., 2001. p70S6 kinase signals cell survival as well as growth, inactivating the pro-apoptotic molecule BAD. *Proceedings of the National Academy of Sciences*, 98(17), pp.9666–9670. Available at: http://www.ncbi.nlm.nih.gov/pubmed/11493700 [Accessed July 26, 2018].

Hashimoto, N. et al., 2010. Endothelial-mesenchymal transition in bleomycin-induced pulmonary fibrosis. *American journal of respiratory cell and molecular biology*, 43(2), pp.161–72. Available at: http://www.ncbi.nlm.nih.gov/pubmed/19767450 [Accessed February 17, 2018].

Hegen, M. et al., 2006. MAPKAP kinase 2-deficient mice are resistant to collagen-induced arthritis. *Journal of immunology (Baltimore, Md. : 1950)*, 177(3), pp.1913–7. Available at: http://www.ncbi.nlm.nih.gov/pubmed/16849504 [Accessed September 6, 2018].

Heldin, C.H. & ten Dijke, P., 1999. SMAD destruction turns off signalling. *Nature cell biology*, 1(8), pp.E195-7. Available at: http://www.nature.com/ncb/journal/v1/n8/full/ncb1299_E195.html#B1 [Accessed April 14, 2016].

Higashiyama, H. et al., 2007. Receptor-activated Smad localisation in bleomycin-induced pulmonary fibrosis. *Journal of clinical pathology*, 60(3), pp.283–9. Available at: http://www.ncbi.nlm.nih.gov/pubmed/16751304 [Accessed August 17, 2018].

Hilberg, F. et al., 2008. BIBF 1120: triple angiokinase inhibitor with sustained receptor blockade and good antitumor efficacy. *Cancer research*, 68(12), pp.4774–82. Available at: http://www.ncbi.nlm.nih.gov/pubmed/18559524 [Accessed January 29, 2018].

Hilinski, M.K. et al., 2012. Analogs of the RSK inhibitor SL0101: optimization of in vitro biological stability. *Bioorganic & medicinal chemistry letters*, 22(9), pp.3244–7. Available at: http://www.ncbi.nlm.nih.gov/pubmed/22464132 [Accessed August 22, 2018].

Hinault, C. et al., 2004. Amino acids and leucine allow insulin activation of the PKB/mTOR pathway in normal adipocytes treated with wortmannin and in adipocytes from db/db mice. *FASEB journal : official publication of the Federation of American Societies for Experimental Biology*, 18(15), pp.1894–6. Available at: http://www.ncbi.nlm.nih.gov/pubmed/15479767 [Accessed April 10, 2017].

Holtmann, H. et al., 2001. The MAPK kinase kinase TAK1 plays a central role in coupling the interleukin-1 receptor to both transcriptional and RNA-targeted mechanisms of gene regulation. *The Journal of biological chemistry*, 276(5), pp.3508–16. Available at: http://www.ncbi.nlm.nih.gov/pubmed/11050078 [Accessed September 6, 2018].

Holz, M.K. et al., 2005. mTOR and S6K1 Mediate Assembly of the Translation Preinitiation

Complex through Dynamic Protein Interchange and Ordered Phosphorylation Events. *Cell*, 123(4), pp.569–580. Available at: http://www.ncbi.nlm.nih.gov/pubmed/16286006 [Accessed August 28, 2018].

Holz, M.K. & Blenis, J., 2005. Identification of S6 kinase 1 as a novel mammalian target of rapamycin (mTOR)-phosphorylating kinase. *The Journal of biological chemistry*, 280(28), pp.26089–93. Available at: http://www.ncbi.nlm.nih.gov/pubmed/15905173 [Accessed March 16, 2017].

Howell, D.C.J. et al., 2005. Absence of Proteinase-Activated Receptor-1 Signaling Affords Protection from Bleomycin-Induced Lung Inflammation and Fibrosis. *The American Journal of Pathology*, 166(5), pp.1353–1365. Available at: http://www.ncbi.nlm.nih.gov/pubmed/15855637 [Accessed August 30, 2018].

Hsu, Y.-C. et al., 2007. Drosophila TCTP is essential for growth and proliferation through regulation of dRheb GTPase. *Nature*, 445(7129), pp.785–788. Available at: http://www.ncbi.nlm.nih.gov/pubmed/17301792 [Accessed August 27, 2018].

Huang, J. et al., 2008. The TSC1-TSC2 complex is required for proper activation of mTOR complex 2. *Molecular and cellular biology*, 28(12), pp.4104–15. Available at: http://www.ncbi.nlm.nih.gov/pubmed/18411301 [Accessed September 4, 2017].

Huang, J. & Manning, B.D., 2008. The TSC1-TSC2 complex: a molecular switchboard controlling cell growth. *The Biochemical journal*, 412(2), pp.179–90. Available at: http://www.pubmedcentral.nih.gov/articlerender.fcgi?artid=2735030&tool=pmcentrez&rendertype=abstract [Accessed April 17, 2016].

Hung, C. et al., 2013. Role of lung pericytes and resident fibroblasts in the pathogenesis of pulmonary fibrosis. *American journal of respiratory and critical care medicine*, 188(7), pp.820–30. Available at: http://www.ncbi.nlm.nih.gov/pubmed/23924232 [Accessed January 29, 2018].

Ikenoue, T. et al., 2008. Essential function of TORC2 in PKC and Akt turn motif phosphorylation, maturation and signalling. *The EMBO journal*, 27(14), pp.1919–31. Available at: http://www.ncbi.nlm.nih.gov/pubmed/18566587 [Accessed July 26, 2018].

Imoto, S. et al., 2005. Roles for lysine residues of the MH2 domain of Smad3 in transforming growth factor-β signaling. *FEBS Letters*, 579(13), pp.2853–2862. Available at: https://www.sciencedirect.com/science/article/pii/S0014579305004989 [Accessed August 30, 2018].

Imoto, S. et al., 2004. The RING domain of PIASy is involved in the suppression of bone morphogenetic protein-signaling pathway. *Biochemical and Biophysical Research Communications*, 319(1), pp.275–282. Available at: http://www.ncbi.nlm.nih.gov/pubmed/15158472 [Accessed September 6, 2018].

Inoki, K. et al., 2003. Rheb GTPase is a direct target of TSC2 GAP activity and regulates mTOR signaling. *Genes & development*, 17(15), pp.1829–34. Available at: http://www.ncbi.nlm.nih.gov/pubmed/12869586 [Accessed August 14, 2018].

Inoki, K., 2003. Rheb GTPase is a direct target of TSC2 GAP activity and regulates mTOR signaling. *Genes & Development*, 17(15), pp.1829–1834. Available at: http://www.genesdev.org/cgi/doi/10.1101/gad.1110003 [Accessed March 16, 2017].

Inoki, K. et al., 2006. TSC2 Integrates Wnt and Energy Signals via a Coordinated Phosphorylation by AMPK and GSK3 to Regulate Cell Growth. *Cell*, 126(5), pp.955–968.

Jenkins, G., 2008. The role of proteases in transforming growth factor-β activation. *The International Journal of Biochemistry & Cell Biology*, 40(6–7), pp.1068–1078. Available at: http://www.ncbi.nlm.nih.gov/pubmed/18243766 [Accessed August 30, 2018].

Jenkins, R.G. et al., 2006. Ligation of protease-activated receptor 1 enhances v 6 integrin-dependent TGF- activation and promotes acute lung injury. *Journal of Clinical*

Investigation, 116(6), pp.1606–1614. Available at: http://www.ncbi.nlm.nih.gov/pubmed/16710477 [Accessed August 30, 2018].

Jewell, J.L. et al., 2015. Metabolism. Differential regulation of mTORC1 by leucine and glutamine. *Science (New York, N.Y.)*, 347(6218), pp.194–8. Available at: http://www.ncbi.nlm.nih.gov/pubmed/25567907 [Accessed August 28, 2018].

Jiang, L. et al., 2013. Rheb/mTORC1 signaling promotes kidney fibroblast activation and fibrosis. *Journal of the American Society of Nephrology : JASN*, 24(7), pp.1114–26. Available at: http://www.ncbi.nlm.nih.gov/pubmed/23661807 [Accessed August 21, 2018].

Jin, F. et al., 1996. Suppression of tumorigenicity by the wild-type tuberous sclerosis 2 (Tsc2) gene and its C-terminal region. *Proceedings of the National Academy of Sciences of the United States of America*, 93(17), pp.9154–9. Available at: http://www.ncbi.nlm.nih.gov/pubmed/8799170 [Accessed August 28, 2018].

Jin, X. et al., 2014. Rapamycin attenuates bleomycin-induced pulmonary fibrosis in rats and the expression of metalloproteinase-9 and tissue inhibitors of metalloproteinase-1 in lung tissue. *Chinese medical journal*, 127(7), pp.1304–9. Available at: http://www.ncbi.nlm.nih.gov/pubmed/24709185 [Accessed August 31, 2018].

Jung, J., Genau, H.M. & Behrends, C., 2015. Amino Acid-Dependent mTORC1 Regulation by the Lysosomal Membrane Protein SLC38A9. *Molecular and cellular biology*, 35(14), pp.2479–94. Available at: http://www.ncbi.nlm.nih.gov/pubmed/25963655 [Accessed August 27, 2018].

Jung, S.M. et al., 2013. Smad6 inhibits non-canonical TGF-β1 signalling by recruiting the deubiquitinase A20 to TRAF6. *Nature communications*, 4, p.2562. Available at: http://www.nature.com/ncomms/2013/131007/ncomms3562/full/ncomms3562.html [Accessed October 8, 2015].

Kakugawa, T. et al., 2004. Pirfenidone attenuates expression of HSP47 in murine bleomycin-induced pulmonary fibrosis. *The European respiratory journal*, 24(1), pp.57–65.

Kamaraju, A.K. & Roberts, A.B., 2005. Role of Rho/ROCK and p38 MAP kinase pathways in transforming growth factor-beta-mediated Smad-dependent growth inhibition of human breast carcinoma cells in vivo. *The Journal of biological chemistry*, 280(2), pp.1024–36. Available at: http://www.ncbi.nlm.nih.gov/pubmed/15520018 [Accessed August 30, 2018].

Kang, H.-R. et al., 2007. Transforming growth factor (TGF)-beta1 stimulates pulmonary fibrosis and inflammation via a Bax-dependent, bid-activated pathway that involves matrix metalloproteinase-12. *The Journal of biological chemistry*, 282(10), pp.7723–32. Available at: http://www.ncbi.nlm.nih.gov/pubmed/17209037 [Accessed August 30, 2018].

Kang, S.A. et al., 2013. mTORC1 phosphorylation sites encode their sensitivity to starvation and rapamycin. *Science (New York, N.Y.)*, 341(6144), p.1236566. Available at: http://www.pubmedcentral.nih.gov/articlerender.fcgi?artid=3771538&tool=pmcentrez&rendertype=abstract [Accessed February 7, 2017].

Karsenty, G. & de Crombrugghe, B., 1991. Conservation of binding sites for regulatory factors in the coordinately expressed alpha 1 (I) and alpha 2 (I) collagen promoters. *Biochemical and biophysical research communications*, 177(1), pp.538–44. Available at: http://www.ncbi.nlm.nih.gov/pubmed/2043139 [Accessed August 31, 2018].

Katzenstein, A.-L.A. & Myers, J.L., 1998. Idiopathic Pulmonary Fibrosis. *American Journal of Respiratory and Critical Care Medicine*, 157(4), pp.1301–1315. Available at: http://www.atsjournals.org/doi/abs/10.1164/ajrccm.157.4.9707039 [Accessed January 12, 2018].

Kawabata, M., Chytil, A. & Moses, H.L., 1995. Cloning of a novel type II serine/threonine

kinase receptor through interaction with the type I transforming growth factor-beta receptor. *The Journal of biological chemistry*, 270(10), pp.5625–30. Available at: http://www.ncbi.nlm.nih.gov/pubmed/7890683 [Accessed August 31, 2018].

Kayyali, U. et al., 2009. MK2 Regulates Fibroblast Biology and Pulmonary Fibrosis. In *B29. TRANSLATIONAL INVESTIGATION INTO MECHANISMS OF LUNG FIBROSIS*. American Thoracic Society, p. A2708. Available at: http://www.atsjournals.org/doi/abs/10.1164/ajrccm-conference.2009.179.1_MeetingAbstracts.A2708 [Accessed September 6, 2018].

Keerthisingam, C.B. et al., 2001. Cyclooxygenase-2 Deficiency Results in a Loss of the Anti-Proliferative Response to Transforming Growth Factor-β in Human Fibrotic Lung Fibroblasts and Promotes Bleomycin-Induced Pulmonary Fibrosis in Mice. *The American Journal of Pathology*, 158(4), pp.1411–1422. Available at: http://www.sciencedirect.com/science/article/pii/S0002944010640928?via%3Dihub [Accessed January 9, 2018].

Kelly, M. et al., 2003. Re-evaluation of fibrogenic cytokines in lung fibrosis. *Current pharmaceutical design*, 9(1), pp.39–49. Available at: http://www.ncbi.nlm.nih.gov/pubmed/12570673 [Accessed August 30, 2018].

Khalil, N., 1999. TGF-beta: from latent to active. *Microbes and infection*, 1(15), pp.1255–63. Available at: http://www.ncbi.nlm.nih.gov/pubmed/10611753 [Accessed August 30, 2018].

Khalil, N. et al., 1996. TGF-beta 1, but not TGF-beta 2 or TGF-beta 3, is differentially present in epithelial cells of advanced pulmonary fibrosis: an immunohistochemical study. *American journal of respiratory cell and molecular biology*, 14(2), pp.131–8. Available at: http://www.ncbi.nlm.nih.gov/pubmed/8630262 [Accessed April 3, 2018].

Kim, D.-H. et al., 2002. mTOR Interacts with Raptor to Form a Nutrient-Sensitive Complex that Signals to the Cell Growth Machinery. *Cell*, 110(2), pp.163–175. Available at: https://www.sciencedirect.com/science/article/pii/S0092867402008085 [Accessed July 27, 2018].

Kim, K. et al., 2010. Blockade of the MEK/ERK signalling cascade by AS703026, a novel selective MEK1/2 inhibitor, induces pleiotropic anti-myeloma activity in vitro and in vivo. *British Journal of Haematology*, 149(4), pp.537–549. Available at: http://www.ncbi.nlm.nih.gov/pubmed/20331454 [Accessed August 22, 2018].

Kim, S. Il et al., 2007. TGF-beta-activated kinase 1 and TAK1-binding protein 1 cooperate to mediate TGF-beta1-induced MKK3-p38 MAPK activation and stimulation of type I collagen. *American journal of physiology. Renal physiology*, 292(5), pp.F1471-8. Available at: http://ajprenal.physiology.org/content/292/5/F1471.long [Accessed September 10, 2015].

Kim, S. Il et al., 2009. Transforming growth factor-beta (TGF-beta1) activates TAK1 via TAB1-mediated autophosphorylation, independent of TGF-beta receptor kinase activity in mesangial cells. *The Journal of biological chemistry*, 284(33), pp.22285–96. Available at: http://www.pubmedcentral.nih.gov/articlerender.fcgi?artid=2755952&tool=pmcentrez&rendertype=abstract [Accessed September 10, 2015].

King, T.E. et al., 2014. A Phase 3 Trial of Pirfenidone in Patients with Idiopathic Pulmonary Fibrosis. *New England Journal of Medicine*, 370(22), pp.2083–2092. Available at: http://www.nejm.org/doi/10.1056/NEJMoa1402582 [Accessed January 28, 2018].

Kohrman, M.H., 2012. Emerging treatments in the management of tuberous sclerosis complex. *Pediatric neurology*, 46(5), pp.267–75. Available at: http://www.ncbi.nlm.nih.gov/pubmed/22520346 [Accessed August 14, 2018].

Kok, K., Geering, B. & Vanhaesebroeck, B., 2009. Regulation of phosphoinositide 3-kinase expression in health and disease. *Trends in Biochemical Sciences*, 34(3), pp.115–127. Available at: http://www.ncbi.nlm.nih.gov/pubmed/19299143 [Accessed August 31,

2018].

Kovacina, K.S. et al., 2003. Identification of a proline-rich Akt substrate as a 14-3-3 binding partner. *The Journal of biological chemistry*, 278(12), pp.10189–94. Available at: http://www.ncbi.nlm.nih.gov/pubmed/12524439 [Accessed July 27, 2018].

Krementsov, D.N. et al., 2013. The emerging role of p38 mitogen-activated protein kinase in multiple sclerosis and its models. *Molecular and cellular biology*, 33(19), pp.3728–34. Available at: http://www.ncbi.nlm.nih.gov/pubmed/23897428 [Accessed October 29, 2018].

Kretzschmar, M. et al., 1999. A mechanism of repression of TGFbeta/ Smad signaling by oncogenic Ras. *Genes & development*, 13(7), pp.804–16. Available at: http://www.ncbi.nlm.nih.gov/pubmed/10197981 [Accessed August 30, 2018].

Kropski, J.A. et al., 2014. A Novel Dyskerin (DKC1) Mutation Is Associated With Familial Interstitial Pneumonia. *Chest*, 146(1), pp.e1–e7. Available at: http://www.ncbi.nlm.nih.gov/pubmed/24504062 [Accessed August 29, 2018].

Kuk, H. et al., 2015. 5Z-7-Oxozeanol Inhibits the Effects of TGFβ1 on Human Gingival Fibroblasts P. C. Trackman, ed. *PLOS ONE*, 10(4), p.e0123689. Available at: http://dx.plos.org/10.1371/journal.pone.0123689 [Accessed August 3, 2018].

Lama, V. et al., 2002. Prostaglandin E $_2$ Synthesis and Suppression of Fibroblast Proliferation by Alveolar Epithelial Cells Is Cyclooxygenase-2–Dependent. *American Journal of Respiratory Cell and Molecular Biology*, 27(6), pp.752–758. Available at: http://www.atsjournals.org/doi/abs/10.1165/rcmb.4857 [Accessed January 9, 2018].

Lamming, D.W. et al., 2012. Rapamycin-induced insulin resistance is mediated by mTORC2 loss and uncoupled from longevity. *Science (New York, N.Y.)*, 335(6076), pp.1638–43. Available at: http://www.ncbi.nlm.nih.gov/pubmed/22461615 [Accessed July 26, 2018].

Lampa, M. et al., 2017. Glutaminase is essential for the growth of triple-negative breast cancer cells with a deregulated glutamine metabolism pathway and its suppression synergizes with mTOR inhibition. *PloS one*, 12(9), p.e0185092. Available at: http://www.ncbi.nlm.nih.gov/pubmed/28950000 [Accessed August 16, 2018].

Last, J.A., Siefkin, A.D. & Reiser, K.M., 1983. Type I collagen content is increased in lungs of patients with adult respiratory distress syndrome. *Thorax*, 38, pp.364–368. Available at: http://thorax.bmj.com/ [Accessed August 31, 2018].

Lawler, S. et al., 1997. The type II transforming growth factor-beta receptor autophosphorylates not only on serine and threonine but also on tyrosine residues. *The Journal of biological chemistry*, 272(23), pp.14850–9. Available at: http://www.ncbi.nlm.nih.gov/pubmed/9169454 [Accessed August 22, 2018].

Lear, T. et al., 2016. Ubiquitin E3 ligase FIEL1 regulates fibrotic lung injury through SUMO-E3 ligase PIAS4. *The Journal of experimental medicine*, 213(6), pp.1029–46. Available at: http://www.ncbi.nlm.nih.gov/pubmed/27162139 [Accessed September 6, 2018].

LEASK, A. & ABRAHAM, D.J., 2004. TGF-β signaling and the fibrotic response. *The FASEB Journal*, 18(7), pp.816–827. Available at: http://www.ncbi.nlm.nih.gov/pubmed/15117886 [Accessed August 30, 2018].

Lee, D.-F. et al., 2007. IKK beta suppression of TSC1 links inflammation and tumor angiogenesis via the mTOR pathway. *Cell*, 130(3), pp.440–55. Available at: http://www.sciencedirect.com/science/article/pii/S0092867407007623 [Accessed May 2, 2016].

Li, H. et al., 2016. MicroRNAs in idiopathic pulmonary fibrosis: involvement in pathogenesis and potential use in diagnosis and therapeutics. *Acta pharmaceutica Sinica. B*, 6(6), pp.531–539. Available at: http://www.ncbi.nlm.nih.gov/pubmed/27818919 [Accessed January 9, 2018].

Li, J. et al., 2017. TAK1 inhibition attenuates both inflammation and fibrosis in experimental

pneumoconiosis. *Cell Discovery*, 3, p.17023. Available at: http://www.nature.com/articles/celldisc201723 [Accessed August 3, 2018].

Li, X. et al., 2014. MicroRNA-26a modulates transforming growth factor beta-1-induced proliferation in human fetal lung fibroblasts. *Biochemical and Biophysical Research Communications*, 454(4), pp.512–517. Available at: http://www.ncbi.nlm.nih.gov/pubmed/25451270 [Accessed August 29, 2018].

Li, X., Rayford, H. & Uhal, B.D., 2003. Essential Roles for Angiotensin Receptor AT1a in Bleomycin-Induced Apoptosis and Lung Fibrosis in Mice. *The American Journal of Pathology*, 163(6), pp.2523–2530. Available at: http://www.ncbi.nlm.nih.gov/pubmed/14633624 [Accessed October 1, 2018].

Li, Y. et al., 2003. The p38 and MK2 kinase cascade phosphorylates tuberin, the tuberous sclerosis 2 gene product, and enhances its interaction with 14-3-3. *The Journal of biological chemistry*, 278(16), pp.13663–71. Available at: http://www.ncbi.nlm.nih.gov/pubmed/12582162 [Accessed February 22, 2018].

Liang, J. et al., 2018. MK2 Inhibition Attenuates Fibroblast Invasion and Severe Lung Fibrosis. *American Journal of Respiratory Cell and Molecular Biology*, p.rcmb.2018-0033OC. Available at: https://www.atsjournals.org/doi/10.1165/rcmb.2018-0033OC [Accessed September 6, 2018].

Lim, I.J. et al., 2003. Synchronous activation of ERK and phosphatidylinositol 3-kinase pathways is required for collagen and extracellular matrix production in keloids. *The Journal of biological chemistry*, 278(42), pp.40851–8. Available at: http://www.ncbi.nlm.nih.gov/pubmed/12907681 [Accessed August 22, 2018].

Liu, W. et al., 2018. Activation of TGF-β-activated kinase 1 (TAK1) restricts Salmonella Typhimurium growth by inducing AMPK activation and autophagy. *Cell Death & Disease*, 9(5), p.570. Available at: http://www.nature.com/articles/s41419-018-0612-z [Accessed August 9, 2018].

Liu, Y. et al., 2005. Wortmannin, a widely used phosphoinositide 3-kinase inhibitor, also potently inhibits mammalian polo-like kinase. *Chemistry & biology*, 12(1), pp.99–107. Available at: http://www.ncbi.nlm.nih.gov/pubmed/15664519 [Accessed July 21, 2018].

Long, J. et al., 2003. Repression of Smad transcriptional activity by PIASy, an inhibitor of activated STAT. *Proceedings of the National Academy of Sciences of the United States of America*, 100(17), pp.9791–6. Available at: http://www.ncbi.nlm.nih.gov/pubmed/12904571 [Accessed September 6, 2018].

Long, X., Ortiz-Vega, S., et al., 2005. Rheb binding to mammalian target of rapamycin (mTOR) is regulated by amino acid sufficiency. *The Journal of biological chemistry*, 280(25), pp.23433–6. Available at: http://www.ncbi.nlm.nih.gov/pubmed/15878852 [Accessed August 24, 2018].

Long, X., Lin, Y., et al., 2005. Rheb Binds and Regulates the mTOR Kinase. *Current Biology*, 15(8), pp.702–713. Available at: http://www.ncbi.nlm.nih.gov/pubmed/15854902 [Accessed August 28, 2018].

Lu, Z. & Xu, S., 2006. ERK1/2 MAP kinases in cell survival and apoptosis. *IUBMB Life (International Union of Biochemistry and Molecular Biology: Life)*, 58(11), pp.621–631. Available at: http://www.ncbi.nlm.nih.gov/pubmed/17085381 [Accessed August 22, 2018].

Luo, J.Q. et al., 1998. Functional association between Arf and RalA in active phospholipase D complex. *Proceedings of the National Academy of Sciences of the United States of America*, 95(7), pp.3632–7. Available at: http://www.ncbi.nlm.nih.gov/pubmed/9520417 [Accessed August 23, 2018].

Lv, D. et al., 2017. PRAS40 signaling in tumor. *Oncotarget*, 8(40), pp.69076–69085. Available at: http://www.ncbi.nlm.nih.gov/pubmed/28978182 [Accessed July 27, 2018].

Ma, L. et al., 2005. Phosphorylation and functional inactivation of TSC2 by Erk implications for tuberous sclerosis and cancer pathogenesis. *Cell*, 121(2), pp.179–93. Available at: http://www.ncbi.nlm.nih.gov/pubmed/15851026 [Accessed August 22, 2018].

Madri, J.A. & Furthmayr, H., 1980. Collagen polymorphism in the lung. An immunochemical study of pulmonary fibrosis. *Human pathology*, 11(4), pp.353–66. Available at: http://www.ncbi.nlm.nih.gov/pubmed/6997183 [Accessed October 15, 2018].

Maher, T.M. et al., 2010. PGE2 Paradoxically Increases Fibroblast Apoptosis But Reduces Airway Epithelial Cell Apoptosis In Response To FasL Via Activation Of The EP4 Receptor. In *C28. AUTOPHAGY VERSUS APOPTOSIS: TWIN SONS OF A DIFFERENT MOTHER?*. American Thoracic Society, pp. A4182–A4182. Available at: http://www.atsjournals.org/doi/abs/10.1164/ajrccm-conference.2010.181.1_MeetingAbstracts.A4182 [Accessed October 15, 2018].

Mahoney, S.J. et al., 2018. A small molecule inhibitor of Rheb selectively targets mTORC1 signaling. *Nature Communications*, 9(1), p.548. Available at: http://www.nature.com/articles/s41467-018-03035-z [Accessed April 28, 2019].

Martinez, F.J. et al., 2017. Idiopathic pulmonary fibrosis. *Nature Reviews Disease Primers*, 3, p.17074. Available at: http://www.nature.com/articles/nrdp201774 [Accessed December 2, 2017].

Massagué, J., 2012. TGFβ signalling in context. Available at: https://www.nature.com/articles/nrm3434.pdf [Accessed April 15, 2018].

Massagué, J., Seoane, J. & Wotton, D., 2005. Smad transcription factors. *Genes & development*, 19(23), pp.2783–810. Available at: http://www.ncbi.nlm.nih.gov/pubmed/16322555 [Accessed April 22, 2018].

McNamara, C.R. & Degterev, A., 2011. Small-molecule inhibitors of the PI3K signaling network. *Future medicinal chemistry*, 3(5), pp.549–65. Available at: http://www.ncbi.nlm.nih.gov/pubmed/21526896 [Accessed July 21, 2018].

Menon, S. et al., 2014. Spatial Control of the TSC Complex Integrates Insulin and Nutrient Regulation of mTORC1 at the Lysosome. *Cell*, 156(4), pp.771–785. Available at: http://www.ncbi.nlm.nih.gov/pubmed/24529379 [Accessed August 27, 2018].

Mercer, P.F. et al., 2016. Exploration of a potent PI3 kinase/mTOR inhibitor as a novel anti-fibrotic agent in IPF. *Thorax*, 71(8), pp.701–11. Available at: http://www.ncbi.nlm.nih.gov/pubmed/27103349 [Accessed April 9, 2018].

Mishra, D.K. et al., 2018. Translationally controlled tumor protein (TCTP) is required for TGF-β1 induced epithelial to mesenchymal transition and influences cytoskeletal reorganization. *Biochimica et Biophysica Acta (BBA) - Molecular Cell Research*, 1865(1), pp.67–75. Available at: http://www.ncbi.nlm.nih.gov/pubmed/28958626 [Accessed August 27, 2018].

Mori, S. et al., 2004. TGF-β and HGF transmit the signals through JNK-dependent Smad2/3 phosphorylation at the linker regions. *Oncogene*, 23(44), pp.7416–7429. Available at: http://www.ncbi.nlm.nih.gov/pubmed/15326485 [Accessed August 30, 2018].

Navé, B.T. et al., 1999. Mammalian target of rapamycin is a direct target for protein kinase B: identification of a convergence point for opposing effects of insulin and amino-acid deficiency on protein translation. *The Biochemical journal*, 344 Pt 2(Pt 2), pp.427–31. Available at: http://www.ncbi.nlm.nih.gov/pubmed/10567225 [Accessed April 27, 2017].

Nellist, M. et al., 1993. Identification and characterization of the tuberous sclerosis gene on chromosome 16. *Cell*, 75(7), pp.1305–1315. Available at: http://www.ncbi.nlm.nih.gov/pubmed/8269512 [Accessed August 28, 2018].

Neveu, W.A. et al., 2015. TGF-β1 epigenetically modifies Thy-1 expression in primary lung fibroblasts. *American journal of physiology. Cell physiology*, 309(9), pp.C616-26. Available at: http://www.ncbi.nlm.nih.gov/pubmed/26333597 [Accessed October 15,

2018].

Nho, R.S. et al., 2013. FoxO3a (Forkhead Box O3a) Deficiency Protects Idiopathic Pulmonary Fibrosis (IPF) Fibroblasts from Type I Polymerized Collagen Matrix-Induced Apoptosis via Caveolin-1 (cav-1) and Fas E. Katz, ed. *PLoS ONE*, 8(4), p.e61017. Available at: http://dx.plos.org/10.1371/journal.pone.0061017 [Accessed August 31, 2018].

Ninomiya-Tsuji, J. et al., 2003. A resorcylic acid lactone, 5Z-7-oxozeaenol, prevents inflammation by inhibiting the catalytic activity of TAK1 MAPK kinase kinase. *The Journal of biological chemistry*, 278(20), pp.18485–90. Available at: http://www.jbc.org/content/278/20/18485.full [Accessed August 6, 2015].

Nojima, H. et al., 2003. The mammalian target of rapamycin (mTOR) partner, raptor, binds the mTOR substrates p70 S6 kinase and 4E-BP1 through their TOR signaling (TOS) motif. *The Journal of biological chemistry*, 278(18), pp.15461–4. Available at: http://www.ncbi.nlm.nih.gov/pubmed/12604610 [Accessed July 27, 2018].

Nozaki, Y. et al., 2000. Induction of Telomerase Activity in Fibroblasts from Bleomycin-Injured Lungs. *American Journal of Respiratory Cell and Molecular Biology*, 23(4), pp.460–465. Available at: http://www.ncbi.nlm.nih.gov/pubmed/11017910 [Accessed October 15, 2018].

Oh, C.K., Murray, L. a & Molfino, N. a, 2012. Smoking and idiopathic pulmonary fibrosis. *Pulmonary medicine*, 2012, p.808260. Available at: http://www.pubmedcentral.nih.gov/articlerender.fcgi?artid=3289849&tool=pmcentrez&rendertype=abstract [Accessed October 20, 2014].

Ohori, M. et al., 2007. Role of a cysteine residue in the active site of ERK and the MAPKK family. *Biochemical and biophysical research communications*, 353(3), pp.633–7. Available at: http://www.sciencedirect.com/science/article/pii/S0006291X06027240 [Accessed December 15, 2015].

Ono, K. et al., 2003. A dominant negative TAK1 inhibits cellular fibrotic responses induced by TGF-β. *Biochemical and Biophysical Research Communications*, 307(2), pp.332–337. Available at: http://www.sciencedirect.com/science/article/pii/S0006291X03012075 [Accessed September 10, 2015].

Oshiro, N. et al., 2007. The proline-rich Akt substrate of 40 kDa (PRAS40) is a physiological substrate of mammalian target of rapamycin complex 1. *The Journal of biological chemistry*, 282(28), pp.20329–39. Available at: http://www.ncbi.nlm.nih.gov/pubmed/17517883 [Accessed July 27, 2018].

Pandit, K. V. et al., 2010. Inhibition and Role of let-7d in Idiopathic Pulmonary Fibrosis. *American Journal of Respiratory and Critical Care Medicine*, 182(2), pp.220–229. Available at: http://www.ncbi.nlm.nih.gov/pubmed/20395557 [Accessed August 29, 2018].

Pardo, A. et al., 2016. Role of matrix metalloproteinases in the pathogenesis of idiopathic pulmonary fibrosis. *Respiratory Research*, 17. Available at: https://www.ncbi.nlm.nih.gov/pmc/articles/PMC4779202/ [Accessed August 30, 2018].

Park, Y. et al., 2017. mTORC1 Balances Cellular Amino Acid Supply with Demand for Protein Synthesis through Post-transcriptional Control of ATF4. *Cell reports*, 19(6), pp.1083–1090. Available at: http://www.ncbi.nlm.nih.gov/pubmed/28494858 [Accessed August 1, 2018].

Parmigiani, A. et al., 2014. Sestrins inhibit mTORC1 kinase activation through the GATOR complex. *Cell reports*, 9(4), pp.1281–91. Available at: http://www.ncbi.nlm.nih.gov/pubmed/25457612 [Accessed August 27, 2018].

Patel, P.H. et al., 2003. Drosophila Rheb GTPase is required for cell cycle progression and cell growth. *Journal of cell science*, 116(Pt 17), pp.3601–10. Available at:

http://www.ncbi.nlm.nih.gov/pubmed/12893813 [Accessed August 27, 2018].

Pearce, L.R. et al., 2007. Identification of Protor as a novel Rictor-binding component of mTOR complex-2. *The Biochemical journal*, 405(3), pp.513–22. Available at: http://www.ncbi.nlm.nih.gov/pubmed/17461779 [Accessed July 26, 2018].

Pearson, G. et al., 2001. ERK5 and ERK2 Cooperate to Regulate NF-κB and Cell Transformation. *Journal of Biological Chemistry*, 276(11), pp.7927–7931. Available at: http://www.ncbi.nlm.nih.gov/pubmed/11118448 [Accessed August 22, 2018].

Pende, M. et al., 2004. S6K1(-/-)/S6K2(-/-) mice exhibit perinatal lethality and rapamycin-sensitive 5'-terminal oligopyrimidine mRNA translation and reveal a mitogen-activated protein kinase-dependent S6 kinase pathway. *Molecular and cellular biology*, 24(8), pp.3112–24. Available at: http://www.ncbi.nlm.nih.gov/pubmed/15060135 [Accessed July 26, 2018].

Peterson, T.R. et al., 2009. DEPTOR is an mTOR inhibitor frequently overexpressed in multiple myeloma cells and required for their survival. *Cell*, 137(5), pp.873–86. Available at: http://www.ncbi.nlm.nih.gov/pubmed/19446321 [Accessed July 26, 2018].

Phan, S.H., 2008. Biology of fibroblasts and myofibroblasts. *Proceedings of the American Thoracic Society*, 5(3), pp.334–7. Available at: http://www.pubmedcentral.nih.gov/articlerender.fcgi?artid=2645244&tool=pmcentrez&rendertype=abstract [Accessed June 22, 2015].

Phillips, R.J. et al., 2004. Circulating fibrocytes traffic to the lungs in response to CXCL12 and mediate fibrosis. *The Journal of clinical investigation*, 114(3), pp.438–46. Available at: http://www.ncbi.nlm.nih.gov/pubmed/15286810 [Accessed April 4, 2016].

Pociask, D.A., Sime, P.J. & Brody, A.R., 2004. Asbestos-derived reactive oxygen species activate TGF-β1. *Laboratory Investigation*, 84(8), pp.1013–1023. Available at: http://www.nature.com/articles/3700109 [Accessed April 5, 2018].

Poncelet, A.-C. et al., 2007. Cell phenotype-specific down-regulation of Smad3 involves decreased gene activation as well as protein degradation. *The Journal of biological chemistry*, 282(21), pp.15534–40. Available at: http://www.ncbi.nlm.nih.gov/pubmed/17400544 [Accessed August 17, 2018].

Pullen, N. et al., 1998. Phosphorylation and activation of P70S6K by PDK1. *Science (New York, N.Y.)*, 279(5351), pp.707–10. Available at: http://www.ncbi.nlm.nih.gov/pubmed/9445476 [Accessed July 26, 2018].

Raghu, G. et al., 2011. An Official ATS/ERS/JRS/ALAT Statement: Idiopathic Pulmonary Fibrosis: Evidence-based Guidelines for Diagnosis and Management. *American Journal of Respiratory and Critical Care Medicine*, 183(6), pp.788–824. Available at: http://www.atsjournals.org/doi/abs/10.1164/rccm.2009-040GL [Accessed January 7, 2018].

Ramírez-Valle, F. et al., 2010. Mitotic raptor promotes mTORC1 activity, G(2)/M cell cycle progression, and internal ribosome entry site-mediated mRNA translation. *Molecular and cellular biology*, 30(13), pp.3151–64. Available at: http://www.ncbi.nlm.nih.gov/pubmed/20439490 [Accessed July 27, 2018].

Rebsamen, M. et al., 2015. SLC38A9 is a component of the lysosomal amino acid sensing machinery that controls mTORC1. *Nature*, 519(7544), pp.477–481. Available at: http://www.ncbi.nlm.nih.gov/pubmed/25561175 [Accessed August 27, 2018].

Refaat, A. et al., 2015. Inhibition of p38 mitogen-activated protein kinase potentiates the apoptotic effect of berberine/tumor necrosis factor-related apoptosis-inducing ligand combination therapy. *Oncology letters*, 10(3), pp.1907–1911. Available at: http://www.ncbi.nlm.nih.gov/pubmed/26622773 [Accessed November 1, 2018].

Reiser, K.M. & Last, J.A., 1981. Pulmonary fibrosis in experimental acute respiratory disease. *The American review of respiratory disease*, 123(1), pp.58–63. Available at:

http://www.ncbi.nlm.nih.gov/pubmed/6161575 [Accessed October 16, 2018].

Reynolds, H.Y., 1978. The Biochemical Basis of Pulmonary Function. *The Yale Journal of Biology and Medicine*, 51(1), p.97. Available at: https://www.ncbi.nlm.nih.gov/pmc/articles/PMC2595646/ [Accessed October 15, 2018].

Reynolds, T.H., Bodine, S.C. & Lawrence, J.C., 2002. Control of Ser2448 phosphorylation in the mammalian target of rapamycin by insulin and skeletal muscle load. *The Journal of biological chemistry*, 277(20), pp.17657–62. Available at: http://www.ncbi.nlm.nih.gov/pubmed/11884412 [Accessed July 18, 2018].

Richeldi, L. et al., 2014. Efficacy and Safety of Nintedanib in Idiopathic Pulmonary Fibrosis — NEJM. *The New England journal of medicine*, 370(22), pp.2071–82. Available at: http://www.nejm.org/doi/full/10.1056/NEJMoa1402584 [Accessed August 7, 2015].

Roach, K.M. et al., 2015. Human lung myofibroblast TGFβ1-dependent Smad2/3 signalling is Ca2+-dependent and regulated by KCa3.1 K+ channels. *Fibrogenesis & Tissue Repair*, 8(1), p.5. Available at: http://www.fibrogenesis.com/content/8/1/5 [Accessed October 20, 2015].

Romeo, Y. et al., 2013. RSK regulates activated BRAF signalling to mTORC1 and promotes melanoma growth. *Oncogene*, 32(24), pp.2917–2926. Available at: http://www.ncbi.nlm.nih.gov/pubmed/22797077 [Accessed August 22, 2018].

Rosas, I.O. et al., 2008. MMP1 and MMP7 as Potential Peripheral Blood Biomarkers in Idiopathic Pulmonary Fibrosis P. Barnes, ed. *PLoS Medicine*, 5(4), p.e93. Available at: http://www.ncbi.nlm.nih.gov/pubmed/18447576 [Accessed August 30, 2018].

Rosner, M. & Hengstschläger, M., 2011. Nucleocytoplasmic localization of p70 S6K1, but not of its isoforms p85 and p31, is regulated by TSC2/mTOR. *Oncogene*, 30(44), pp.4509–4522. Available at: http://www.nature.com/articles/onc2011165 [Accessed July 26, 2018].

Roux, P.P. et al., 2004. Tumor-promoting phorbol esters and activated Ras inactivate the tuberous sclerosis tumor suppressor complex via p90 ribosomal S6 kinase. *Proceedings of the National Academy of Sciences of the United States of America*, 101(37), pp.13489–94. Available at: http://www.ncbi.nlm.nih.gov/pubmed/15342917 [Accessed August 22, 2018].

Roybal, C.N. et al., 2005. The oxidative stressor arsenite activates vascular endothelial growth factor mRNA transcription by an ATF4-dependent mechanism. *The Journal of biological chemistry*, 280(21), pp.20331–9. Available at: http://www.ncbi.nlm.nih.gov/pubmed/15788408 [Accessed August 1, 2018].

Rozen-Zvi, B. et al., 2013. TGF-β/Smad3 activates mammalian target of rapamycin complex-1 to promote collagen production by increasing HIF-1α expression. *American journal of physiology. Renal physiology*, 305(4), pp.F485-94. Available at: http://www.ncbi.nlm.nih.gov/pubmed/23761672 [Accessed July 24, 2018].

Sakurai, H., 2012. Targeting of TAK1 in inflammatory disorders and cancer. *Cell Press*, 33(10), pp.522–530. Available at: http://dx.doi.org/10.1016/j.tips.2012.06.007 [Accessed September 6, 2018].

Sancak, Y. et al., 2007. PRAS40 Is an Insulin-Regulated Inhibitor of the mTORC1 Protein Kinase. *Molecular Cell*, 25(6), pp.903–915. Available at: http://linkinghub.elsevier.com/retrieve/pii/S1097276507001487 [Accessed March 16, 2017].

Sancak, Y. et al., 2010. Ragulator-Rag complex targets mTORC1 to the lysosomal surface and is necessary for its activation by amino acids. *Cell*, 141(2), pp.290–303. Available at: http://www.pubmedcentral.nih.gov/articlerender.fcgi?artid=3024592&tool=pmcentrez&rendertype=abstract [Accessed September 27, 2016].

Sanchez Canedo, C. et al., 2010. Activation of the cardiac mTOR/p70 ^{S6K} pathway by leucine requires PDK1 and correlates with PRAS40 phosphorylation. *American Journal of Physiology-Endocrinology and Metabolism*, 298(4), pp.E761–E769. Available at: http://www.physiology.org/doi/10.1152/ajpendo.00421.2009 [Accessed July 27, 2018].

Sanders, Y.Y. et al., 2015. SMAD-Independent Down-Regulation of Caveolin-1 by TGF-β: Effects on Proliferation and Survival of Myofibroblasts R. Johnson, ed. *PLOS ONE*, 10(2), p.e0116995. Available at: http://dx.plos.org/10.1371/journal.pone.0116995 [Accessed October 15, 2018].

Sapkota, G. et al., 2006. Dephosphorylation of the linker regions of Smad1 and Smad2/3 by small C-terminal domain phosphatases has distinct outcomes for bone morphogenetic protein and transforming growth factor-beta pathways. *The Journal of biological chemistry*, 281(52), pp.40412–9. Available at: http://www.ncbi.nlm.nih.gov/pubmed/17085434 [Accessed August 30, 2018].

Sapkota, G.P., 2013. The TGFβ-induced phosphorylation and activation of p38 mitogen-activated protein kinase is mediated by MAP3K4 and MAP3K10 but not TAK1. *Open biology*, 3(6), p.130067. Available at: http://rsob.royalsocietypublishing.org/content/3/6/130067 [Accessed May 15, 2015].

Sarbassov, D.D. et al., 2006. Prolonged rapamycin treatment inhibits mTORC2 assembly and Akt/PKB. *Molecular cell*, 22(2), pp.159–68. Available at: http://www.ncbi.nlm.nih.gov/pubmed/16603397 [Accessed July 26, 2018].

Sato, T. et al., 2009. Specific Activation of mTORC1 by Rheb G-protein *in Vitro* Involves Enhanced Recruitment of Its Substrate Protein. *Journal of Biological Chemistry*, 284(19), pp.12783–12791. Available at: http://www.ncbi.nlm.nih.gov/pubmed/19299511 [Accessed August 27, 2018].

Saxton, R.A. et al., 2016. Mechanism of arginine sensing by CASTOR1 upstream of mTORC1. *Nature*, 536(7615), pp.229–233. Available at: http://www.ncbi.nlm.nih.gov/pubmed/27487210 [Accessed August 27, 2018].

Saxton, R.A. et al., 2017. mTOR Signaling in Growth, Metabolism, and Disease. *Cell*, 168(6), pp.960–976. Available at: http://www.ncbi.nlm.nih.gov/pubmed/28283069 [Accessed July 7, 2017].

Schalm, S.S. & Blenis, J., 2002. Identification of a conserved motif required for mTOR signaling. *Current biology : CB*, 12(8), pp.632–9. Available at: http://www.ncbi.nlm.nih.gov/pubmed/11967149 [Accessed July 27, 2018].

Schmelzle, T. & Hall, M.N., 2000. TOR, a central controller of cell growth. *Cell*, 103(2), pp.253–62. Available at: http://www.ncbi.nlm.nih.gov/pubmed/11057898 [Accessed July 25, 2018].

Seibold, M.A. et al., 2011. A Common *MUC5B* Promoter Polymorphism and Pulmonary Fibrosis. *New England Journal of Medicine*, 364(16), pp.1503–1512. Available at: http://www.ncbi.nlm.nih.gov/pubmed/21506741 [Accessed August 29, 2018].

Sekulić, A. et al., 2000. A Direct Linkage between the Phosphoinositide 3-Kinase-AKT Signaling Pathway and the Mammalian Target of Rapamycin in Mitogen-stimulated and Transformed Cells. *Cancer Research*, 60(13).

Selman, M., 2006. Role of Epithelial Cells in Idiopathic Pulmonary Fibrosis: From Innocent Targets to Serial Killers. *Proceedings of the American Thoracic Society*, 3(4), pp.364–372. Available at: http://pats.atsjournals.org/cgi/doi/10.1513/pats.200601-003TK [Accessed August 29, 2018].

Selman, M. et al., 2000. TIMP-1, -2, -3, and -4 in idiopathic pulmonary fibrosis. A prevailing nondegradative lung microenvironment? *American Journal of Physiology-Lung Cellular and Molecular Physiology*, 279(3), pp.L562–L574. Available at: http://www.ncbi.nlm.nih.gov/pubmed/10956632 [Accessed January 10, 2018].

Selvarajah, B. et al., 2019. mTORC1 amplifies the ATF4-dependent de novo serine-glycine pathway to supply glycine during TGF-β1-induced collagen biosynthesis. *Science signaling*, 12(582), p.eaav3048. Available at: http://www.ncbi.nlm.nih.gov/pubmed/31113850 [Accessed June 21, 2019].

Seo, J. et al., 2009. Atf4 regulates obesity, glucose homeostasis, and energy expenditure. *Diabetes*, 58(11), pp.2565–73. Available at: http://www.ncbi.nlm.nih.gov/pubmed/19690063 [Accessed August 1, 2018].

Shi, M. et al., 2007. Phospholipase D provides a survival signal in human cancer cells with activated H-Ras or K-Ras. *Cancer letters*, 258(2), pp.268–75. Available at: http://www.ncbi.nlm.nih.gov/pubmed/17949898 [Accessed August 27, 2018].

Shi, Y., 2006. Structural Insights into Smad Function and Specificity. In *Smad Signal Transduction*. Dordrecht: Springer Netherlands, pp. 215–233. Available at: http://link.springer.com/10.1007/1-4020-4709-6_11 [Accessed August 30, 2018].

Shou, J. et al., 2018. SIS3, a specific inhibitor of smad3, attenuates bleomycin-induced pulmonary fibrosis in mice. *Biochemical and Biophysical Research Communications*, 503(2), pp.757–762. Available at: http://www.ncbi.nlm.nih.gov/pubmed/29913150 [Accessed August 31, 2018].

Shuda, M. et al., 2015. CDK1 substitutes for mTOR kinase to activate mitotic cap-dependent protein translation. *Proceedings of the National Academy of Sciences*, 112(19), pp.5875–5882. Available at: http://www.ncbi.nlm.nih.gov/pubmed/25883264 [Accessed August 21, 2018].

Siu, M.K. et al., 2015. Transforming growth factor-β promotes prostate bone metastasis through induction of microRNA-96 and activation of the mTOR pathway. *Oncogene*, 34(36), pp.4767–4776. Available at: http://www.nature.com/articles/onc2014414 [Accessed July 27, 2018].

van Slegtenhorst, M. et al., 1997. Identification of the tuberous sclerosis gene TSC1 on chromosome 9q34. *Science (New York, N.Y.)*, 277(5327), pp.805–8. Available at: http://www.ncbi.nlm.nih.gov/pubmed/9242607 [Accessed August 28, 2018].

Smith, E.M. et al., 2005. The Tuberous Sclerosis Protein TSC2 Is Not Required for the Regulation of the Mammalian Target of Rapamycin by Amino Acids and Certain Cellular Stresses. *Journal of Biological Chemistry*, 280(19), pp.18717–18727. Available at: http://www.ncbi.nlm.nih.gov/pubmed/15772076 [Accessed August 24, 2018].

Smith, G.C.M. & Jackson, S.P., 2010. The PIKK Family of Protein Kinases. *Handbook of Cell Signaling*, pp.575–580. Available at: https://www.sciencedirect.com/science/article/pii/B9780123741455000772 [Accessed July 25, 2018].

Souchelnytskyi, S. et al., 1996. Phosphorylation of Ser165 in TGF-beta type I receptor modulates TGF-beta1-induced cellular responses. *The EMBO journal*, 15(22), pp.6231–40. Available at: http://www.ncbi.nlm.nih.gov/pubmed/8947046 [Accessed August 30, 2018].

Stanley, S.E. et al., 2016. Loss-of-function mutations in the RNA biogenesis factor *NAF1* predispose to pulmonary fibrosis–emphysema. *Science Translational Medicine*, 8(351), p.351ra107-351ra107. Available at: http://www.ncbi.nlm.nih.gov/pubmed/27510903 [Accessed August 29, 2018].

Strieter, R.M. & Mehrad, B., 2009. New mechanisms of pulmonary fibrosis. *Chest*, 136(5), pp.1364–1370. Available at: http://www.ncbi.nlm.nih.gov/pubmed/19892675 [Accessed February 3, 2018].

Stuart, B.D. et al., 2015. Exome sequencing links mutations in PARN and RTEL1 with familial pulmonary fibrosis and telomere shortening. *Nature Genetics*, 47(5), pp.512–517. Available at: http://www.ncbi.nlm.nih.gov/pubmed/25848748 [Accessed August 29, 2018].

Sullivan, D.E. et al., 2008. The Latent Form of TGFβ 1 is Induced by TNFα Through an ERK Specific Pathway and is Activated by Asbestos-Derived Reactive Oxygen Species *In Vitro* and *In Vivo*. *Journal of Immunotoxicology*, 5(2), pp.145–149. Available at: http://www.tandfonline.com/doi/full/10.1080/15476910802085822 [Accessed April 5, 2018].

Sun, Y. et al., 2008. Phospholipase D1 is an effector of Rheb in the mTOR pathway. *Proceedings of the National Academy of Sciences of the United States of America*, 105(24), pp.8286–91. Available at: http://www.ncbi.nlm.nih.gov/pubmed/18550814 [Accessed March 27, 2017].

Sun, Y. & Chen, J., 2008. mTOR signaling: PLD takes center stage. *Cell Cycle*, 7(20), pp.3118–3123. Available at: http://www.tandfonline.com/doi/abs/10.4161/cc.7.20.6881 [Accessed March 27, 2017].

Sutherland, J.J. et al., 2011. A robust high-content imaging approach for probing the mechanism of action and phenotypic outcomes of cell-cycle modulators. *Molecular cancer therapeutics*, 10(2), pp.242–54. Available at: http://www.ncbi.nlm.nih.gov/pubmed/21216932 [Accessed August 21, 2018].

Tager, A.M. et al., 2008. The lysophosphatidic acid receptor LPA1 links pulmonary fibrosis to lung injury by mediating fibroblast recruitment and vascular leak. *Nature Medicine*, 14(1), pp.45–54. Available at: http://www.ncbi.nlm.nih.gov/pubmed/18066075 [Accessed August 30, 2018].

Tan, L. et al., 2017. Studies of TAK1-centered polypharmacology with novel covalent TAK1 inhibitors. *Bioorganic & medicinal chemistry*, 25(4), pp.1320–1328. Available at: http://www.ncbi.nlm.nih.gov/pubmed/28038940 [Accessed August 7, 2018].

Tanjore, H., Blackwell, T.S. & Lawson, W.E., 2012. Emerging evidence for endoplasmic reticulum stress in the pathogenesis of idiopathic pulmonary fibrosis. *American journal of physiology. Lung cellular and molecular physiology*, 302(8), pp.L721-9. Available at: http://www.ncbi.nlm.nih.gov/pubmed/22287606 [Accessed January 9, 2018].

Tatler, A.L. & Jenkins, G., 2012. TGF-β Activation and Lung Fibrosis. *Proceedings of the American Thoracic Society*, 9(3), pp.130–136. Available at: http://www.atsjournals.org/doi/abs/10.1513/pats.201201-003AW [Accessed April 5, 2018].

Tavares, M.R. et al., 2015. The S6K protein family in health and disease. *Life Sciences*, 131, pp.1–10. Available at: https://www.sciencedirect.com/science/article/pii/S0024320515001538?via%3Dihub#bb0420 [Accessed July 26, 2018].

Thoreen, C.C. et al., 2009. An ATP-competitive Mammalian Target of Rapamycin Inhibitor Reveals Rapamycin-resistant Functions of mTORC1. *Journal of Biological Chemistry*, 284(12), pp.8023–8032. Available at: http://www.ncbi.nlm.nih.gov/pubmed/19150980 [Accessed August 16, 2018].

Toschi, A. et al., 2009. Regulation of mTORC1 and mTORC2 complex assembly by phosphatidic acid: competition with rapamycin. *Molecular and cellular biology*, 29(6), pp.1411–20. Available at: http://www.ncbi.nlm.nih.gov/pubmed/19114562 [Accessed August 24, 2018].

Tsakiri, K.D. et al., 2007. Adult-onset pulmonary fibrosis caused by mutations in telomerase. *Proceedings of the National Academy of Sciences of the United States of America*, 104(18), pp.7552–7. Available at: http://www.ncbi.nlm.nih.gov/pubmed/17460043 [Accessed August 29, 2018].

Tsuchida, K.-I. et al., 2003. Role of Smad4 on TGF-β–induced extracellular matrix stimulation in mesangial cells. *Kidney International*, 63(6), pp.2000–2009. Available at: https://www.sciencedirect.com/science/article/pii/S0085253815491173 [Accessed August 17, 2018].

Velásquez, C. et al., 2016. Mitotic protein kinase CDK1 phosphorylation of mRNA translation regulator 4E-BP1 Ser83 may contribute to cell transformation. *Proceedings of the National Academy of Sciences of the United States of America*, 113(30), pp.8466–71. Available at: http://www.ncbi.nlm.nih.gov/pubmed/27402756 [Accessed July 26, 2018].

Verrecchia, F., Chu, M.L. & Mauviel, A., 2001. Identification of novel TGF-beta /Smad gene targets in dermal fibroblasts using a combined cDNA microarray/promoter transactivation approach. *The Journal of biological chemistry*, 276(20), pp.17058–62. Available at: http://www.ncbi.nlm.nih.gov/pubmed/11279127 [Accessed September 13, 2017].

Verrecchia, F. & Mauviel, A., 2002. Transforming Growth Factor-β Signaling Through the Smad Pathway: Role in Extracellular Matrix Gene Expression and Regulation. *Journal of Investigative Dermatology*, 118(2), pp.211–215. Available at: https://www.sciencedirect.com/science/article/pii/S0022202X15415520 [Accessed April 22, 2018].

Vilella-Bach, M. et al., 1999. The FKBP12-rapamycin-binding domain is required for FKBP12-rapamycin-associated protein kinase activity and G1 progression. *The Journal of biological chemistry*, 274(7), pp.4266–72. Available at: http://www.ncbi.nlm.nih.gov/pubmed/9933627 [Accessed July 25, 2018].

Walker, N.M. et al., 2016. Mechanistic Target of Rapamycin Complex 1 (mTORC1) and mTORC2 as Key Signaling Intermediates in Mesenchymal Cell Activation. *Journal of Biological Chemistry*, 291(12), pp.6262–6271. Available at: http://www.ncbi.nlm.nih.gov/pubmed/26755732 [Accessed August 16, 2018].

Wang, R. et al., 1999. Angiotensin II induces apoptosis in human and rat alveolar epithelial cells. *The American journal of physiology*, 276(5 Pt 1), pp.L885-9. Available at: http://www.ncbi.nlm.nih.gov/pubmed/10330045 [Accessed October 15, 2018].

Wang, R. et al., 1999. Human lung myofibroblast-derived inducers of alveolar epithelial apoptosis identified as angiotensin peptides. *American Journal of Physiology-Lung Cellular and Molecular Physiology*, 277(6), pp.L1158–L1164. Available at: http://www.ncbi.nlm.nih.gov/pubmed/10600886 [Accessed October 15, 2018].

Wang, S. et al., 2015. Metabolism. Lysosomal amino acid transporter SLC38A9 signals arginine sufficiency to mTORC1. *Science (New York, N.Y.)*, 347(6218), pp.188–94. Available at: http://www.pubmedcentral.nih.gov/articlerender.fcgi?artid=4295826&tool=pmcentrez&rendertype=abstract [Accessed January 23, 2017].

Wang, X. et al., 1998. Amino acid availability regulates p70 S6 kinase and multiple translation factors. *The Biochemical journal*, 334 (Pt 1), pp.261–7. Available at: http://www.ncbi.nlm.nih.gov/pubmed/9693128 [Accessed August 24, 2018].

Wang, X. et al., 2008. Re-evaluating the Roles of Proposed Modulators of Mammalian Target of Rapamycin Complex 1 (mTORC1) Signaling. *Journal of Biological Chemistry*, 283(45), pp.30482–30492. Available at: http://www.ncbi.nlm.nih.gov/pubmed/18676370 [Accessed August 27, 2018].

Wang, X. et al., 2003. The C terminus of initiation factor 4E-binding protein 1 contains multiple regulatory features that influence its function and phosphorylation. *Molecular and cellular biology*, 23(5), pp.1546–57. Available at: http://www.ncbi.nlm.nih.gov/pubmed/12588975 [Accessed July 26, 2018].

Wang, X.M. et al., 2006. Caveolin-1: a critical regulator of lung fibrosis in idiopathic pulmonary fibrosis. *The Journal of Experimental Medicine*, 203(13), pp.2895–2906. Available at: http://www.ncbi.nlm.nih.gov/pubmed/17178917 [Accessed October 15, 2018].

Wells, A.U., 2013. The revised ATS/ERS/JRS/ALAT diagnostic criteria for idiopathic pulmonary fibrosis (IPF)--practical implications. *Respiratory research*, 14 Suppl 1, p.S2.

Wienecke, R., König, A. & DeClue, J.E., 1995. Identification of tuberin, the tuberous sclerosis-2 product. Tuberin possesses specific Rap1GAP activity. *The Journal of biological chemistry*, 270(27), pp.16409–14. Available at: http://www.ncbi.nlm.nih.gov/pubmed/7608212 [Accessed August 28, 2018].

Wilborn, J. et al., 1995. Cultured lung fibroblasts isolated from patients with idiopathic pulmonary fibrosis have a diminished capacity to synthesize prostaglandin E2 and to express cyclooxygenase-2. *Journal of Clinical Investigation*, 95(4), pp.1861–1868. Available at: http://www.ncbi.nlm.nih.gov/pubmed/7706493 [Accessed October 15, 2018].

Willis, B.C. et al., 2005. Induction of epithelial-mesenchymal transition in alveolar epithelial cells by transforming growth factor-beta1: potential role in idiopathic pulmonary fibrosis. *The American journal of pathology*, 166(5), pp.1321–32. Available at: http://www.ncbi.nlm.nih.gov/pubmed/15855634 [Accessed February 17, 2018].

Wollin, L. et al., 2014. Antifibrotic and anti-inflammatory activity of the tyrosine kinase inhibitor nintedanib in experimental models of lung fibrosis. *The Journal of pharmacology and experimental therapeutics*, 349(2), pp.209–20. Available at: http://www.ncbi.nlm.nih.gov/pubmed/24556663 [Accessed January 29, 2018].

Wollin, L. et al., 2015. Mode of action of nintedanib in the treatment of idiopathic pulmonary fibrosis. *The European respiratory journal*, 45(5), pp.1434–45. Available at: http://www.ncbi.nlm.nih.gov/pubmed/25745043 [Accessed January 29, 2018].

Wolters, P.J., Collard, H.R. & Jones, K.D., 2014. Pathogenesis of idiopathic pulmonary fibrosis. *Annual review of pathology*, 9, pp.157–79. Available at: http://www.pubmedcentral.nih.gov/articlerender.fcgi?artid=4116429&tool=pmcentrez&rendertype=abstract [Accessed April 15, 2015].

Woodcock, H. V. et al., 2019. The mTORC1/4E-BP1 axis represents a critical signaling node during fibrogenesis. *Nature Communications*, 10(1), p.6. Available at: http://www.nature.com/articles/s41467-018-07858-8 [Accessed January 5, 2019].

Woodford, M.R. et al., 2017. Tumor suppressor Tsc1 is a new Hsp90 co-chaperone that facilitates folding of kinase and non-kinase clients. *The EMBO journal*, 36(24), pp.3650–3665. Available at: http://www.ncbi.nlm.nih.gov/pubmed/29127155 [Accessed August 28, 2018].

Wu, J. et al., 2013. Mechanism and in vitro pharmacology of TAK1 inhibition by (5Z)-7-Oxozeaenol. *ACS chemical biology*, 8(3), pp.643–50. Available at: http://dx.doi.org/10.1021/cb3005897 [Accessed June 18, 2015].

Xiao, G.H. et al., 1997. The tuberous sclerosis 2 gene product, tuberin, functions as a Rab5 GTPase activating protein (GAP) in modulating endocytosis. *The Journal of biological chemistry*, 272(10), pp.6097–100. Available at: http://www.ncbi.nlm.nih.gov/pubmed/9045618 [Accessed August 28, 2018].

Xie, N. et al., 2015. Glycolytic Reprogramming in Myofibroblast Differentiation and Lung Fibrosis. *American journal of respiratory and critical care medicine*, 192(12), pp.1462–74. Available at: http://www.ncbi.nlm.nih.gov/pubmed/26284610 [Accessed August 16, 2018].

Xu, L., Chen, S. & Bergan, R.C., 2006. MAPKAPK2 and HSP27 are downstream effectors of p38 MAP kinase-mediated matrix metalloproteinase type 2 activation and cell invasion in human prostate cancer. *Oncogene*, 25(21), pp.2987–98. Available at: http://dx.doi.org/10.1038/sj.onc.1209337 [Accessed May 16, 2016].

Yamaguchi, K. et al., 1995. Identification of a member of the MAPKKK family as a potential mediator of TGF-beta signal transduction. *Science (New York, N.Y.)*, 270(5244), pp.2008–11. Available at: http://www.ncbi.nlm.nih.gov/pubmed/8533096 [Accessed September 6, 2018].

Yamashita, A. et al., 2001. Human SMG-1, a novel phosphatidylinositol 3-kinase-related

protein kinase, associates with components of the mRNA surveillance complex and is involved in the regulation of nonsense-mediated mRNA decay. *Genes and Development*, 15(17), pp.2215–2228. Available at: http://www.ncbi.nlm.nih.gov/pubmed/11544179 [Accessed July 25, 2018].

Yang, C. et al., 2014. Glutamine Oxidation Maintains the TCA Cycle and Cell Survival during Impaired Mitochondrial Pyruvate Transport. *Molecular Cell*, 56(3), pp.414–424. Available at: https://www.sciencedirect.com/science/article/pii/S1097276514007825#undfig1 [Accessed April 10, 2019].

Yang, H. et al., 2013. mTOR kinase structure, mechanism and regulation. *Nature*, 497(7448), pp.217–23. Available at: http://www.ncbi.nlm.nih.gov/pubmed/23636326 [Accessed July 24, 2018].

Yang, S. et al., 2012. Participation of miR-200 in pulmonary fibrosis. *The American journal of pathology*, 180(2), pp.484–93. Available at: http://www.ncbi.nlm.nih.gov/pubmed/22189082 [Accessed August 29, 2018].

Yang, X. et al., 2004. ATF4 is a substrate of RSK2 and an essential regulator of osteoblast biology; implication for Coffin-Lowry Syndrome. *Cell*, 117(3), pp.387–98. Available at: http://www.ncbi.nlm.nih.gov/pubmed/15109498 [Accessed August 1, 2018].

Yang, Y. et al., 2011. A cytosolic ATM/NEMO/RIP1 complex recruits TAK1 to mediate the NF-kappaB and p38 mitogen-activated protein kinase (MAPK)/MAPK-activated protein 2 responses to DNA damage. *Molecular and cellular biology*, 31(14), pp.2774–86. Available at: http://www.ncbi.nlm.nih.gov/pubmed/21606198 [Accessed September 6, 2018].

Yoon, M.-S. et al., 2011. Class III PI-3-kinase activates phospholipase D in an amino acid-sensing mTORC1 pathway. *The Journal of cell biology*, 195(3), pp.435–47. Available at: http://jcb.rupress.org/content/195/3/435.abstract [Accessed February 1, 2017].

Yoon, M.-S. et al., 2015. Rapid Mitogenic Regulation of the mTORC1 Inhibitor, DEPTOR, by Phosphatidic Acid. *Molecular Cell*, 58(3), pp.549–556. Available at: http://www.ncbi.nlm.nih.gov/pubmed/25936805 [Accessed July 27, 2018].

Young, J. & Povey, S., 1998. The genetic basis of tuberous sclerosis. *Molecular Medicine Today*, 4(7), pp.313–319. Available at: https://www.sciencedirect.com/science/article/pii/S1357431098012453 [Accessed August 28, 2018].

Zaru, R. et al., 2015. The PDK1-Rsk Signaling Pathway Controls Langerhans Cell Proliferation and Patterning. *Journal of immunology (Baltimore, Md. : 1950)*, 195(9), pp.4264–72. Available at: http://www.ncbi.nlm.nih.gov/pubmed/26401001 [Accessed August 22, 2018].

Zawel, L. et al., 1998. Human Smad3 and Smad4 are sequence-specific transcription activators. *Molecular cell*, 1(4), pp.611–7. Available at: http://www.ncbi.nlm.nih.gov/pubmed/9660945 [Accessed August 31, 2018].

Zhang, H.Y. et al., 1996. Lung fibroblast alpha-smooth muscle actin expression and contractile phenotype in bleomycin-induced pulmonary fibrosis. *The American journal of pathology*, 148(2), pp.527–37. Available at: http://www.ncbi.nlm.nih.gov/pubmed/8579115 [Accessed October 15, 2018].

Zhang, J. et al., 2011. Smad2 and Smad3 as mediators of the response of adventitial fibroblasts induced by transforming growth factor β1. *Molecular Medicine Reports*, 4(3), pp.561–567. Available at: http://www.spandidos-publications.com/10.3892/mmr.2011.458 [Accessed August 17, 2018].

Zhang, Y.E., 2009. Non-Smad pathways in TGF-beta signaling. *Cell research*, 19(1), pp.128–39. Available at: http://www.ncbi.nlm.nih.gov/pubmed/19114990 [Accessed August 9, 2018].

Zhao, J. et al., 2002. Smad3 deficiency attenuates bleomycin-induced pulmonary fibrosis in mice. *American Journal of Physiology-Lung Cellular and Molecular Physiology*, 282(3), pp.L585–L593. Available at: http://www.physiology.org/doi/10.1152/ajplung.00151.2001 [Accessed April 22, 2018].

Zhao, Y. & Geverd, D.A., 2002. Regulation of Smad3 expression in bleomycin-induced pulmonary fibrosis: a negative feedback loop of TGF-β signaling. *Biochemical and Biophysical Research Communications*, 294(2), pp.319–323. Available at: http://www.ncbi.nlm.nih.gov/pubmed/12051713 [Accessed August 31, 2018].

Zhao, Y., Xiong, X. & Sun, Y., 2011. DEPTOR, an mTOR inhibitor, is a physiological substrate of SCF(βTrCP) E3 ubiquitin ligase and regulates survival and autophagy. *Molecular cell*, 44(2), pp.304–16. Available at: http://www.ncbi.nlm.nih.gov/pubmed/22017876 [Accessed July 27, 2018].

Zhu, K. et al., 2013. ATF4 promotes bone angiogenesis by increasing VEGF expression and release in the bone environment. *Journal of bone and mineral research : the official journal of the American Society for Bone and Mineral Research*, 28(9), pp.1870–1884. Available at: http://www.ncbi.nlm.nih.gov/pubmed/23649506 [Accessed August 1, 2018].

Zoncu, R. et al., 2011. mTORC1 senses lysosomal amino acids through an inside-out mechanism that requires the vacuolar H(+)-ATPase. *Science (New York, N.Y.)*, 334(6056), pp.678–83. Available at: http://science.sciencemag.org/content/334/6056/678.abstract [Accessed February 1, 2017].

Zoz, D.F., Lawson, W.E. & Blackwell, T.S., 2011. Idiopathic pulmonary fibrosis: a disorder of epithelial cell dysfunction. *The American journal of the medical sciences*, 341(6), pp.435–8. Available at: http://www.ncbi.nlm.nih.gov/pubmed/21613930 [Accessed August 29, 2018].

Zuo, F. et al., 2002. Gene expression analysis reveals matrilysin as a key regulator of pulmonary fibrosis in mice and humans. *Proceedings of the National Academy of Sciences of the United States of America*, 99(9), pp.6292–7. Available at: http://www.ncbi.nlm.nih.gov/pubmed/11983918 [Accessed April 8, 2018].

Appendix

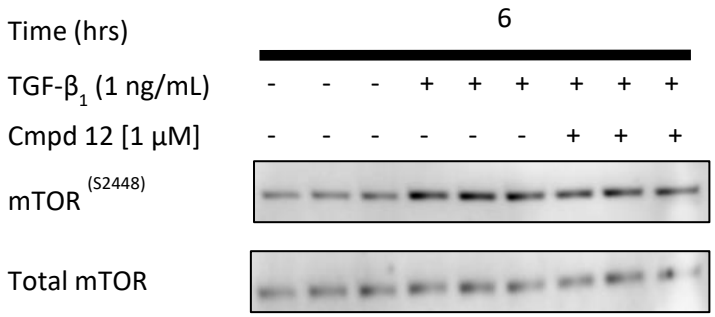

Appendix 1: The effect on PI3K inhibition on TGF-β$_1$ stimulated mTOR^{S2448} phosphorylation in pHLFs

pHLFs were serum-starved prior to treatment, the cells were incubated for 1 hour with and without compound 12 (cmpd) prior to stimulation with 1ng/ml TGF- β1 for 6 hours. The mTOR S2448 phosphorylation site was assessed by western blot.

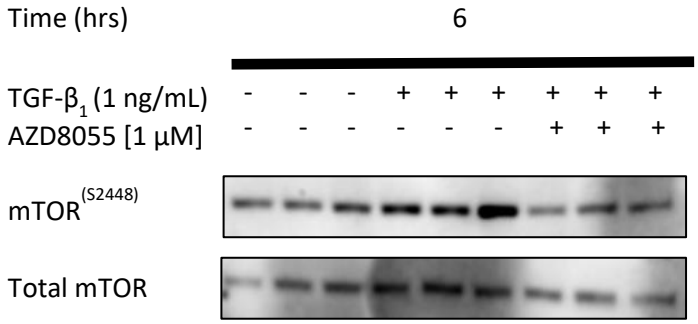

Appendix 2: The effects of mTOR kinase activity inhibition on TGF-β$_1$ stimulated mTOR^{S2448} phosphorylation in pHLFs

pHLFs were serum-starved prior to treatment, the cells were incubated for 1 hour with and without AZD8055 prior to stimulation with 1ng/ml TGF- β1 for 6 hours. The mTOR S2448 phosphorylation site was assessed by western blot.

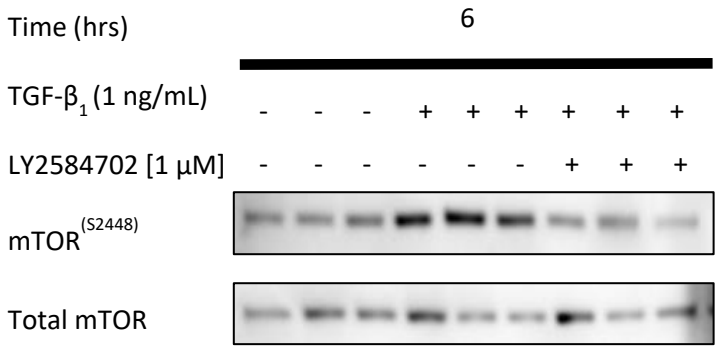

Appendix 3: The effects of P70S6K inhibition on TGF-β_1 stimulated mTOR^{S2448} phosphorylation in pHLFs

pHLFs were serum-starved prior to treatment, the cells were incubated for 1 hour with and without LY2584702 prior to stimulation with 1ng/ml TGF- β1 for 6 hours. The mTOR S2448 phosphorylation site was assessed by western blot.

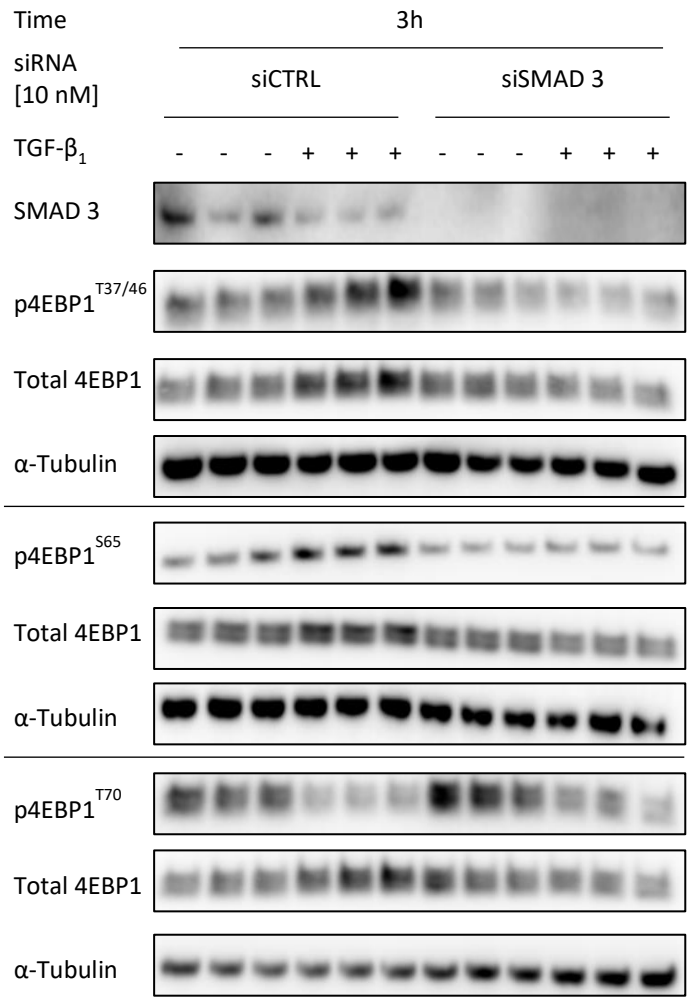

Appendix 4: The effect of SMAD 3 knock-down on TGF-β_1 stimulated 4E-BP1 phosphorylation in pHLFs

At 60-80% confluence pHLFs were transfected with SMAD 3 siRNA for 24 hours prior to starvation with 0% DMEM. Cells were starved for 24 hours prior to treatment with or without 1 ng/mL TGF-β_1. The cells were harvested 3 hours post stimulation. The lysates were assessed by either western blotting investigating four 4E-BP1 phosphorylation sites. Protein loading was verified by blotting with an anti-α-Tubulin antibody.

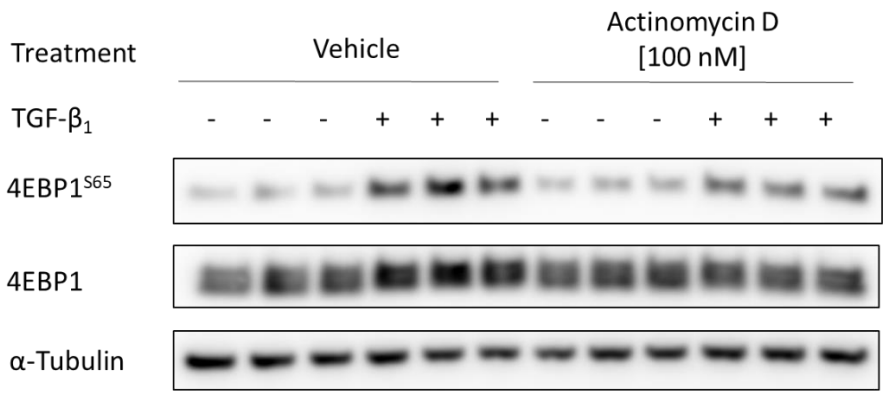

Appendix 5: The effect of Actinomycin D on TGF-β1 signalling in pHLFs

Confluent pHLFs were serum-starved prior for 24 hours prior to incubation with Actinomycin D for 1 hours followed by stimulation with 1 ng/mL TGF-β_1 for 3 hours. The phosphorylation of 4E-BP1^{S65} was assessed by western blotting.

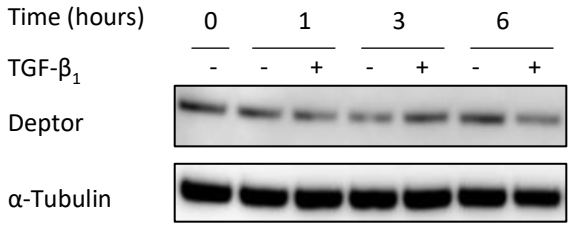

Appendix 6: The effect of TGF-β1 stimulation on DEPTOR protein expression over 6 hours in pHLFs

Confluent pHLFs were serum-starved prior to stimulation with 1 ng/mL TGF-β_1 for the indicated time-periods. DEPTOR was assessed by western blotting. Protein loading was verified by blotting with anti- α-tubulin antibody. The densitometry was calculated and plotted as DEPTOR to α-tubulin antibody ratio. The data is representative of two independent experiments. See Appendix 6 for the repeat.

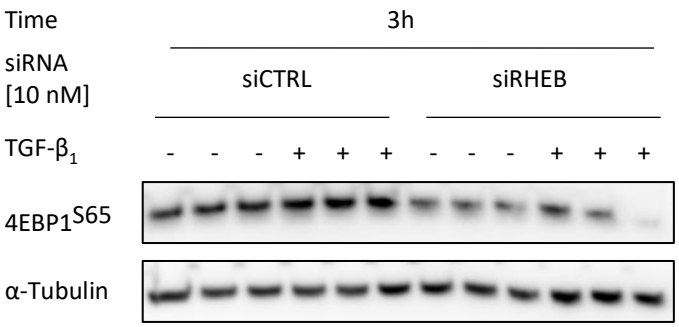

Appendix 7: The effect of RHEB knock-down on TGF-β_1 stimulated 4E-BP1 phosphorylation in pHLFs

At 60-80% confluence pHLFs were transfected with RHEB siRNA for 24 hours prior to starvation with 0% DMEM. Cells were starved for 24 hours prior to treatment with or without 1 ng/mL TGF-β_1. The cells were harvested 3 hours post stimulation. The lysates were assessed by western blotting investigating the 4E-BP1^{S65} phosphorylation site. Protein loading was verified by blotting with an anti-α-Tubulin antibody.

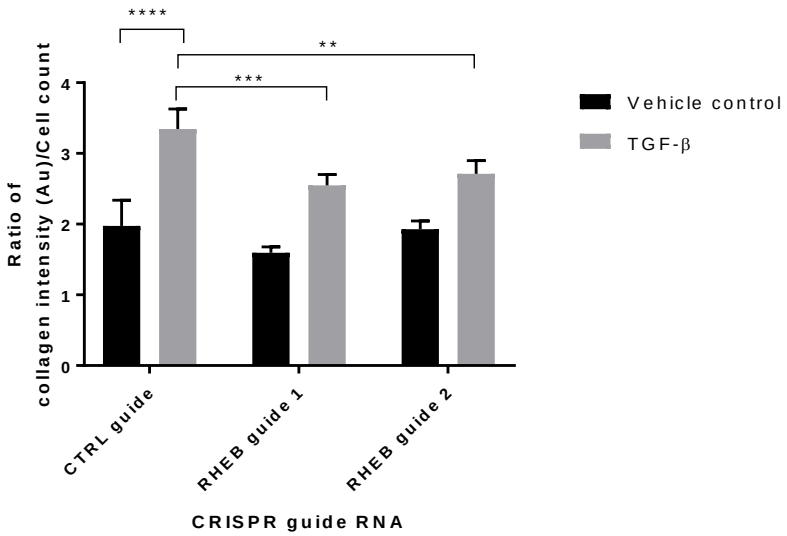

Appendix 8: The effect of RHEB knock-out on TGF-β_1 stimulated collagen I synthesis in pHLFs

pHLFs were electroporated with individual RHEB guide1/CAS9 complex. The cells were then seeded into a T25 cultured until confluence. The cells were treated with trypsin and re-seeded in 96 well plates in 10% DMEM. At confluence the pHLFs were starved for 24 hours prior to treatment. After starvation cells were incubated with DMEM containing Ficoll for 1 hour. Following incubation cells were treated with or without TGF-β_1 [1 ng/mL] which was spiked into the wells and incubated for 48 hours, prior to fixation and staining for type1 collagen (left column) and cell counts (right column) were obtained from a DAPI counter stain. Data are expressed as mean fluorescent intensity or cell count (n=4 reads per well) averaged across 4 replicates. Differences between groups were evaluated with two-way ANOVA and Tukey multiple comparison testing.

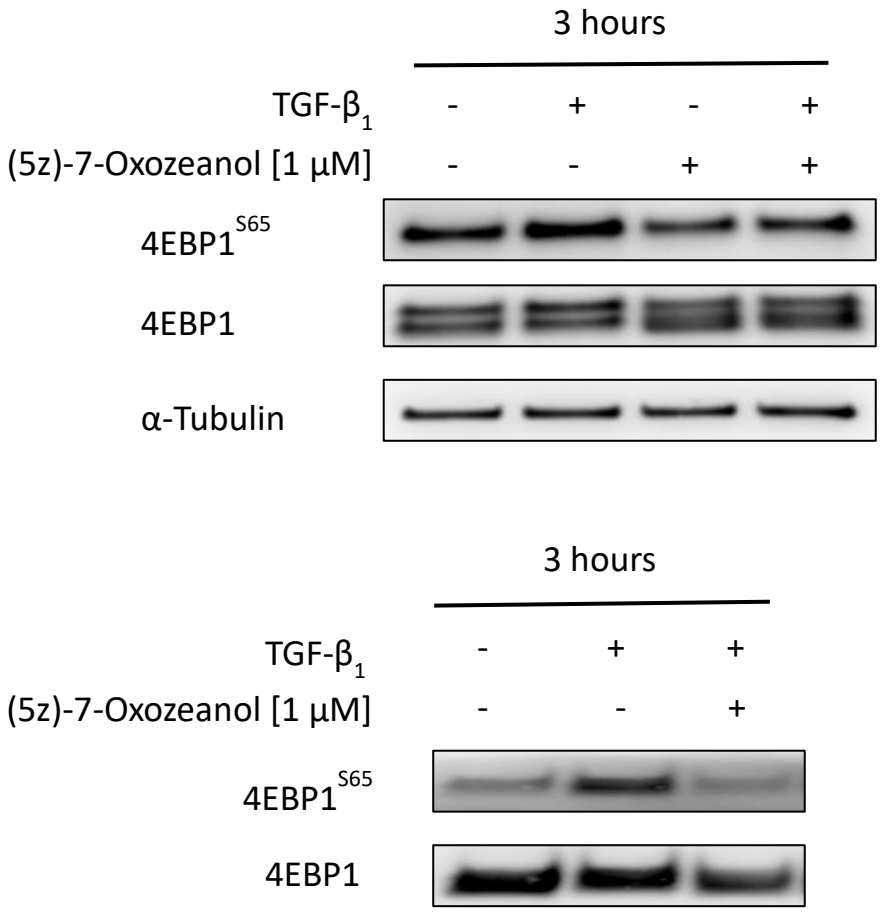

Appendix 9: The effect of (5z)-7-Oxozeaenol on TGF-β_1 stimulated mTORC1 phosphorylation at 3 hours in pHLFs

Confluent pHLFs were serum-starved prior for 24 hours prior to incubation with (5z)-7-Oxozeaenol for 1 hours and then stimulation with 1 ng/mL TGF-β_1 for 3 hours. Phosphorylation of 4E-BP1^{S65} was assessed by western blotting.

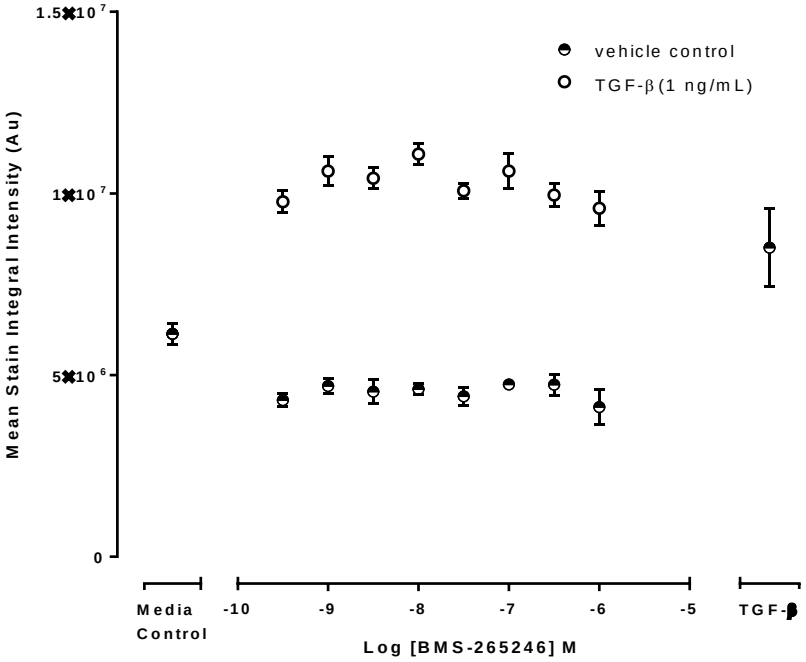

Appendix 10: The effect of BMS-256246 on TGF-β_1 stimulated collagen I synthesis in pHLF

Confluent pHLFs were starved for 24 hours before being incubated with increasing concentrations of BSM-256246 (vehicle controls were incubated with 0.1% DMSO) in DMEM containing Ficoll for 1 hour. Following incubation cells were treated with or without TGF-β_1 [1 ng/mL] which was spiked into the wells and incubated for 48 hours, prior to fixation and staining for type1 collagen (left column) and cell counts (right column) were obtained from a DAPI counter stain. Data are expressed as mean fluorescent intensity or cell count (n=4 reads per well) averaged across 4 replicates.

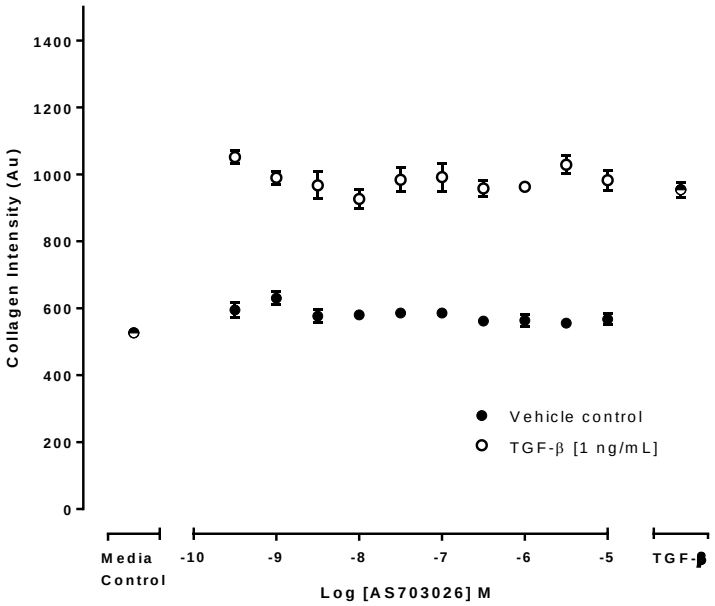

Appendix 11: The effect of AS703026 on TGF-β_1 stimulated collagen I synthesis in pHLF

Confluent pHLFs were starved for 24 hours before being incubated with increasing concentrations of AS703026 (vehicle controls were incubated with 0.1% DMSO) in DMEM containing Ficoll for 1 hour. Following incubation cells were treated with or without TGF-β_1 [1 ng/mL] which was spiked into the wells and incubated for 48 hours, prior to fixation and staining for type1 collagen (left column) and cell counts (right column) were obtained from a DAPI counter stain. Data are expressed as mean fluorescent intensity or cell count (n=4 reads per well) averaged across 4 replicates.

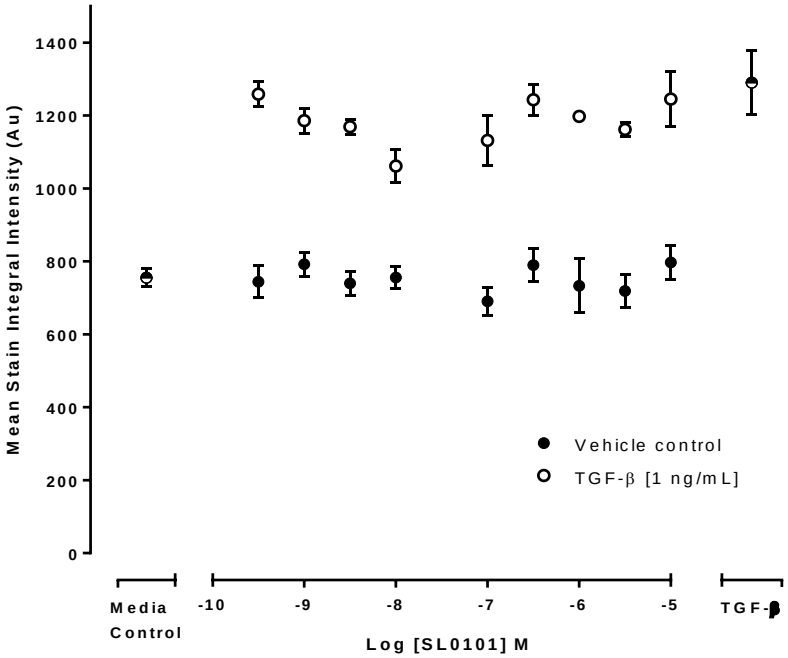

Appendix 12: The effect of SL0101 on TGF-β_1 stimulated collagen I synthesis in pHLF

Confluent pHLFs were starved for 24 hours before being incubated with increasing concentrations of AS703026 (vehicle controls were incubated with 0.1% DMSO) in DMEM containing Ficoll for 1 hour. Following incubation cells were treated with or without TGF-β_1 [1 ng/mL] which was spiked into the wells and incubated for 48 hours, prior to fixation and staining for type1 collagen (left column) and cell counts (right column) were obtained from a DAPI counter stain. Data are expressed as mean fluorescent intensity or cell count (n=4 reads per well) averaged across 4 replicates. This is representative of two independent experiments. See Appendix 12 for replicate data

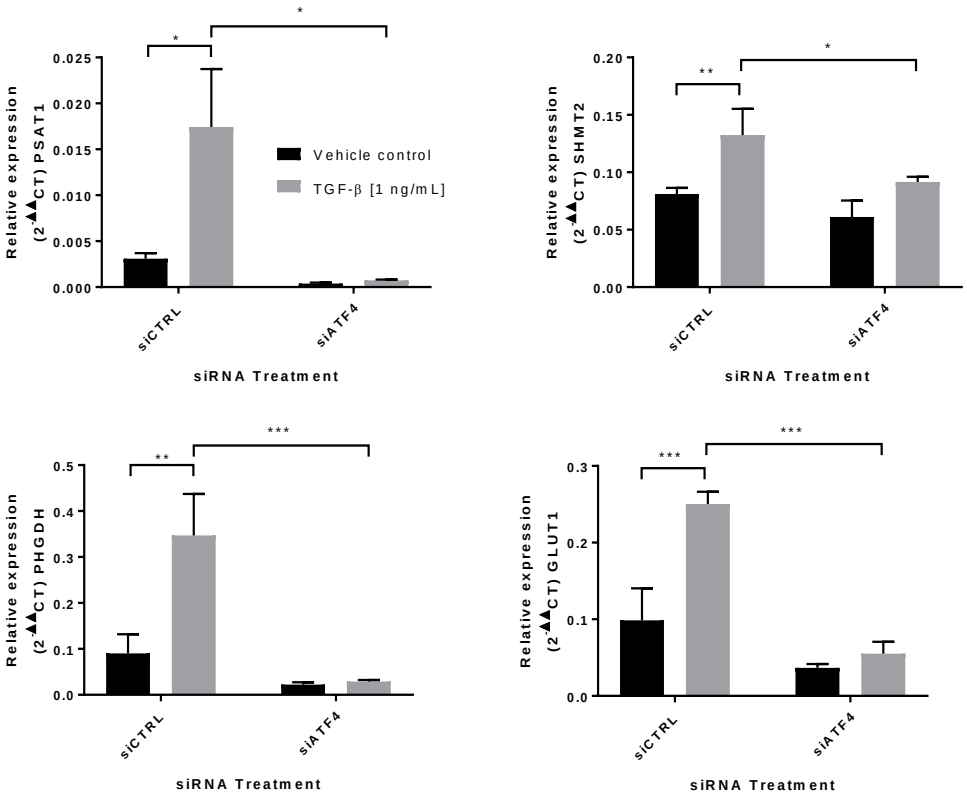

Appendix 14: The effect of ATF4 knock-down on TGF-β_1 induced glycolytic enzyme gene expression in pHLFs

At 60-80% confluence pHLFs were transfected with ATF4 siRNA for 24 hours prior to starvation with 0% DMEM. Cells were starved for 24 hours prior to treatment with or without 1 ng/mL TGF-β_1. The cells were harvested 24 hours post stimulation. The lysates were assessed by rt-qPCR. Data are shown as gene expression of PSAT1, SHMT2, PHDGH and GLUT1 expression relative to the geometric mean of two housekeeping genes (mean ± SEM, n=3 replicates). This data is representative of two independent experiments performed. Differences between groups were evaluated with two-way ANOVA and Tukey multiple comparison testing. This was made in collaboration with Dr Selvarajah

Chemical structures

AZD8055

- IC50 0.8 nM

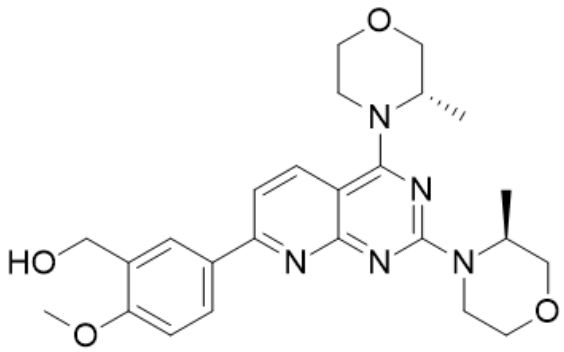

Rapamycin

- IC50 0.1 nM

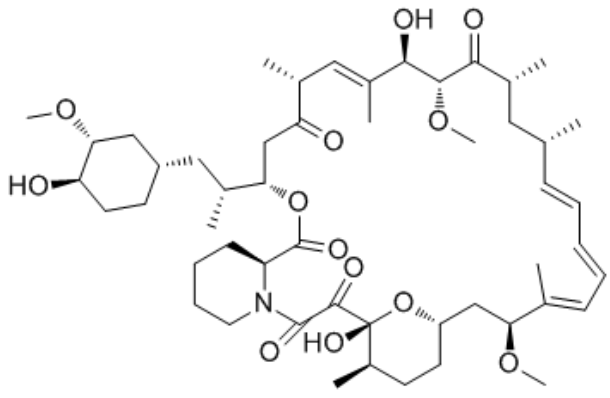

AS703026

- IC50 5 nM – 2 μM

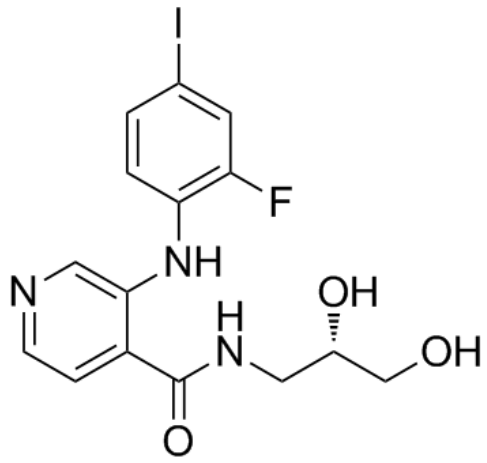

SL0101

- IC50 85 nM

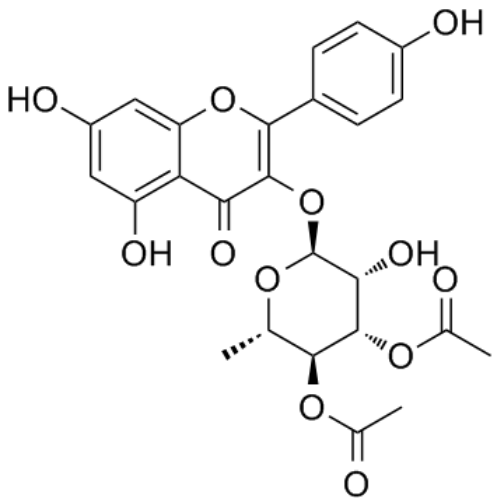

MKIV

- IC50 110 nM

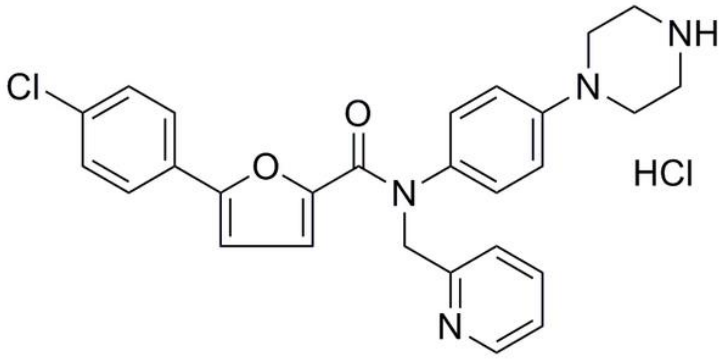

PF 3644022

- 5.2 nM

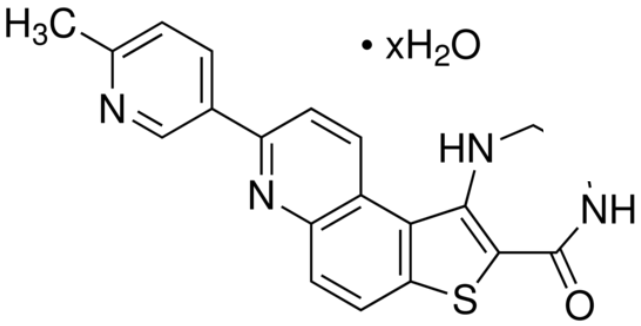

BMS-265246

- IC50 6-9 nM

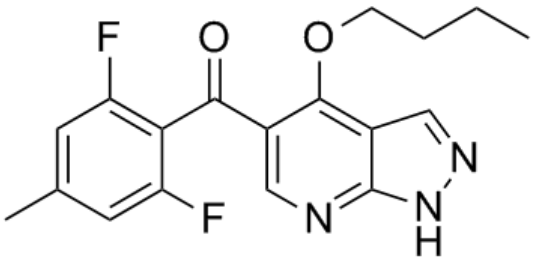

(5z)-7-Oxozeaenol

- IC50 8 nM

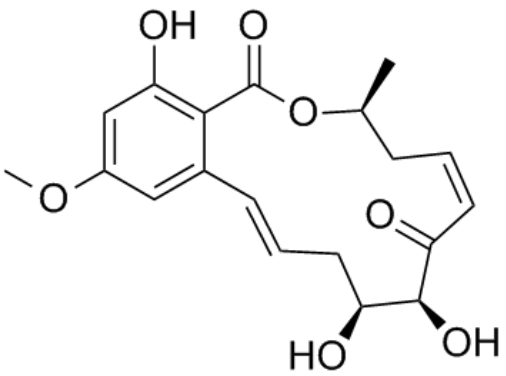

TAK-715

- IC50 7.1 nM (p38α)

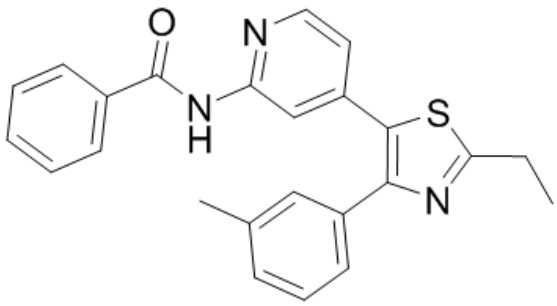

SB 202190

- IC50 50 nM (p38α) and 100 nM (p38β)

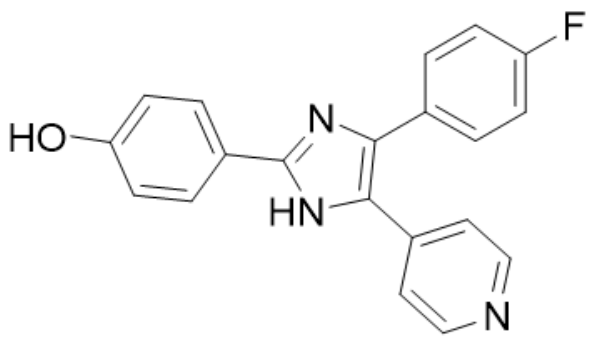

BIRB796

- IC50 50 nM (p38α) and 100 nM (p38β) 38 nM (p38α), 65 nM (p38β), 200 nM (p38δ), and 520 nM (p38γ)

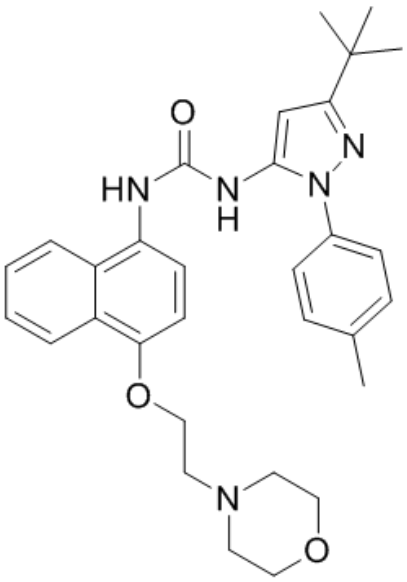

LY-2584702

- IC50 4 nM

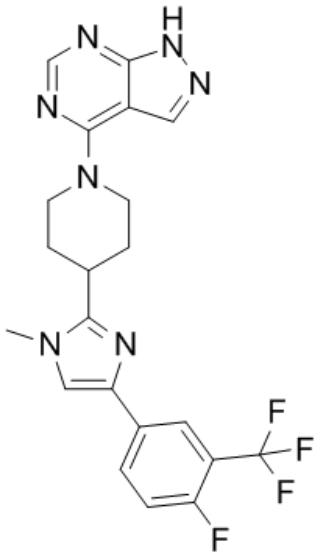

GSK2334470

- IC50 10 nM

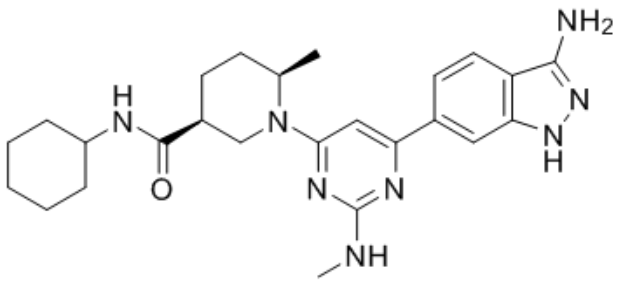

SB525334

- IC50 14.3 nM

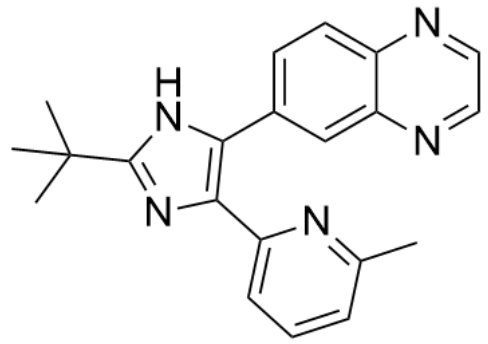

CB-839

- IC50 24 nM